

**New Applications of TEMPO in Organic  
Synthesis**

**Joseph P. Atkin**

**PhD**

**University of York**

**Chemistry**

**September 2015**

## Abstract

This thesis contains a number of projects investigating the use of TEMPO in organic synthesis, developing new methodologies for radical reactions and synthesising new TEMPO derivatives. Chapter 1 outlines the current status quo of radical chemistry and some of the uses of TEMPO in synthesis.

Chapter 2 details the TEMPO/Lewis acid mediated oxidation of acetals to form esters, in particular focussing on the optimisation of a TEMPO/MgBr<sub>2</sub> system, examining its scope and mechanism. The TEMPO/MgBr<sub>2</sub> system was shown to oxidise phenyl acetals with electron donating groups to form esters in moderate to good yield, but phenyl acetals with electron withdrawing groups and alkyl acetals gave considerably lower yields of esters.

Chapter 3 explores the use of TEMPO as an initiator in the radical addition of diphenylphosphine sulfide to alkenes and alkynes. The scope of this reaction has been explored in the form of both simple additions to C-C unsaturated bonds and C-C bond forming reactions in the cyclisation of dienes. A mechanism for these addition reactions has been proposed. Also investigated was the addition of diphenylphosphine sulfide to Michael acceptors at room temperature in the absence of a radical initiator. The chapter includes speculation on the mechanism of the uninitiated additions.

Chapter 4 discusses the synthesis of two novel nitroxide ionic liquids with the aim of using them as recyclable catalysts. The first of these, [BMIM][Carboxy-TEMPO], was synthesised in 17% yield and preliminary results show that it is capable of oxidising benzyl alcohol in [BMIM][BF<sub>4</sub>] and that both the solvent and the catalyst can be recycled. Benzyl-2-(2,2,6,6-tetramethylpiperidin-4-ylidene)acetate has been synthesised via a Horner-Wadsworth-Emmons reaction in 29% yield with aim of synthesising the second ionic liquid from it.

Chapter 5 outlines efforts to use TEMPO in the chiral resolution of 1-phenylethanol with camphorsulfonate and amino acid based ionic liquids as chiral auxiliaries.

## Table of Contents

Abstract .....	2
Table of Contents .....	3
List of Figures .....	8
List of Tables.....	16
Acknowledgements.....	18
Declaration .....	20
1. Introduction .....	21
1.1. General Radical Chemistry .....	22
1.1.1. What is a Radical? .....	22
1.1.2. Organic Radicals .....	23
1.1.3 Radical Stability .....	25
1.2. Initiation .....	28
1.2.1. Photolysis .....	29
1.2.2. Peroxide Initiators.....	30
1.2.3. Azo Initiators .....	31
1.2.4. Triethylborane.....	33
1.3. Radical Reactions .....	35
1.3.1. Radical Polarity.....	35
1.3.2. Baldwin's Rules .....	37
1.3.3. Radical Mediators .....	39
1.4. Tributyltin Hydride .....	40
1.4.1. Stannanes.....	40
1.4.2. Tributyltin Hydride Mediated Halogen Reductions .....	40
1.4.3. Tributyltin Hydride Mediated Cyclisations .....	41
1.4.4. Tributyltin Hydride Mediated Ring Expansions .....	42
1.4.5. Barton-McCombie Deoxygenation .....	43
1.4.6. Hydrostannation .....	44

1.4.7. Problems with Organostannanes.....	45
1.4.8. Alternative Tin Based Methods.....	46
1.5. Germanium Hydride.....	48
1.6. Silanes .....	49
1.6.1. Trialkylsilane Mediated Barton-McCombie Deoxygenation.....	50
1.6.2. Trialkylsilanes with Polarity Reversal Catalysts .....	50
1.6.3. Tris(trimethylsilyl)silane .....	53
1.6.4. Tris(trimethylsilyl)silane Mediated Reductions .....	53
1.7. Phosphorus Hydride Reagents .....	57
1.7.1. Hypophosphorus Acid and its Salts.....	57
1.8. TEMPO.....	62
1.8.1. Nitroxides .....	63
1.8.2. TEMPO.....	63
1.8.3. Synthesis of TEMPO .....	65
1.8.4. TEMPO Oxidations .....	68
1.8.5. TEMPO Mediated Polymerisation.....	72
1.8.6. Ionic Liquids.....	73
1.9. Aims.....	74
2. Acetal Oxidation .....	76
2.1. Acetal Introduction .....	77
2.1.1. Terminology .....	77
2.1.2. Acetals in Synthesis .....	78
2.1.3. Esters.....	82
2.1.4. Aims.....	83
2.2. Preliminary Investigations.....	83
2.2.1. Lewis Acid Screen.....	84
2.2.2. Mechanism.....	87
2.2.3. EPR Studies.....	88
2.2.4. TEMPO and Magnesium Bromide.....	91

2.3. Acetal Optimisation.....	94
2.3.1. Oxoammonium as a Possible Oxidant .....	95
2.3.2. Solvent.....	96
2.3.3. Reaction Stoichiometry.....	97
2.3.4. Time.....	99
2.3.5. Oxygen and Water .....	100
2.3.6. Temperature .....	101
2.3.7. Scale .....	103
2.3.8. Optimal Conditions .....	103
2.4. Acetal Scope .....	104
2.4.1. Steric Effects.....	104
2.4.2. Conjugation .....	106
2.4.3. Electronic Effects.....	107
2.4.4. Acetal Ring.....	110
2.4.5. Mechanism.....	111
2.4.6. Formation of a Primary Radical.....	113
2.4.7. Regioselectivity .....	116
3. Phosphorus Hydrides .....	119
3.1. Phosphorus Hydride Addition .....	120
3.1.1. Introduction .....	120
3.1.2. Horner-Wadsworth-Emmons.....	121
3.1.3. Different Phosphorus Hydrides.....	122
3.1.4. TEMPO Initiated Phosphorus Hydride Addition .....	125
3.1.5. Trapping with TEMPO .....	125
3.1.6. Phosphorus Hydride Stoichiometry .....	127
3.1.8. Cyclisations.....	129
3.1.9. Uninitiated Phosphorus Hydride Addition .....	132
4. TEMPO Ionic Liquids.....	137
4.1. Introduction .....	138
4.1.1. Nitroxide Ionic Liquids.....	138

4.1.2. Aims.....	141
4.2. Synthesis of Nitroxide Ionic Liquids .....	141
4.2.1. [BMIM][Carboxy-TEMPO] .....	141
4.2.2. Horner-Wadsworth-Emmons.....	143
5. Kinetic Resolution of Secondary Alcohols.....	146
5.1. Introduction .....	147
5.2. Kinetic Resolution .....	147
5.2.1. Camphorsulfonic Acid .....	147
5.2.2. Ionic Liquids.....	151
6. Conclusions .....	154
6.1 Acetal Oxidation.....	155
6.2 Phosphorus Hydrides .....	155
6.3 TEMPO Ionic Liquids.....	156
6.4 Kinetic Resolution of Secondary Alcohols.....	156
7. Future Work .....	157
7.1 Acetal Oxidation.....	158
7.2 Phosphorus Hydrides .....	159
7.3 TEMPO Ionic Liquids.....	160
7.4 Kinetic Resolution of Secondary Alcohols.....	160
8. Experimental .....	161
8.1. General Methods .....	162
8.2. Acetal Oxidation.....	162
8.3 Phosphorus Hydrides .....	182
8.4. TEMPO Ionic Liquids.....	192
8.5. Chiral Resolution of Secondary Alcohols .....	196
Appendices.....	201

<i>tert</i> -Butyl 3-[(diphenylphosphorothioyl)methyl]-4-methylpyrrolidine-1-carbamate (77) .....	202
<sup>1</sup> H NMR.....	202
<sup>13</sup> C NMR.....	203
COSY .....	204
HMQC .....	205
135 DEPT .....	206
[(4-Methyltetrahydrofuran-3-yl)methyl](diphenyl)phosphane sulfide (78).....	207
<sup>1</sup> H NMR.....	207
<sup>13</sup> C NMR.....	208
COSY .....	209
HMQC .....	210
135 DEPT .....	211
<i>tert</i> -Butyl 3-[(diphenylphosphorothioyl)methyl]-4-methylpyrrolidine-1-carbamate (80) .....	212
<sup>1</sup> H NMR.....	212
<sup>13</sup> C NMR.....	213
COSY .....	214
HMQC .....	215
Benzyl-2-(2,2,6,6-tetramethylpiperidin-4-ylidene)acetate (90) .....	216
<sup>1</sup> H NMR.....	216
<sup>13</sup> C NMR.....	217
COSY .....	218
HMQC .....	219
135 DEPT .....	220
Abbreviations .....	221
References.....	227

## List of Figures

Figure 1.1: Molecular orbital diagram of O <sub>2</sub> . .....	22
Figure 1.2: Attempted synthesis of hexaphenylethane. ....	23
Figure 1.3: Synthesis of triphenylmethyl radical. ....	23
Figure 1.4: Markovnikov and Anti-Markovnikov addition of HBr to allyl bromide. ..	24
Figure 1.5: Ionic addition of HBr to allyl bromide. ....	24
Figure 1.6: Radical addition of HBr to allyl bromide. ....	25
Figure 1.7: Methyl substituted radicals in decreasing order of stability. ....	25
Figure 1.8: Graphical representation of hyperconjugation. ....	26
Figure 1.9: Mesomeric stabilisation of a benzyl radical and an allyl radical. ....	26
Figure 1.10: Stabilisation of radicals by electron donating and withdrawing substituents. ....	26
Figure 1.11: Molecular orbital diagram of SOMO stabilisation by overlap with a LUMO. ....	27
Figure 1.12: Molecular orbital diagram of SOMO stabilisation by overlap with a HOMO. ....	27
Figure 1.13: Methyl, vinyl, ethenyl and phenyl radicals. ....	28
Figure 1.14: 3D structure of the triphenylmethyl radical ( <b>4</b> ). ....	28
Figure 1.15: Radical addition of chlorine to methane. ....	29
Figure 1.16: Thermolysis of a peroxide bond. ....	30
Figure 1.17: Radical dissociation of benzoyl peroxide and tert-butyl peroxide with their O-O bond strengths. <sup>9,10</sup> .....	30
Figure 1.18: Fragmentation of phenyl carboxy radical and tert-butoxy radical. ....	31
Figure 1.19: Fragmentation of AIBN to form isobutyronitrile radicals ( <b>7</b> ). ....	31
Figure 1.20: Recombination of isobutyronitrile radicals. ....	32
Figure 1.21: Reaction mechanism of the Wohl-Ziegler reaction. ....	32
Figure 1.22: Bromination of alkenes by Br <sub>2</sub> . ....	33
Figure 1.23: Asymmetric synthesis of (S)-(-)-acromelobinic acid from 2,5-dimethylpyridine. ....	33
Figure 1.24: Fragmentation of Et <sub>3</sub> B to form ethyl and peroxy radicals. ....	34



Figure 1.25: Molecular orbital diagrams of an electron rich and an electron poor radical interacting with the HOMO and LUMO of an alkene.....	36
Figure 1.26: Examples of favoured cyclisations as described by Baldwin's rules.....	37
Figure 1.27: Example of a 5-endo-trig cyclisation.....	38
Figure 1.28: Tautomeric forms which allow a 5-endo-trig cyclisation. ....	39
Figure 1.29: BDE of tin halides. ....	40
Figure 1.30: Formation of the tributyltin radical and a halogen-atom abstraction reaction. ....	40
Figure 1.31: Tributyltin hydride mediated reduction of an aryl bromide. ....	41
Figure 1.32: Mechanism of a tributyltin hydride mediated 5-exo-trig cyclisation ....	41
Figure 1.33: Tributyltin hydride mediated formation of bicyclic carbocycles .....	41
Figure 1.34: Tributyltin hydride mediated 5-exo-trig cyclisation. ....	42
Figure 1.35: Tributyltin hydride mediated 5-exo-trig cyclisation mechanism.....	42
Figure 1.36: Tributyltin mediated ring expansion of cyclic $\beta$ -keto esters.....	43
Figure 1.37: Mechanism of a tributyltin hydride mediated ring expansion. ....	43
Figure 1.38: Mechanism of the Barton-McCombie deoxygenation. ....	44
Figure 1.39: Synthesis of (-)-cyclonerodiol including the Barton-McCombie deoxygenation.....	44
Figure 1.40: Hydrostannation of phenyl acetylene. ....	45
Figure 1.41: Catalytic cycle of the Stille cross coupling. ....	45
Figure 1.42: Regeneration of the tributyltin radical by sodium borohydride. ....	46
Figure 1.43: Radical cyclisation with catalytic tin and stoichiometric silane.....	47
Figure 1.44 Structures of some tin containing tributyltin hydride alternatives. ....	47
Figure 1.45: Radical trapping of CO mediated by catalytic triphenylgermanium hydride. ....	49
Figure 1.46: Competing hydrogermylation and termolecular radical addition.....	49
Figure 1.47: Triethylsilane mediated Barton-McCombie deoxygenation.....	50
Figure 1.48: Starting materials of triethylsilane mediated Barton-McCombie deoxygenation and yields of deoxygenated products. ....	50
Figure 1.49: Triethylsilane with thiol polarity reversal catalyst.....	51
Figure 1.50: Reduction of alkyl halides by triethylsilane with thiol polarity reversal catalyst. ....	51

Figure 1.51: Addition of triethylsilane to alkenes with thiol polarity reversal catalyst. ....	52
Figure 1.52: Triethylsilane addition products. ....	53
Figure 1.53: BDEs of tributyltin hydride, tris(trimethylsilyl)silane and trimethylsilane. ....	53
Figure 1.54: Tris(trimethylsilyl)silane mediated reduction and addition products. ...	54
Figure 1.55: Tris(trimethylsilyl)silane mediated C-C bond forming reactions. ....	55
Figure 1.56: Products of tris(trimethylsilyl)silane mediated C-C bond forming reactions. ....	55
Figure 1.57: Comparison of tributyltin hydride and tris(trimethylsilyl)silane mediated 5-exo-trig cyclisation. ....	56
Figure 1.58: Structure of hypophosphorus acid. ....	57
Figure 1.59: Reduction of halo-adamantane mediated by hypophosphorus acid. ...	57
Figure 1.60: Hypophosphorus acid mediated 5-exo-trig cyclisation. ....	60
Figure 1.61: 2,2'-azobis[2-(2-imidazolin-2-yl)propane] ( <b>23</b> ) and 1-ethylpiperidine hypophosphite ( <b>24</b> ).....	61
Figure 1.62: Hypophosphorus acid mediated 5-exo-trig cyclisation in aqueous medium. ....	61
Figure 1.63: Trimethyl pentadecyl ammonium hypophosphite. ....	62
Figure 1.64: Trimethyl pentadecyl ammonium hypophosphite mediated Barton-McCombie reaction. ....	62
Figure 1.65: General structure of a nitroxide. ....	63
Figure 1.66: Structure of Fremy's salt. ....	63
Figure 1.67: Different nitroxides. ....	63
Figure 1.68: Structures of TEMPO and its derivatives. TEMPO ( <b>27</b> ), 4-oxo-TEMPO ( <b>28</b> ), 4-hydroxy-TEMPO ( <b>29</b> ), 4-amino-TEMPO ( <b>30</b> ) and 4-acetamido-TEMPO ( <b>31</b> ). ...	64
Figure 1.69: Resonance stabilisation of TEMPO. ....	64
Figure 1.70: Disproportionation of a nitroxide with an alpha hydrogen. ....	64
Figure 1.71: 2-Azaadamantane-N-oxyl and Bredt's rule. ....	65
Figure 1.72: Synthesis of triacetoneamine ( <b>33</b> ). ....	65
Figure 1.73: Mechanism for the synthesis of triacetoneamine ( <b>33</b> ). ....	66
Figure 1.74: Oxidation of tetramethyl piperidine to form TEMPO. ....	66

Figure 1.75: Mechanism for the synthesis of chiral piperidones from acetoinin ( <b>34</b> ). .....	67
Figure 1.76: Chiral piperidones synthesised from acetoinin ( <b>34</b> ). .....	67
Figure 1.77: Structure of TEMPO oxoammonium ( <b>35</b> ). .....	68
Figure 1.78: Oxidation of primary alcohols by oxoammonium ( <b>35</b> ). .....	68
Figure 1.79: Acid catalysed disproportionation of TEMPO. .....	68
Figure 1.80: Oxidation of alcohols by disproportionated TEMPO. .....	69
Figure 1.81: Mechanism of the TEMPO mediated oxidation of alcohols. .....	69
Figure 1.82: Oxidation of alcohols by TEMPO/Cu with O <sub>2</sub> as the terminal oxidant. .	70
Figure 1.83: Conditions for the oxidation of 4-hexene-1-ol by TEMPO/Cu(OTf). .....	70
Figure 1.84: Laccase/TEMPO mediated oxidation of 4-methoxybenzyl alcohol. ....	70
Figure 1.85: The yields of 4-methoxybenzaldehyde from 4-methoxybenzyl alcohol as achieved by certain mediators of Laccase. ....	71
Figure 1.86: Oxidation of substituted benzaldehydes by TEMPO/Laccase with O <sub>2</sub> as the terminal oxidant. ....	71
Figure 1.87: Trapping of carbon centred radicals by TEMPO. ....	72
Figure 1.88: Formation of block copolymers by nitroxide mediated polymerisation. .....	72
Figure 1.89: Structures and melting points of ionic liquids [BMIM][PF <sub>6</sub> ] and [BMIM][Cl]. .....	73
Figure 1.90: The oxidation of alcohols by TEMPO in [BMIM][PF <sub>6</sub> ]. .....	74
Figure 1.91: The structure of [Bmpyrd][NTf <sub>2</sub> ] and the yields of aldehydes and ketones oxidised from the corresponding alcohols by TEMPO in [Bmpyrd][NTf <sub>2</sub> ]. .	74
Figure 2.1: General structure of an acetal. ....	77
Figure 2.2: General structures (from left to right) of an acetal, a ketal, a hemi-acetal and a hemi-ketal. ....	77
Figure 2.3: Decomposition of a hemi-acetal to an aldehyde and an alcohol. ....	78
Figure 2.4: Acetal formation. ....	78
Figure 2.5: Formation of a cyclic acetal. ....	78
Figure 2.6: Reduction of a cyclic acetal. .....	79
Figure 2.7: Reduction of acetals via S <sub>N</sub> 1 and S <sub>N</sub> 2 reactions. ....	79
Figure 2.8: Oxidation of acetals by NBS. ....	80

Figure 2.9: Products and yields of NBS mediated oxidation of acetals. <sup>a</sup> In CCl <sub>4</sub> . <sup>b</sup> In benzene.....	80
Figure 2.10: Oxidation of acetals by NHPI. ....	80
Figure 2.11: Mechanism of NHPI ( <b>38</b> ) mediated oxidation of acetals. ....	81
Figure 2.12: Products and yields of NHPI ( <b>38</b> ) mediated acetal oxidations. ....	82
Figure 2.13: Hydrolysis of aspirin. ....	82
Figure 2.14: Oxidation of dihydroanthracene by TEMPO/AlCl <sub>3</sub> .....	83
Figure 2.15: Oxidation of acetal <b>39</b> to benzoate ester <b>40</b> by TEMPO/AlCl <sub>3</sub> . ....	83
Figure 2.16: Oxidation of acetal <b>39</b> to benzoate esters. ....	84
Figure 2.17: Acid-catalysed hydrolysis of acetal <b>39</b> . ....	86
Figure 2.18: Initially proposed mechanism for the TEMPO/LA mediated oxidation of acetal <b>39</b> . ....	88
Figure 2.19: Non-degeneracy of the magnetic spin components of paramagnetic compound in a magnetic field. ....	89
Figure 2.20: EPR spectra of TEMPO with and without exposure to BF <sub>3</sub> •OEt <sub>2</sub> .....	90
Figure 2.21: Structure of 2-bromoethyl benzoate ( <b>41</b> ).....	92
Figure 2.22: Synthesis of acetal <b>39</b> . ....	94
Figure 2.23: Initial conditions for the oxidation of acetal <b>39</b> into bromo ester <b>41</b> . ..	94
Figure 2.24: Inhibition of rotation of acetal by ortho substituents. ....	105
Figure 2.25: Mesomeric stabilisation of radical <b>50</b> from acetal <b>39</b> . ....	106
Figure 2.26: Mesomeric stabilisation of radical by acetal <b>48</b> . ....	109
Figure 2.27: Mesomeric stabilisation of radical by acetal <b>59</b> . ....	110
Figure 2.28: Mechanisms for the formation of a primary or secondary radical from acetal <b>61</b> . ....	111
Figure 2.29: TEMPO/MgBr <sub>2</sub> mediated hydrogen abstraction from acetal <b>39</b> . ....	112
Figure 2.30: Mesomeric stabilisation of acetal radical <b>39</b> . ....	112
Figure 2.31: Oxidation of dihydroanthracene to anthracene.....	112
Figure 2.32: Possible locations for Lewis acid coordination in hydrogen abstraction from an acetal by TEMPO. ....	113
Figure 2.33: Ring opening of an acetal radical.....	113
Figure 2.34: Trapping of primary radical by TEMPO and subsequent substitution by bromide ion.....	114

Figure 2.35: Anchimeric assisted bromide substitution. ....	114
Figure 2.36: Trapping of primary radical by molecular bromine and bromine radical .....	115
Figure 2.37: Oxidation of primary radical by TEMPO and subsequent trapping by bromide ion.....	115
Figure 2.38: Mesomeric stabilisation of ethyl benzoate cation. ....	115
Figure 2.39: Stereoselective oxidation of acetal <b>62</b> .....	116
Figure 2.40: Mechanism proposed by McNulty for the formation of <b>62</b> . ....	116
Figure 2.41: Possible mechanisms for the formation of <b>62</b> . ....	117
Figure 3.1: Radical addition of phosphorus hydrides to alkenes.....	120
Figure 3.2: Mechanism of Michael addition of phosphorus hydrides to Michael acceptors.....	121
Figure 3.3: One pot cyclisation then HWE reaction starting from diallyl ether.....	121
Figure 3.4: Mechanism of the HWE reaction.....	122
Figure 3.5: Addition of a phosphorus hydride to an alkene initiated by TEMPO/MgBr <sub>2</sub> .....	122
Figure 3.7: Addition of different phosphorus hydrides to methyl methacrylate. ...	122
Figure 3.8: BDEs of some phosphorus hydrides. ....	123
Figure 3.9: Equilibrium of TEMPO and diphenylphosphine sulfide. ....	124
Figure 3.6: Initially proposed mechanism for the TEMPO initiated addition of diphenylphosphine sulfide to methyl methacrylate.....	124
Figure 3.10: Mechanism for the trapping of the adduct formed from the addition of Ph <sub>2</sub> P(S) <sup>•</sup> to methyl methacrylate by TEMPO.....	126
Figure 3.11: The proposed adduct formed on trapping Ph <sub>2</sub> P(S) <sup>•</sup> with TEMPO. ....	126
Figure 3.12: Trapping of diphenylphosphine oxide radical by TEMPO. ....	126
Figure 3.13: Relative stability of alkyl and vinyl radicals. ....	129
Figure 3.14: Hydrogen atom donation to E and Z vinyl radicals.....	129
Figure 3.15: Mechanism of phosphorous sulfide mediated cyclisation. ....	131
Figure 3.16: Chair-like transition state.....	131
Figure 3.17: Boat-like transition state.....	132
Figure 3.18: Reversible 5-exo-trig cyclisation. ....	132

Figure 3.19: Addition of diphenylphosphine sulfide to methyl methacrylate in the absence of TEMPO. ....	133
Figure 3.20: EM radiation initiated addition of diphenylphosphine sulfide to alkenes. ....	134
Figure 3.21: Addition of diphenylphosphine sulfide to alkenes by Trofimov et al..	135
Figure 3.22: Radical cyclisation at elevated temperatures.....	135
Figure 3.23: Tautomerism of diphenylphosphine sulfide. ....	136
Figure 3.24: Addition of diphenylphosphinothionous ( <b>84</b> ) acid to Michael acceptors. ....	136
Figure 4.1: TEMPO ionic liquid <b>86</b> . ....	138
Figure 4.2: Synthesis of TEMPO ionic liquid <b>86</b> by Click chemistry.....	139
Figure 4.3: TEMPO ionic liquid <b>87</b> . ....	139
Figure 4.4: Imidazolium TEMPO sulfonates. ....	140
Figure 4.5: Synthesis of cyano-TEMPO. ....	141
Figure 4.6: Hydrolysis of cyano-TEMPO ( <b>88</b> ).....	142
Figure 4.7: Synthesis of [BMIM][Carboxy-TEMPO] ( <b>89</b> ). ....	142
Figure 4.8: Mechanism of the HWE of triacetoneamine ( <b>33</b> ).....	144
Figure 4.9: Proposed route for the formation of <b>91</b> . ....	144
Figure 4.10: HWE of triacetoneamine ( <b>33</b> ). ....	145
Figure 5.1: Kinetic resolution of secondary alcohols by (R)-CF <sub>3</sub> -PIP.....	147
Figure 5.2: Formation of oxoammonium/camphorsulfonate ion pair ( <b>92</b> ) by disproportionation of TEMPO. ....	148
Figure 5.3: Scheme for the kinetic resolution of 1-phenylethanol ( <b>93</b> ). ....	148
Figure 5.4: Chiral HPLC trace of 1-phenylethanol ( <b>93</b> ). ee = 0.1%. Chiralcel OD-H column (95:5 hexane:IPA, 0.5 mL/min). R and S assignments determined by use of commercial (S)-1-phenylethanol.....	149
Figure 5.5: Acid catalysed racemization of (S)-1-phenylethanol. ....	150
Figure 5.6: Synthesis of [BMIM][Leu] ( <b>94</b> ) from [BMIM][Cl]. ....	151
Figure 5.7: Structure of [BMIM][BocLeu] and [BMIM][AcLeu]. ....	152
Figure 5.8: Structure of [BIMIM][AcO] ( <b>97</b> ). ....	153
Figure 7.1: One pot TEMPO/Lewis acid mediated synthesis of esters from aldehydes. ....	158

Figure 7.2: Oxidation of acetals to esters with catalytic TEMPO.....	159
Figure 7.3: One pot TEMPO initiated phosphorous hydride addition and HWE reaction. ....	159
Figure 7.4: Route to ionic liquid <b>91</b> .....	160

## List of Tables

Table 1.1.: Reduction of alkyl halides by tributyltin hydride and triethylborane.....	34
Table 1.2: Summary of Baldwin's rules. Green represents favoured cyclisations while red represents disfavoured. ....	38
Table 1.3: Reduction of organo-halides by triethylsilane with a thiol polarity reversal catalyst. ....	52
Table 1.4: Reduction of organo-halides by tris(trimethylsilyl)silane. ....	54
Table 1.5: Reduction of organo-halides by catalytic tris(trimethylsilyl)silane and stoichiometric sodium borohydride. ....	56
Table 1.6: Reduction of functionalised-adamantane by hypophosphorus acid.....	58
Table 1.7: Reduction of water soluble organohalides by hypophosphorus acid in water. ....	59
Table 2.1: Screen of Lewis acids for mediation of acetal oxidation in conjunction with TEMPO.....	85
Table 2.2: Comparing methods of determining yields using TEMPO/BF <sub>3</sub> •OEt <sub>2</sub> mediated oxidation of acetal <b>39</b> . ....	92
Table 2.3: Comparison of large and small scale TEMPO/MgBr <sub>2</sub> mediated oxidations of acetal <b>39</b> to form 2-bromoethylbenzoate ( <b>41</b> ).....	93
Table 2.4: Comparing TEMPO and TEMPO oxoammonium chloride as mediators of acetal oxidation.....	95
Table 2.5: Comparison of different solvents in the oxidation of acetal <b>39</b> . ....	96
Table 2.6: Comparing yield of <b>41</b> to increase in TEMPO and MgBr <sub>2</sub> . ....	97
Table 2.7: Comparing yield of ester <b>41</b> to increase in TEMPO. ....	98
Table 2.8: Comparing yield of ester <b>41</b> to increase in MgBr <sub>2</sub> . ....	99
Table 2.9: Effect of reaction time on yield of ester <b>41</b> . ....	100
Table 2.10: Effect of water and oxygen on yield of ester <b>41</b> . ....	101
Table 2.11: Effect of temperature of yield of ester <b>41</b> . ....	102
Table 2.12: Effect of scale on the yield of ester <b>41</b> .....	103
Table 2.13: Optimised conditions for the TEMPO/MgBr <sub>2</sub> mediated oxidation of acetal <b>39</b> to ester <b>41</b> . ....	104



Table 2.14: TEMPO/MgBr <sub>2</sub> mediated oxidation of methyl and methoxy substituted phenylacetals. ....	105
Table 2.15: TEMPO/MgBr <sub>2</sub> mediated oxidation of acetals <b>39</b> , <b>51</b> and <b>53</b> . ....	107
Table 2.16: TEMPO/MgBr <sub>2</sub> mediated oxidation of phenyl acetals with electron donating and electron withdrawing substituents.....	108
Table 2.17: TEMPO/MgBr <sub>2</sub> mediated oxidation of <b>61</b> and <b>63</b> . ....	110
Table 3.1: Addition of different phosphorus hydrides to methyl methacrylate. ....	123
Table 3.2: Comparing the TEMPO initiated addition of diphenylphosphine sulfide to methyl methacrylate with and without MgBr <sub>2</sub> .....	125
Table 3.3: Investigating the effect of phosphorus hydride stoichiometry on the TEMPO initiated addition of diphenylphosphine sulfide to methyl methacrylate..	127
Table 3.4: TEMPO initiated additions of diphenylphosphine sulfide to different alkenes and alkynes. ....	128
Table 3.5: TEMPO initiated, diphenylphosphine mediated cyclisations of dienes..	130
Table 3.6: Non-initiated addition of diphenylphosphine sulfide to Michael acceptors.....	133
Table 4.1: Oxidation of aldehydes by TEMPO ionic liquid <b>87</b> . <sup>147</sup> .....	140
Table 4.2: Oxidation of benzyl alcohol by [BMIM][Carboxy-TEMPO] ( <b>89</b> ). ....	143
Table 5.1: Yields and enantiomeric excesses of chiral oxidations. ....	150
Table 5.2: Oxidation of 1-phenylethanol in ionic liquids. ....	152
Table 5.3: Oxidation of 1-phenylethanol in protected amino acid ionic liquids. ....	153

## Acknowledgements

First of all thanks to Victor and Andy for all their help throughout the course of this project, both for their aid in matters of chemistry and encouragement in the face of pessimism.

I would also like thank the members of the VC group (Sindhu, Yury, Zhou, Tom, Chris, Andrew, Rob Thatcher, Rob Smith, Chiara, Phil, Brenden and Kazim), for their input during group meetings and for attempting to hide their yawns during my presentations.

My gratitude goes to the members of D215 past and present (POB group members: Donald 'James' Firth, Giacomo 'Guacamole' Gelardi, Pete Rayner, Xiao 'X-Dubz' Wu, Nah Haji-Cheteh, Mary 'Jesus Christ' Wheldon, Adam 'Pies' Islip, Alice Kwong, Will 'Spare Capacity' Duckworth, Masakazu Atobe and Paola Ruggeri and my MChem/summer students: Laura Blunt, Jess Vaughan, Mark James and Tom Sheridan), for their support, encouragement and occasional mocking. In particular I would like to thank Pete Birch for showing me the ropes and David 'D2' Creighton for showing me that no matter how mad I think I am there is always someone worse.

Thanks go to the RJKT group whose office I shared/gate-crashed (Will, Sarah, Mickey, Ronson, Tim, Ryan, Dave Burns, Graeme Coulthard, Aimee, Monique, Pauline, Phil, Jimmy, Doveston, Lucia and Laura) for providing technical help, chemicals and amusement at coffee time.

Thanks also go to Heather for running the NMR service, to Karl for the Mass Spec service, Steve and Mike in Stores and Graeme McAllister for ensuring everything in D-Block worked. In addition I would like to thank the teaching lab staff (Phil, Helen, David, Charlotte and Julia) for allowing me to use/pilfer equipment.

Special thanks go to Kate 'CG' Horner, Julia Sarju and Helen Robinson for listening to my chemistry and wine induced ranting and where appropriate, telling me to shut up and get on with it.

Finally I would like to thank Sophie for enduring my constant chemistry based complaints, Anthony and Kate for their advice on how to survive a PhD and my parents David and Hilary for their continued support.

## **Declaration**

I, Joseph Atkin, declare that this thesis is a presentation of original work and I am the sole author. This work has not previously been presented for an award at this, or any other, University. All sources are acknowledged as References.

## **1. Introduction**

# 1. Introduction

## 1.1. General Radical Chemistry

### 1.1.1. What is a Radical?

A radical is an atom or molecule with one or more unpaired electrons. Most radicals are extremely reactive with very short half-lives. Some radicals however are persistent and can be found in nature. Molecular oxygen is a classic example of a persistent di-radical. Figure 1.1 shows the molecular orbital diagram of the ground state of  $O_2$  with two unpaired electrons in the two degenerate  $2p \sigma^*$  orbitals. Oxygen exists in this state in order to negate the pairing energy required to have two electrons in the same orbital.

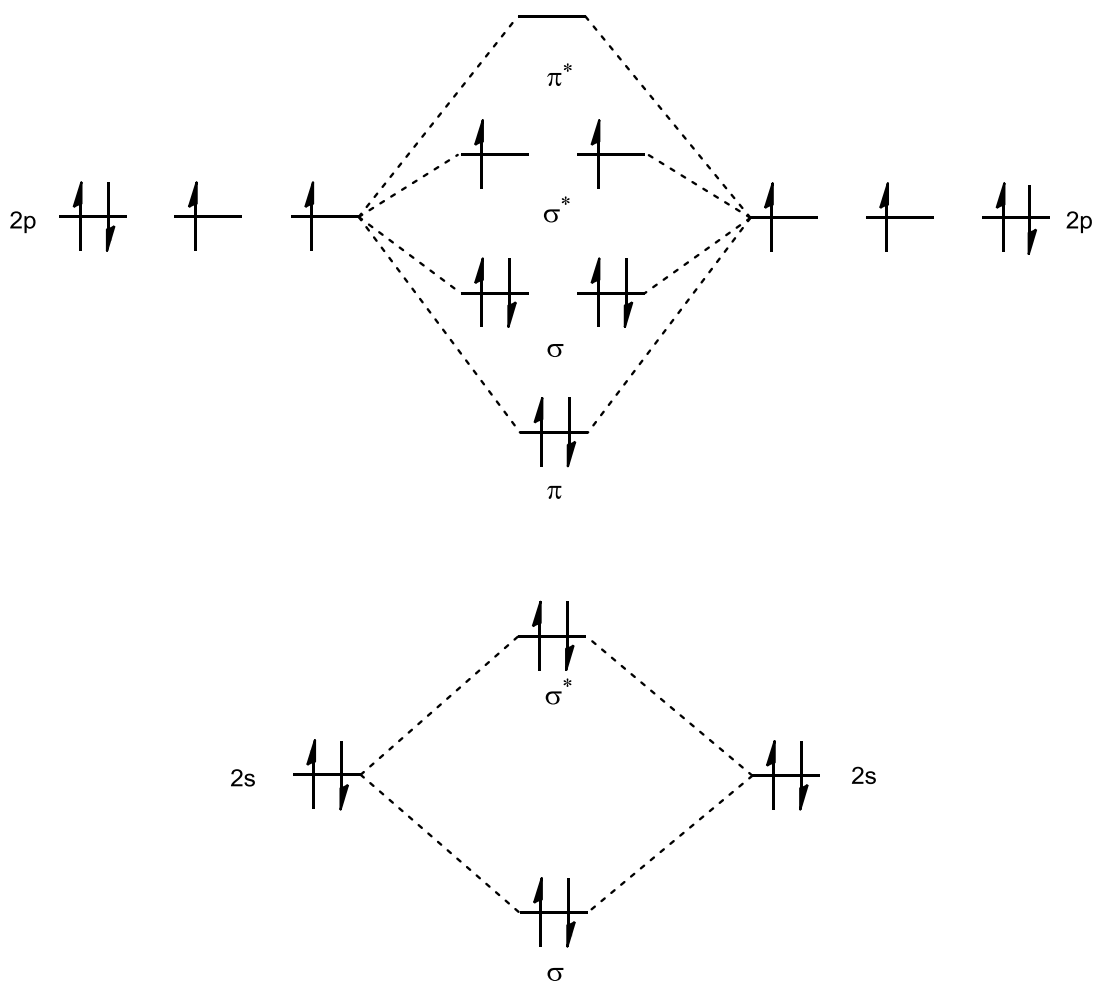


Figure 1.1: Molecular orbital diagram of  $O_2$ .

### 1.1.2. Organic Radicals

The first recorded discovery of a persistent organic radical is attributed to Moses Gomberg in 1900. Gomberg was attempting to synthesise hexaphenylethane (**1**) by reducing a triphenylmethyl halide (**2**) with elemental silver (Figure 1.2).

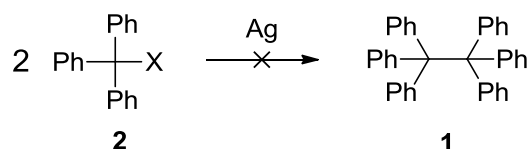


Figure 1.2: Attempted synthesis of hexaphenylethane.

Upon analysis however he found the elemental composition lacking in carbon and evidence for oxygen present in the compound. Concluding that the oxygen came from the atmosphere Gomberg repeated his reaction under an inert atmosphere using zinc as the reducing agent and isolated what proved to be the triphenylmethyl or trityl radical (**4**) (Figure 1.3).<sup>1</sup>

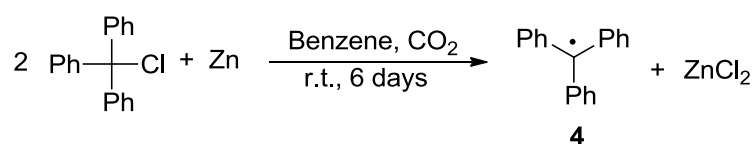


Figure 1.3: Synthesis of triphenylmethyl radical.

It was initially believed that due to their high reactivity radicals were too indiscriminate and not selective enough for use as organic intermediates. Since then the field of organic radical chemistry has grown increasingly useful and varied.<sup>2-5</sup> Thanks to the aforementioned reactivity, radical reactions often proceed under fairly mild conditions. In addition to this, the reactivity of radical intermediates is notably different from ionic intermediates meaning that radicals often don't interfere with functional groups which otherwise usually require protecting groups. This lessened interaction between radical and ionic intermediates also allows multi-step, one-pot reactions where radical and ionic steps occur alongside each other.<sup>6</sup> The lack of charged intermediates also lessens solvent effects due to varying polarity allowing a greater choice of solvent and negating development time relating to solvent selection.

Another distinct advantage of using radicals in synthesis is that radical reactions sometimes give rise to different regioisomers to their ionic counterparts. This was demonstrated by Kharasch in 1933 when he showed that in the presence of peroxides, addition of HBr to alkenes proceeded in an anti-Markovnikov fashion instead of the Markovnikov addition observed in the absence of radical initiators (Figure 1.4).<sup>7</sup>

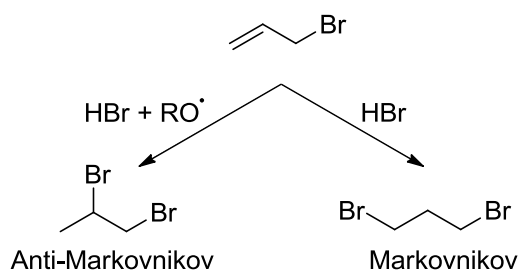


Figure 1.4: Markovnikov and Anti-Markovnikov addition of HBr to allyl bromide.

In Markovnikov addition the product formed is determined by the most stable intermediate. In this case the most substituted cation (**5**) is favoured due to the stabilising +I effect from the two alkyl groups (Figure 1.5).

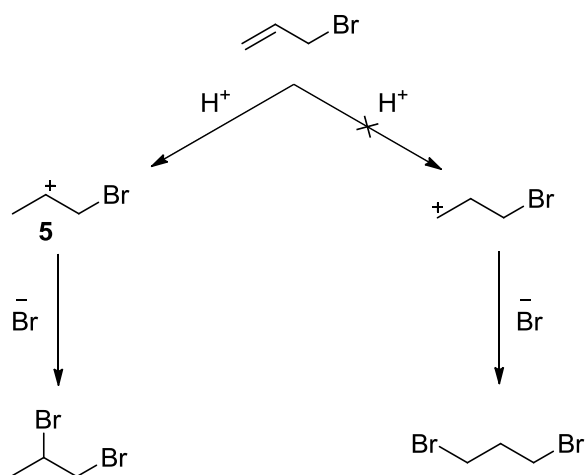


Figure 1.5: Ionic addition of HBr to allyl bromide.

In the radical addition of HBr, a bromine atom attacks the double bond first creating a carbon centred radical. Like the cation this radical is stabilised by electron donation and so the formation of the anti-Markovnikov product from the more stable intermediate (**6**) dominates (Figure 1.6). In addition to the electronic



effects, in the case of bulky substituents the bromine radical will also be directed to attack the least substituted position by steric effects.

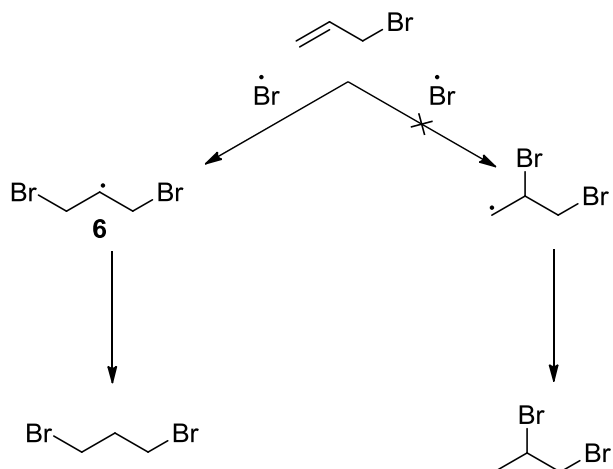


Figure 1.6: Radical addition of HBr to allyl bromide.

Having touched on the subject of radical stability it is worth exploring the factors that determine the stability and therefore the reactivity and likelihood of forming particular radicals.

### 1.1.3 Radical Stability

In the previous section it was stated that radicals are stabilised by +I substituents, this is due to the fact that neutral radicals are electron deficient and therefore benefit from inductive electron donation. As one would expect, the greater the number of +I groups, the more stable the radical becomes (Figure 1.7).

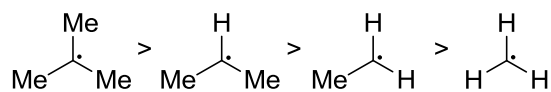


Figure 1.7: Methyl substituted radicals in decreasing order of stability.

It should also be obvious at this point that substituents with a -I effect have a destabilising effect on radical species.

As well as the inductive effects offered by greater substitution, a radical is also stabilised by hyperconjugation effects. Hyperconjugation is the donation of electron

density from (in this case) the C-H bonding orbital into the partially filled non-bonding SOMO (Figure 1.8).



Figure 1.8: Graphical representation of hyperconjugation.

Just like cations and anions, radicals benefit from delocalisation around a conjugated  $\pi$  system. This means radicals adjacent to unsaturated C=C bonds and phenyl rings show an increased level of stability (Figure 1.9).

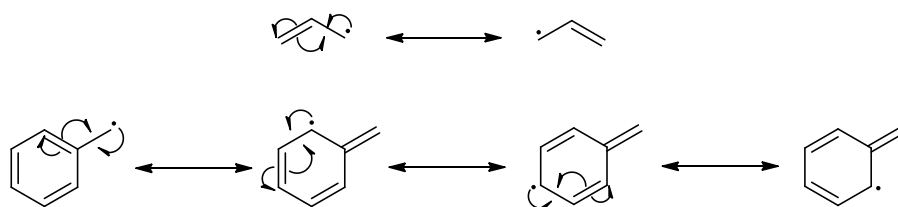


Figure 1.9: Mesomeric stabilisation of a benzyl radical and an allyl radical.

In ionic chemistry cations are stabilised by +M groups and anions are stabilised by -M groups. Radicals on the other hand can be stabilised by both electron donating and withdrawing mesomeric effects. This effect can be demonstrated by drawing the appropriate mesomeric forms (Figure 1.10).

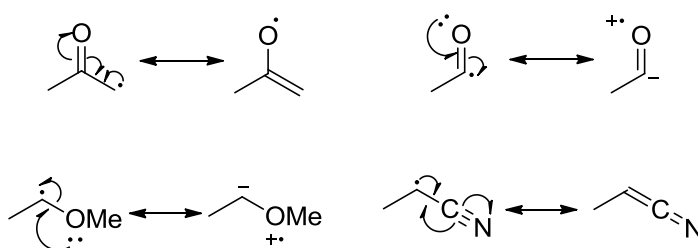
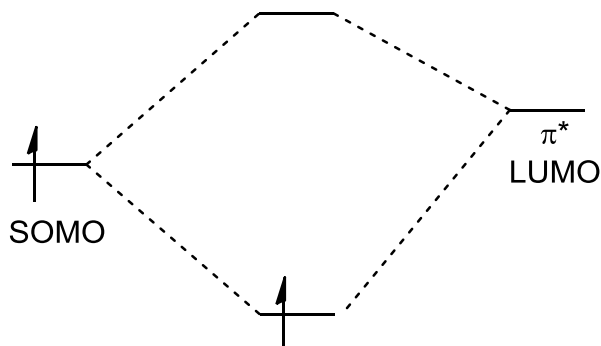


Figure 1.10: Stabilisation of radicals by electron donating and withdrawing substituents.

In order to get a better understanding of why radicals are stabilised by both +M and -M groups it is helpful to look at the molecular orbital diagrams of radical orbitals which overlap with electron withdrawing and donating groups. Functional groups with a -M effect are characterised by an unoccupied, low energy  $\pi^*$  orbital with

which nearby occupied orbitals overlap, hence the electron withdrawing effect. When a singly occupied orbital (SOMO) overlaps with this  $\pi^*$  orbital the effect is to lower the energy of the SOMO and thus stabilise the radical (Figure 1.11).



*Figure 1.11: Molecular orbital diagram of SOMO stabilisation by overlap with a LUMO.*

Functional groups with a +M effect possess a high energy occupied orbital containing a non-bonding electron lone pair. When this orbital overlaps with the SOMO, the radical electron is raised in energy. This change on its own would have the effect of destabilising the radical but it is outweighed by the fact that both electrons of the lone pair are lowered in energy resulting in a net stabilising effect (Figure 1.12).

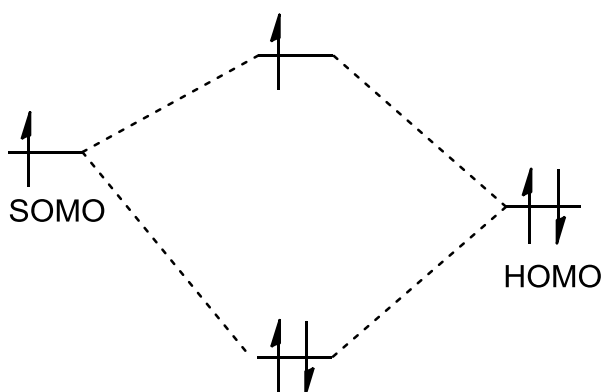


*Figure 1.12: Molecular orbital diagram of SOMO stabilisation by overlap with a HOMO.*

The hybridisation of the carbon atom on which the radical is centred also plays a role in its stability as evidenced by  $sp^2$  and  $sp$  hybridised radicals being less stable than  $sp^3$  (Figure 1.13).

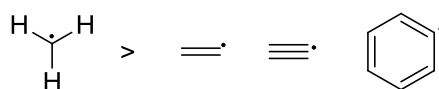


Figure 1.13: Methyl, vinyl, ethenyl and phenyl radicals.

As the level of s character increases, the atom becomes more electronegative and forms stronger C-H bonds making radical formation less favourable and the radical less stable.

The final factor in the stability of carbon centred radicals is steric hindrance. For example it is thought that the trityl radical (**4**) discussed earlier is not as easily delocalised around the aromatic rings as one would expect because the steric clash between the rings prevents them from lying in the correct plane (Figure 1.14).

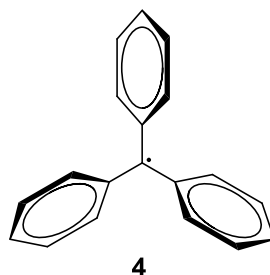


Figure 1.14: 3D structure of the triphenylmethyl radical (**4**).

Since there is not a strong mesomeric effect to delocalise the radical much of the stabilisation comes from +I effects and steric shielding of the radical carbon atom.<sup>8</sup>

## 1.2. Initiation

Synthetically useful radical reactions are often chain reactions comprising three distinct steps: initiation, propagation and termination, each of which can consist of multiple steps. Initiation consists of turning a non-radical initiator into a reactive radical species which then starts the reaction chain. Propagation is the step in which the radical created in the initiation reacts with a non-radical species to form and/or break bonds, giving a new radical product. Finally, the reaction pathway is terminated by combination of two radical species, disproportionation or redox processes. One of the main aims of this thesis is to devise new methods of initiation

for radical reactions and as such we will be examining the different methods of initiation and classes of initiator.

### 1.2.1. Photolysis

Many radical reactions are initiated by photolysis where high energy UV light is used to selectively break a weak covalent bond. The reaction commonly used as an example of this is the radical chlorination of methane. Figure 1.15 shows some but by no means all of the reactions which take place when  $\text{Cl}_2$  and  $\text{CH}_4$  are exposed to UV light.

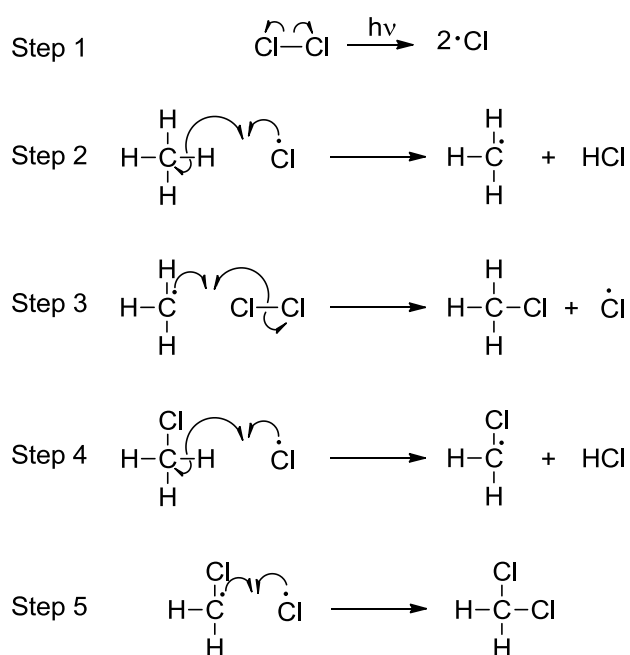


Figure 1.15: Radical addition of chlorine to methane.

This reaction shows quite clearly the three stages of a radical reaction. Step 1 shows the initiation step with two chlorine atoms produced by the homolytic cleavage of the weak Cl-Cl bond. Steps 2-4 show some of the possible propagation steps where a radical and non-radical species interact to form new radical and non-radical species. Finally, step 5 shows an example of a termination step, where two radicals combine to form a non-radical product (DCM).

### 1.2.2. Peroxide Initiators

The weak oxygen-oxygen bonds found in peroxides (RO-OR) are easily broken, often by thermolysis, to form oxygen centred radicals, RO<sup>•</sup> (Figure 1.16).

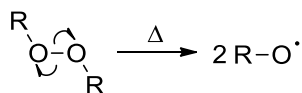


Figure 1.16: Thermolysis of a peroxide bond.

Two examples of peroxide initiators are *tert*-butyl peroxide and benzoyl peroxide. These peroxides have substantially different O-O BDEs due to the mesomeric stabilisation of the benzoyl radical which is absent in the *tert*-butoxy radical (Figure 1.17).

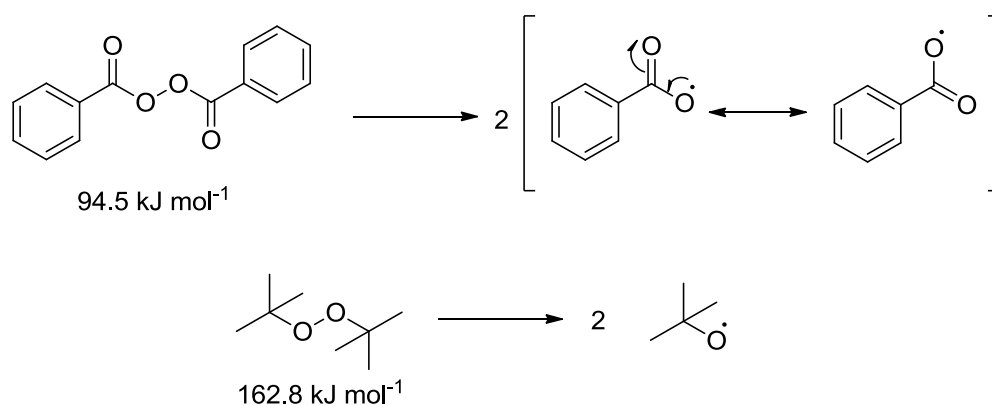


Figure 1.17: Radical dissociation of benzoyl peroxide and *tert*-butyl peroxide with their O-O bond strengths.<sup>9,10</sup>

Depending on their structure the oxygen centred radicals can then fragment to form carbon centred radicals. Benzoyl peroxide, an acyl peroxide, fragments to form a phenyl radical and carbon dioxide whereas *tert*-butyl peroxide, an alkyl peroxide, forms acetone and a methyl radical (Figure 1.18).

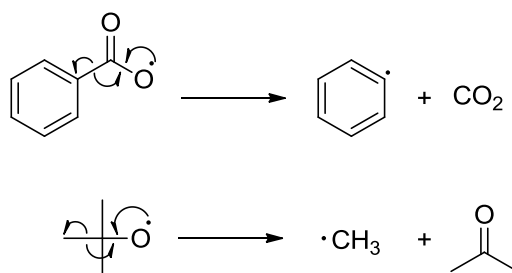


Figure 1.18: Fragmentation of phenyl carboxy radical and tert-butoxy radical.

Initiation can be caused by the oxygen or carbon centred radicals. Whilst they are effective as radical initiators, peroxides must be handled with care since they can explode at high temperatures or high concentrations. Peroxide initiators are predominantly used as initiators for radical polymerisations.<sup>11-14</sup>

### 1.2.3. Azo Initiators

Of the various azo initiators available azobisisobutyronitrile (AIBN) is the most commonly used in synthesis. AIBN can be converted into radicals either by heating or photolysis as shown in Figure 1.19.

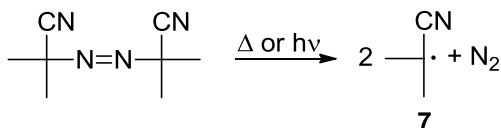


Figure 1.19: Fragmentation of AIBN to form isobutyronitrile radicals (**7**).

This process is both enthalpically and entropically favoured thanks to the formation of gaseous  $N_2$  with a strong  $N\equiv N$  bond (BDE  $945 \text{ kJ mol}^{-1}$ ). This strong driving force comes with its downsides though as the exothermic production of gas makes azo initiators an explosion risk. Despite this, however, they are generally considered safer to use and handle than peroxides.

Care must be taken when using AIBN to avoid recombination of the isobutyronitrile radicals (**7**) which can be caught in a solvent cage and react with each other forming an inactive compound (**8**) (Figure 1.20). This effect is largely dependent on the viscosity of the solvent.

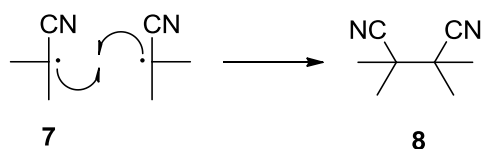


Figure 1.20: Recombination of isobutyronitrile radicals.

AIBN is a common initiator for the Wohl-Ziegler reaction in which *N*-bromosuccinimide (NBS) is used to generate bromine radicals, which selectively react with hydrogen atoms at allylic or benzylic positions (Figure 1.21).

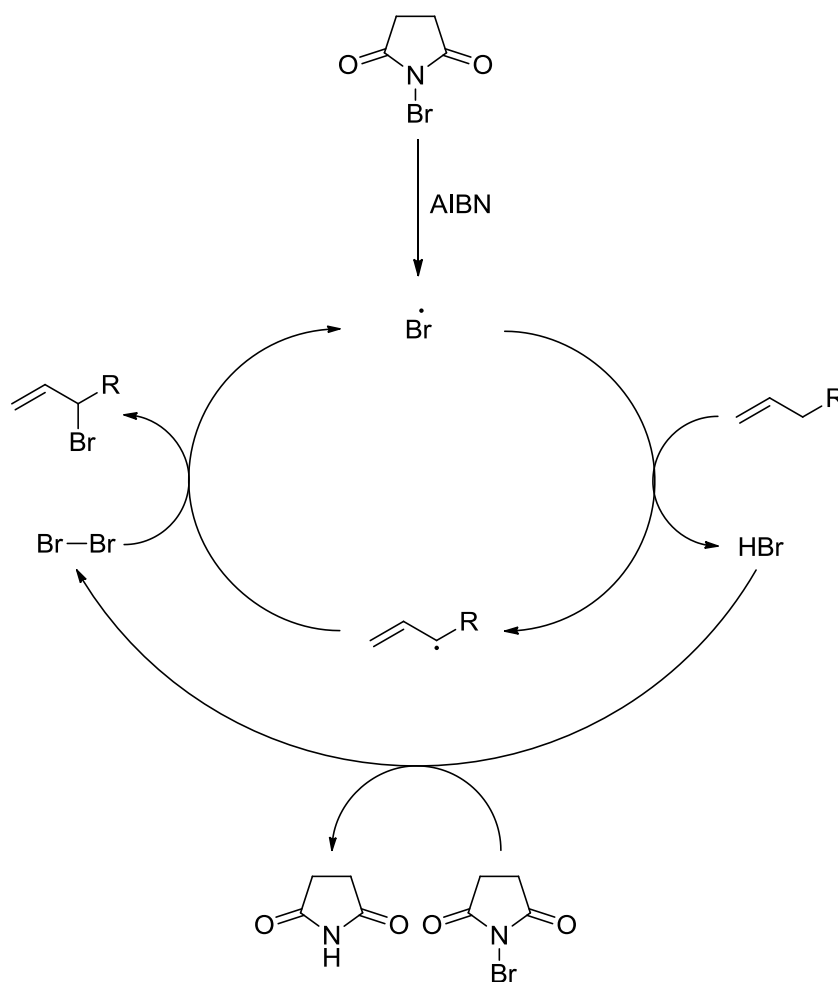


Figure 1.21: Reaction mechanism of the Wohl-Ziegler reaction.

It might be expected that since  $\text{Br}_2$  is present, a major side product would be the addition of  $\text{Br}_2$  across the double bond (Figure 1.22), but the formation of this product is limited by the very low steady state concentrations of  $\text{Br}_2$ .



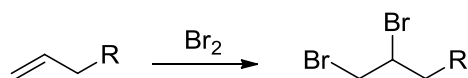


Figure 1.22: Bromination of alkenes by  $\text{Br}_2$ .

The asymmetric synthesis of (*S*)-(-)-acromelobinic acid (**9**) from 2,5-dimethylpyridine (**10**) by Adamczyk et al. is an example of the Wohl-Ziegler reaction in action (Figure 1.23).<sup>15</sup>

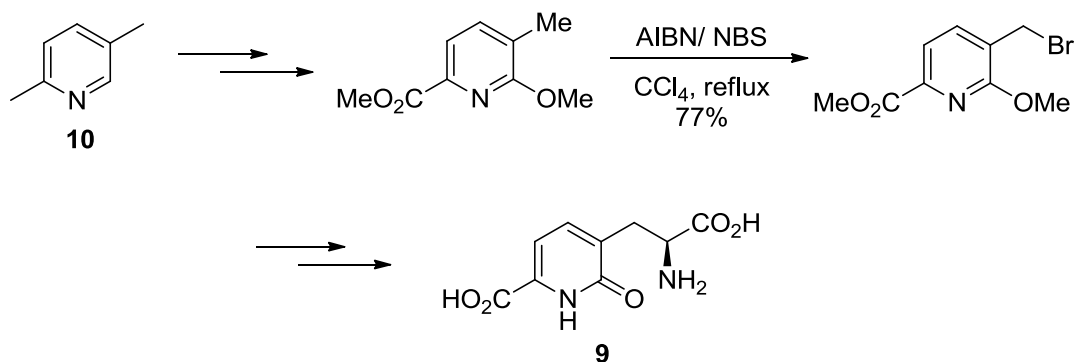


Figure 1.23: Asymmetric synthesis of (*S*)-(-)-acromelobinic acid from 2,5-dimethylpyridine.

This example shows the selectivity of the NBS system for the benzylic type methyl group over the ester and ether methyl groups leading to a high yield of the desired product.

#### 1.2.4. Triethylborane

Triethylborane is a pyrophoric liquid, usually supplied in a hexane, diethyl ether or THF solution, which reacts with molecular oxygen to form ethyl and peroxy radicals which can then act as radical initiators (Figure 1.24).

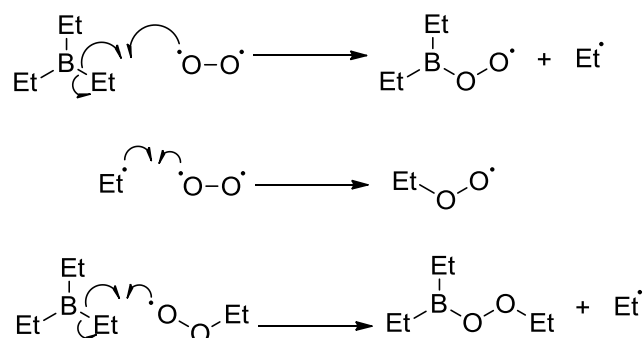


Figure 1.24: Fragmentation of  $\text{Et}_3\text{B}$  to form ethyl and peroxy radicals.

Triethylborane is a useful initiator for reactions which are light and/or heat sensitive since it does not require thermal or electromagnetic energy to activate. In 1989 Oshima et al. used  $\text{Et}_3\text{B}$  as an initiator in conjunction with  $\text{Bu}_3\text{SnH}$  to reduce a variety of organo-halides to alkanes at  $-78\text{ }^\circ\text{C}$  (Table 1.1)<sup>16</sup>

Table 1.1.: Reduction of alkyl halides by tributyltin hydride and triethylborane.

Entry	Substrate	Yield of dodecane (%)
1	1-Iodododecane	95
2	2-Iodododecane	90
3	1-Bromododecane	100
4	2-Bromododecane	98

Conditions: alkyl halide 1 eq,  $\text{Bu}_3\text{SnH}$ , 1.1 eq,  $\text{Et}_3\text{B}$  0.1 eq, toluene,  $-78\text{ }^\circ\text{C}$ , 0.5 h.

The main disadvantage of triethylborane is the need for oxygen to produce the ethyl and peroxy radicals since  $\text{O}_2$  will often inhibit reactions by trapping radical intermediates.<sup>17</sup> Luckily only small quantities of  $\text{O}_2$  are needed but optimising and controlling the amount of  $\text{O}_2$  in a lab reaction isn't always quick or trivial.

## 1.3. Radical Reactions

### 1.3.1. Radical Polarity

In ionic chemistry a nucleophile will preferentially attack the most electron deficient electrophile and an electrophile will preferentially react with the most electron rich nucleophile. In terms of molecular orbitals, this is due to a larger difference in energy between the HOMO of the nucleophile and the LUMO of the electrophile which results in a greater change in energy when they react, making the process more thermodynamically favoured. A similar effect is observed in radical chemistry where reactions between electron rich radicals and electron poor substrates or between electron poor radicals and electron rich substrates are favoured over reactions between radicals and substrates of similar polarity. Figure 1.25 shows the molecular orbital diagrams of an electron rich and an electron poor radical interacting with the HOMO and LUMO of an alkene.

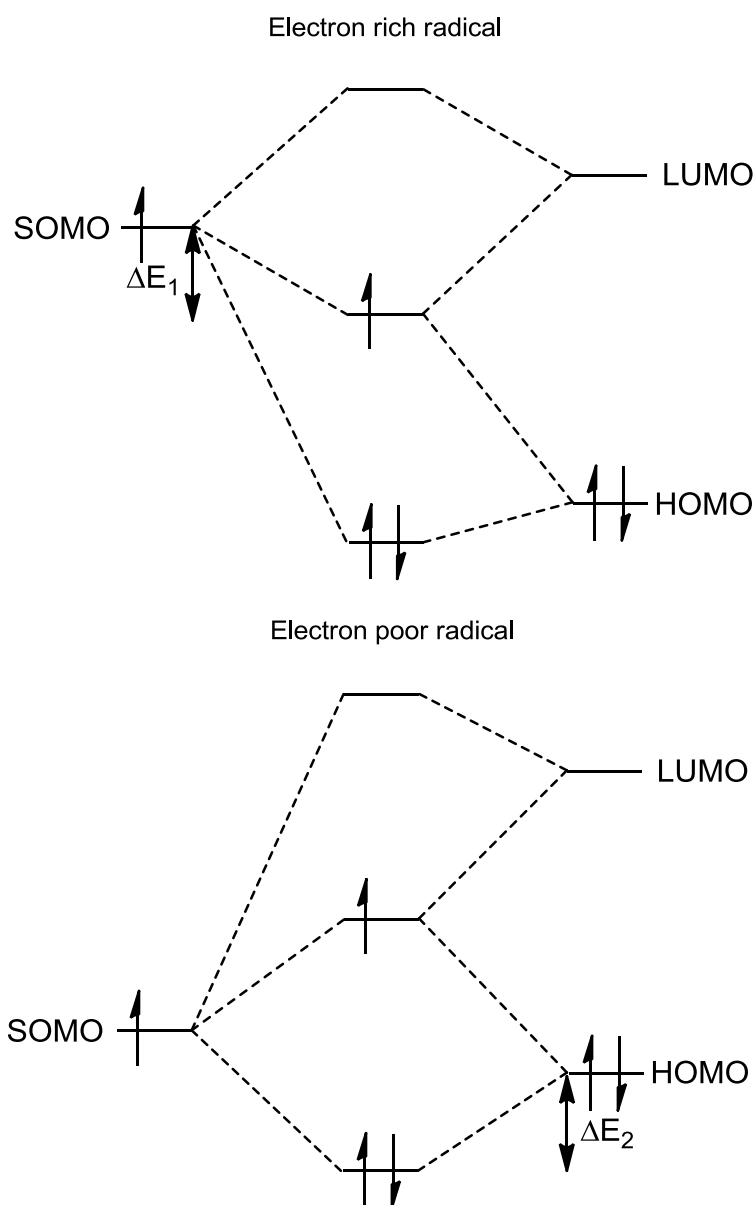


*Figure 1.25: Molecular orbital diagrams of an electron rich and an electron poor radical interacting with the HOMO and LUMO of an alkene.*

The SOMO of an electron rich radical is high in energy and interacts predominantly with the LUMO of the alkene. In this instance raising the energy of the SOMO (by creating a more electron rich radical) or lowering the LUMO (by creating a more electron poor alkene) will increase the difference in energy ( $\Delta E_1$ ) between the SOMO of the original radical and the SOMO of the adduct, making the interaction thermodynamically more favourable. The SOMO of an electron poor radical is much lower in energy and mainly interacts with the HOMO of the alkene. Therefore lowering the energy of the SOMO or raising the energy of the HOMO will have the

effect of increasing  $\Delta E_2$  and making the interaction thermodynamically more favourable. These MO diagrams show that for both electron rich and electron poor radicals, the overall change in energy becomes more favourable when they interact with an alkene of opposite polarity.

### 1.3.2. Baldwin's Rules

Throughout the course of this thesis we will be discussing both radical and ionic cyclisations. Certain cyclisations are favoured whilst others are not, a phenomenon described by Baldwin's rules. In 1976 Jack Baldwin presented an empirically determined set of guidelines describing the likelihood of cyclisations occurring based on the stereochemical properties of the starting material and product.<sup>18</sup> Baldwin outlined three terms for the description of a cyclisation reaction. The first of these was a numerical reference to the size of ring being formed. The second referred to the position of the bond being broken to form the cyclic product. If the bond being broken is external to the ring being formed it is classified as *exo* and if it is internal then it is *endo*. Finally a term is used to describe the hybridisation of the carbon undergoing nucleophilic or radical attack that leads to cyclisation: *tet* for  $sp^3$ , *trig* for  $sp^2$  and *dig* for  $sp$  hybridised carbons. Examples of each of these terms are shown in Figure 1.26.

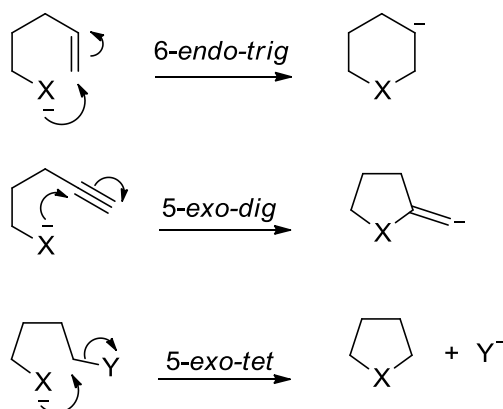


Figure 1.26: Examples of favoured cyclisations as described by Baldwin's rules.

Baldwin noticed that certain combinations of these three characteristics did not cyclise while others did. These observations are summarised in Table 1.2.

Table 1.2: Summary of Baldwin's rules. Green represents favoured cyclisations while red represents disfavoured.

Ring size	3		4		5		6		7	
	<i>endo</i>	<i>exo</i>	<i>endo</i>	<i>exo</i>	<i>endo</i>	<i>exo</i>	<i>endo</i>	<i>exo</i>	<i>endo</i>	<i>exo</i>
<i>tet</i>		Y		Y	N	Y	N	Y	N	Y
<i>trig</i>	N	Y	N	Y	N	Y	Y	Y	Y	Y
<i>dig</i>	Y	N	Y	N	Y	Y	Y	Y	Y	Y

The rationalisation behind Baldwin's rules is that, in the transition state, good orbital overlap between the HOMO of the nucleophile and the LUMO of the electrophile only occurs for certain combinations of ring size and hybridisation.

Baldwin's rules are a good guide for whether a particular cyclisation is likely to be favoured or disfavoured but they are not absolute. In 1977 Baldwin et al. showed that certain disfavoured cyclisations could be carried out in particular circumstances such as the 5-*endo-trig* cyclisation shown in Figure 1.27.<sup>19</sup>

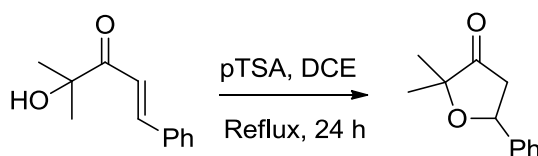


Figure 1.27: Example of a 5-*endo-trig* cyclisation.

In this example Baldwin et al. rationalise this violation of their rules by proposing that the acid catalyst enolises the enone, thereby reducing barriers to rotation and allowing a greater degree of flexibility than would normally be expected (Figure 1.28). This allows the HOMO and LUMO to overlap more favourably and the reaction is able to proceed.

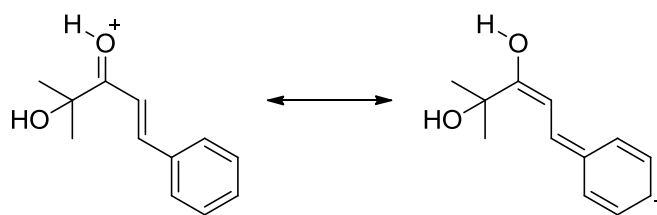


Figure 1.28: Tautomeric forms which allow a 5-endo-trig cyclisation.

More recent publications throw into question the validity of classifying 5-endo-trig cyclisations as unfavourable and state that 4-exo-trig is less favourable despite being classed as favourable by Baldwin.<sup>20</sup> Despite this, Baldwin's rules are generally held to be a good rule of thumb when studying cyclisations. In addition to Baldwin's rules Beckwith also published some guidelines in 1980 for radical cyclisations stating that:<sup>21</sup>

Intramolecular addition under kinetic control in lower alkenyl and alkynyl radicals and related species occurs preferentially in the *exo*-mode.

Substituents on an olefinic bond disfavour homolytic addition at the substituted position.

Homolytic cleavage is favoured when the bond concerned lies close to the plane of an adjacent semi-occupied orbital or of an adjacent filled non-bonding or  $\pi$ -orbital.

1,5-ring closures of substituted hex-5-enyl and related radicals are stereoselective. 1- or 3-substituted systems afford mainly *cis*-disubstituted products, whereas 2- or 4-substituted systems give mainly *trans*-products.

### 1.3.3. Radical Mediators

As well as an initiator an important component of a successful radical reaction is a radical mediator. Often the radicals created by the fragmentation of initiators do not interact favourably with the selected starting materials of a reaction. Therefore mediators are used to react with the radical created by the initiator, generating a new radical which is capable of interacting selectively with a chosen starting material. Usually radical mediators are part of a chain process where the

termination of the desired reaction generates a new radical to begin the cycle again. Arguably the most well-known radical mediator is tributyltin hydride.

## 1.4. Tributyltin Hydride

### 1.4.1. Stannanes

Stannanes ( $R_3SnH$ ) have been one of the most versatile and ubiquitous groups of radical mediators for many years.<sup>22-26</sup> Of the readily available stannanes in synthesis the most commonly used is tributyltin hydride ( $Bu_3SnH$ ). Tributyltin hydride contains a weak Sn-H bond (BDE  $308 \text{ kJ mol}^{-1}$ )<sup>27</sup> and carbon-centred radicals can abstract a hydrogen atom from tributyltin hydride to form a new, strong C-H bond and a tin-centred radical. This tributyltin radical can reduce a variety of different functional groups in a chain process and is often used to promote radical cyclisations by atom abstraction, or addition to unsaturated bonds such as those in alkenes and alkynes. Typical initiators used with tin hydrides include AIBN,  $Et_3B$  or EM radiation.

### 1.4.2. Tributyltin Hydride Mediated Halogen Reductions

Tributyltin hydride has a high affinity for abstraction of halogen atoms due to the strength of the resulting tin halide bond (Figure 1.29).<sup>28</sup>

Sn—I	Sn—Br	Sn—Cl
$234 \text{ kJ mol}^{-1}$	$339 \text{ kJ mol}^{-1}$	$406 \text{ kJ mol}^{-1}$

Figure 1.29: BDE of tin halides.

This affinity for halogen atoms allows the conversion of organo-halides into a range of carbon-centred radicals (Figure 1.30).

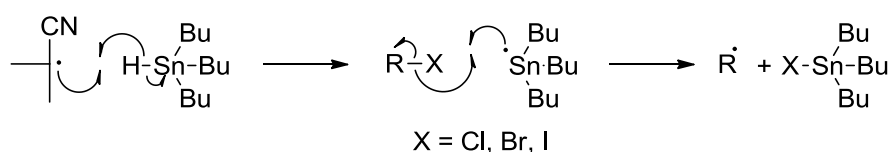


Figure 1.30: Formation of the tributyltin radical and a halogen-atom abstraction reaction.



Carbon centred radicals generated in this way can be reduced further by H-atom abstraction from tributyltin hydride, thereby replacing a halogen atom with a hydrogen atom. For example, the radical initiator AIBN and tributyltin hydride were used for a simple halide reduction in the final step of Dobbs' synthesis of a naturally occurring indole (**11**) isolated from *Tricholoma* fungi (Figure 1.31).<sup>29</sup>

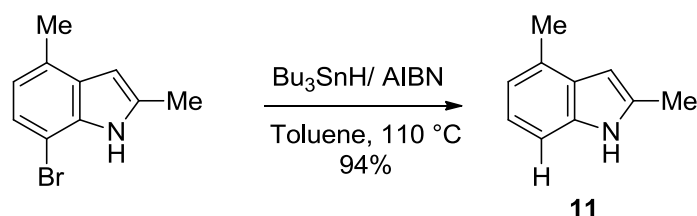


Figure 1.31: Tributyltin hydride mediated reduction of an aryl bromide.

#### 1.4.3. Tributyltin Hydride Mediated Cyclisations

In the presence of an internal alkene or alkyne, a carbon-centred radical generated by halogen atom abstraction can be used to form a new C-C bond in a radical cyclisation (Figure 1.32).

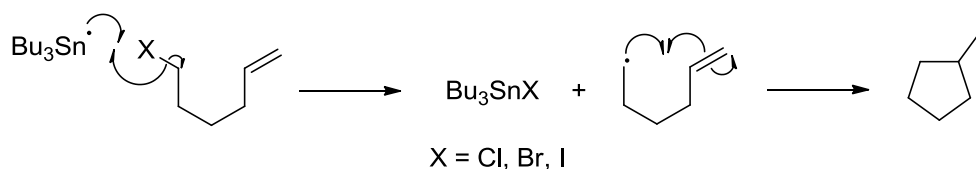


Figure 1.32: Mechanism of a tributyltin hydride mediated 5-exo-trig cyclisation

For example, Mohanakrishnan et al. used this method to form bicyclic carbocycles (Figure 1.33).<sup>30</sup>

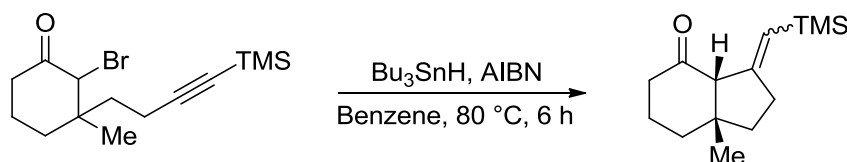


Figure 1.33: Tributyltin hydride mediated formation of bicyclic carbocycles

Tributyltin hydride can also be used to generate radicals from functional groups other than organo-halides. This includes aldehydes and ketones as shown in the formation of a cyclopentane ring developed by Chen et al. (Figure 1.34).<sup>31</sup>

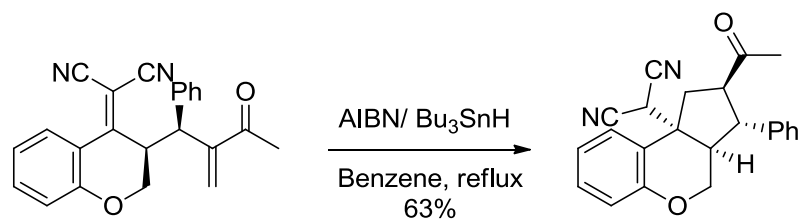


Figure 1.34: Tributyltin hydride mediated 5-*exo-trig* cyclisation.

In this example, the initial carbon centred radical is formed by addition of the tin-centred radical to the oxygen atom in the  $\alpha,\beta$ -unsaturated carbonyl. Subsequent 5-*exo* cyclisation then reduction forms the cyclopentane ring (**12**) as shown in Figure 1.35.

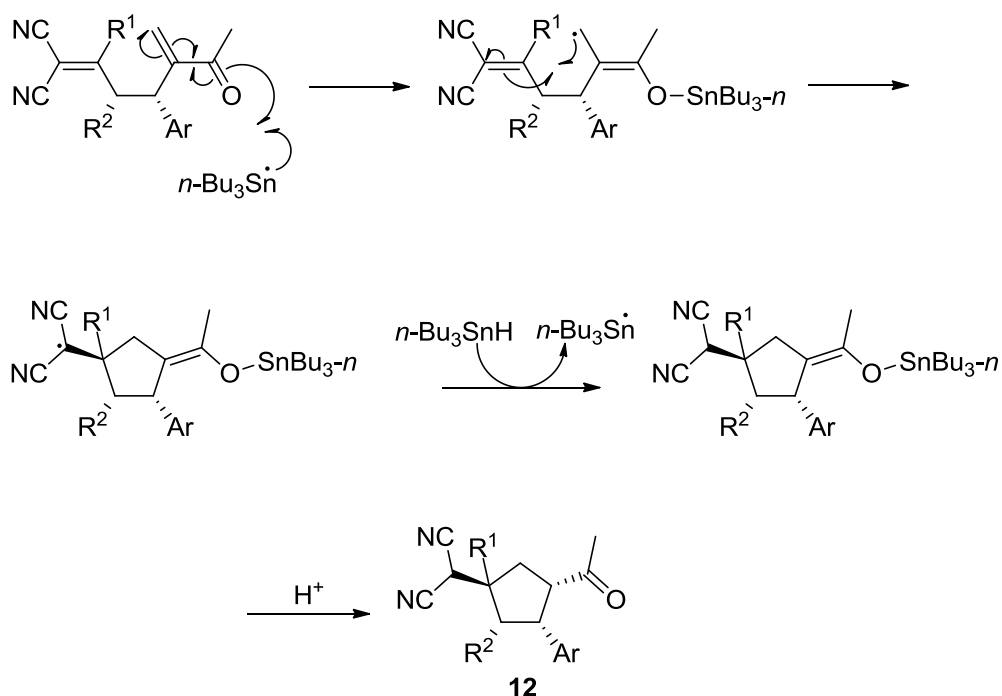


Figure 1.35: Tributyltin hydride mediated 5-*exo-trig* cyclisation mechanism.

#### 1.4.4. Tributyltin Hydride Mediated Ring Expansions

In addition to cyclisation reactions tributyltin hydride has been used to perform one-carbon ring expansions, which has proved to be a good way of synthesising 7- and 8-membered rings from more commonly available starting materials. This was demonstrated by Dowd et al. in 1987 in their ring expansion of  $\beta$ -keto esters (Figure 1.36).<sup>32</sup>

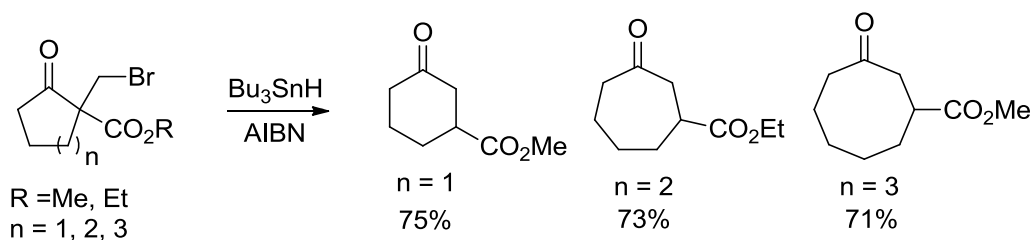


Figure 1.36: Tributyltin mediated ring expansion of cyclic  $\beta$ -keto esters.

In these ring expansions the radical generated from abstraction of a bromine atom by tributyltin hydride adds to the carbonyl in a 3-*exo-trig* cyclisation to form a strained bicyclic intermediate (**13**). This bicyclic intermediate breaks open to relieve the strain and form a resonance stabilised tertiary radical (**14**) (Figure 1.37).

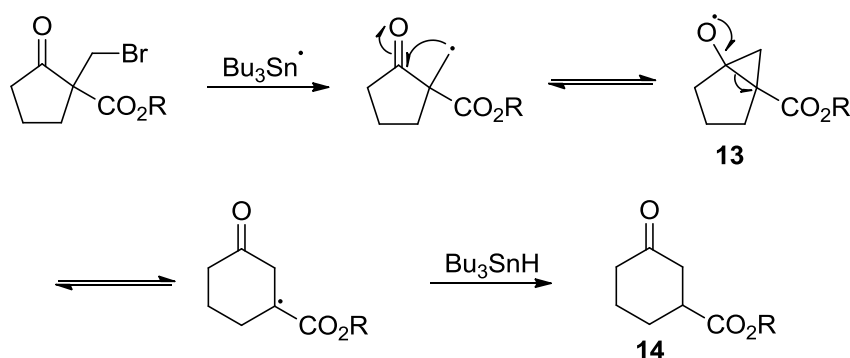


Figure 1.37: Mechanism of a tributyltin hydride mediated ring expansion.

#### 1.4.5. Barton-McCombie Deoxygenation

The Barton-McCombie deoxygenation uses the strength of the Sn-S bond and C=O bond to reduce hydroxy groups into alkanes.<sup>33</sup> First the alcohol is converted into a xanthate (ROC(S)SR), which is then reduced by the radical process shown in Figure 1.38.

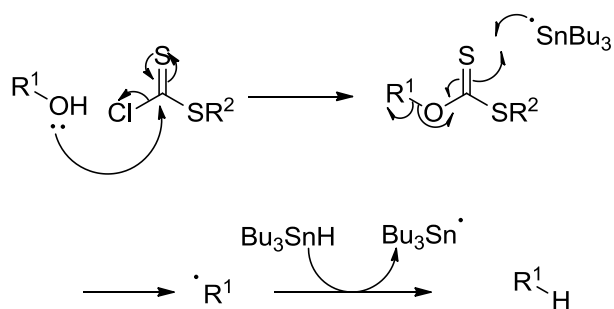


Figure 1.38: Mechanism of the Barton-McCombie deoxygenation.

The fragmentation of the xanthate forms a strong C=O bond in preference to the weaker C=S bond. The R group on the xanthate ( $R^2$ ) is often chosen to be a methyl group to ensure that there is not a good radical leaving group on sulfur.

This method of generating carbon centred radicals was used by Opatz et al. in 2014 in the total synthesis of (-)-cyclonerodiol **15**, which has been identified as a potential starting point for novel asthma therapeutics (Figure 1.39).<sup>34</sup>

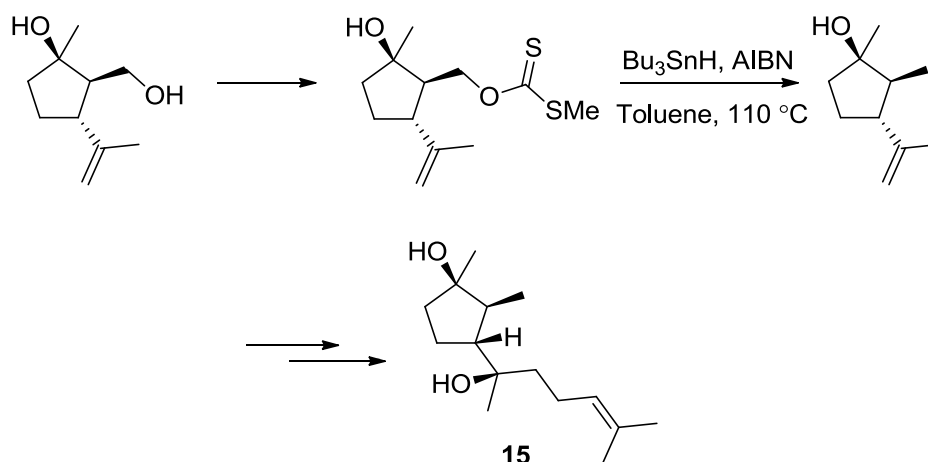


Figure 1.39: Synthesis of (-)-cyclonerodiol including the Barton-McCombie deoxygenation.

#### 1.4.6. Hydrostannation

Hydrostannation is the addition of a hydrogen-tin bond across an unsaturated C=C bond or C≡C bond. In 1996 Yamamoto demonstrated the use of Lewis acids as catalysts for the hydrostannation of alkynes to form *cis*-vinyl stannanes in moderate yields and in high regio- and stereo-selectivity (Figure 1.40).<sup>35</sup>

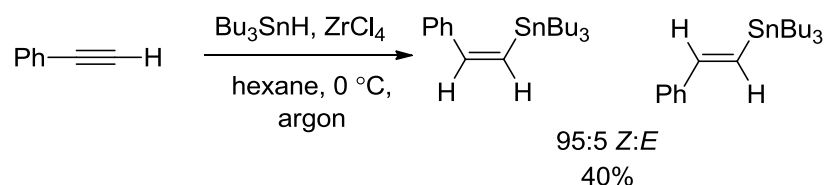


Figure 1.40: Hydrostannation of phenyl acetylene.

Vinyl stannanes are useful reagents for organic synthesis as they are used, for example, in the Stille cross coupling reaction. A Stille cross coupling typically joins together an  $sp^2$  hybridised stannane and an organohalide using a palladium catalyst (Figure 1.41).

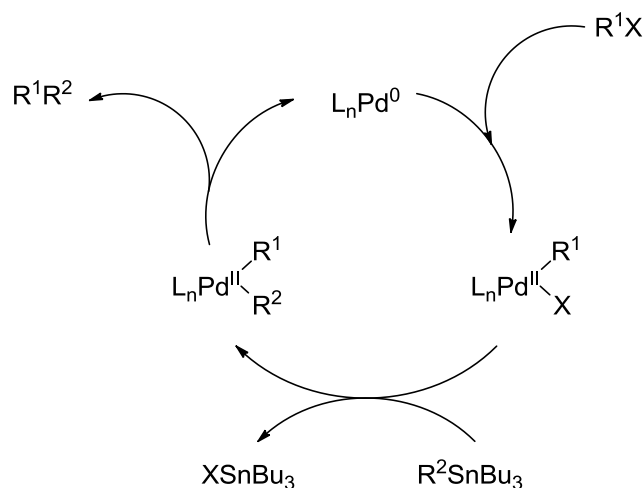


Figure 1.41: Catalytic cycle of the Stille cross coupling.

#### 1.4.7. Problems with Organostannanes

The big problem with the use of organo-tin hydrides is their high toxicity and detrimental environmental impact. Tributyltin hydride is a flammable liquid which is toxic by ingestion, harmful on contact with skin, damages organs on prolonged or repeated exposure and is toxic to aquatic life. It is also notoriously difficult to remove all traces of tin-containing compounds from a final product making it an unsuitable reagent for the manufacture of pharmaceuticals. An additional issue is the stability of tributyltin hydride which decomposes steadily over time making it less than ideal for use after long term storage. Over the last few years there have been numerous attempts to create alternative methods of mediating radical

reactions as well as ways of improving the use of tin hydrides some of which we will explore in the following sections.<sup>36</sup>

#### 1.4.8. Alternative Tin Based Methods

The by-products of alkyl tin mediated reactions, such as tin halides, tend to slowly hydrolyse when a mixture is purified by flash column chromatography making their separation from the rest of the crude mixture a difficult task. In 1996 Crich et al. proposed an alternative work up procedure to improve the removal of stannanes from crude reaction mixtures thereby removing a large downside to their use.<sup>37</sup> By using sodium cyanoborohydride in *tert*-butanol Crich reduced the tin halide back to the original tin hydride. This not only improves the ease with which tin compounds can be removed from the reaction mixture by column chromatography but allows the reagent to be recovered and reused, reducing its environmental impact.

The regeneration of tin hydrides from tin halides can be taken one step further and used to create a catalytic cycle such as that presented by Corey et al. who used an equivalent of sodium borohydride to regenerate a catalytic quantity of tributyltin hydride *in situ* (Figure 1.42).<sup>38</sup>

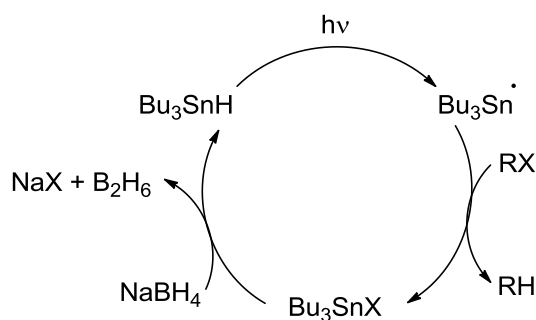


Figure 1.42: Regeneration of the tributyltin radical by sodium borohydride.

An alternative catalytic method uses an exchange process to convert an alkoxy tin species (**16**) into a silyl ether (**17**) and regenerate the tin hydride (Figure 1.43).<sup>39</sup> This allows stoichiometric tin to be replaced with a much more environmentally benign silane.

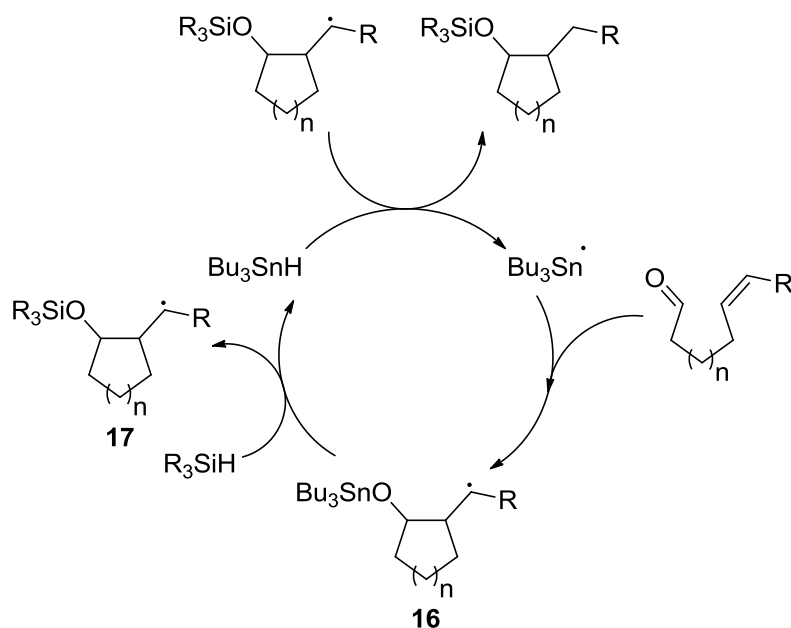


Figure 1.43: Radical cyclisation with catalytic tin and stoichiometric silane.

The silyl ether is then hydrolysed on work up to yield the corresponding alcohol.

Another method by which people have tried to improve the use of tin reagents is by replacing the butyl groups on tributyltin hydride with groups which improve the removal of stannanes by work up or purification techniques. Figure 1.44 shows a few of these modified stannanes.

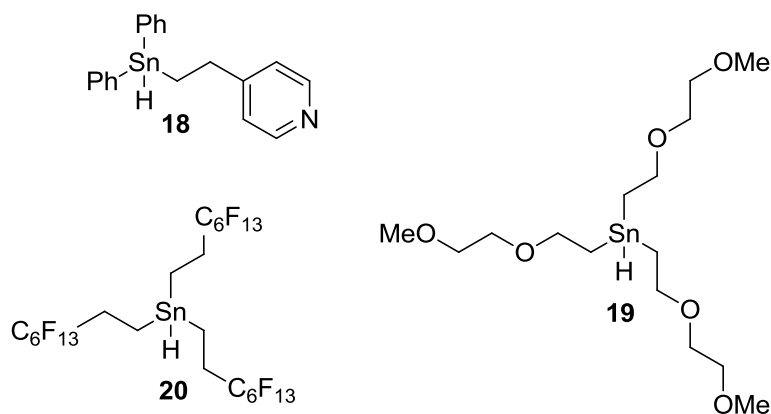


Figure 1.44 Structures of some tin containing tributyltin hydride alternatives.

Stannane **18** incorporates a pyridine ring which greatly lowers the  $R_f$  value of any left-over tin reagents or side products allowing them to be easily removed by flash column chromatography on silica. This variation on tributyltin hydride is

synthesised from 4-vinylpyridine in a three step process with a rather low overall yield of 27%.<sup>40</sup> Compound **19** is synthesised via a five step process with a comparable yield of 25%. The high oxygen content in **19** makes it water soluble and therefore easy to remove with an aqueous wash and even perform reactions in aqueous media.<sup>41</sup> Alternatively the fluorous stannane **20** can be prepared in three steps with a 65% yield.<sup>42</sup> This compound makes use of the fact that highly fluorinated organic substances don't mix with water or with many organic solvents allowing the stannane derivatives to be extracted into a separate fluorous layer during the work up procedure.

Although all of these methods improve on the traditional use of tin-containing compounds, alternative reagents have been increasingly sought to address the issues associated with tin.

### 1.5. Germanium Hydride

Tributylgermanium hydride ( $\text{Bu}_3\text{GeH}$ ) is a considerably safer alternative to tributyltin hydride which is classified as harmful rather than toxic. In addition to this there is currently nothing to suggest it has any significant environmental impact. In practical terms one of the main advantages of germanium hydrides is their significantly increased stability and shelf life compared to tin hydrides.<sup>43</sup> Germanium is a group 14 element one place above tin in the periodic table giving it similar chemical properties. The Ge-H bond in tributylgermanium hydride (BDE  $346 \text{ kJ mol}^{-1}$ )<sup>44</sup> is somewhat stronger than tributyltin hydride (BDE  $308 \text{ kJ mol}^{-1}$ )<sup>27</sup> which means that germanium hydrides are less likely to perform direct reductions than the equivalent tin compounds.<sup>45,46</sup> This was used to good effect by Kahne et al. who found that the reaction of saccharide **21** with carbon monoxide proceeded with only 5% yield of **22** when mediated by tributyltin hydride since direct reduction of the iodine atom to hydrogen dominated. Replacement of tributyltin hydride with catalytic triphenyl germanium hydride and sodium cyanoborohydride however gave the desired product in much higher yield (Figure 1.45).<sup>47</sup> As with tributyltin hydride, a hydride source, in this case sodium cyanoborohydride, can be used to regenerate the germanium hydride from the germanium halide.



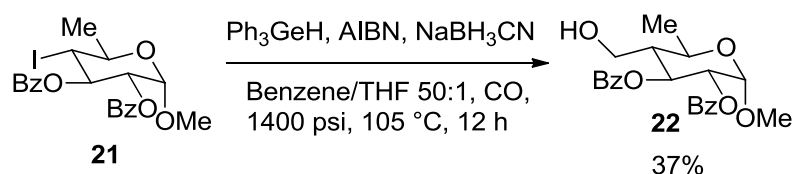


*Figure 1.45: Radical trapping of CO mediated by catalytic triphenylgermanium hydride.*

The CO preferentially adds to the carbon radical in the less sterically hindered equatorial position and is then reduced by cyanoborohydride to the alcohol to selectively form **22**.

While germanium hydrides have specific applications where they have an advantage over tin hydrides, Hershberger et al. noted that tributylgermanium hydride had a lower reactivity towards halides than its tin counterpart and could only be used for organo-iodides or in some circumstances organo-bromides.<sup>48</sup> Competing hydrogermylation of unsaturated C-C bonds is another significant problem when dealing with reactions containing alkenes, such as when attempting to perform a cyclisation or intermolecular addition (Figure 1.46).<sup>48</sup>

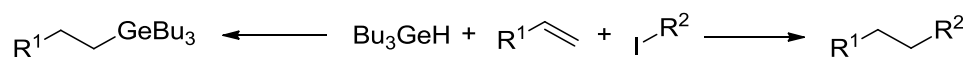


*Figure 1.46: Competing hydrogermylation and termolecular radical addition.*

## 1.6. Silanes

One place above germanium in the periodic table, silicon, is another obvious choice for a tin replacement. Alkyl-silane reagents such as triethylsilane contain a very strong Si-H bond ( $377 \text{ kJ mol}^{-1}$ )<sup>27</sup> approximately  $70 \text{ kJ mol}^{-1}$  stronger than the Sn-H bond in tributyltin hydride and about  $30 \text{ kJ mol}^{-1}$  stronger than the Ge-H bond in tributylgermanium hydride. This can make alkyl-silanes difficult reagents to use for chain processes because although silyl radicals are highly reactive to a range of functional groups, carbon centred radicals will not readily abstract a hydrogen atom from silanes due to the strong Si-H bond.

### 1.6.1. Trialkylsilane Mediated Barton-McCombie Deoxygenation

Despite the difficulties of using triethylsilane some examples do exist in the literature such as Barton's variation on the Barton-McCombie reaction (Figure 1.47).<sup>49</sup>

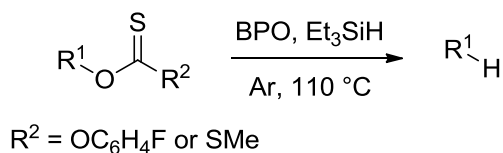


Figure 1.47: Triethylsilane mediated Barton-McCombie deoxygenation.

This methodology was used to deoxygenate a number of compounds with high yields and reasonably short reaction times (Figure 1.48).

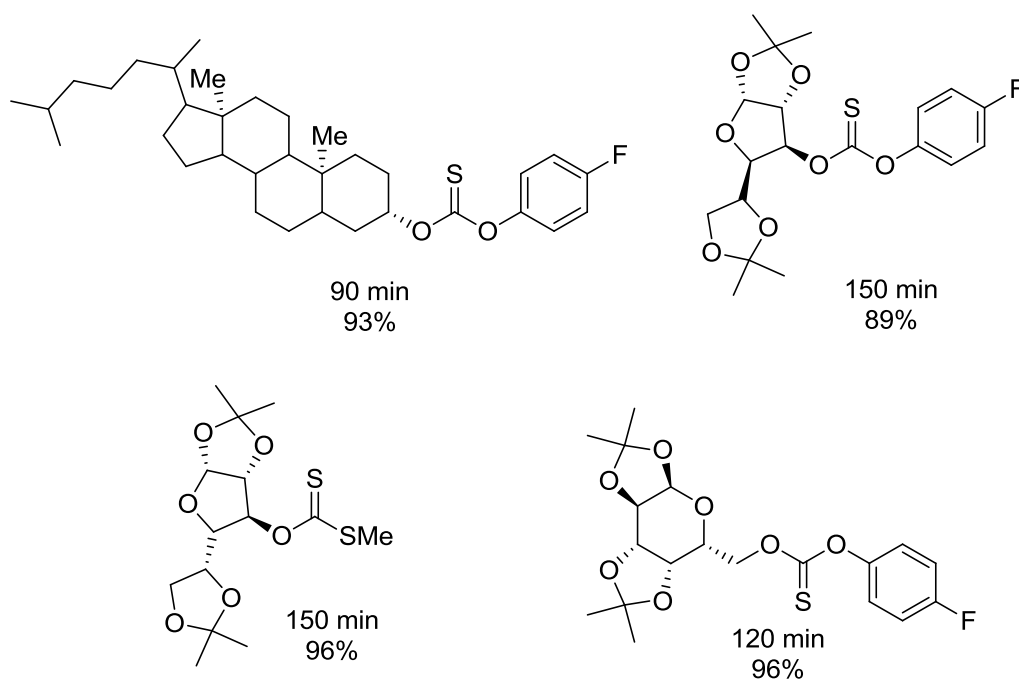


Figure 1.48: Starting materials of triethylsilane mediated Barton-McCombie deoxygenation and yields of deoxygenated products.

### 1.6.2. Trialkylsilanes with Polarity Reversal Catalysts

On the whole trialkyl-silanes have a limited scope and require high temperatures to achieve meaningful results. In order to overcome these issues trialkyl silanes have been used in conjunction with thiols as polarity reversal catalysts. This allows the

slow abstraction of hydrogen from the silane by a nucleophilic alkyl radical to be replaced by a faster abstraction by an electrophilic sulfur-centred radical (Figure 1.49).

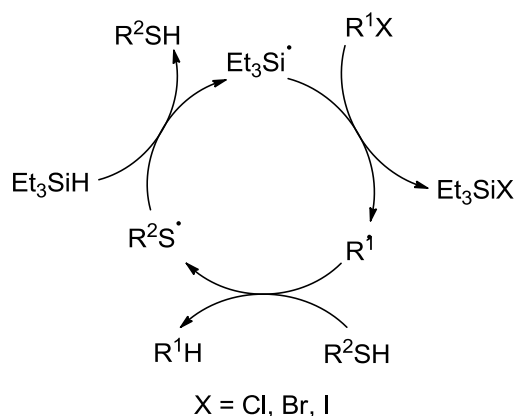


Figure 1.49: Triethylsilane with thiol polarity reversal catalyst.

In 1991 Roberts et al. developed a methodology using *tert*-dodecanethiol as a polarity reversal catalyst to reduce alkyl halides (Figure 1.50).<sup>50</sup>

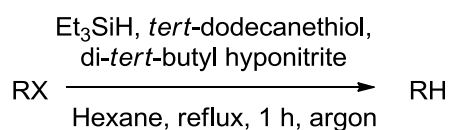


Figure 1.50: Reduction of alkyl halides by triethylsilane with thiol polarity reversal catalyst.

Roberts et al. used this polarity reversal methodology to reduce a number of alkyl halides in excellent yields (Table 1.3).

Table 1.3: Reduction of organo-halides by triethylsilane with a thiol polarity reversal catalyst.

Entry	Organo-halide (RX)	Yield of RH (%)
1	1-Bromooctane	99
2	1-Bromooctane	10 <sup>a</sup>
3	1-Chlorooctane	96
4	1-Iodoctane	91
5	2-Bromooctane	96
6	1-Bromoadamantane	99
7	1-Bromo-1-methyl cyclohexane	95

Conditions: organo-halide 1 eq, triethylsilane 2 eq, *tert*-dodecanethiol 0.02 eq, *di-tert*-butyl hyponitrite 0.02 eq reflux in hexane for 1 h under argon. <sup>a</sup>Without *t*-dodecanethiol

Entry 2 of Table 1.3 demonstrates that in the absence of dodecanethiol the observed yield is considerably lower proving the validity of using a polarity reversal catalyst in this instance.

As well as in halide reductions, thiols have been used in conjunction with triethylsilane by Roberts et al. to perform hydrosilylations (Figure 1.51).<sup>51</sup>

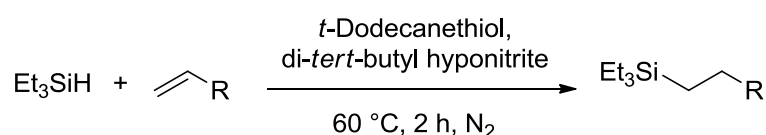


Figure 1.51: Addition of triethylsilane to alkenes with thiol polarity reversal catalyst.

Although the introduction of *tert*-dodecanethiol as a catalyst improves the hydrosilylation of alkyl substituted alkenes the methodology still requires

triethylsilane to be used as a solvent in order to achieve the necessary excess of reagent and produces mostly moderate yields (Figure 1.52).

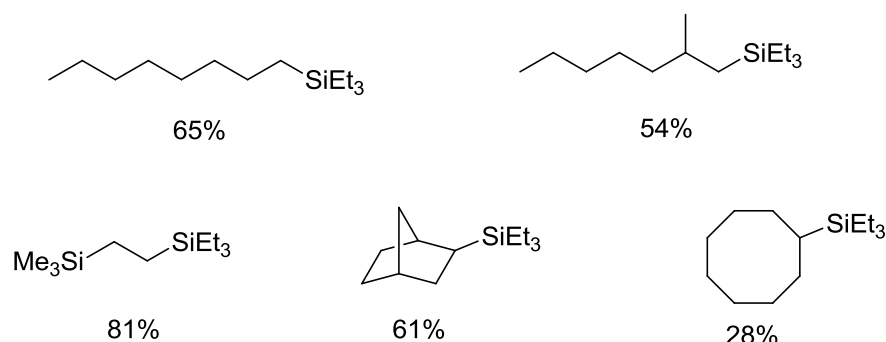


Figure 1.52: Triethylsilane addition products.

Triethylsilane has been shown to perform a few different reactions both on its own and with a polarity reversal catalyst but its high Si-H bond strength limits its versatility. As a result people have looked to other silanes with weaker bonds as potential replacements for organo-tin reagents.

### 1.6.3. *Tris(trimethylsilyl)silane*

Tris(trimethylsilyl)silane has been put forward as a versatile and environmentally friendly alternative to organotin reagents with a considerable weaker Si-H bond than trimethylsilane (Figure 1.53).<sup>27,52</sup>

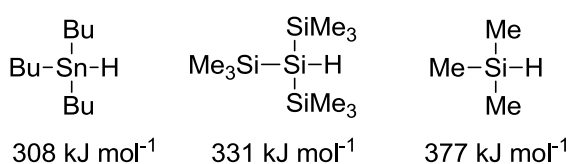


Figure 1.53: BDEs of tributyltin hydride, tris(trimethylsilyl)silane and trimethylsilane.

The reason behind the significantly weaker bond is the  $\beta$  silicon effect also known as hyperconjugation where electron density from the silicon d orbitals is donated into the SOMO of the radical.<sup>52</sup> This stabilises the radical and favours its formation.

### 1.6.4. *Tris(trimethylsilyl)silane Mediated Reductions*

In 1988 Chatgililoglu et al. showed that on photolytic or chemical initiation tris(trimethylsilyl)silane could reduce alkyl halides in excellent yields (Table 1.4).<sup>53</sup>

Table 1.4: Reduction of organo-halides by tris(trimethylsilyl)silane.

Entry	Organo-halide (RX)	Yield of RH (%)
1	1-Chlorooctadecane	93 <sup>a</sup>
2	<i>exo</i> -2-Chloronorbornane	95 <sup>a</sup>
3	3-Chloro-2-norbornanone	100 <sup>a</sup>
4	Benzyl bromide	100 <sup>b</sup>
5	1-Bromo hexadecane	100 <sup>b</sup>
6	1-Bromo hexadecane	100 <sup>a</sup>
7	1-Iodoctadecane	100 <sup>a</sup>

Conditions: <sup>a</sup>Photolysis of RX and  $(\text{Me}_3\text{Si})_3\text{SiH}$  in hydrocarbon solvent 0.25-1 h.

<sup>b</sup>Initiated with benzoyl peroxide at 50 °C with no solvent.

Since then tris(trimethylsilyl)silane has been shown to reduce a range of functional groups and add to a number of different unsaturated bonds some of which were summarised in a review by Chatgililoglu (Figure 1.54).<sup>54</sup>

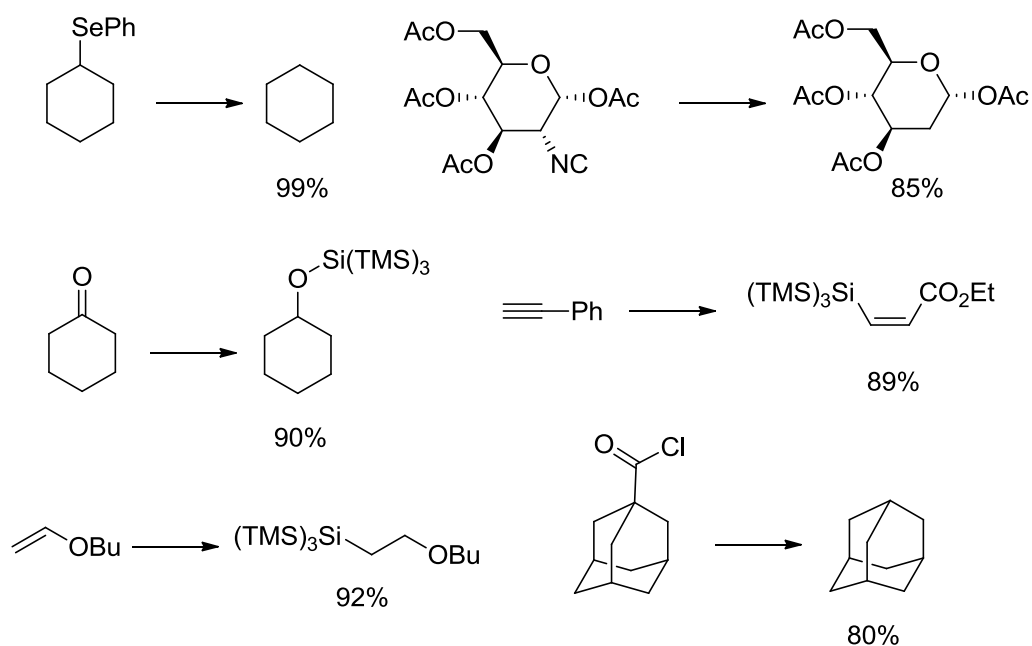


Figure 1.54: Tris(trimethylsilyl)silane mediated reduction and addition products.

Figure 1.53 shows the versatility of tris(trimethylsilyl)silane in its ability to reduce selenides,<sup>55</sup> isocyanides,<sup>56</sup> and acid chlorides<sup>57</sup> as well as add to alkenes<sup>54</sup> and alkynes.<sup>54</sup>

As well as the reduction of functional groups such as alkenes, alkynes and carbonyls, tris(trimethylsilyl)silane can also be used to generate carbon centred radicals from organohalides which can then undergo inter- or intra-molecular addition to unsaturated C=C bonds (Figure 1.55).<sup>56</sup>

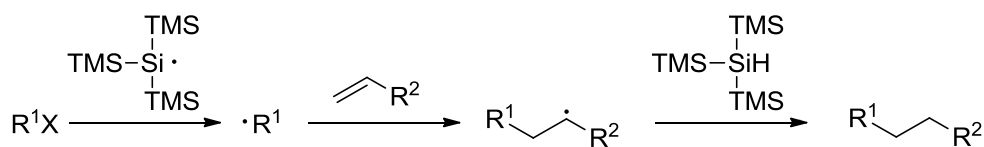


Figure 1.55: Tris(trimethylsilyl)silane mediated C-C bond forming reactions.

Giese et al. used tris(trimethylsilyl)silane to create a hexyl radical from iodohexane, which then added to various C=C bonds prior to reduction (Figure 1.56).<sup>56</sup>

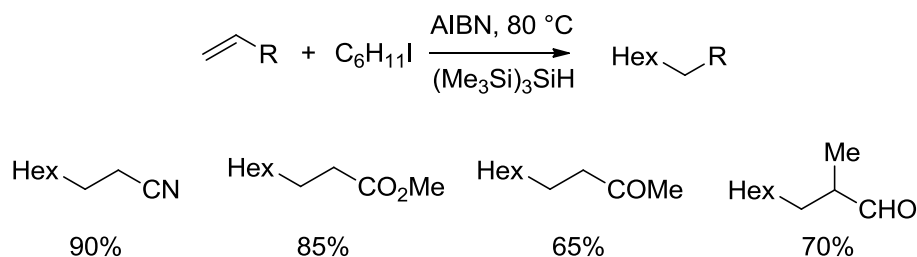


Figure 1.56: Products of tris(trimethylsilyl)silane mediated C-C bond forming reactions.

It can be seen in Figure 1.56 that the more electron deficient alkenes gave higher yields, presumably due to the more favourable match in polarity between them and the relatively electron rich (nucleophilic) hexyl radical.

As well as performing intermolecular additions Giese et al. showed that tris(trimethylsilyl)silane can be used to perform radical cyclisations more effectively than tributyltin hydride under the same conditions (Figure 1.57).<sup>56</sup>

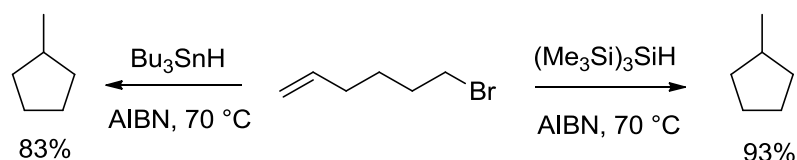


Figure 1.57: Comparison of tributyltin hydride and tris(trimethylsilyl)silane mediated 5-exo-trig cyclisation.

Methods have been developed to regenerate tris(trimethylsilyl)silane *in situ*. As with the tributyltin hydride methods this takes the form of a sacrificial hydride source such as sodium borohydride. In 1989 Griller et al. showed that stoichiometric tris(trimethylsilyl)silane could be replaced with stoichiometric sodium borohydride and 0.1 equivalents of tris(trimethylsilyl)silane with little or no loss of product yield (Table 1.5).<sup>58</sup>

Table 1.5: Reduction of organo-halides by catalytic tris(trimethylsilyl)silane and stoichiometric sodium borohydride.

Entry	Substrate	Yield with 0.1 eq tris(trimethylsilyl)silane, 1 eq NaBH <sub>4</sub> (%)	Yield with 1 eq tris(trimethylsilyl)silane (%)
1	1-Iodoctadecane	68	78
2	1-Bromooctadecane	85	86
3	1-Bromonaphthalene	88	91
4	1-Bromoadamantane	90	99
5	Cholesteryl iodide	55	75

Conditions: Organo-halide (1 eq), sodium borohydride (5 eq), tris(trimethylsilyl)silane (0.1 eq), *p*-methoxybenzoyl peroxide (0.02 eq), photolysis, in DME.



The disadvantages of using tris(trimethylsilyl)silane are its high cost, the need for it to be handled under argon and its high propensity to add to alkenes and alkynes, reducing its functional group tolerance.

## 1.7. Phosphorus Hydride Reagents

Much work has been done to investigate the possibility of using phosphorus hydride reagents as a replacement for tin hydrides in radical chemistry.<sup>59,60</sup>

### 1.7.1. Hypophosphorus Acid and its Salts

Hypophosphorus acid also known as phosphinic acid is a monoprotic acid with the structure shown in Figure 1.58.

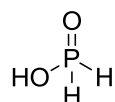


Figure 1.58: Structure of hypophosphorus acid.

Salts of hypophosphorus acid are called hypophosphites or phosphinates. Hypophosphorus acid and its salts are water soluble and highly hygroscopic and as such are often supplied and used as aqueous solutions.

In 1993 Barton et al. developed a method for using hypophosphorus acid to perform radical reductions (Figure 1.59).<sup>61</sup>

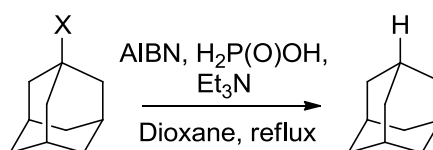


Figure 1.59: Reduction of halo-adamantane mediated by hypophosphorus acid.

Table 1.6 shows some of the scope of the hypophosphorus acid mediated reduction.

Table 1.6: Reduction of functionalised-adamantane by hypophosphorus acid.

Entry	X	Yield of adamantane (%)
1	I	100 <sup>a</sup>
2	Br	95 <sup>a</sup>
3	Cl	0 <sup>b</sup>
4	OC(S)SMe	100 <sup>b</sup>
5	NC	97 <sup>b</sup>
6	SePh	21 <sup>b</sup>
7	NO <sub>2</sub>	0 <sup>b</sup>

Conditions: <sup>a</sup>functionalised-adamantane (1 eq), hypophosphorus acid (5 eq), Et<sub>3</sub>N (5.5 eq), AIBN in refluxing dioxane, 90-160 min. <sup>b</sup>functionalised-adamantane (1 eq), hypophosphorus acid (10 eq), Et<sub>3</sub>N (11 eq), AIBN in refluxing dioxane, 90-200 min.

Not all of the functional groups investigated were reduced, such as chloroadamantane (Table 1.6, Entry 3). While this does somewhat limit the range of reductions that can be performed it does allow for other functional groups (e.g. organo-bromides or iodides) to be selectively reduced in the presence of chloroalkanes potentially allowing access to chemoselective synthetic routes.

Shortly after, in 1996, Jang developed this method further by reducing, water soluble alkyl bromides and iodides with hypophosphorus acid in water, removing the necessity of an organic solvent (Table 1.7).<sup>62</sup>

*Table 1.7: Reduction of water soluble organohalides by hypophosphorus acid in water.*

Entry	Substrate	Time (min)	Yield of reduced product (%)
1	3-Iodobenzoic acid	60	95
2	2-Iodobenzoic acid	60	94
3	5-Iodosalicylic acid	60	91
4	3-Bromobenzoic acid	300	53
5	3-Iodopropionic acid	60	45
6	5-Bromo uracil	150	50
7	5-Iodo uracil	90	89
8	2-Bromo-3-methyl butyric acid	90	98

*Conditions: Organohalide (1 eq), hypophosphorus acid (5 eq), NaHCO<sub>3</sub> (6.6 eq) and AIBN refluxed in water.*

Table 1.7 shows that while bromo-alkanes can be reduced by hypophosphorus acid in water in high yields (Table 1.7, Entry 8), aryl bromides are much less susceptible to reduction even with extended reaction times reflecting the difficulty in breaking a stronger C-Br bond (Table 1.7, Entry 4).

A number of research groups have shown that hypophosphorus acid and its salts, like tin hydrides, can be used to perform radical cyclisations as well as simple reductions.<sup>63</sup> For example in 2000 Murphy et al. showed that aryl iodides could be used to synthesise 5-membered heterocycles in moderate to good yields (Figure 1.60).<sup>64</sup>

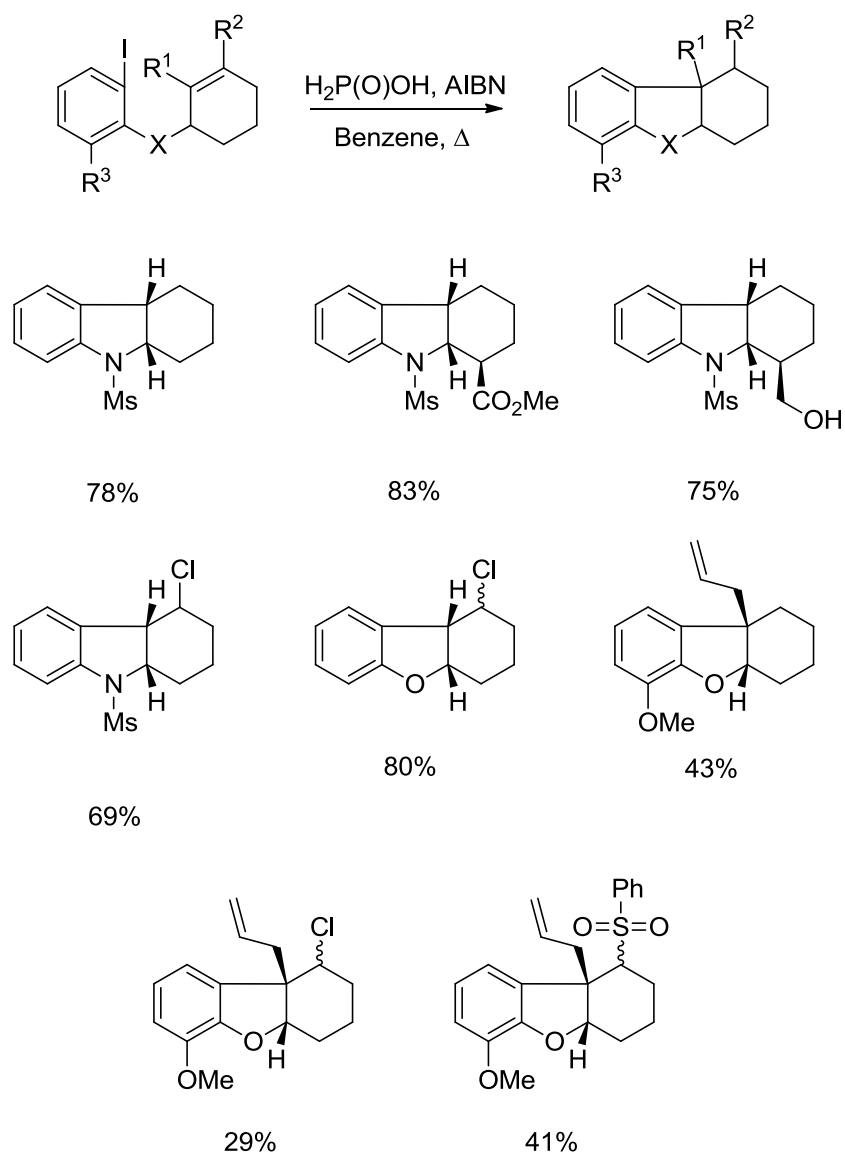
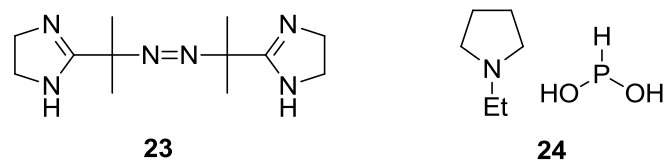


Figure 1.60: Hypophosphorus acid mediated 5-exo-trig cyclisation.

Once again hypophosphorus acid has been shown to work well in water, this time by Kita et al. who investigated the radical cyclisation of hydrophobic substrates.<sup>65</sup> This was achieved by using a water soluble initiator 2,2'-azobis[2-(2-imidazolin-2-yl)propane] (**23**), the hypophosphorus acid salt 1-ethylpiperidine hypophosphite (**24**) and a surfactant, cetyltrimethylammonium bromide (CTAB).



*Figure 1.61: 2,2'-azobis[2-(2-imidazolin-2-yl)propane] (**23**) and 1-ethylpiperidine hypophosphite (**24**)*

A number of compounds were cyclised with high yields (Figure 1.62).

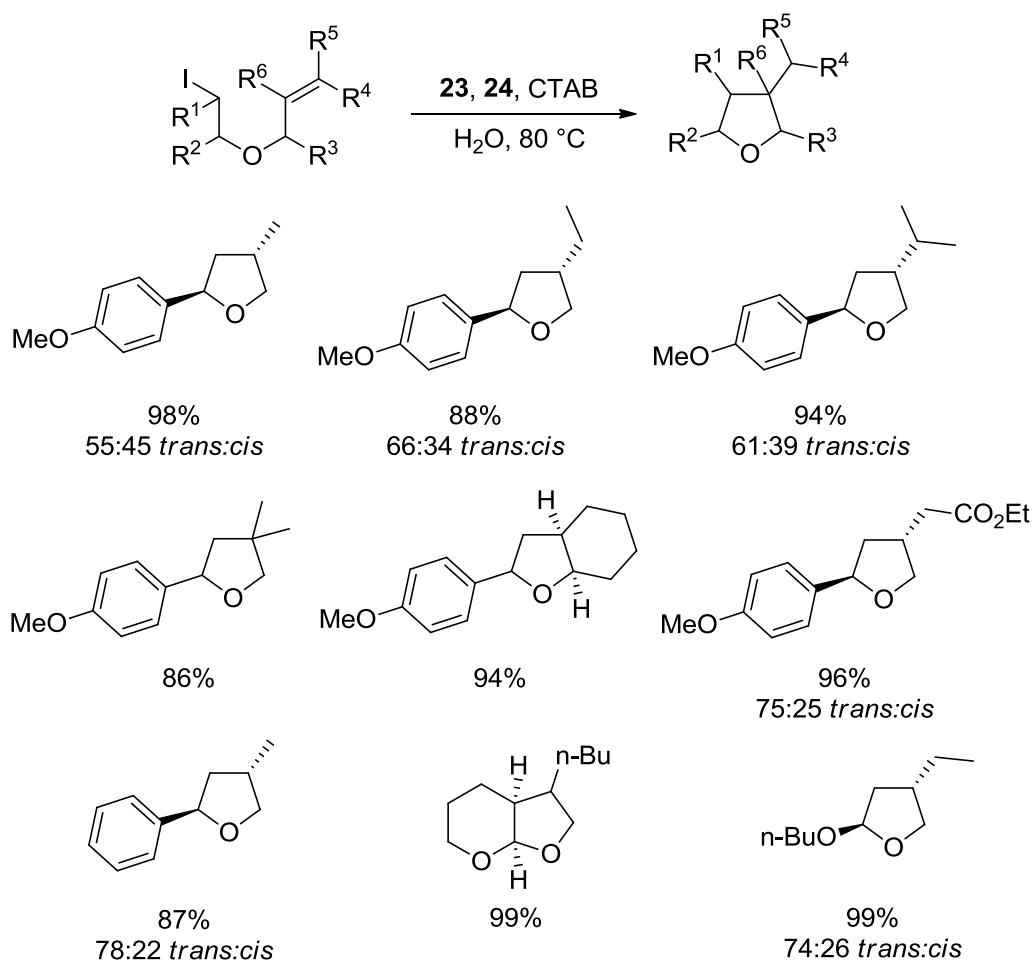


*Figure 1.62: Hypophosphorus acid mediated 5-exo-trig cyclisation in aqueous medium.*

Kita et al. attributed the reaction of these hydrophobic substrates in water to the formation of micelles aiding the solubilisation of the unsaturated iodides. In 2005 Jang et al. took this idea one step further and created a surfactant type hypophosphorus acid salt (**25**) (Figure 1.63).<sup>66</sup>

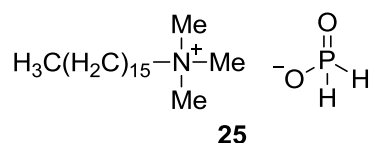


Figure 1.63: Trimethyl pentadecyl ammonium hypophosphite.

Jang et al. used the hypophosphite surfactant **25** with the water soluble azo initiator 4,4-azobis(4-cyanovaleric acid) **26** to deoxygenate alcohols, via xanthates to good effect (Figure 1.64).<sup>66</sup>

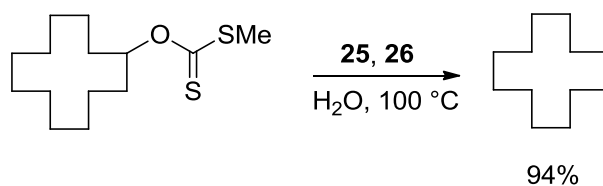


Figure 1.64: Trimethyl pentadecyl ammonium hypophosphite mediated Barton-McCombie reaction.

Like the tin, silicon and germanium agents mentioned previously phosphorus hydride reagents are also capable of radical addition to unsaturated C-C bonds which will be discussed in greater detail in Chapter 3.

Hypophosphorus acid and its salts have been shown to be effective at reducing certain function groups such as alkyl iodides and bromides but do not have the same range as tin hydrides. The upside to this lowered reactivity is that hypophosphorus acids can be used for selective reductions. For example alkyl bromides can be selectively reduced in the presence of aryl bromides. One significant disadvantage arises from the hygroscopic nature of hypophosphorus acids, making them difficult to use with water sensitive substrates.

## 1.8. TEMPO

The work described in this thesis predominantly revolves around the use of nitroxides in radical reactions and the synthesis of novel nitroxides.

### 1.8.1. Nitroxides

Nitroxides are a class of stable organic radical with the general structure shown in Figure 1.65.



Figure 1.65: General structure of a nitroxide.

The first nitroxide to be discovered was Fremy's salt (**27**) which was discovered by Edmund Fremy in 1845 (Figure 1.66).<sup>67</sup>

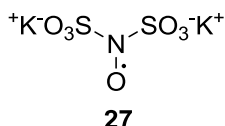


Figure 1.66: Structure of Fremy's salt.

Since Fremy's discovery a variety of related nitroxides have been prepared (Figure 1.67) and shown to have a range of applications such as oxidising agents,<sup>68,69</sup> radical inhibitors,<sup>70</sup> spin labels,<sup>71</sup> and polymerisation mediators.<sup>72</sup>

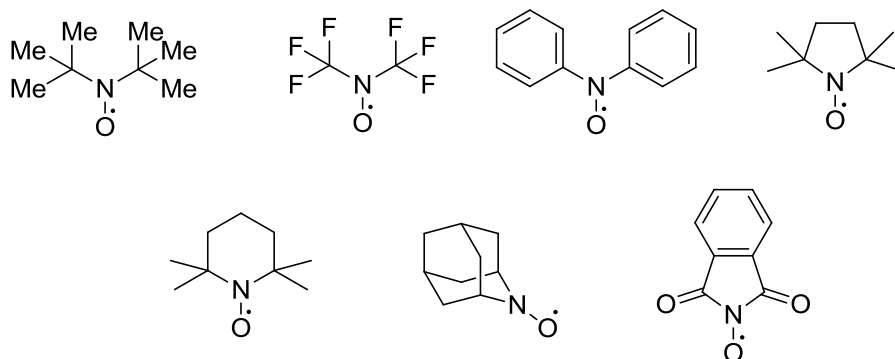


Figure 1.67: Different nitroxides.

### 1.8.2. TEMPO

Probably the most widely used and recognised nitroxide is 2,2,6,6-tetramethylpiperidine-*N*-oxyl, commonly known as TEMPO, and its derivatives (Figure 1.68).

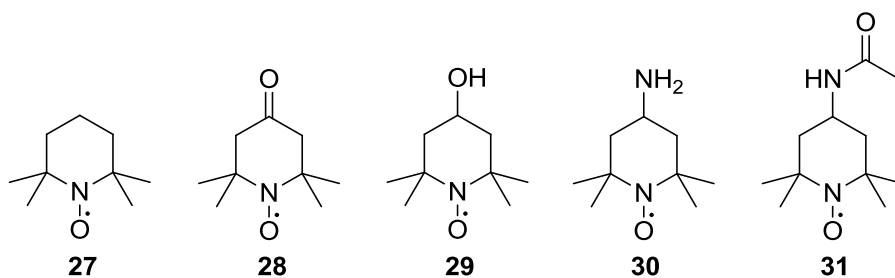


Figure 1.68: Structures of TEMPO and its derivatives. TEMPO (**27**), 4-oxo-TEMPO (**28**), 4-hydroxy-TEMPO (**29**), 4-amino-TEMPO (**30**) and 4-acetamido-TEMPO (**31**).

TEMPO is an orange persistent organic radical which is shelf stable for long periods at room temperature without the necessity of storage under an inert atmosphere. Like all nitroxides the oxygen radical is stabilised by electron donation from the nitrogen lone pair (Figure 1.69).

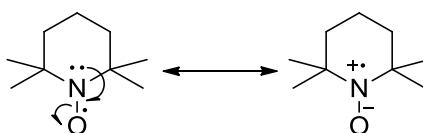


Figure 1.69: Resonance stabilisation of TEMPO.

Some claim that the four methyl groups adjacent to the nitroxide also provide stabilisation through steric hindrance however since TEMPO is reactive in the right circumstances it seems unlikely that the steric effect of these methyl groups is all that significant. What the methyl groups do achieve is the prevention of self-decomposition through hydrogen abstraction which is why nitroxides with alpha hydrogens are unstable (Figure 1.70).<sup>73</sup>

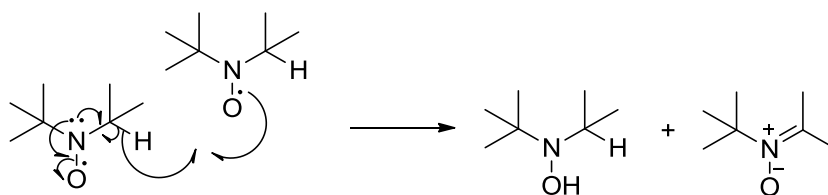


Figure 1.70: Disproportionation of a nitroxide with an alpha hydrogen.



2-Azaadamantane-*N*-oxyl (**32**) is an exception to this general rule since abstraction of the alpha hydrogen to form the nitron requires the formation of a double bond at a bridgehead (Figure 1.71).<sup>74</sup>

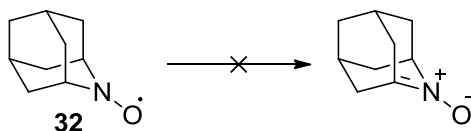


Figure 1.71: 2-Azaadamantane-*N*-oxyl and Bredt's rule.

This would violate Bredt's rule which states that for small ring systems, a double bond cannot be situated on a bridgehead carbon due to the ring and bond angle strains it would cause.<sup>75</sup>

### 1.8.3. Synthesis of TEMPO

TEMPO and its common derivatives are synthesised from 2,2,6,6-tetramethyl piperidone (triacetoneamine) (**33**), which is formed from the condensation of ammonia with acetone in the presence of an acid catalyst (Figure 1.72).

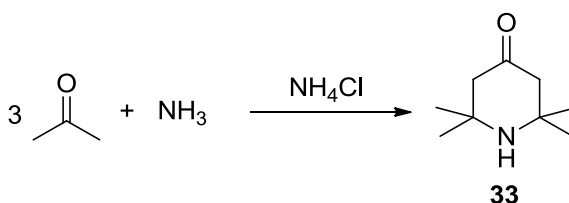


Figure 1.72: Synthesis of triacetoneamine (**33**).

The mechanism of this condensation reaction involves the formation acetonin (**34**) which ring opens to incorporate another molecule of acetone and then ring closes again to form **35** (Figure 1.73). Finally **35** hydrolyses on workup to yield triacetoneamine (**33**).

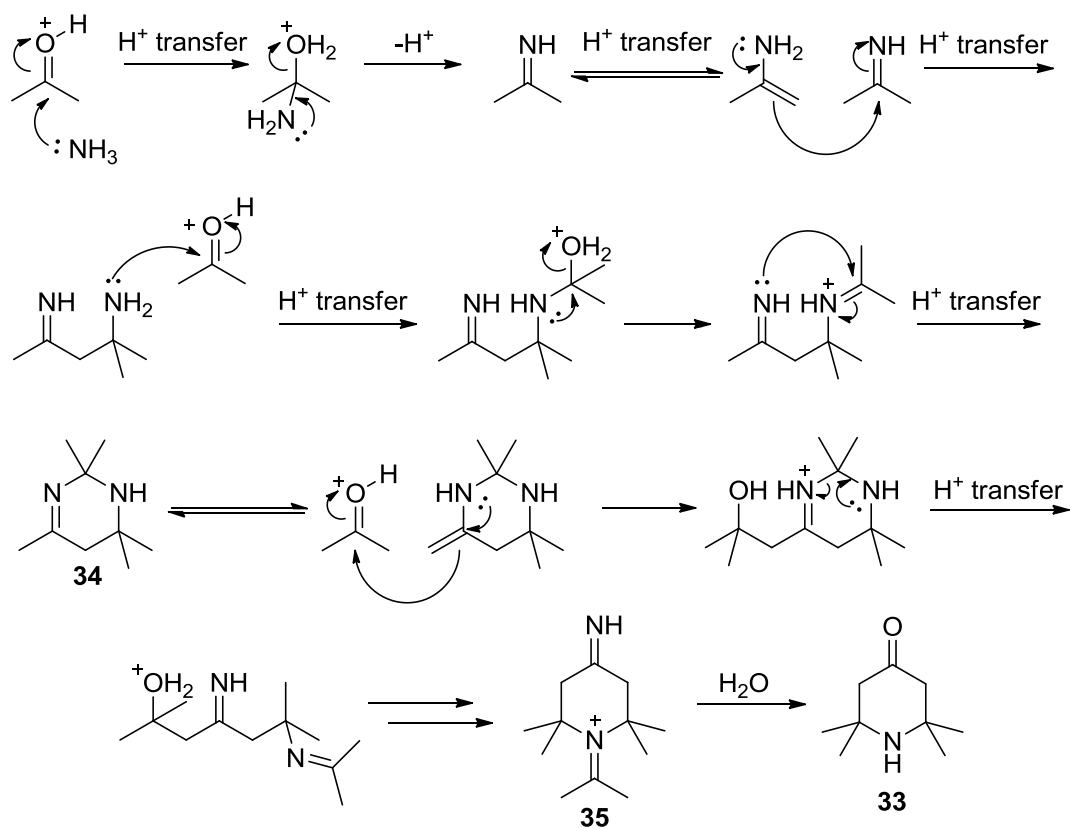


Figure 1.73: Mechanism for the synthesis of triacetoneamine (33).

The ketone group in triacetoneamine (33) can then be altered through functional group interconversions or removed completely to form the basis for the different TEMPO variations. The final step is the formation of the nitroxide functionality which is commonly achieved using hydrogen peroxide and a sodium tungstate catalyst (Figure 1.74).

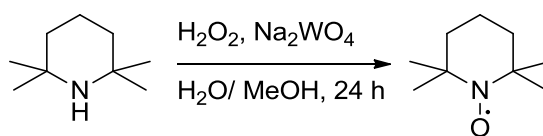


Figure 1.74: Oxidation of tetramethyl piperidine to form TEMPO.

In 1993 Bobbit et al. discovered that using a thiocyanate catalyst allowed the isolation of acetoinin (34) which could then be reacted with a different ketone to create a TEMPO derivative with a chiral centre adjacent to the nitroxide group (Figure 1.75).

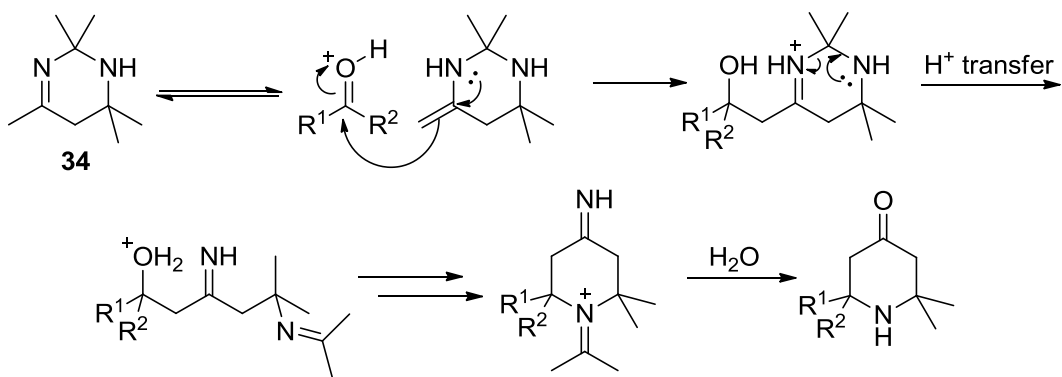


Figure 1.75: Mechanism for the synthesis of chiral piperidones from acetonin (**34**).

Bobbitt et al. used this method to synthesise a number of differently substituted chiral piperidones (Figure 1.76) which were then converted into nitroxides or oxoammonium salts. These were then used to perform chiral oxidations of alcohols with moderate yields but low enantioselectivity.

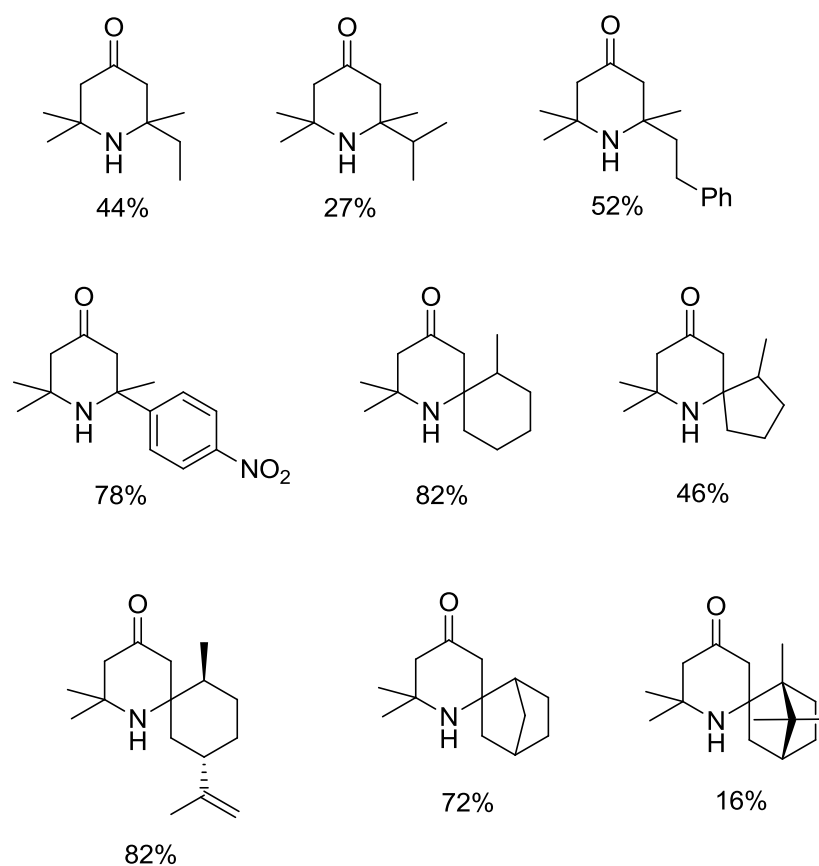


Figure 1.76: Chiral piperidones synthesised from acetonin (**34**).

#### 1.8.4. TEMPO Oxidations

One of the many uses of TEMPO is as a mild oxidising agent. TEMPO systems are capable of oxidising primary alcohols to form aldehydes without over-oxidation to carboxylic acids. In addition to this, TEMPO will preferentially oxidise primary alcohols in the presence of secondary alcohols allowing the selective formation of aldehydes over ketones.

In the case of alcohol oxidations TEMPO is not the active agent but rather it is the oxidised form of TEMPO, oxoammonium (**35**) (Figure 1.77) which performs the oxidation.

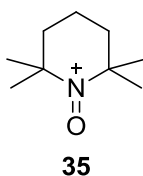


Figure 1.77: Structure of TEMPO oxoammonium (**35**).

Initially Golubev et al. used stoichiometric quantities of oxoammonium (**35**) to perform oxidations (Figure 1.78).<sup>76</sup>

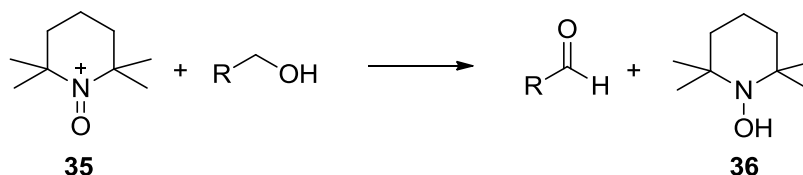


Figure 1.78: Oxidation of primary alcohols by oxoammonium (**35**).

Under acidic conditions TEMPO disproportionates to form the oxoammonium ion (**35**) and a hydroxylamine (**36**) (Figure 1.79).

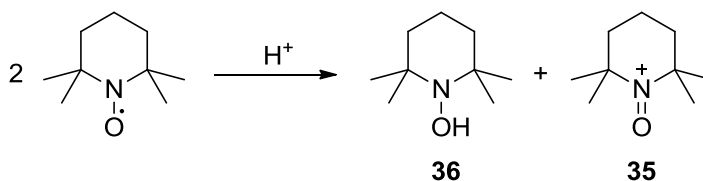


Figure 1.79: Acid catalysed disproportionation of TEMPO.

In 1991 Bobbit et al. used this disproportionation to bypass the necessity of synthesising an oxoammonium salt, instead creating it *in situ* by disproportionation of two equivalents of TEMPO (Figure 1.80).<sup>77</sup>

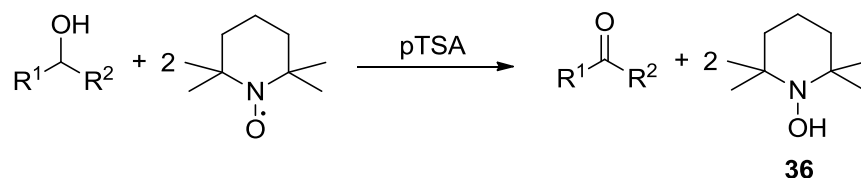


Figure 1.80: Oxidation of alcohols by disproportionated TEMPO.

Since then a number of different methods have been developed that use catalytic quantities of TEMPO to perform primary alcohol oxidations when accompanied by a stoichiometric co-oxidant, this generates and then regenerates the active oxoammonium **35** as shown in Figure 1.81.

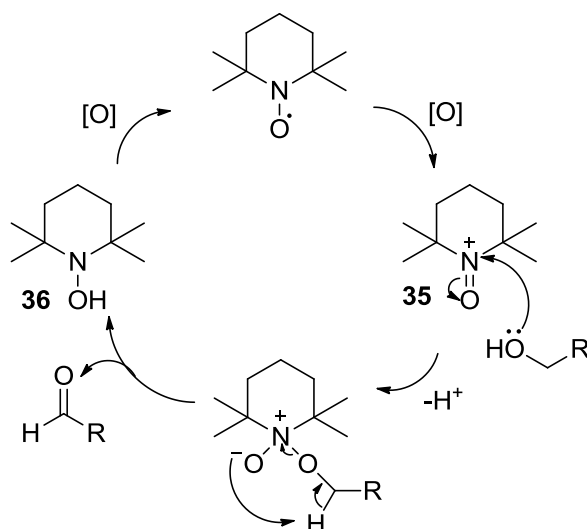


Figure 1.81: Mechanism of the TEMPO mediated oxidation of alcohols.

Examples of stoichiometric co-oxidants include NaOCl,<sup>78</sup> potassium hexacyanoferrate(III),<sup>79</sup> iodine,<sup>80</sup> oxone,<sup>81</sup> iodobenzene dichloride,<sup>82</sup> trichloroisocyanuric acid<sup>83</sup> and *N*-chlorosuccinimide<sup>84</sup>.

In order to do away with wasteful stoichiometric co-oxidants, methods have been developed to utilise O<sub>2</sub> as the terminal oxidant. One example developed by Stahl et al. in 2011 is the use of copper(II) salts which regenerate from copper(I) in an oxygen-rich atmosphere and oxidise TEMPO to oxoammonium **35** (Figure 1.82).<sup>85</sup>

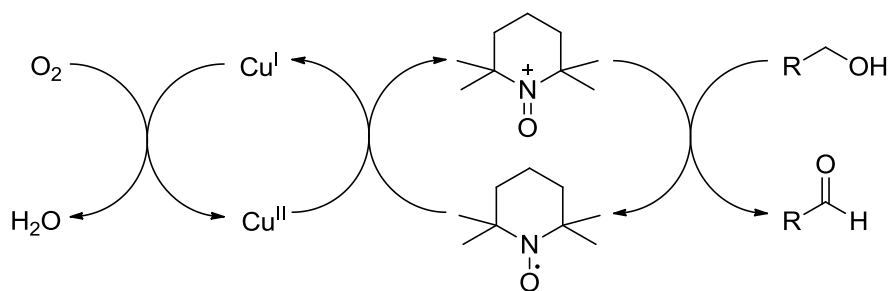


Figure 1.82: Oxidation of alcohols by TEMPO/Cu with  $O_2$  as the terminal oxidant.

Stahl tried using different ligands and bases to help mediate this reaction before settling on bipyridine and *N*-methylimidazole (Figure 1.83).

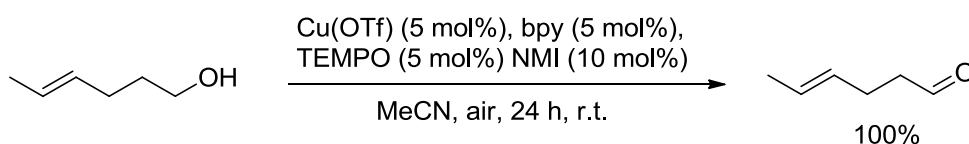


Figure 1.83: Conditions for the oxidation of 4-hexene-1-ol by TEMPO/Cu(OTf).

In an effort to be even more environmentally friendly, Galli et al. discovered that Laccase, an enzyme found in white rot fungi could be used as a co-oxidant. This is illustrated by the oxidation of 4-methoxybenzyl alcohol to 4-methoxybenzaldehyde (Figure 1.84).<sup>86</sup>

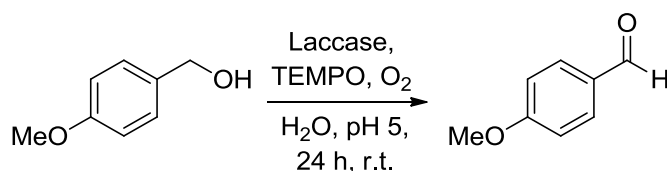


Figure 1.84: Laccase/TEMPO mediated oxidation of 4-methoxybenzyl alcohol.

Of the mediators tested by Galli et al. TEMPO and some of its derivatives were found to be the most efficient (Figure 1.85).

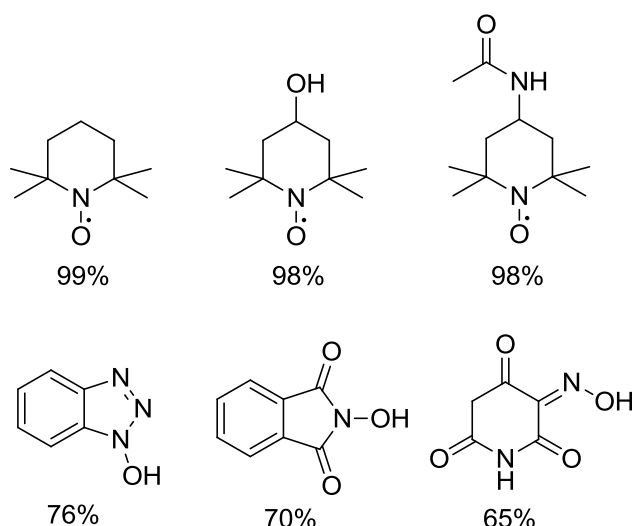


Figure 1.85: The yields of 4-methoxybenzaldehyde from 4-methoxybenzyl alcohol as achieved by certain mediators of Laccase.

Similar to the use of copper(II) salts mentioned above, the terminal oxidant in this reaction is molecular oxygen as shown in Figure 1.86.

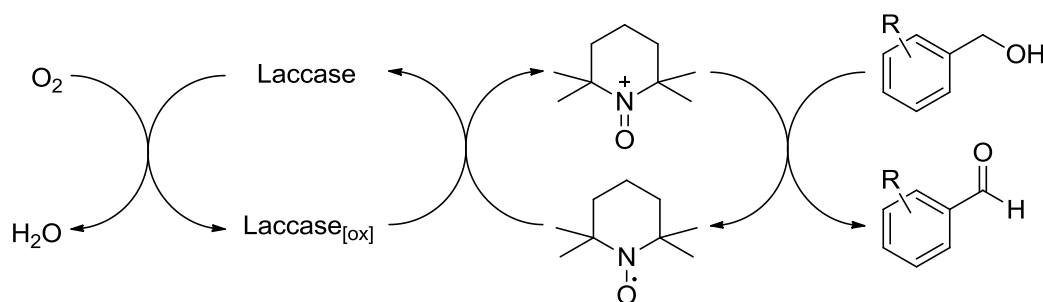


Figure 1.86: Oxidation of substituted benzaldehydes by TEMPO/Laccase with  $O_2$  as the terminal oxidant.

What Galli et al. developed is a superb example of taking an existing process and reducing its environmental impact by using water as a solvent, using catalytic TEMPO instead of stoichiometric oxoammonium and replacing a metal catalyst with a common, naturally occurring, enzymatic co-oxidant with molecular oxygen as the terminal oxidant.

It should be mentioned at this point that TEMPO is not the only nitroxide used for mild oxidations. For example 2-azaadamantane-*N*-oxyl and 1-methyl-2-azaadamantane-*N*-oxyl have been shown by Iwabuchi et al. to exceed the oxidative

capacity of TEMPO at low catalyst loadings.<sup>74</sup> In addition to this they oxidise secondary alcohols much more readily due to reduced steric hindrance around the nitroxide group.

### 1.8.5. TEMPO Mediated Polymerisation

Nitroxide mediated polymerisation (NMP) is a form of living radical polymerisation which uses a reversible deactivation step to help control molecular weight and molecular weight distribution. By adding a nitroxide like TEMPO the growing radical polymer chains are trapped by the oxygen-centred radical to form a deactivated chain which is in equilibrium with the free radical (Figure 1.87).

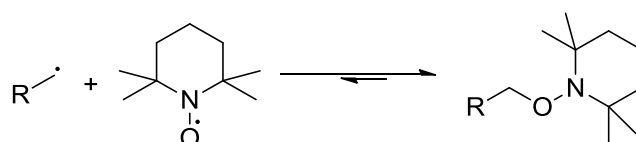


Figure 1.87: Trapping of carbon centred radicals by TEMPO.

This equilibrium favours the adduct which leaves only a small proportion of radical chains present in the reaction mixture. With such a low concentration of active chains the odds of two carbon centred radicals combining in a non-reversible termination is significantly reduced. This allows all of the polymer chains to grow at a similar rate without premature termination leading to a polymer with a low polydispersity. Living polymers like this continue to grow until no more monomer remains and will remain dormant until more monomer is introduced. This coupled with the low polydispersity allows for the controlled synthesis of block co-polymers (Figure 1.88).

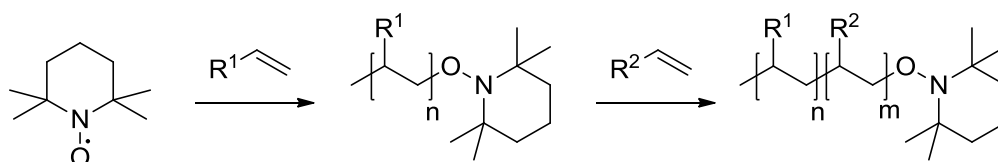


Figure 1.88: Formation of block copolymers by nitroxide mediated polymerisation.



### 1.8.6. Ionic Liquids

Ionic liquids have received a lot of attention recently due to their potential as environmentally benign solvents and they came under our scrutiny as a potential way of improving TEMPO based methodology.

An ionic liquid is usually defined as an ionic compound with a melting point below 100 °C. The class of ionic liquids most often used as solvents are room temperature ionic liquids which, as the name suggests are ionic compounds which are liquid at room temperature. Ionic liquids consist of a large, soft, often delocalised ion paired with a small, hard counterion. This mismatch of size and charge density leads to a poor interaction between the ions and results in an ionic compound with a low melting point (Figure 1.89).

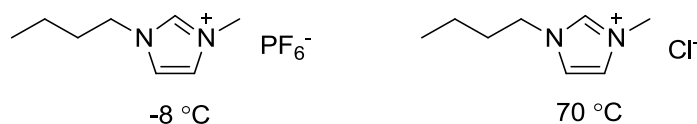


*Figure 1.89: Structures and melting points of ionic liquids [BMIM][PF<sub>6</sub>] and [BMIM][Cl].*

Ionic liquids have an incredibly low vapour pressure since the intermolecular interactions present are considerably stronger than in traditional organic solvents. This is a desirable characteristic for a reaction solvent since it reduces pollution due to volatile organic compounds and increases the ease with which the solvent can be reused. Low volatility also lowers the risk of accidental ignition making ionic liquids safer to use.

TEMPO mediated reactions are among the large variety of chemical processes which have been modified to work in ionic liquids. For example in 2002 Gree et al. performed TEMPO mediated aerobic oxidations of primary and secondary alcohols in the ionic liquid [BMIM][PF<sub>6</sub>] (Figure 1.90).<sup>87</sup>

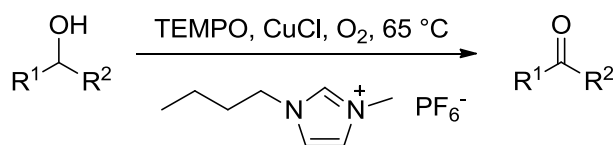


Figure 1.90: The oxidation of alcohols by TEMPO in [BMIM][PF<sub>6</sub>].

In 2007 TEMPO in [Bmpyrd][NTf<sub>2</sub>] was shown to mediate the oxidation of alcohols into aldehydes or ketones under electrochemical conditions (Figure 1.91).<sup>88</sup>

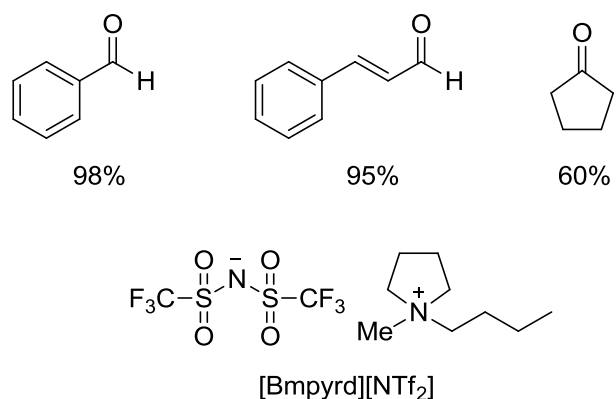


Figure 1.91: The structure of [Bmpyrd][NTf<sub>2</sub>] and the yields of aldehydes and ketones oxidised from the corresponding alcohols by TEMPO in [Bmpyrd][NTf<sub>2</sub>].

Although the desire to use a non-volatile, reusable solvent is an understandable one, there are some who question whether ionic liquids are as green as many claim. In 2005 Scammells, Scott and Singer published a review collating a number of concerns over the use of ionic liquids including issues with purification, toxicity and biodegradability which call into question the environmental impact of ionic liquids.<sup>89</sup>

## 1.9. Aims

The overall aim of this project is to further investigate the use of TEMPO in synthesis, in particular as a radical initiator. The following sections detail the results of this investigation, specifically describing the TEMPO initiated oxidation of acetals to esters, the TEMPO initiated addition of phosphorus sulfides to unsaturated C-C bonds, the synthesis of TEMPO ionic liquids and the TEMPO mediated chiral resolution of 1-phenylethanol. TEMPO was used in these projects in the hope of

creating new, milder and more environmentally friendly methodologies than those already in existence.

## **2. Acetal Oxidation**

## 2. Acetal Oxidation

### 2.1. Acetal Introduction

This chapter will examine some of the existing synthetic uses of acetals before continuing to discuss the novel TEMPO/Lewis acid mediated oxidation of acetals to form esters.

#### 2.1.1. Terminology

Acetals are a functional group consisting of an  $sp^3$  carbon with single bonds to two OR groups, where R is an alkyl or aryl group (Figure 2.1).

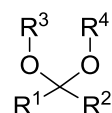


Figure 2.1: General structure of an acetal.

The term acetal is often used as a general term for any molecule of this type but technically acetals come in four distinct forms. Acetal refers to a species derived from an aldehyde where one of the groups on the acetal carbon is a hydrogen atom. Ketals are derived from ketones and contain two carbon based groups on the acetal carbon. When one of the OR groups is an OH it is referred to as a hemi-acetal or hemi-ketal (Figure 2.2). From this point on the term acetals will be used to describe only the aldehyde derived variant.

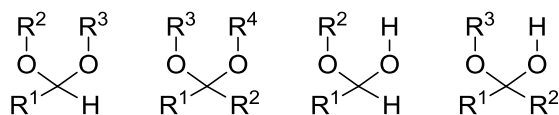


Figure 2.2: General structures (from left to right) of an acetal, a ketal, a hemi-acetal and a hemi-ketal.

Generally hemi-acetals are fairly unstable and readily revert to their parent aldehyde and alcohol under acidic or basic conditions as shown in Figure 2.3.

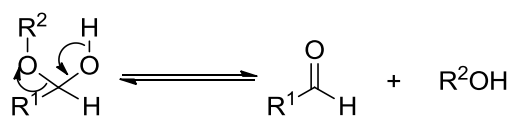


Figure 2.3: Decomposition of a hemi-acetal to an aldehyde and an alcohol.

Acetals are formed by the acid catalysed, reversible reaction between an aldehyde and an alcohol (Figure 2.4).

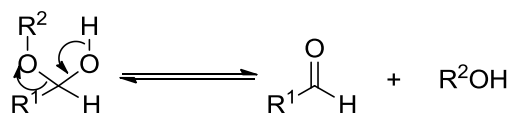


Figure 2.4: Acetal formation.

In order to obtain a high yield, the equilibrium needs to be drawn to the right. This is achieved by removing water from the reaction. This can be achieved by chemical means, or by molecular sieves, but perhaps the most common method is by azeotroping with a solvent like toluene using a Dean-Stark apparatus.

Acetals are commonly used as protecting groups for aldehydes, ketones or diols. In these cases it is often a 5 or 6 membered cyclic acetal (Figure 2.5).

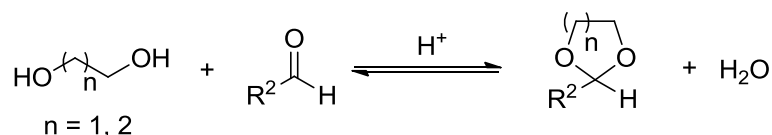


Figure 2.5: Formation of a cyclic acetal.

### 2.1.2. Acetals in Synthesis

Although commonly used as protecting groups, our interest lies in using acetals as synthetically useful intermediates or starting materials in their own right. The literature pertaining to acetals as reagents is mostly concerned with oxidation or reduction of acetals. For example Rerick et al. demonstrated that combining a Lewis acid with a strong reducing agent could be used to form hydroxy ethers from cyclic acetals (Figure 2.6).<sup>90</sup>

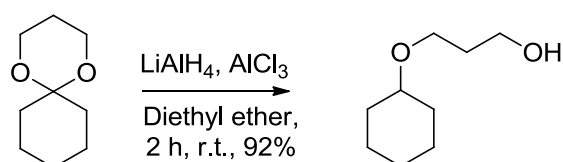


Figure 2.6: Reduction of a cyclic acetal.

In this reduction the Lewis acid coordinates to an oxygen atom, drawing electron density away from the acetal carbon and rendering it more susceptible to nucleophilic attack. The nucleophilic substitution could proceed via an  $S_N1$  or an  $S_N2$  process (Figure 2.7).

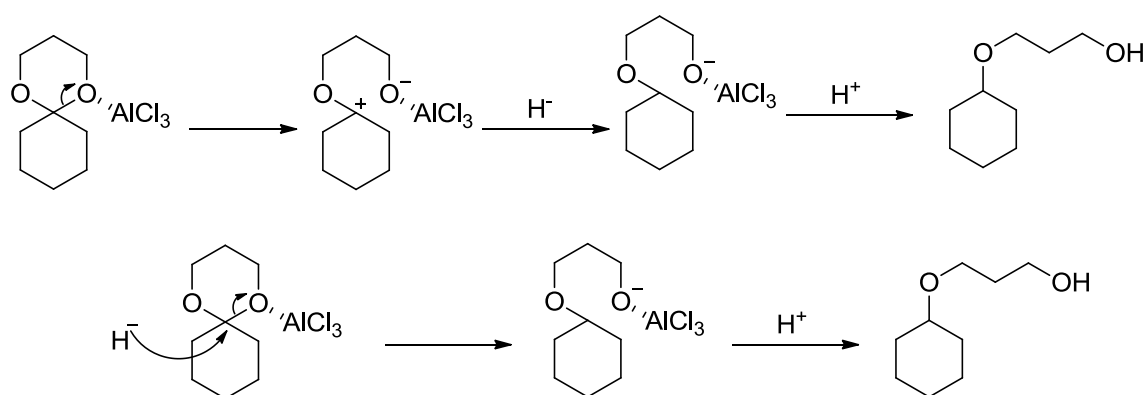


Figure 2.7: Reduction of acetals via  $S_N1$  and  $S_N2$  reactions.

Oxidation to esters is a more common use for cyclic acetals and a number of different reagents have been used for this transformation including ozone,<sup>91,92</sup> Co(II),<sup>93</sup> and  $V_2O_5/H_2O_2$ .<sup>94</sup> Common issues with these reactions include the use of toxic or environmentally hazardous metals and potentially explosive peroxides. Of the different reagents used for the oxidation of acetals two in particular are relevant to the work carried out in this research program, namely *N*-bromosuccinimide (NBS) and *N*-hydroxyphthalimide (NHPI).

In 1966 Prugh et al. used NBS initiated by AIBN to oxidise cyclic acetals into bromo esters (Figure 2.8).<sup>95</sup>

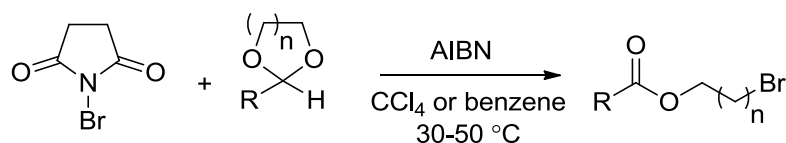


Figure 2.8: Oxidation of acetals by NBS.

In general, they found that phenyl acetals gave higher yields than alkyl acetals, presumably due to resonance stabilisation of radical intermediates. (Figure 2.9).<sup>95</sup>

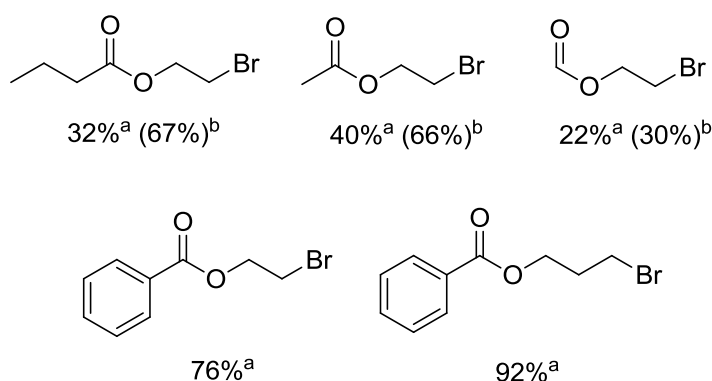


Figure 2.9: Products and yields of NBS mediated oxidation of acetals. <sup>a</sup>In  $\text{CCl}_4$ . <sup>b</sup>In benzene.

Although this is a fairly mild reaction with only a little heat needed to encourage the oxidation, NBS is not the best of reagents to work with. NBS itself is relatively harmless but it decomposes over time to generate  $\text{Br}_2$ , a toxic liquid. In addition, NBS will brominate allylic and benzylic positions under certain conditions (as discussed in section 1.2.3.) which limits its use in some circumstances.

In 2003 Karimi et al. used the transient nitroxide phthalimide-N-oxyl (PINO) (**37**) generated from *N*-hydroxyphthalimide (NHPI) (**38**) to oxidise various acetals into esters, a method which they improved upon in 2005 by replacing the cobalt acetate catalyst with cobalt hexanoate (Figure 2.10).<sup>17,96</sup>

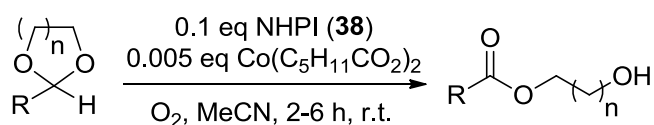


Figure 2.10: Oxidation of acetals by NHPI.



Their proposed mechanism involved hydrogen atom abstraction by the PINO nitroxide followed by trapping with molecular oxygen to form a peroxy radical which is oxidised by Co(III) to form the desired ester and an alcohol (Figure 2.11).

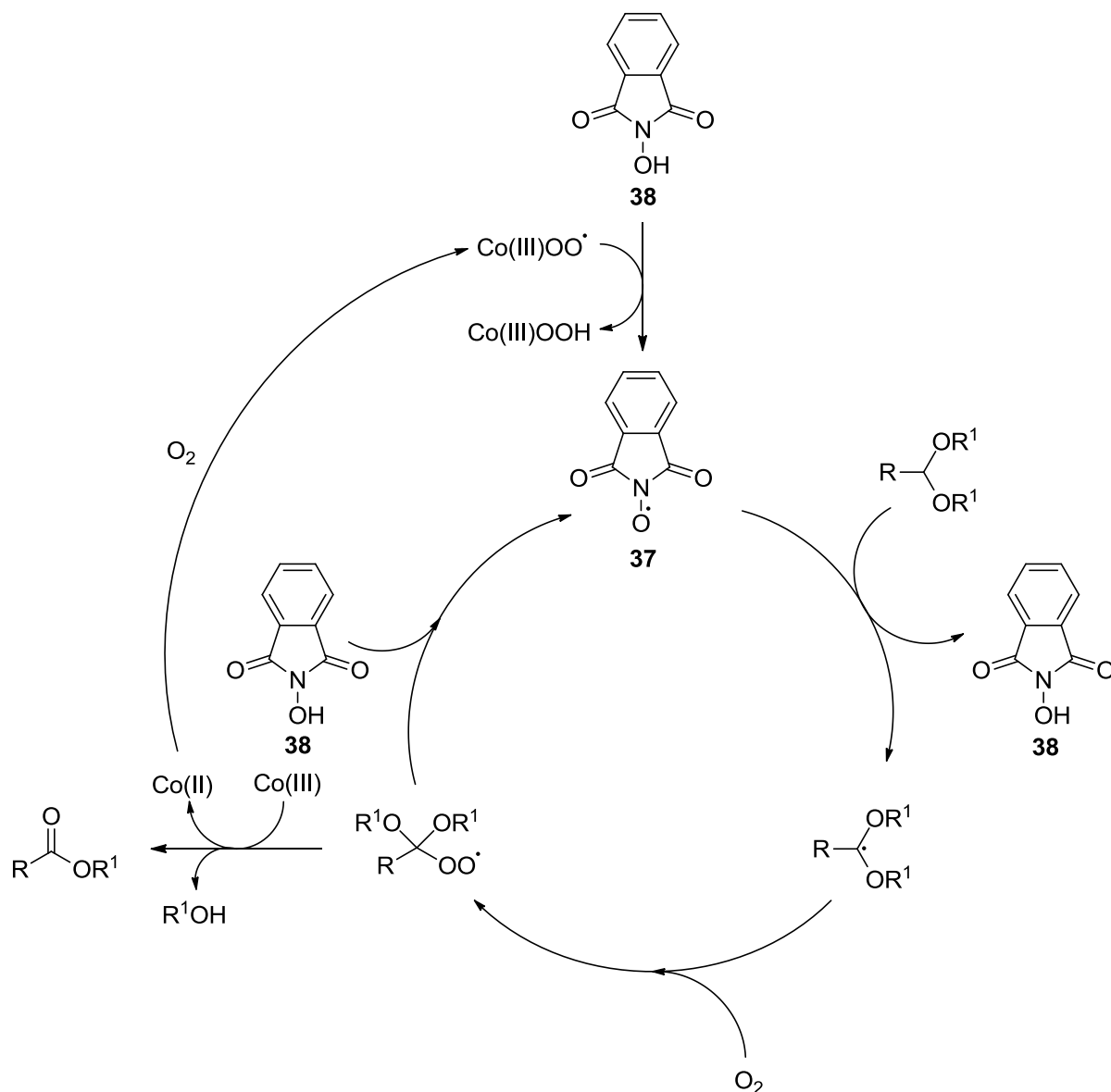


Figure 2.11: Mechanism of NHPI (**38**) mediated oxidation of acetals.

Overall they found that both 5- and 6-membered acetals were oxidised in high yields, but when R was a phenyl ring with a strong electron withdrawing NO<sub>2</sub> group, the reaction did not proceed. Aliphatic acetals also gave high yields of oxidised product but starting materials containing C=C bonds gave complex mixtures of unidentified products which were attributed to radical intermediates reacting with the double bonds (Figure 2.12).

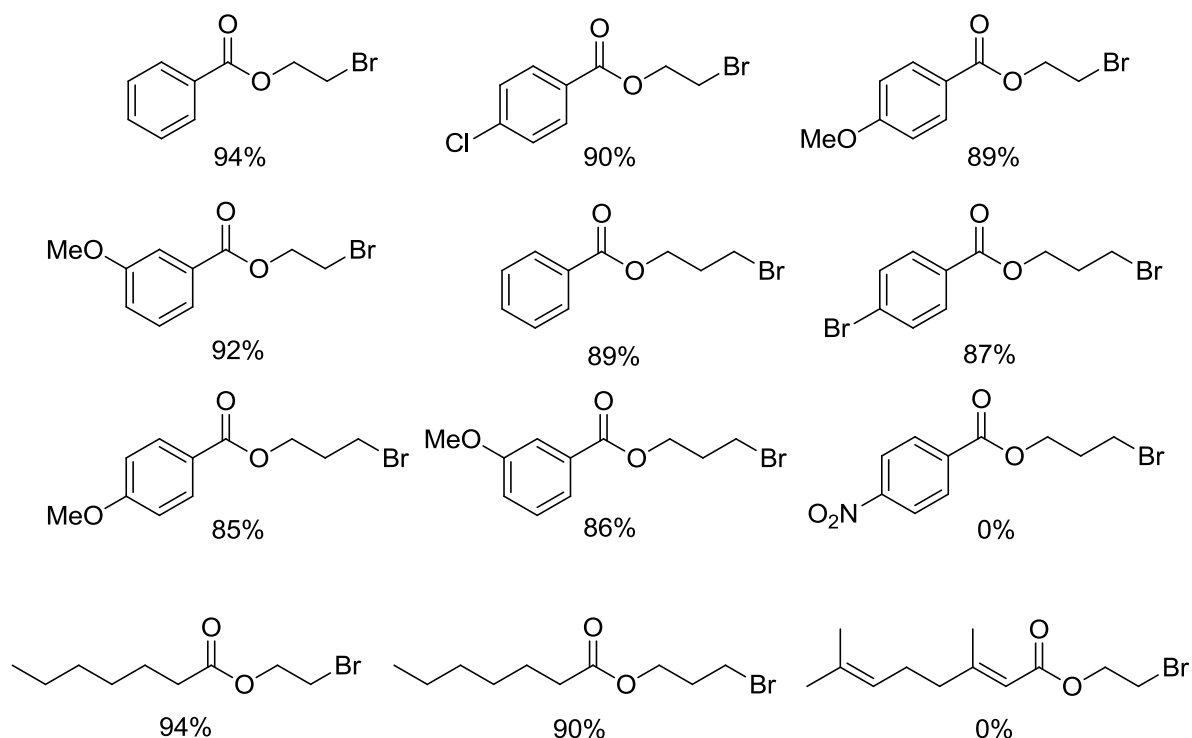


Figure 2.12: Products and yields of NHPI (**38**) mediated acetal oxidations.

Advantages of this method include short reaction times, ambient temperatures and fairly low catalyst loadings. The use of cobalt salts is problematic however due to their acute toxicity, long term health risks and environmental impact.

### 2.1.3. Esters

Esters are a very common functional group with a wide range of applications. Their most notable characteristic is probably their sweet smell making them ideal for use in perfumes, indeed many are naturally found in flowers.<sup>97</sup> In pharmaceuticals esters are sometimes used as prodrugs since they can be readily hydrolysed in the body to form the active drug, the classic example being aspirin acting as a masked form of salicylic acid (Figure 2.13).<sup>98</sup>

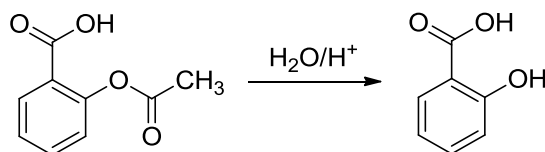


Figure 2.13: Hydrolysis of aspirin.

All in all esters are such a ubiquitous functional group that new synthetic pathways to their formation will always be useful.

#### 2.1.4. Aims

Investigations by Hayton et al. have shown that the TEMPO exhibits an increased ability to perform hydrogen atom abstractions in the presence of Lewis acids.<sup>99</sup> This was demonstrated by the oxidation of dihydroanthracene into anthracene in the presence of a TEMPO/ $\text{AlCl}_3$  complex at room temperature, (Figure 2.14)<sup>99</sup> a reaction which does not occur in the absence of Lewis acid.

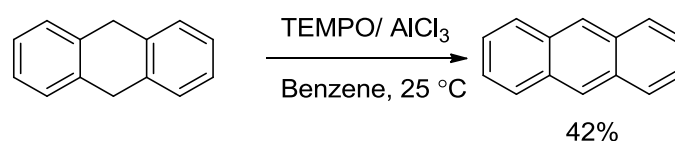


Figure 2.14: Oxidation of dihydroanthracene by TEMPO/ $\text{AlCl}_3$ .

The aim of our investigation was to use TEMPO/Lewis acid complexes to perform oxidations of acetals preferably under mild and non-hazardous conditions.

## 2.2. Preliminary Investigations

It was hoped that a combination of TEMPO and a suitable Lewis acid would be able to oxidise cyclic acetals into esters by hydrogen atom abstraction in a similar manner to PINO. It was quickly confirmed that this was indeed possible and that  $\text{AlCl}_3$  in conjunction with TEMPO was a sufficiently good oxidant to convert acetal **39** into benzoate ester **40** in 86% conversion as estimated from the crude  $^1\text{H}$  NMR spectrum (Figure 2.15). Attempts to oxidise **39** with TEMPO in the absence of a Lewis acid showed no evidence of reaction.

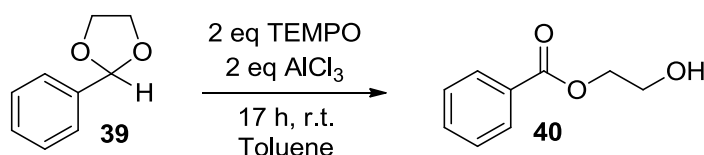


Figure 2.15: Oxidation of acetal **39** to benzoate ester **40** by TEMPO/ $\text{AlCl}_3$ .

### 2.2.1. Lewis Acid Screen

$\text{AlCl}_3$  was the Lewis acid first used to perform the oxidation of 2-phenyl-1,3-dioxolane (**39**) and it was thought that other Lewis acids could be used to perform similar oxidations as shown in Figure 2.16.

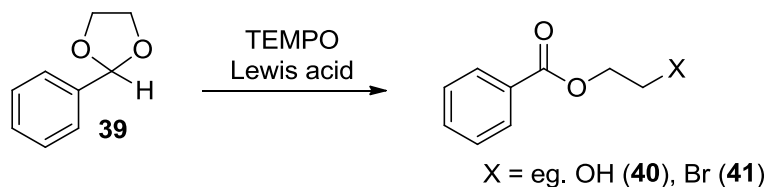


Figure 2.16: Oxidation of acetal **39** to benzoate esters.

It was hoped that different Lewis acids would lead to different products, higher yields or milder reactions and so a number of novel conditions were used to oxidise acetal **39**. Table 2.1 summarises the screen of Lewis acids. Yields were estimated by comparing relative integrations of the ester product, the starting acetal and the side product benzaldehyde in the  $^1\text{H}$  NMR spectra.

Table 2.1: Screen of Lewis acids for mediation of acetal oxidation in conjunction with TEMPO.

Entry	Lewis acid	Benzoate ester (%)	2-Phenyl-1,3-dioxolane ( <b>39</b> ) (%)	Benzaldehyde (%)
1	BF <sub>3</sub> •OEt <sub>2</sub>	91 ( <b>40</b> )	0	9
2	FeCl <sub>3</sub>	89 ( <b>40</b> )	4	7
3	AlCl <sub>3</sub>	86 ( <b>40</b> )	6	7
4	Cu(OTf) <sub>2</sub>	86 ( <b>40</b> )	3	10
5	MgBr <sub>2</sub>	67 ( <b>41</b> )	33	0
6	In(OTf) <sub>3</sub>	64	8	28
7	ZnBr <sub>2</sub>	9	88	4
8	CuCl <sub>2</sub>	8	89	4
9	CuBr <sub>2</sub>	7	93	0
10	ZnCl <sub>2</sub>	4	96	0
11	MgCl <sub>2</sub>	4	96	0
12	Ti(O <sup>i</sup> Pr) <sub>4</sub>	0	96	4
13	SnCl <sub>2</sub> •2H <sub>2</sub> O	0	57	43

Conditions: 2-phenyl-1,3-dioxolane (1 eq), Lewis acid (2 eq), TEMPO (2 eq) in toluene, under argon for 17 h. Yields estimated by comparison of relative integrations of products in the <sup>1</sup>H NMR spectra.

Some Lewis acids (Table 2.1, Entries 1-4) were found to produce hydroxy benzoate esters (**40**) where X = OH. MgBr<sub>2</sub> (Table 2.1, Entry 5) on the other hand was found to produce the bromo ester (**41**) where X = Br as determined by mass spectrometry.

The remaining Lewis acids (Table 2.2, Entries 6-13) produced benzoate esters as determined by  $^1\text{H}$  NMR but determination of the substituent X was not achieved.

It was found that a number of Lewis acids, as well as producing the benzoate esters, gave high levels of benzaldehyde as a side product. This is almost certainly due to unreacted acetal being hydrolysed on aqueous work-up catalysed by Brønsted-Lowry acids formed from the Lewis acids (Figure 2.17) or the Lewis acids themselves.

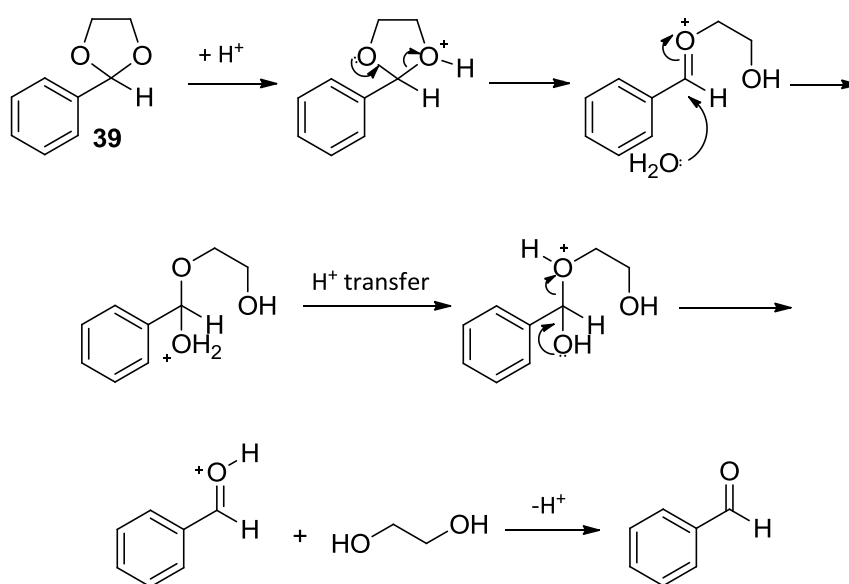


Figure 2.17: Acid-catalysed hydrolysis of acetal **39**.

The most active catalysts, namely  $\text{BF}_3 \cdot \text{OEt}_2$ ,  $\text{FeCl}_3$ ,  $\text{AlCl}_3$  and  $\text{Cu}(\text{OTf})_2$  (Table 2.1, Entries 1-4), are particularly notable as virtually all of the remaining acetal **39** was converted into benzaldehyde.  $\text{SnCl}_2 \cdot 2\text{H}_2\text{O}$  produced the highest levels of benzaldehyde despite not appearing to catalyse the desired reaction at all (Table 2.1, Entry 13). This can be attributed to the water associated with the Lewis acid hydrolysing the acetal throughout the reaction as well as during the work up.<sup>100</sup>

$\text{MgBr}_2$  is worthy of attention at this point as an example of a Lewis acid which oxidises acetal **39** in moderate yield, but gives no sign of hydrolysed starting material (Table 2.1, Entry 5). Although it appears to be less reactive than some of the stronger Lewis acids it is considerably less hazardous and less hygroscopic making it easier and safer to handle. In addition to this, the absence of

benzaldehyde indicates that  $\text{MgBr}_2$  does not hydrolyse acetal **39**, even on aqueous work-up, making it ideal for situations where the starting material is precious and needs to be recovered or where rigorously anhydrous conditions cannot be guaranteed.

Interestingly  $\text{MgCl}_2$  showed almost no activity at all. It seems reasonable to assume that  $\text{MgCl}_2$  would act in a similar way to  $\text{MgBr}_2$ , however this appears not to be the case. It is possible that since the  $\text{MgCl}_2$  was not fresh, that on standing it had become at least partially hydrated which would diminish its Lewis acidity.

Of the four most active Lewis acids ( $\text{BF}_3 \cdot \text{OEt}_2$ ,  $\text{FeCl}_3$ ,  $\text{AlCl}_3$  and  $\text{Cu}(\text{OTf})_2$ )  $\text{BF}_3 \cdot \text{OEt}_2$  was initially chosen as the catalyst to be used for further studies. As a liquid it is considerably easier to transfer without absorption of water than the hygroscopic metal salts and it was hoped this would lead to more consistent results. In addition, metal free reactions make a more attractive proposition for large scale and industrial reactions due to the comparative ease of dealing with non-metallic waste.

### **2.2.2. Mechanism**

Figure 2.18 represents our initially proposed mechanism for the TEMPO/Lewis acid mediated oxidation of acetal **39** by  $\text{BF}_3 \cdot \text{OEt}_2$ .

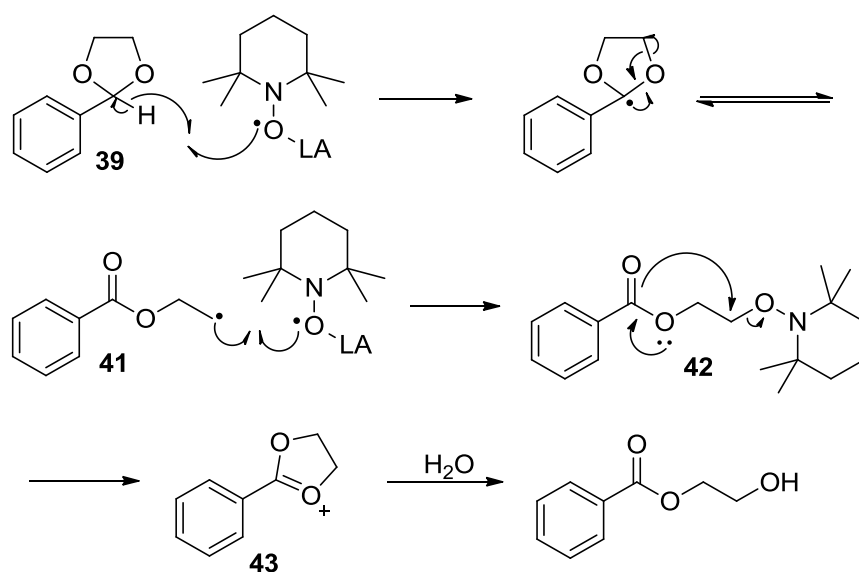


Figure 2.18: Initially proposed mechanism for the TEMPO/LA mediated oxidation of acetal **39**.

First the acetal hydrogen is abstracted by the TEMPO/Lewis acid complex. The ring then fragments, reversibly, to form the primary radical **41** which could be readily trapped by TEMPO. TEMPO adducts such as **42** are very stable and normally require zinc and acetic acid to cleave the N-O bond,<sup>101-103</sup> therefore it was envisioned that for water to displace it by nucleophilic substitution it would require the formation of the resonance stabilised cation **43** to create a more reactive electrophile. This process is known as anchimeric assistance or neighbouring group participation where a substitution reaction is aided by an intramolecular reaction.<sup>104,105</sup>

### 2.2.3. EPR Studies

Electron paramagnetic resonance (EPR) was used to try to observe complexation between TEMPO and the Lewis acids and potentially determine the fate of the TEMPO radical throughout the course of a reaction.

Electron paramagnetic resonance (EPR), also known as electron spin resonance, observes spin transitions of an unpaired electron in a magnetic field. It is an analogous technique to NMR which studies nuclear spin transitions in a magnetic field. EPR relies on the fact that electrons have a magnetic moment and a spin quantum number  $S = \frac{1}{2}$ . The spin has magnetic spin quantum numbers  $m_s = +\frac{1}{2}$  and



$m_s = -\frac{1}{2}$  which under normal conditions are degenerate. When subjected to a magnetic field the magnetic moment can align itself with or against the external field causing the magnetic components of the spin to no longer exist at the same energy (Figure 2.19).

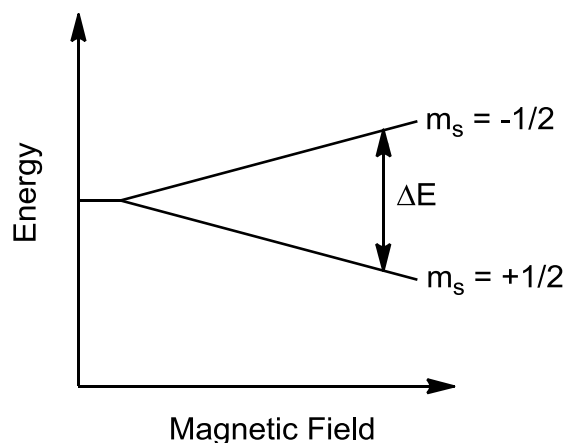


*Figure 2.19: Non-degeneracy of the magnetic spin components of paramagnetic compound in a magnetic field.*

An unpaired electron can switch between energy levels by either emitting or absorbing a photon where  $h\nu = \Delta E$ . The frequency used is ca. 9 GHz which is in the microwave region. At this frequency, spin transitions are observed at around 0.35 T. In an EPR spectrometer a sample is exposed to microwave radiation at a fixed frequency while the magnetic field is swept. When the magnetic field reaches the appropriate strength for the energy gap between spin states to match the energy of the photons, the unpaired electrons change between the two states. Since the lower energy state is more densely populated, more photons are absorbed than emitted and this absorption is detected and gives rise to a signal on a spectrum.

An EPR spectrum of TEMPO ( $1 \times 10^{-5} \text{ mol dm}^{-3}$ ) and  $\text{BF}_3 \cdot \text{OEt}_2$  ( $1 \times 10^{-5} \text{ mol dm}^{-3}$ ) in toluene was recorded. The observed signal was identical to that of TEMPO in solution indicating that no complex was being formed. The concentrations of TEMPO and Lewis acid in the reaction conditions are considerably higher ( $0.13 \text{ mol dm}^{-3}$ ) than those that are optimal for EPR spectroscopy. These higher concentrations would favour complexation but lead to loss of the hyperfine in the EPR spectrum and limit the information that could be gathered. In order to recreate

these conditions without affecting the EPR spectrum, the concentration of  $\text{BF}_3 \cdot \text{OEt}_2$  was raised to that of the standard reaction conditions ( $0.13 \text{ mol dm}^{-3}$ ) whilst the quantity of TEMPO remained at  $1 \times 10^{-5} \text{ mol dm}^{-3}$ . Under these conditions the TEMPO signal remained unchanged except for a decrease in intensity which suggests that the TEMPO radical was somehow being destroyed. The most likely reason for this is disproportionation of the TEMPO radical initiated by small quantities of Brønsted acids present in the Lewis acid.

In order to see if disproportionation of TEMPO was taking place under the reaction conditions two experiments were run; one with the standard oxidation conditions (1 eq acetal **39**, 2 eq  $\text{BF}_3 \cdot \text{OEt}_2$ , 2 eq TEMPO in toluene at r.t. for 17 h) and one without any acetal. After 17 h and before quenching with water a sample was taken from each and submitted for EPR spectroscopy. Both samples gave signals which integrated to ca. 1/8 of the signal of the starting concentration of TEMPO suggesting that the TEMPO is consumed by the Lewis acid even in the absence of the acetal **39** (Figure 2.20).

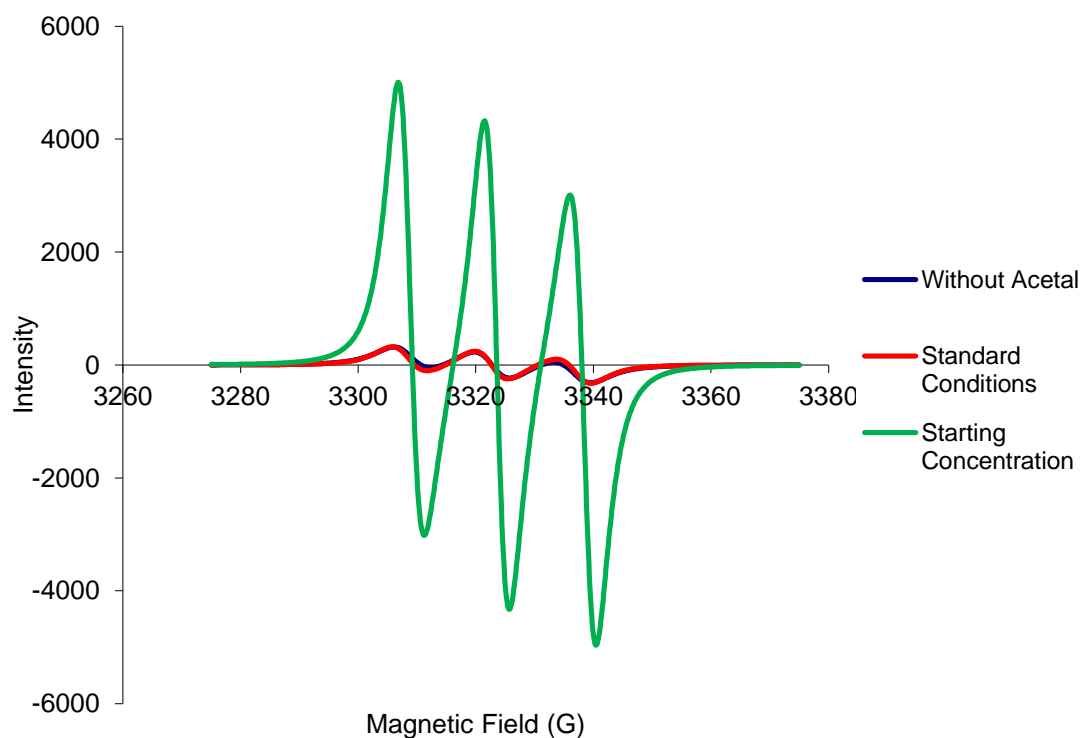


Figure 2.20: EPR spectra of TEMPO with and without exposure to  $\text{BF}_3 \cdot \text{OEt}_2$ .

Although these results look compelling the TEMPO/BF<sub>3</sub>•OEt<sub>2</sub> mixture does not appear to fully dissolve so the heterogeneous nature of these reactions makes taking representative samples from them a difficult task and as a result this data should be treated with caution.

Overall the EPR experiments seem to show that there is little or no complexation occurring between TEMPO and BF<sub>3</sub>•OEt<sub>2</sub> and that TEMPO is decaying in the presence of BF<sub>3</sub>•OEt<sub>2</sub>.

#### **2.2.4. TEMPO and Magnesium Bromide**

Having determined that BF<sub>3</sub>•OEt<sub>2</sub> is a good catalyst, studies were undertaken to optimise the reaction conditions. It quickly became apparent that oxidation of acetal **39** occurred even in the absence of TEMPO, but with lower conversion (49%). It was initially assumed that this was largely due to autoxidation by O<sub>2</sub> on work-up but the yield detected was higher than we expected for this kind of process. As a result of this, the method of estimating the yields was revisited.

To begin with it, was assumed that all of the acetal remained unreacted or was converted into benzoate ester **40** or benzaldehyde and ethane-1,2-diol. The yield of benzoate ester **40** was then estimated from the <sup>1</sup>H NMR spectrum of the crude product by comparing the relative intensities of peaks corresponding to these products. When benzaldehyde and BF<sub>3</sub>•OEt<sub>2</sub> were stirred in EtOAc and H<sub>2</sub>O for 30 min as a recreation of the work-up conditions it was found that between 41% and 76% of benzaldehyde was lost. It was thought that in the presence of Lewis and/or Brønsted acids, benzaldehyde was being oxidised by O<sub>2</sub> to form benzoic acid, which then was removed by aqueous washes. Whatever the reason, it is clear that the yields discussed previously are likely to be overestimates due to disproportionately low quantities of benzaldehyde that are isolated.

Larger scale reactions (5 times larger than previous reactions) were carried out in order to determine the isolated yields of these oxidations, which were compared to the estimated NMR conversions and NMR yields using dry DMF as an internal standard (Table 2.2).<sup>106</sup>

Table 2.2: Comparing methods of determining yields using TEMPO/BF<sub>3</sub>•OEt<sub>2</sub> mediated oxidation of acetal **39**.

Entry	NMR Conversion of <b>40</b> (%) (Estimate)	NMR Yield of <b>40</b> (%) (DMF Internal Standard)	Yield of <b>40</b> (%) (Isolated)
1	44	-	28
2	41	10	12

Conditions: 2-phenyl-1,3-dioxolane (1 eq), BF<sub>3</sub>•OEt<sub>2</sub> (2 eq), TEMPO (2 eq) in toluene, under argon for 17 h.

Table 2.2 shows that the method of estimating the conversion by NMR spectroscopy does not represent the actual yield of the reaction, although NMR spectroscopy with an internal standard does appear to give an acceptable approximation of the actual yield. As expected, the actual yields are lower than the original estimates suggested. It was also unclear at this point how much of the oxidation of acetal **39** was as a result of oxidation by TEMPO and how much was due to autoxidation by O<sub>2</sub> during the work-up. Table 2.2 also demonstrates a significant degree of variability in the product yields.

In order to study a system without the complications associated with BF<sub>3</sub>•OEt<sub>2</sub>, we returned to the original Lewis acid screen to find an alternative and noted that MgBr<sub>2</sub> and TEMPO mediated the oxidation of acetal **39** into bromoethyl benzoate **41** (Figure 2.21) with a reasonable conversion (67%) without hydrolysing the acetal to benzaldehyde (Table 2.1, Entry 5).

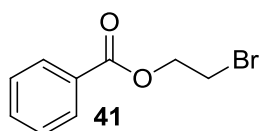


Figure 2.21: Structure of 2-bromoethyl benzoate (**41**).

Since there is no benzaldehyde to alter the figures, the original conversion as estimated by  $^1\text{H}$  NMR spectroscopy is likely to be much more accurate.

*Table 2.3: Comparison of large and small scale TEMPO/MgBr<sub>2</sub> mediated oxidations of acetal **39** to form 2-bromoethylbenzoate (**41**).*

Entry	Scale (mmol)	NMR Yield of <b>41</b> (%) (DMF Internal Standard)	Yield of <b>41</b> (%) (Isolated)
1	0.32	59	-
2	1.5	42	37

*Conditions: 2-phenyl-1,3-dioxolane (1 eq), MgBr<sub>2</sub> (2 eq), TEMPO (2 eq) in toluene, under argon for 17 h.*

Table 2.3 shows that on a small scale the conversion of acetal **39** into benzoate ester **41** proceeds in a reasonable yield. The larger scale reaction gives a lower yield but reaffirms the accuracy of NMR with an internal standard in determining the product yield.

The TEMPO/MgBr<sub>2</sub> system is a much milder one than TEMPO/BF<sub>3</sub>•OEt<sub>2</sub> and suffers none of the autoxidation reactions on work up. In addition to this, the Br functional group is more suitable for substitution reactions than the OH group, making benzoate ester **41** arguably more synthetically useful than benzoate ester **40**. The bromo ester motif occurs regularly in organic chemistry for example in anti-cancer agents<sup>107</sup> and as an intermediate in the synthesis of biologically active molecules,<sup>108–110</sup> The same motif can be synthesised by direct esterification with the toxic and corrosive 2-bromoethanol but this requires high temperatures to achieve or the use of coupling agents such as *N,N'*-dicyclohexylcarbodiimide which is an allergen and sensitizer, making the TEMPO/MgBr<sub>2</sub> system a mild and safe alternative. For these reasons it was decided to further investigate the oxidation of acetals using TEMPO/MgBr<sub>2</sub>.

### 2.3. Acetal Optimisation

Having established that TEMPO and  $\text{MgBr}_2$  were capable of oxidising acetal **39** into benzoate ester **41**, studies were carried out to optimise the reaction conditions. Reactions were performed using acetal **39** which was prepared by refluxing benzaldehyde and ethane-1,2-diol under Dean-Stark conditions in toluene with catalytic pTSA (Figure 2.22).

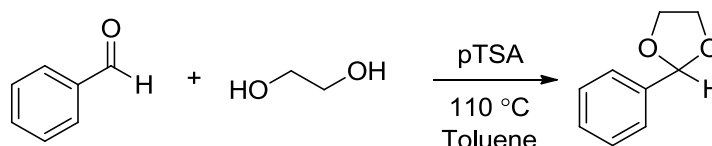


Figure 2.22: Synthesis of acetal **39**.

It was found that the shelf-life of acetal **39** was relatively short and it readily hydrolysed back to benzaldehyde and ethane-1,2-diol on standing at room temperature in a sealed flask. This led to unreliable results where reactions repeated weeks apart from each other had significantly different product yields. In order to account for the variable purity of the starting material the optimisation reactions were performed in batches, each with a standard performed under the conditions described in Figure 2.23 to ensure that each set of reactions could be directly compared within themselves and with the initial conditions.

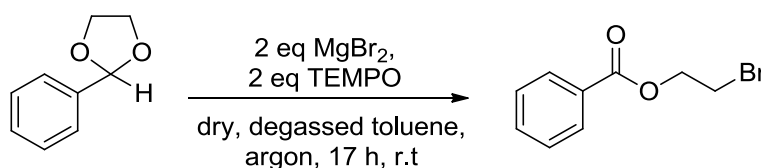


Figure 2.23: Initial conditions for the oxidation of acetal **39** into bromo ester **41**.

Another factor to be considered when comparing the product yields of these reactions is the nature of the Lewis acid. Irregularly sized particles would result in different surface areas changing the rate of reaction.  $\text{MgBr}_2$  is also hygroscopic, absorbing moisture from the air to form magnesium bromide hexahydrate, which will not be as Lewis acidic as the anhydrous salt. As a result of these characteristics a certain level of variability in the yields should be expected.

### 2.3.1. Oxoammonium as a Possible Oxidant

Since nitroxides undergo disproportionation in the presence of Brønsted-Lowry acids to form an oxoammonium and a hydroxylamine, and since TEMPO oxoammonium is known to perform oxidations, it was considered that oxoammonium **35** could be responsible for the observed acetal oxidation. Although we found nothing in the literature to suggest that disproportionation of TEMPO occurs in the presence of Lewis acids it was considered prudent to rule out the possibility of oxoammonium **35** performing a two-electron oxidation of the acetals. Table 2.4 shows the effects of replacing TEMPO with oxoammonium **35**, with and without MgBr<sub>2</sub>.

*Table 2.4: Comparing TEMPO and TEMPO oxoammonium chloride as mediators of acetal oxidation.*

Entry	Oxidising Agent	Eq MgBr <sub>2</sub>	Yield of <b>41</b> (%)
1	TEMPO	2	50
2	Oxoammonium chloride	2	22
3	Oxoammonium chloride	0	0

*Conditions: 2-phenyl-1,3-dioxolane (1 eq), MgBr<sub>2</sub> (2 eq), TEMPO or TEMPO oxoammonium chloride (2 eq) in toluene, under argon for 17 h. Yields were calculated by <sup>1</sup>H NMR spectroscopy in CDCl<sub>3</sub> with dry DMF as an internal standard.*

Oxoammonium chloride in the presence of MgBr<sub>2</sub> oxidised acetal **39** into benzoate ester **41** in a relatively low yield (Table 2.4, Entry 2). In the absence of MgBr<sub>2</sub> however, no reaction occurred and only acetal **39** was observed (Table 2.4, Entry 3). From this it was concluded that oxoammonium **35** was not responsible for the observed oxidation and the small quantity of benzoate ester **41** produced in the presence of MgBr<sub>2</sub> was due to TEMPO formed by the decomposition of the oxoammonium chloride during storage.

### 2.3.2. Solvent

Toluene was used as the solvent in most of the optimisation reactions as this was the solvent used in the original work by Hayton describing TEMPO/Lewis acid complexes.<sup>99</sup> It was hoped that alternative solvents could be used to increase the solubility of the MgBr<sub>2</sub>, or any complexes it may form with TEMPO, or the acetal, and hence increase the yield of **41** (Table 2.5).

Table 2.5: Comparison of different solvents in the oxidation of acetal **39**.

Entry	Solvent	Yield of <b>41</b> (%)
1	Toluene	50
2	DCM	45
3	Diethyl ether	33
4	THF	5
5	Acetonitrile	4
6	Hexane	4

*Conditions: 2-phenyl-1,3-dioxolane (1 eq), MgBr<sub>2</sub> (2 eq), TEMPO (2 eq) under argon for 17 h. Yields were calculated by <sup>1</sup>H NMR spectroscopy in CDCl<sub>3</sub> with dry DMF as an internal standard.*

THF and acetonitrile, as strongly coordinating solvents, proved to be highly unsuitable for this reaction, since even if they do improve solubility this effect is outweighed by their coordination to, and deactivation of, the Lewis acid. Diethyl ether is less coordinating and therefore returned a higher yield of **41**, but it still inhibits the reactivity of MgBr<sub>2</sub> and detrimentally affects the product yield. The use of hexane as a solvent also gave a very poor yield. DCM was the only solvent found to be nearly as effective as toluene and it was the solvent used for investigating the scope of the oxidation due to ease of solvent removal on work-up after reaction completion.



### 2.3.3. Reaction Stoichiometry

To begin with, it was assumed that a TEMPO/MgBr<sub>2</sub> complex mediated the oxidation of **39** to form **41**. As a one-electron oxidant, two equivalents of TEMPO are needed and two equivalents of MgBr<sub>2</sub> were used to maintain a 1:1 ratio of oxidant to Lewis acid. This combination of reagents gave moderate yields of product **41**, but it was hoped that these could be improved upon by changing the relative quantities of the reagents with respect to acetal **39** or that the atom efficiency could be increased.

Table 2.6: Comparing yield of **41** to increase in TEMPO and MgBr<sub>2</sub>.

Entry	Eq TEMPO	Eq MgBr <sub>2</sub>	Yield of <b>41</b> (%)
1	1	1	25
2	2	2	59
3	3	3	74

Conditions: 2-phenyl-1,3-dioxolane (1 eq), MgBr<sub>2</sub>, TEMPO in toluene under argon for 17 h. Yields were calculated by <sup>1</sup>H NMR spectroscopy in CDCl<sub>3</sub> with dry DMF as an internal standard.

Table 2.6 clearly shows that increasing the equivalents of TEMPO and MgBr<sub>2</sub>, while maintaining a 1:1 ratio, increases the yield of benzoate ester **41**. However, in order to maximise both product yield and atom efficiency, further tests were carried out to determine which of the reagents was responsible for the increased yield.

Table 2.7: Comparing yield of ester **41** to increase in TEMPO.

Entry	Eq TEMPO	Eq MgBr <sub>2</sub>	Yield of <b>43</b> (%)
1	1	2	46
2	2	2	59
3	3	2	50

Conditions: 2-phenyl-1,3-dioxolane (1 eq), MgBr<sub>2</sub>, TEMPO in toluene under argon for 17 h. Yields were calculated by <sup>1</sup>H NMR spectroscopy in CDCl<sub>3</sub> with dry DMF as an internal standard.

In Table 2.7 the quantity of MgBr<sub>2</sub> was kept constant while TEMPO was increased from 1 eq to 3 eq. As expected 2 eq of TEMPO proved to be more effective than one due to the need for two 1-electron oxidations to occur. However, it transpired that increasing the equivalents of TEMPO from 2 to 3 had a slight negative effect on the yield of **41**. This could be explained by considering TEMPO's common usage as a spin trap. It is possible that TEMPO may be trapping radical intermediates formed in the reaction, hence lowering the yield. It is interesting to note that when 3 eq of TEMPO is matched by 3 eq of MgBr<sub>2</sub> (Table 2.6, Entry 4) the yield is considerably higher. Perhaps then the quantity of MgBr<sub>2</sub> is the key to obtaining higher yields.

Given that 2 eq of TEMPO seems to be ideal and the amount of Lewis acid is clearly a key parameter, the number of equivalents of MgBr<sub>2</sub> were varied to determine the optimal quantity (Table 2.8). It is worth noting at this point that since this is a heterogeneous reaction, the equivalents of MgBr<sub>2</sub> do not relate exactly to the stoichiometry but have been used here as a measure of the quantity of MgBr<sub>2</sub>.

Table 2.8: Comparing yield of ester **41** to increase in MgBr<sub>2</sub>.

Entry	Eq TEMPO	Eq MgBr <sub>2</sub>	Yield of <b>41</b> (%)
1	2	1	37
2	2	2	59
3	2	3	72
4	2	4	76 <sup>a</sup>
5	2	8	82 <sup>a</sup>

Conditions: 2-phenyl-1,3-dioxolane (1 eq), MgBr<sub>2</sub>, TEMPO in toluene under argon for 17 h. <sup>a</sup>DCM was used as solvent. Yields were calculated by <sup>1</sup>H NMR spectroscopy in CDCl<sub>3</sub> with dry DMF as an internal standard.

Keeping the equivalents of TEMPO at 2 and increasing the equivalents of MgBr<sub>2</sub> from 1 to 8 had the effect of more than doubling the yield of **41** as seen in Table 2.8. Despite 8 eq of MgBr<sub>2</sub> giving the highest yield, 4 eq were chosen as the standard for the rest of the project for the sake of atom efficiency. The need for such large quantities of Lewis acid is most likely due to the lack of solubility of any MgBr<sub>2</sub> complexes in organic solvents and/or the low surface area of MgBr<sub>2</sub>. Increasing the surface area of the solid reagent by grinding or sonication could potentially mitigate this.<sup>111,112</sup>

#### 2.3.4. Time

Initial reactions were stirred for 17 h but shorter reaction times would make this methodology a more attractive proposition to industry or academia. In an attempt to determine the optimal reaction time, oxidations of differing lengths were carried out (Table 2.9).

Table 2.9: Effect of reaction time on yield of ester **41**.

Entry	Time (h)	Yield of <b>41</b> (%)
1	4	21
2	8	48
3	17	59
4	24	53

Conditions: 2-phenyl-1,3-dioxolane (1 eq), MgBr<sub>2</sub> (2 eq), TEMPO (2 eq) in toluene under argon. Yields were calculated by <sup>1</sup>H NMR spectroscopy in CDCl<sub>3</sub> with dry DMF as an internal standard.

Reactions performed at different times show the yield of **41** increasing up to a reaction time of 17 h (Table 2.9, Entries 1, 2 and 3). Reactions stirred for 24 h showed no improvement in yield. This could be down to one of the starting materials being fully consumed by the 17 h mark and/or the surface of the MgBr<sub>2</sub> becoming contaminated and deactivated.

### 2.3.5. Oxygen and Water

To begin with, reactions were performed under an inert atmosphere in dry, degassed solvent. It was thought that excluding water from the reaction would prevent MgBr<sub>2</sub> hydrates from forming, which would reduce its efficiency as a reagent. Acetals are also prone to hydrolysis to form aldehydes and diols, particularly in the presence of Brønsted-Lowry or Lewis acids.<sup>113–116</sup> Oxygen, as a di-radical, is often a problem for radical reactions due its ability to trap intermediates with unpaired electrons, particularly carbon-centred radicals and so this was also excluded.<sup>117</sup> Experiments were carried out to test how robust the acetal oxidation was and whether dry conditions and an inert atmosphere were necessary (Table 2.10).

Table 2.10: Effect of water and oxygen on yield of ester **41**.

Entry	Atmosphere	Solvent	Yield of <b>41</b> (%)
1	Argon	Dry, degassed (argon)	50
2	Air	Dry	48
3	Oxygen	Dry, degassed (O <sub>2</sub> )	57
4	Argon	Non-dry, degassed (argon)	57

Conditions: 2-phenyl-1,3-dioxolane (1 eq), MgBr<sub>2</sub> (2 eq), TEMPO (2 eq) in toluene under argon for 17 h. Yields were calculated by <sup>1</sup>H NMR spectroscopy in CDCl<sub>3</sub> with dry DMF as an internal standard.

Changing from reactions performed under inert atmospheres to those under air and oxygen (Table 2.10, Entries 1, 2 and 3) did not have the anticipated effect of reducing the yield of benzoate ester **41** (due to trapping of intermediates by O<sub>2</sub>). In fact, if anything, the yield of **41** increases slightly. A similar effect is observed when changing from dry solvent to non-dry solvent (Table G, Entries 1 and 4). The expected inhibition of the Lewis acid reagent did not happen and the yield of **41** appears to even increase a little. There isn't an obvious reason why the addition of water or oxygen should increase the observed yield, but it is clear that rigorously dry and anaerobic conditions are not required for these reactions.

### 2.3.6. Temperature

An obvious method for increasing the yield of **41** further would be to increase the temperature of the reaction. Hence a reaction at an elevated temperature was compared to a reaction at room temperature (Table 2.11).

Table 2.11: Effect of temperature of yield of ester **41**.

Entry	Temperature	Yield of <b>41</b> (%)
1	r.t.	39
2	50 °C	49

*Conditions: 2-phenyl-1,3-dioxolane (1 eq), MgBr<sub>2</sub> (2 eq), TEMPO (2 eq) in toluene under argon for 17 h. Yields were calculated by <sup>1</sup>H NMR spectroscopy in CDCl<sub>3</sub> with dry DMF as an internal standard.*

Table 2.11 shows that increasing the temperature from r.t. to 50 °C had the effect of increasing the yield of **41**, but only slightly. The increased temperature would increase the rate of collisions within the reaction and provide the reagents with more energy, which would increase the reaction rate and hopefully impact positively on the yield. However at the same time the increased energy in the system would also result in the breaking the dative bond between the reagents and the Lewis acid. This would decrease the activity of the reagents and potentially decrease the yield.

An often quoted rule of thumb is that in simple systems a 10 °C increase in temperature corresponds to a doubling of the rate. This is not always the case however and the chance of that increase in rate corresponding to an increased yield is even less reliable. As was seen with the optimisation of reaction time the yield seemed to be limited to a certain point regardless of extra time so even if the elevated temperature increased the reaction rate it might not be observed in the yield. In order to determine if an elevated temperature is truly beneficial, further kinetic studies would be required.

All things considered, the increase in yield of **41** was not considered substantial enough to warrant the increase in energy consumption and subsequent reactions were carried out at room temperature.

### 2.3.7. Scale

For a reaction to be a viable in a synthetic route it should be capable of being scaled up. In order to see how well the reaction coped with increased scale the oxidation of acetal **39** was scaled up five times and compared to the standard scale reaction.

Table 2.12: Effect of scale on the yield of ester **41**.

Entry	Scale (mmol)	NMR Yield of <b>41</b> (%)	Isolated Yield of <b>41</b> (%)
1	0.32	59	-
2	1.6	42	37

*Conditions: 2-phenyl-1,3-dioxolane (1 eq), MgBr<sub>2</sub> (2 eq), TEMPO (2 eq) in toluene under argon for 17 h. Yields were calculated by <sup>1</sup>H NMR spectroscopy in CDCl<sub>3</sub> with dry DMF as an internal standard.*

Table 2.12 clearly shows a loss of yield of **41** on scale up, which can be attributed to reduced stirring efficiency. It is worth noting, however, that the isolated yield of the larger scale reaction is fairly close to the NMR yield, reaffirming the accuracy of the yields determined by NMR spectroscopy.

### 2.3.8. Optimal Conditions

Table 2.13 shows the conditions determined as being optimal for use in the rest of the project.

Table 2.13: Optimised conditions for the TEMPO/MgBr<sub>2</sub> mediated oxidation of acetal **39** to ester **41**.

Entry	Variable	Initial conditions	Optimised conditions
1	Oxidant	TEMPO	TEMPO
2	Solvent	Toluene	DCM
3	Eq TEMPO	2	2
4	Eq MgBr <sub>2</sub>	2	4
5	Atmosphere	Argon	Air
6	Dry solvent	Yes	No
7	Time	17 h	17 h

Having decided on a suitable set of conditions for the oxidation of acetal **39** the next step is to investigate which other substrates will oxidise under these conditions.

## 2.4. Acetal Scope

With an optimised set of conditions in place we set about testing the scope of the oxidation reaction with a variety of different acetals designed to probe the effects of sterics, electronics, conjugation and changes to the acetal ring.

### 2.4.1. Steric Effects

The initially presumed reaction mechanism for the formation of the benzoate ester involves the abstraction of a hydrogen atom from the acetal carbon adjacent to the phenyl ring. An ortho substituent of sufficient size may inhibit rotation around the bond connecting the phenyl ring to the dioxolane. This will force the molecule into a conformation where the hydrogen is close in space to the ortho substituent,



potentially sterically blocking it and slowing the rate of hydrogen abstraction (Figure 2.24).

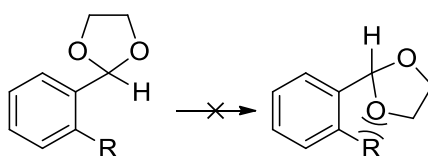
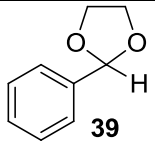
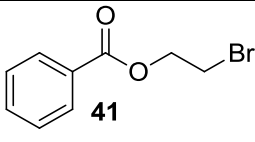
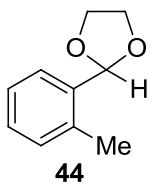
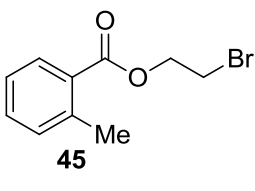
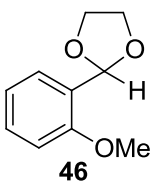
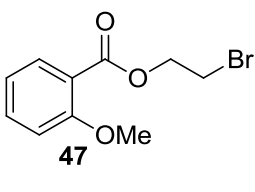
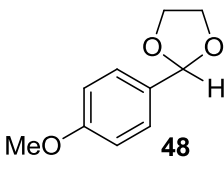
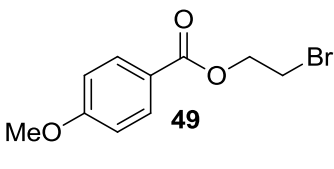


Figure 2.24: Inhibition of rotation of acetal by ortho substituents.

Acetals with ortho substituents were used to probe the effect of steric hindrance on their oxidation to benzoate esters (Table 2.14).

Table 2.14: TEMPO/MgBr<sub>2</sub> mediated oxidation of methyl and methoxy substituted phenylacetals.

Entry	Starting Material	Product	NMR Yield (%)
1	 39	 41	76
2	 44	 45	80 <sup>a</sup>
3	 46	 47	60 <sup>a</sup>
4	 48	 49	54

Conditions: Conditions: 2-phenyl-1,3-dioxolane (1 eq), MgBr<sub>2</sub> (4 eq), TEMPO (2 eq) in DCM for 17 h. Yields were calculated by <sup>1</sup>H NMR spectroscopy in CDCl<sub>3</sub> with dry DMF as an internal standard. <sup>a</sup>Novel compounds.

Comparison of Entries 1 and 2 in Table 2.14 show a very small difference in the yields of the unsubstituted and the ortho-methyl benzoate esters. If one assumes a negligible electronic effect from the ortho methyl group this suggests no steric hindrance from the methyl group. This is supported by Entries 3 and 4 where the electronic effects of the ortho and para methoxy substituents would be expected to be broadly the same and the position on the aromatic ring has had no significant effect on the product yield. From this we can suggest that relatively small substituents on the phenyl ring do not have a significant effect on the reactivity of the acetals.

#### 2.4.2. Conjugation

It was assumed that the rate-determining step in the formation of the benzoate esters from acetals would involve the formation of a benzylic radical on the acetal carbon. This would make the presence of the phenyl group key in stabilising the radical intermediate by resonance (Figure 2.25).

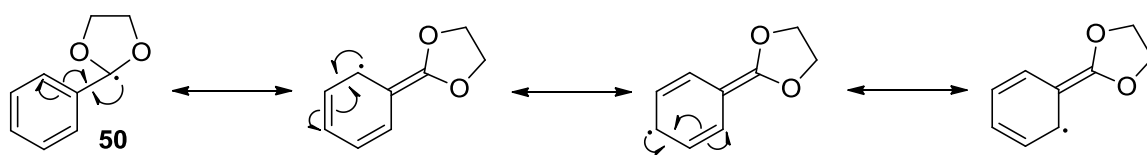
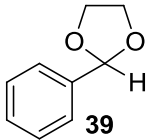
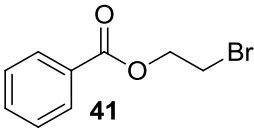
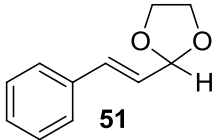
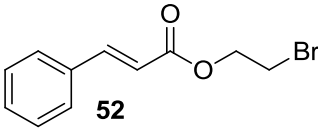
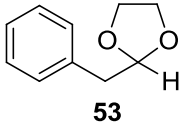
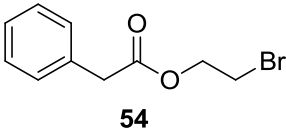


Figure 2.25: Mesomeric stabilisation of radical **50** from acetal **39**.

Table 2.15: TEMPO/MgBr<sub>2</sub> mediated oxidation of acetals **39**, **51** and **53**.

Entry	Starting Material	Product	NMR Yield (%)
1			76
2			47
3			27 39 <sup>a</sup>

Conditions: Conditions: 2-phenyl-1,3-dioxolane (1 eq), MgBr<sub>2</sub> (4 eq), TEMPO (2 eq) in DCM for 17 h. Yields were calculated by <sup>1</sup>H NMR spectroscopy in CDCl<sub>3</sub> with dry DMF as an internal standard. <sup>a</sup>48 h.

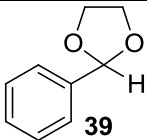
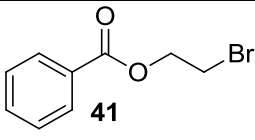
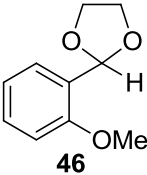
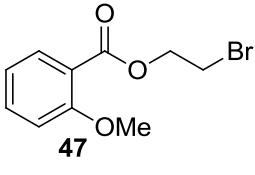
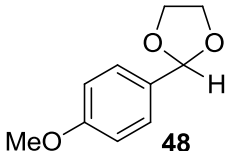
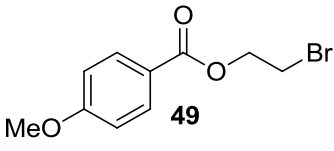
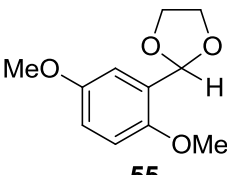
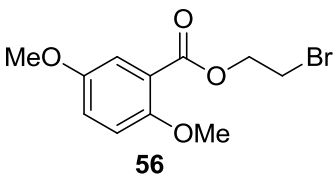
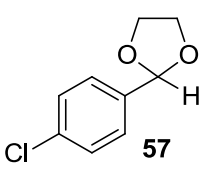
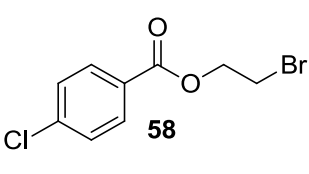
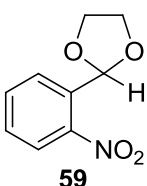
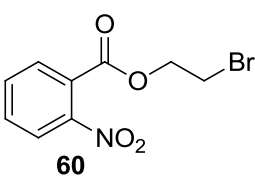
Table 2.15 shows that increasing the distance between the reaction centre and the phenyl ring, while still allowing conjugation to any electron deficient intermediates that may form, produces the (*E*)-cinnamyl ester **52** in a lower yield than those observed when the phenyl ring is adjacent to the acetal carbon (Table A, Entries 1 and 2). If the phenyl ring is separated from the acetal carbon by a CH<sub>2</sub> group, thereby preventing delocalisation of charged or radical intermediates, then the yield of the benzoate ester drops yet again, further supporting the idea that stabilisation of an intermediate by delocalisation around an aromatic ring is key in the efficient conversion of acetals into esters. The yields of non-benzylic acetals can be improved however with extended reaction times meaning this could still be a viable route to synthesise alkyl esters (Table 2.15, Entry 3).

### 2.4.3. Electronic Effects

The effect of electron donating and withdrawing substituents on the phenyl ring is an important consideration since it will determine how widely applicable the

methodology is and potentially give some insight into the reaction mechanism (Table 2.16).

Table 2.16: TEMPO/MgBr<sub>2</sub> mediated oxidation of phenyl acetals with electron donating and electron withdrawing substituents.

Entry	Starting Material	Product	NMR Yield (%)
1			76
2			60 <sup>a</sup>
3			54
4			41 <sup>a</sup>
5			35
6			0

Conditions: Conditions: 2-phenyl-1,3-dioxolane (1 eq), MgBr<sub>2</sub> (4 eq), TEMPO (2 eq) in DCM for 17 h. Yields were calculated by <sup>1</sup>H NMR spectroscopy in CDCl<sub>3</sub> with dry DMF as an internal standard. <sup>a</sup>Novel compounds.

It can be seen that adding electron donating substituents to the phenyl ring in the form of methoxy groups has a slightly detrimental effect on the yield of benzoate ester compared to the unsubstituted product (Table 2.16, Entries 1, 2 and 3). This effect is compounded by introducing a second methoxy group on the ring (Table 2.16, Entry 4). It would be expected that electron donating groups, especially those capable of conjugating to the acetal carbon, would help to stabilise a radical or cation formed there and thereby improve the yield of product (Figure 2.26).

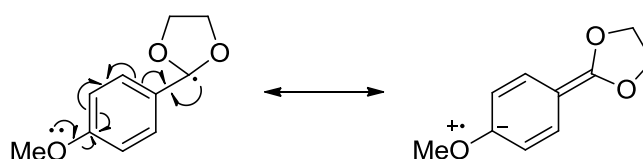


Figure 2.26: Mesomeric stabilisation of radical by acetal **48**.

It seems likely that, as seen with coordinating solvents, the methoxy groups are interfering with the ability of  $\text{MgBr}_2$  to catalyse the reaction by competing for binding to the Lewis acid.

The *para*-chloro substituted acetal **57** yielded a significantly lower quantity of benzoate ester than the unsubstituted system, which is consistent with the  $-I$  effect of the chlorine outweighing the  $+M$  effect and thereby Cl destabilising the electron deficient radical intermediate. Due to the strong electronegativity of chlorine there is little danger of lone pair donation to  $\text{MgBr}_2$  and competitive binding. This idea is supported by the fact that DCM was used as a solvent in this reaction without significantly decreasing the ester yield (Table 2.5, Entry 2).

As seen with certain other methods of oxidising acetals,<sup>118</sup> the introduction of  $\text{NO}_2$ , a strong electron-withdrawing group, stops the reaction completely (Table 2.16, Entry 6). If the key intermediate is a radical centred on the acetal carbon then an ortho-nitro group would be expected to have a stabilising effect as show in Figure 2.27.

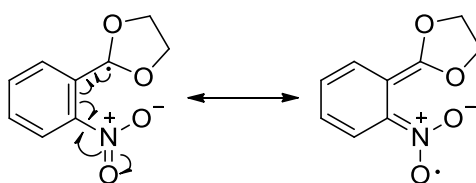


Figure 2.27: Mesomeric stabilisation of radical by acetal **59**.

Although this is beneficial for the formation of the radical intermediate it could have the effect of slowing the trapping of the radical and allowing an alternative route to dominate and quench the radical without forming the desired product. It is also possible that the nitro group is coordinating to  $\text{MgBr}_2$  in the same way that the methoxy groups are suspected of doing.

#### 2.4.4. Acetal Ring

Until now we have focussed mainly on the effects of changing the phenyl ring but changes to the acetal ring could lead to synthetically interesting products (Table 2.17).

Table 2.17: TEMPO/ $\text{MgBr}_2$  mediated oxidation of **61** and **63**.

Entry	Starting Material	Product	NMR Yield (%)
1	 <b>61</b>	 <b>62</b>	73
2	 <b>63</b>	 <b>64</b>	19

Conditions: Conditions: Acetal (1 eq),  $\text{MgBr}_2$  (4 eq), TEMPO (2 eq) in DCM for 17 h. Yields were calculated by  $^1\text{H}$  NMR spectroscopy in  $\text{CDCl}_3$  with dry DMF as an internal standard.

The addition of an extra  $\text{CH}_2$  group between the ester and the bromide is easily achieved by using a 6-membered 1,3-dioxane **63** instead of the 5-membered 1,3-

dioxolane **39** albeit with a significantly reduced yield. In contrast the presence of a methyl group on a 5-membered ring has little effect on the reactivity giving benzyl ester **62** in high yield. Interestingly, the regioisomer observed (as evidenced by a CH<sub>3</sub> doublet in the <sup>1</sup>H NMR spectrum) is not the one that might be predicted from the mechanism in Figure 2.18 since it would mean the preferential formation of a primary radical over a secondary radical (Figure 2.28).

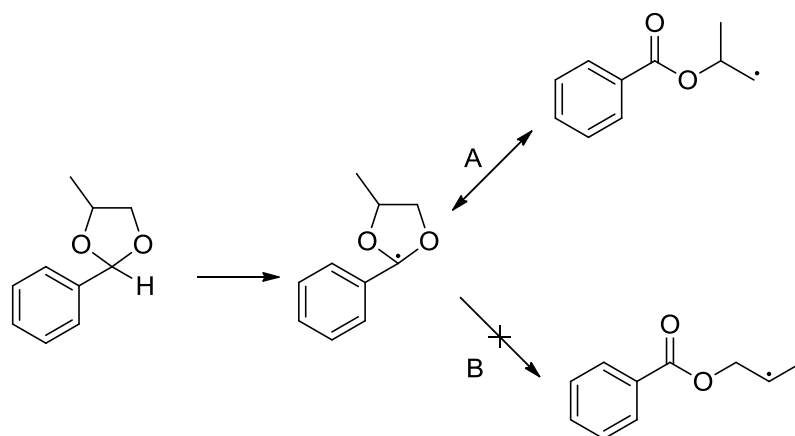


Figure 2.28: Mechanisms for the formation of a primary or secondary radical from acetal **61**.

Given that secondary radicals are more stable than primary radicals due to the +I effect of alkyl groups it would be expected that route B would be favoured not route A as is observed although the respective rates of trapping primary and secondary radicals could be playing a role here.

Considering this piece of information and the others garnered from the optimisation and scope investigations, it would now be worth revisiting and possibly revising the proposed mechanism.

#### 2.4.5. Mechanism

The investigations into the scope and the optimisation have thrown up a number of points, which may indicate a potential mechanism of the TEMPO/MgBr<sub>2</sub> mediated oxidation of acetal **39**. The first thing to note is that oxoammonium **35** does not appear to be the oxidising agent in this reaction. This means that rather than a single 2-electron oxidation occurring we are instead observing two 1-electron

oxidations. This coupled with observations of Hayton et al. regarding the oxidation of dihydroanthracene by TEMPO/LA systems means the most likely first step is the abstraction of the hydrogen atom from the acetal carbon (Figure 2.29).<sup>99</sup>

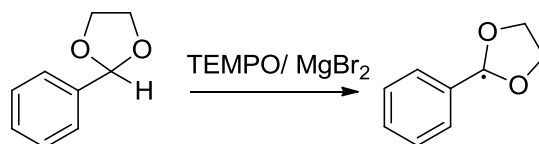


Figure 2.29: TEMPO/MgBr<sub>2</sub> mediated hydrogen abstraction from acetal **39**.

This tertiary radical is well stabilised by delocalisation onto the phenyl ring and both of the oxygen atoms (Figure 2.30).

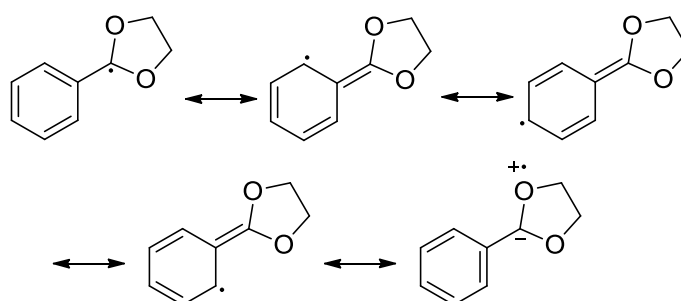


Figure 2.30: Mesomeric stabilisation of acetal radical **39**.

In Hayton's work he demonstrated that the ability of TEMPO to abstract a hydrogen atom was improved by coordination of the Lewis acid AlCl<sub>3</sub> to the oxygen on TEMPO by performing the oxidation of dihydroanthracene (Figure 2.31).<sup>99</sup>

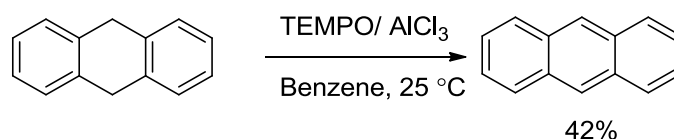
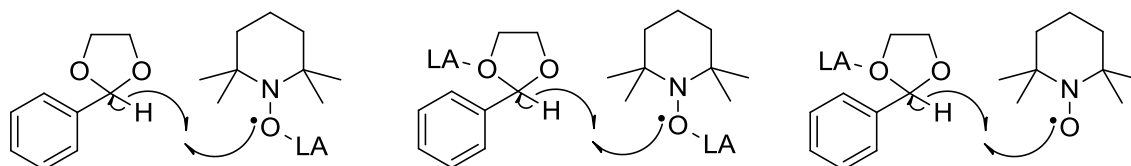


Figure 2.31: Oxidation of dihydroanthracene to anthracene.

Since AlCl<sub>3</sub> will not coordinate to dihydroanthracene it must be coordination to TEMPO which makes the difference in its reactivity. In our system however it is possible for MgBr<sub>2</sub> to coordinate not only to TEMPO but to the oxygen atoms in the acetal ring. Therefore the role of MgBr<sub>2</sub> may be to coordinate to TEMPO and destabilise the nitroxyl radical by withdrawing electron density, increasing its ability



to perform hydrogen atom abstractions. Alternatively  $\text{MgBr}_2$  could coordinate to one or more of the acetal oxygen atoms and weaken the C-H bond on the acetal carbon making it more susceptible to abstraction. In reality it is likely to be a combination of either or both of these effects that occurs (Figure 2.32).



*Figure 2.32: Possible locations for Lewis acid coordination in hydrogen abstraction from an acetal by TEMPO.*

#### **2.4.6. Formation of a Primary Radical**

Having formed a radical intermediate there are a number of ways in which it could then reversibly ring open and acquire a bromine atom. The mechanism presented in section 2.2.2. proposed that the ring opened via a radical route to form a primary carbon centred radical (**65**) as shown in Figure 2.33.

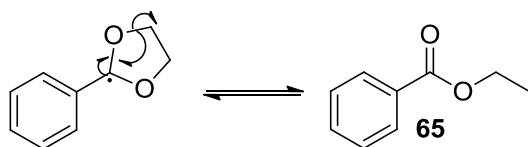


*Figure 2.33: Ring opening of an acetal radical.*

The formation of a primary radical from a tertiary one is not going to be favourable since primary radicals are less stable. Also, since the tertiary radical benefits from the additional stabilisation shown in Figure 2.30 the radical intermediate will preferentially exist in its most substituted form. It is conceivable however that if the radical intermediate is long lived enough and the equilibrium far enough to the right this could be a possible route. If the primary radical is formed it could be trapped by TEMPO (Figure 2.34).

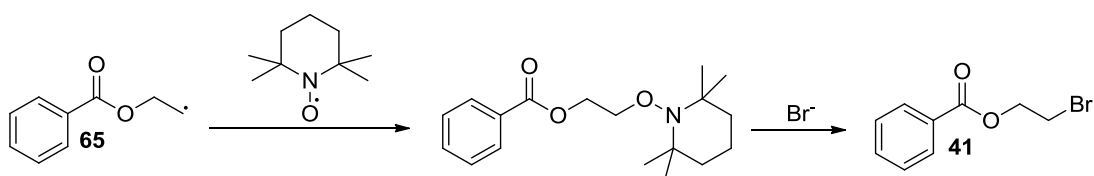


Figure 2.34: Trapping of primary radical by TEMPO and subsequent substitution by bromide ion.

TEMPO is frequently used as a radical trap so the chances of this happening seem quite high. The problem occurs with the next step where a bromide ion replaces the TEMPO group by nucleophilic substitution. TEMPO adducts of this type are generally very stable and for example, require zinc and acetic acid to cleave the N-O bond. Potentially the substitution is enabled by anchimeric assistance as shown in Figure 2.35.

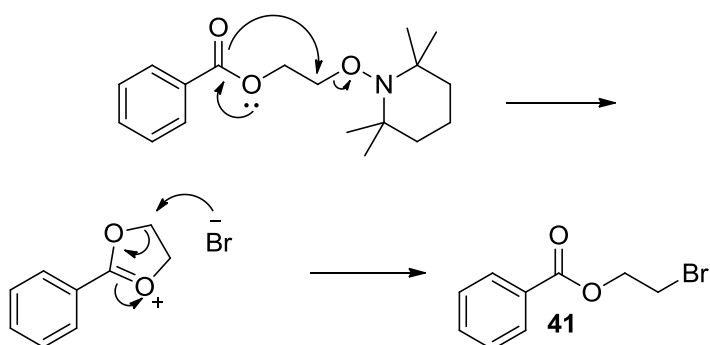


Figure 2.35: Anchimeric assisted bromide substitution.

This is a 5-*exo-tet* cyclisation which is favoured according to Baldwin's rules although it does require the breaking of a strong C-O bond which would not be very thermodynamically favoured.<sup>18</sup>

Perhaps the simplest way to get from the primary radical to the product is a termination step involving Br<sub>2</sub> or a bromine radical (Figure 2.36).

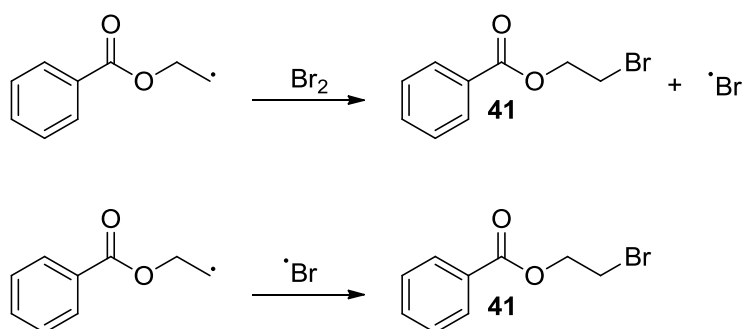


Figure 2.36: Trapping of primary radical by molecular bromine and bromine radical

EPR studies show that the TEMPO radical signal does not degrade in the presence of  $\text{MgBr}_2$ ; therefore TEMPO and  $\text{MgBr}_2$  do not react with each other to form  $\text{Br}_2$  or a bromine radical, rendering this route unlikely.

The only other way to form benzoate ester **43** from the primary radical is for TEMPO to perform another 1-electron oxidation to form a primary cation (**66**), which then reacts with  $\text{Br}^-$  (Figure 2.37).

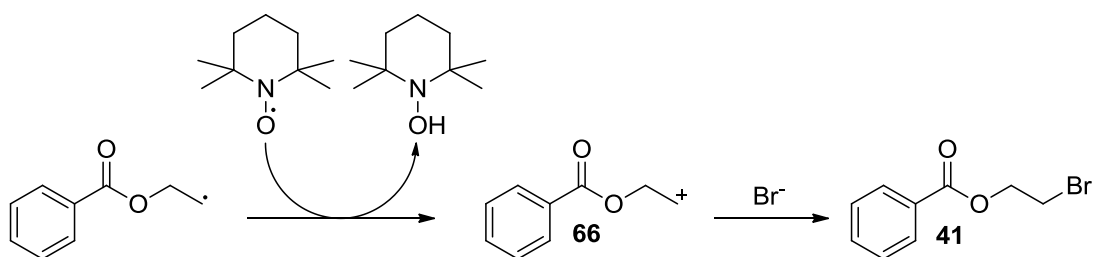


Figure 2.37: Oxidation of primary radical by TEMPO and subsequent trapping by bromide ion.

This mechanism involves the formation of a primary cation, which like the primary radical is a particularly unstable intermediate. In this case however it could perhaps cyclise as shown in Figure 2.38 to form the resonance stabilised cation **67**.

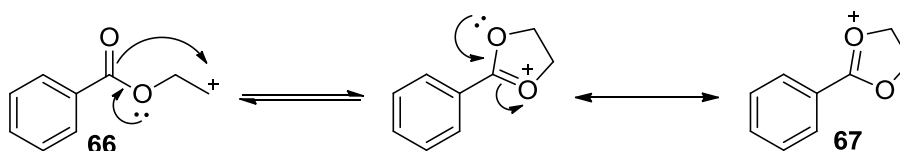


Figure 2.38: Mesomeric stabilisation of ethyl benzoate cation.

### 2.4.7. Regioselectivity

In the scope section we mentioned that acetal **61** was oxidised in the presence of TEMPO/MgBr<sub>2</sub> to form benzoate ester **62** without any of the other regioisomer being observed (Figure 2.39).

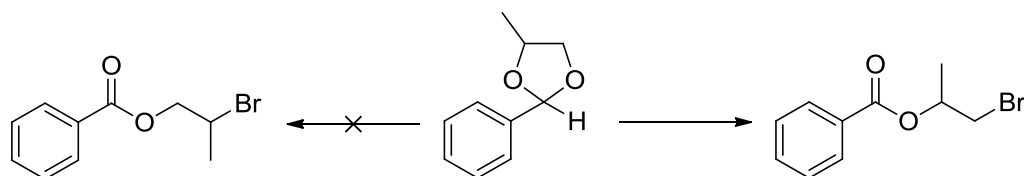


Figure 2.39: Stereoselective oxidation of acetal **62**.

This was unexpected since this would suggest the preferential formation of a primary radical and/or cation over a secondary radical and/or cation. This regioselectivity has also been observed in the oxidation of acetal **61** to form benzoate ester **62** in the presence of NBS. In 2004 McNulty et al. investigated this and proposed the following mechanism to explain the observed selectivity (Figure 2.40).<sup>119</sup>

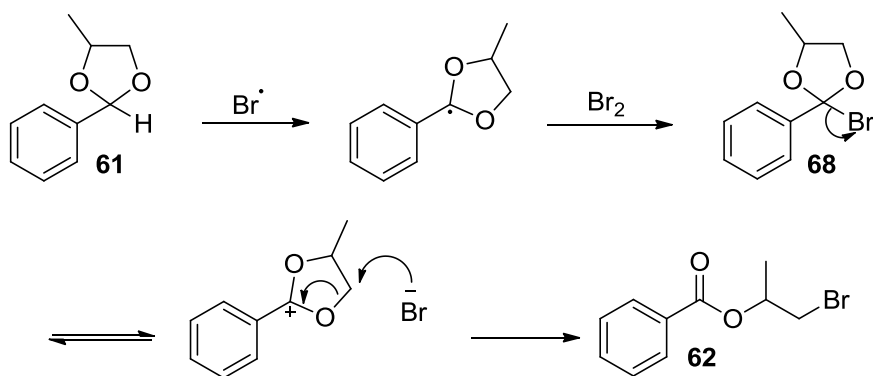


Figure 2.40: Mechanism proposed by McNulty for the formation of **62**.

This mechanism starts with hydrogen atom abstraction in the same manner as the mechanisms discussed previously. The tertiary radical then traps a bromine atom to form an unstable bromide (**68**). The bromide ion then leaves and attacks at the least sterically hindered position, via an S<sub>N</sub>2 process, to form benzoate ester **62**.

McNulty's mechanism can be adapted to fit the conditions in the TEMPO/MgBr<sub>2</sub> mediated oxidation of acetals. As previously mentioned there is no evidence for the

formation of bromine radicals under our conditions, therefore the tertiary radical would have to be either oxidised to a cation or trapped by TEMPO. This gives us two possible mechanisms for the formation of benzoate ester **62** (Figure 2.41).

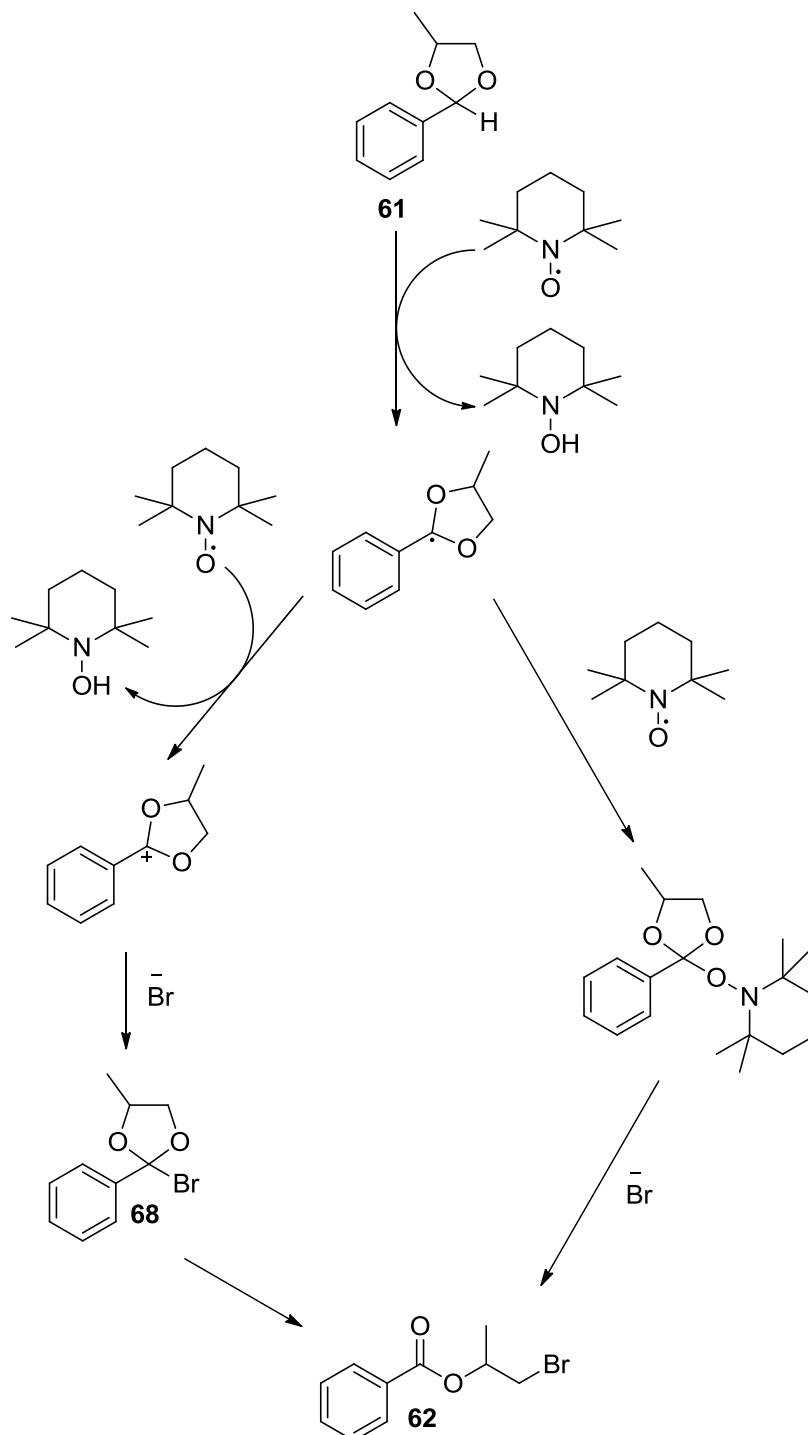


Figure 2.41: Possible mechanisms for the formation of **62**.

In both of these mechanisms the final step can go via an  $S_N1$  or  $S_N2$  process creating four possible routes in total. The fact that the ortho-nitro substituted acetal did not react to form a benzoate ester could be an indication that a cation is being formed in the rate determining step, assuming that it is not just due to catalyst deactivation. Further mechanistic studies are required to determine for sure which of these four routes is correct.

In conclusion, it has been shown that TEMPO/Lewis acid mediated oxidation of acetals proceeds in moderate to good yields and appears to follow a similar mechanism to the equivalent NBS mediated reaction.

### **3. Phosphorus Hydrides**

## 3. Phosphorus Hydrides

### 3.1. Phosphorus Hydride Addition

#### 3.1.1. Introduction

Phosphine sulfides and oxides have a wide range of uses such as metal catalyst ligands,<sup>120–126</sup> heavy metal extraction agents<sup>127</sup> and radical polymerisation mediators.<sup>128,129</sup> One of the ways to synthesise tri-substituted phosphine sulfides and oxides is by radical addition to alkenes or alkynes. The addition of phosphorus hydrides to unsaturated C-C bonds is usually accomplished in one of two ways. A radical initiator such as AIBN or Et<sub>3</sub>B can be used to create a phosphorus-centred radical which then adds to the double bond (Figure 3.1).<sup>130–133</sup>

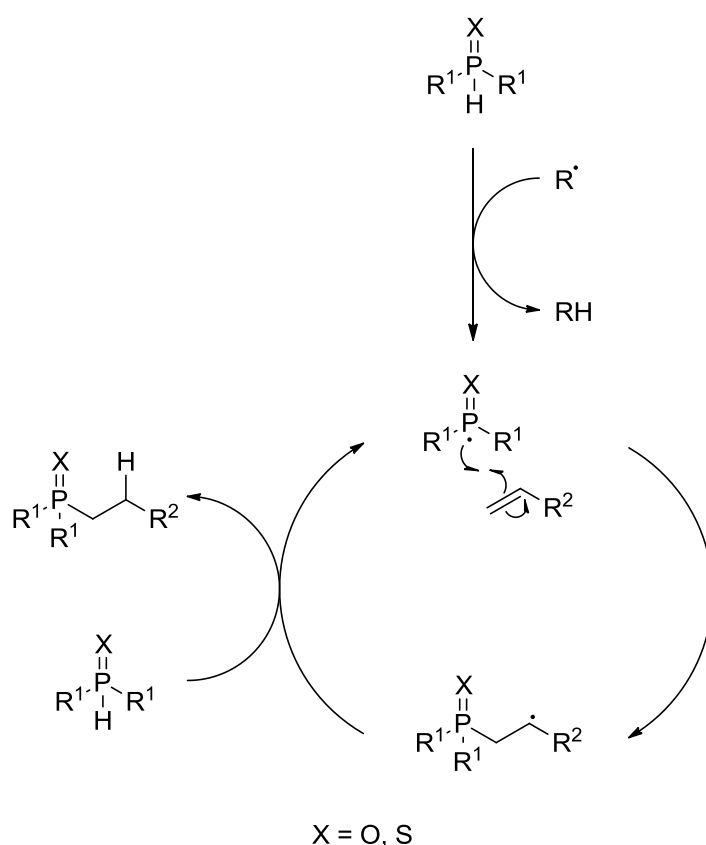


Figure 3.1: Radical addition of phosphorus hydrides to alkenes.

One problem that is sometimes encountered is the breakdown of the chain process. For example several portions of triethylborane are sometimes required to keep the reaction from stalling.<sup>6,131</sup>



Alternatively in the case of Michael acceptors an ionic approach can be used whereby a base deprotonates the phosphorus hydride which then adds to the unsaturated bond in a Michael-type addition (Figure 3.2).<sup>134–136</sup>

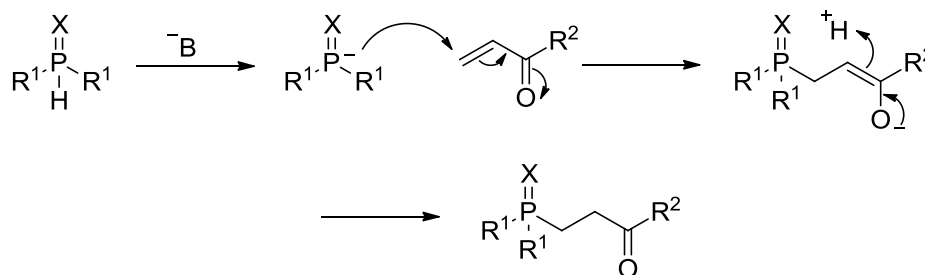


Figure 3.2: Mechanism of Michael addition of phosphorus hydrides to Michael acceptors.

This approach has the disadvantage of requiring stoichiometric base and therefore suffering from lower atom efficiency than the radical method and is restricted to addition to Michael acceptors.

### 3.1.2. Horner-Wadsworth-Emmons

Once phosphorus hydrides have been added to double bonds they can be used for further chemical reactions such as Horner-Wadsworth-Emmons (HWE) style reactions, often in a one-pot reaction as demonstrated by the use of diethyl thiophosphite by Parsons et al. in 2005 (Figure 3.3).<sup>6</sup>

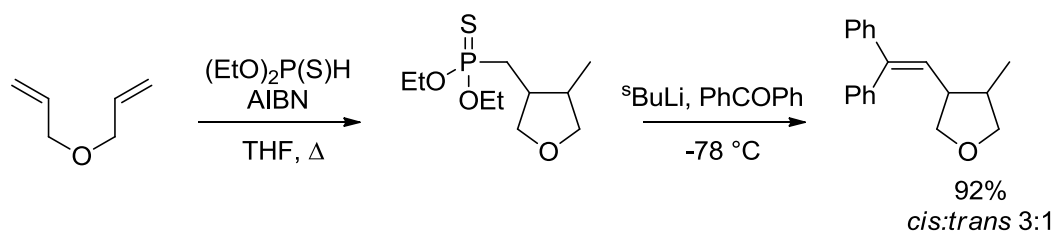


Figure 3.3: One pot cyclisation then HWE reaction starting from diallyl ether.

In the cyclisation example shown in Figure 3.3, two C-C bonds are being formed in a single pot in high yields. The HWE reaction proceeds via a four membered transition state and results in the formation of a strong P=O bond (Figure 3.4).

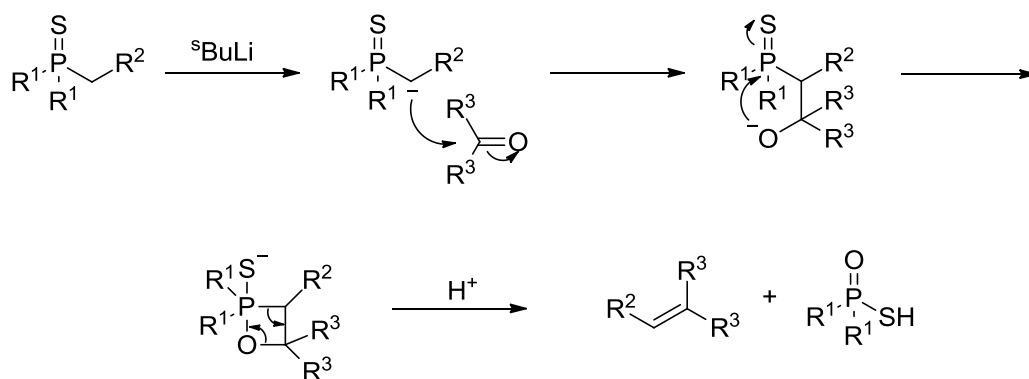


Figure 3.4: Mechanism of the HWE reaction.

### 3.1.3. Different Phosphorus Hydrides

It was hoped that the TEMPO/MgBr<sub>2</sub> radical initiation system developed for the oxidation of acetals could be used to initiate the addition of phosphorus hydrides to unsaturated C-C bonds under mild conditions as shown in Figure 3.5.

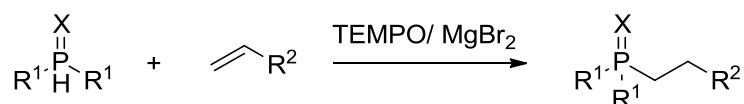


Figure 3.5: Addition of a phosphorus hydride to an alkene initiated by TEMPO/MgBr<sub>2</sub>

An attempt was made to add a number of different phosphorus hydrides to methyl methacrylate using TEMPO/MgBr<sub>2</sub> as an initiator (Figure 3.7).

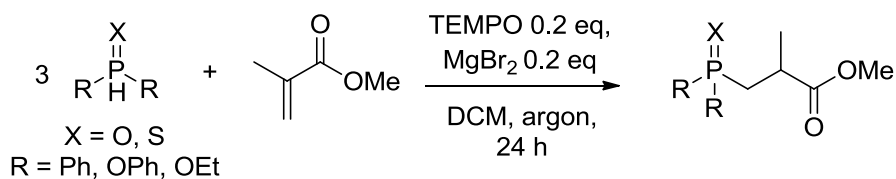
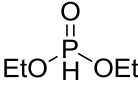
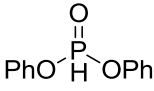
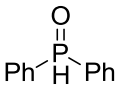
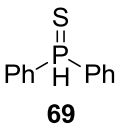


Figure 3.7: Addition of different phosphorus hydrides to methyl methacrylate.

The phosphorus hydrides were all purchased from commercial sources with the exception of diphenylphosphine sulfide which was synthesised by oxidation of diphenylphosphine with sulfur.<sup>137</sup> The results of the additions are summarised in Table 3.1.

Table 3.1: Addition of different phosphorus hydrides to methyl methacrylate.

Entry	Phosphorus Hydride	Isolated Yield (%)
1		0
2		0
3		0
4	 <b>69</b>	75

Conditions: Methyl methacrylate (1 eq), phosphorus hydride (3 eq), TEMPO (0.2 eq), MgBr<sub>2</sub> (0.2 eq) in DCM under argon for 24 h.

Of the four phosphorus hydrides only one produced the desired phosphorus adduct. This can be easily explained by examining the P-H bond dissociation energies (BDE) of the phosphorus hydrides shown in Figure 3.8.<sup>138</sup>

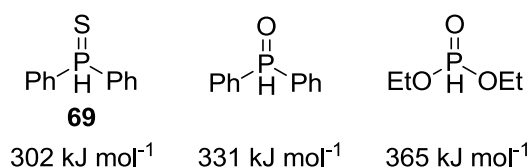


Figure 3.8: BDEs of some phosphorus hydrides.

Diphenylphosphine sulfide (**69**) has a BDE of 302 kJ mol<sup>-1</sup> which is fairly close to the BDE of the O-H bond in TEMPO hydroxylamine (291 kJ mol<sup>-1</sup>).<sup>139</sup> Therefore in a mixture of diphenylphosphine sulfide and TEMPO it would be expected that the equilibrium shown in Figure 3.9 would exist.

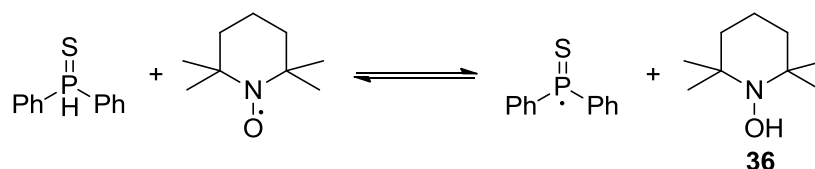


Figure 3.9: Equilibrium of TEMPO and diphenylphosphine sulfide.

For the phosphorus oxides, however, the difference between the P-H BDE and the O-H BDE is considerably greater and as such, the driving force for the formation of the phosphorus radical is greatly diminished.

It was assumed that the reaction proceeded via a hydrogen atom abstraction followed by addition to the unsaturated bond. The secondary carbon-centred radical would then abstract a hydrogen atom from the phosphorus hydride, closing the catalytic cycle (Figure 3.6).

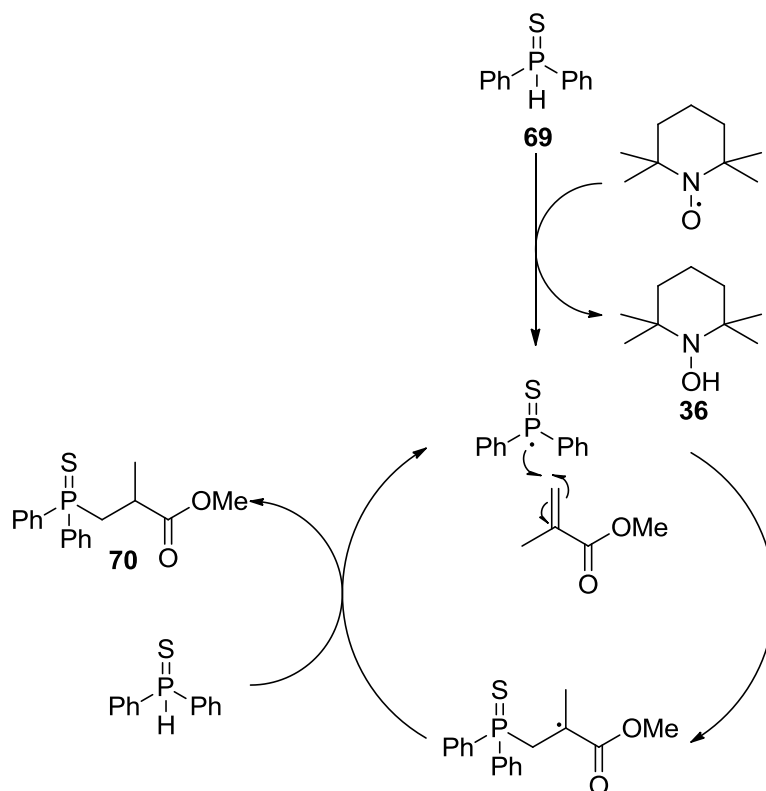


Figure 3.6: Initially proposed mechanism for the TEMPO initiated addition of diphenylphosphine sulfide to methyl methacrylate.

### 3.1.4. TEMPO Initiated Phosphorus Hydride Addition

As shown in the previous chapter,  $\text{MgBr}_2$  can improve the ability of TEMPO to perform hydrogen atom abstractions. In the case of generating  $\text{Ph}_2\text{P}(\text{S})^\bullet$  though it was found to be unnecessary (Table 3.2).

Table 3.2: Comparing the TEMPO initiated addition of diphenylphosphine sulfide to methyl methacrylate with and without  $\text{MgBr}_2$ .

Entry	Eq $\text{MgBr}_2$	Isolated Yield of <b>70</b> (%)
1	0.2	75
2	0	100

Conditions: Methyl methacrylate (1 eq), diphenylphosphine sulfide (3 eq), TEMPO (0.2 eq),  $\text{MgBr}_2$  in DCM under argon for 24 h.

In fact, the presence of  $\text{MgBr}_2$  appears to be hindering the addition of diphenylphosphine sulfide to methyl methacrylate. It is possible that  $\text{MgBr}_2$  is coordinating to the sulfur atom of diphenylphosphine sulfide. This could have the effect of drawing electron density away from the phosphorus atom and preventing the lone pair on sulfur from stabilising the phosphorus centred radical.

### 3.1.5. Trapping with TEMPO

As discussed previously TEMPO is known for efficiently trapping carbon-centred radicals. It was thought that by increasing the quantity of TEMPO from 0.2 eq to 4 eq, the secondary radical formed by the addition of the phosphorus radical would be trapped by the nitroxide to form **71** (Figure 3.10).

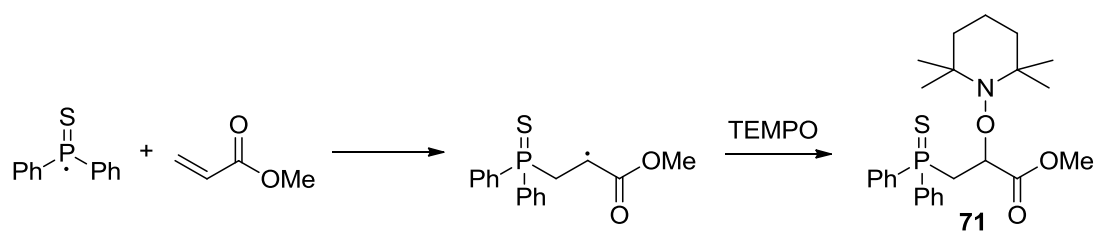


Figure 3.10: Mechanism for the trapping of the adduct formed from the addition of  $Ph_2P(S)^\bullet$  to methyl methacrylate by TEMPO

It was found however that the expected product was not formed. The issue here is that TEMPO was in excess and the phosphorus radical and the nitroxide have a high affinity for each other, forming a strong P-O bond ( $\approx 507.5 \text{ kJ mol}^{-1}$ ). Therefore instead of TEMPO trapping the carbon-centred radical we believe it is trapping the phosphorus radical forming 1-[(diphenylphosphorothioyl)oxy]-2,2,6,6-tetramethylpiperidine (Figure 3.11). This product requires isolation to confirm.

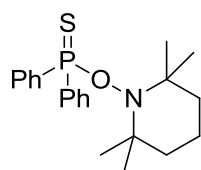


Figure 3.11: The proposed adduct formed on trapping  $Ph_2P(S)^\bullet$  with TEMPO.

In 2014 Li et al. used TEMPO to trap a diphenylphosphine oxide radical in order to demonstrate their reaction proceeded via a radical mechanism (Figure 3.12).<sup>140</sup>

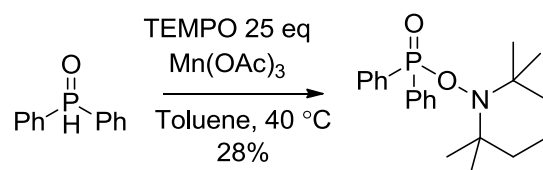


Figure 3.12: Trapping of diphenylphosphine oxide radical by TEMPO.

This demonstrates that large quantities of TEMPO are not compatible with phosphorus hydrides in radical processes.

### 3.1.6. Phosphorus Hydride Stoichiometry

One of the main disadvantages of the initial reaction conditions is the use of three equivalents of diphenylphosphine sulfide. The necessity of using this much phosphorus hydride was tested by reducing the equivalents of diphenylphosphine sulfide from three to one (Table 3.3).

*Table 3.3: Investigating the effect of phosphorus hydride stoichiometry on the TEMPO initiated addition of diphenylphosphine sulfide to methyl methacrylate.*

Entry	Eq of Ph <sub>2</sub> P(S)H	Isolated Yield of <b>70</b> (%)
1	3	100
2	1	52

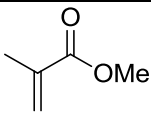
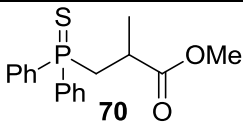
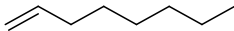
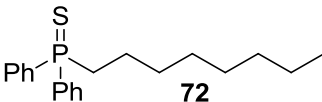
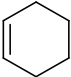
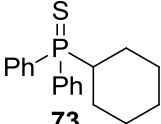
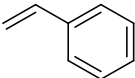
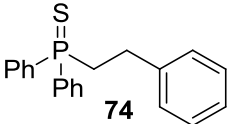
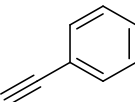
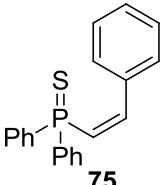
*Conditions: Methyl methacrylate (1 eq), diphenylphosphine sulfide, TEMPO (0.2 eq), in DCM under argon for 24 h.*

The reduction in equivalents of diphenylphosphine sulfide causes a significant drop in the observed yield of **70**. The lowering of the concentration of the phosphorus hydride will have shifted the equilibrium between the phosphorus hydride and phosphorus radical in favour of the phosphorus hydride due to Le Châtelier's principle. This lowers the concentration of the phosphorus-centred radical in the reaction mixture, slowing the rate of the addition reaction. Clearly then, an excess of phosphorus hydride aids the addition to unsaturated bonds.

### 3.1.7. Scope

The optimised conditions were applied to a number of different alkenes and alkynes (Table 3.4).

Table 3.4: TEMPO initiated additions of diphenylphosphine sulfide to different alkenes and alkynes.

Entry	Starting Material	Product	Isolated Yield (%)
1		 70	100
2		 72	95
3		 73	27
4		 74	88
5		 75	43

Conditions: Methyl methacrylate (1 eq), diphenylphosphine sulfide (3 eq), TEMPO (0.2 eq), in DCM under argon for 24 h.

Methyl methacrylate and octene both reacted to give very high yields of adducts (Table 3.4, Entries 1 and 2), but cyclohexene (Table 3.4, Entry 3) gave only a 27% yield. It seems likely that this is due to steric effects but more examples would be needed to confirm this. Comparison of additions to styrene and phenylacetylene (Table 3.4, Entries 4 and 5) suggest that alkenes are more susceptible to addition of  $\text{Ph}_2\text{P}(\text{S})^\bullet$  than alkynes, presumably due to the lower stability of the vinyl radical intermediate (**76**) (Figure 3.13).



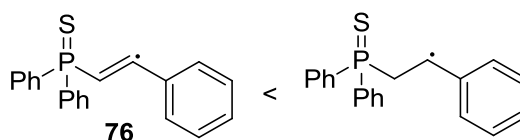


Figure 3.13: Relative stability of alkyl and vinyl radicals.

The alkene formed by addition of diphenylphosphine sulfide to phenylacetylene was identified as exclusively the *Z* isomer due to the 13.5 Hz coupling observed between the two alkene protons which matches with the 13.6 Hz coupling in the literature for the *Z* isomer as opposed to the 16.3 Hz coupling for the *E* isomer.<sup>141,142</sup> This is thought to be due to the interconversion of the vinyl radical intermediate between the *E* and *Z* forms with preferential hydrogen atom donation to the *Z* form due to sterics (Figure 3.14).<sup>143</sup>

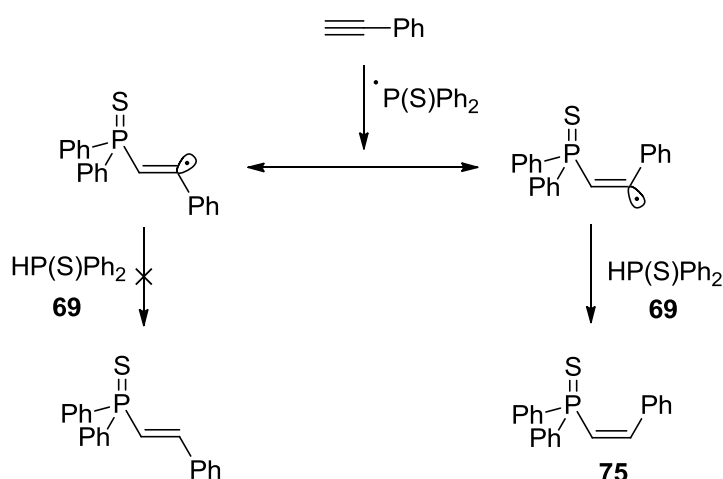


Figure 3.14: Hydrogen atom donation to *E* and *Z* vinyl radicals.

### 3.1.8. Cyclisations

As well simple additions to alkenes and alkynes, several cyclisation reactions were also achieved (Table 3.5).

Table 3.5: TEMPO initiated, diphenylphosphine mediated cyclisations of dienes.

Entry	Starting Material	Product	Isolated Yield (%)	dr <i>cis:trans</i>
1			67 <sup>a</sup>	9.4:1
2			41 <sup>a</sup>	3.7:1
3			51 <sup>a</sup>	2.1:1
4			32	N/A

Conditions: Methyl methacrylate (1 eq), diphenylphosphine sulfide (3 eq), TEMPO (0.2 eq), in DCM under argon for 24 h. <sup>a</sup>Novel compounds.

Diallyl malonate, diallyl ether and *N*-Boc-diallylamine all cyclised in moderate yields confirming the notion that addition occurs via a radical mechanism (Figure 3.15).

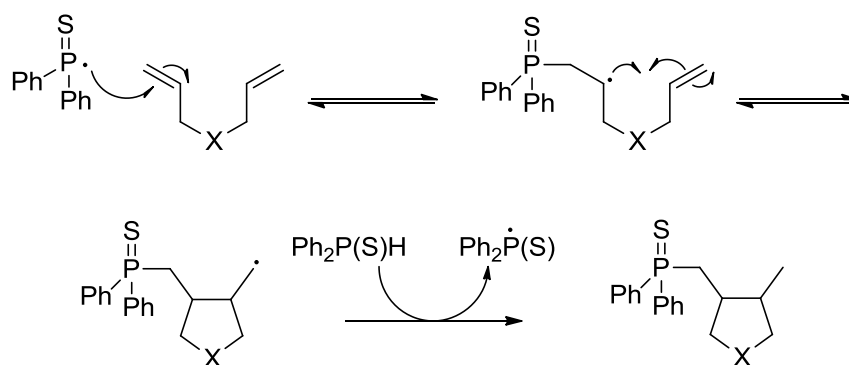


Figure 3.15: Mechanism of phosphorous sulfide mediated cyclisation.

The cyclisation of the malonate is facilitated by the Thorpe-Ingold effect where increasing the size of two geminal substituents forces the molecule into a conformation which is favourable for a particular reaction, in this case bringing the two alkenes together to favour cyclisation over simple addition. A similar effect is observed with the bulky Boc group on the diallylamine and the two lone pairs on the diallyl ether. The octadiene however has nothing to force its two alkenes together and as a result undergoes simple addition instead of cyclisation.

The *cis* isomer was identified as the major isomer due to the characteristic chemical shift of the methyl doublet in the  $^1\text{H}$  NMR spectrum which matches the shift of similar compounds in the literature.<sup>6,133</sup> The formation of the *cis* isomer can be explained by considering the chair-like transition state 5-*exo-trig* cyclisations adopt (Figure 3.16).

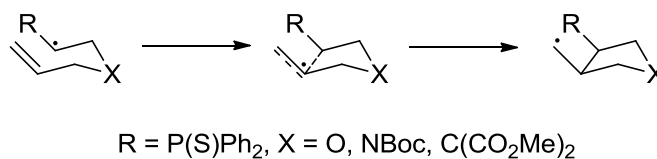


Figure 3.16: Chair-like transition state.

In this transition state the R group and the methyl group preferentially sit in a pseudo axial position which leads to the formation of the *cis*-product. The higher energy boat-like transition state is responsible for the minor *trans*-isomer (Figure 3.17).

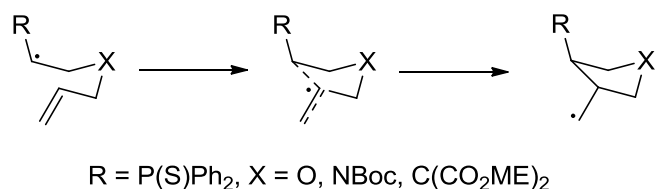


Figure 3.17: Boat-like transition state.

It was noted that the diastereoselectivity of diallyl dimethylmalonate was considerably higher than the other two which was attributed to the greater steric bulk of the two ester groups compared to the oxygen or N-Boc on the other compounds. These bulky groups help force compound into an ideal configuration for a 5-membered ring and lower the rate of the radical fragmentation of the ring (Figure 3.18).<sup>144</sup>

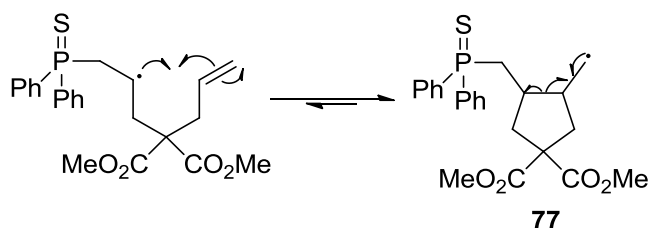


Figure 3.18: Reversible 5-exo-trig cyclisation.

Since the forward reaction is faster, the kinetic (*cis*) product is favoured rather than the thermodynamic (*trans*) product leading to a greater dr.<sup>145</sup> In the other examples where the diester is replaced with N-Boc and oxygen, the rate of the back reaction is higher in comparison to the forward reaction leading to a greater proportion of the thermodynamic (*trans*) product and a lower dr.

### 3.1.9. Uninitiated Phosphorus Hydride Addition

During the course of the investigation into the TEMPO initiated addition of phosphorus hydrides we discovered that Ph<sub>2</sub>P(S)H adds to methyl methacrylate at room temperature in DCM without the need for an initiator (Figure 3.19).

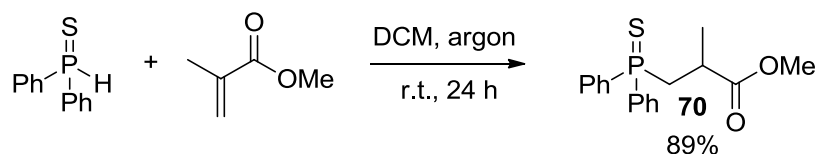


Figure 3.19: Addition of diphenylphosphine sulfide to methyl methacrylate in the absence of TEMPO.

The same reaction with TEMPO as an initiator produced a quantitative yield, suggesting that a radical initiator was beneficial, but clearly high yields of **70** are obtainable in the absence of TEMPO. This ‘uninitiated addition’ was not observed with 1-octene, however, and we began to suspect that only electron-deficient alkenes reacted under these conditions.

Having established that diphenylphosphine sulfide efficiently adds to methyl methacrylate, a number of different electron deficient alkenes were subjected to the same reaction conditions (Table 3.6).

Table 3.6: Non-initiated addition of diphenylphosphine sulfide to Michael acceptors.

Entry	Alkene	Product	Yield (%)
1			89
2			47
3			52

Conditions: Michael acceptor (1 eq), diphenylphosphine sulfide (3 eq), in DCM under argon for 24 h.

It should be noted that not only are the alkenes in Table 3.6 all electron-deficient, they are also all Michael acceptors which could be the key to explaining their reactivity. It is well known in the literature that phosphorus hydrides can add to Michael acceptors such as methyl methacrylate in the presence of an appropriate base as previously shown in Figure 3.2.<sup>136</sup> The problem with this as a possible mechanism is that it requires a base strong enough to deprotonate diphenylphosphine sulfide and such a base is not present in our reaction conditions.

Another possibility is that a radical mechanism occurs where the PH bond homolytically dissociates by absorption of light and then adds to the alkene Figure 3.20.

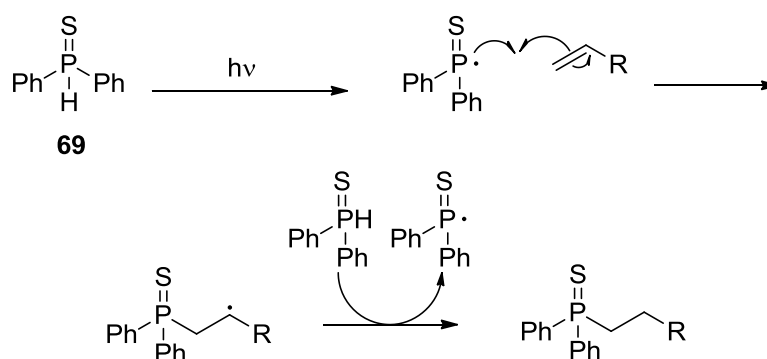


Figure 3.20: EM radiation initiated addition of diphenylphosphine sulfide to alkenes.

If phosphorus centred radicals are formed under these conditions then one would expect that additions to most alkenes would occur as seen with the TEMPO initiated reactions in the previous chapter. What we observe, however, is exclusive addition to Michael acceptors and not to more electron-rich alkenes like 1-octene. In addition to this there does not appear to be any significant degradation of diphenylphosphine sulfide on standing in natural light. This then is also not likely to be the real mechanism.

In related work it was demonstrated by Trofimov et al. that 1 equivalent of diphenylphosphine hydride, at elevated temperatures (80 °C), will add to a variety of electron rich-alkenes in the absence of an initiator or solvent (Figure 3.21).<sup>146</sup>

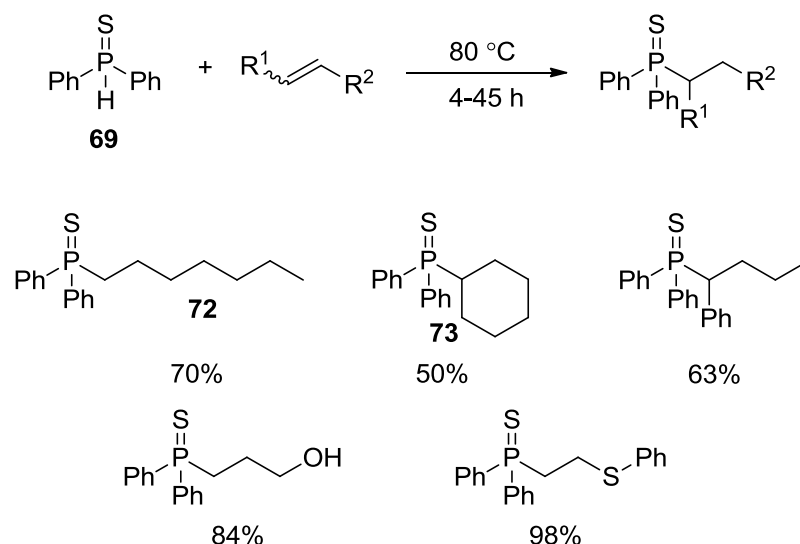


Figure 3.21: Addition of diphenylphosphine sulfide to alkenes by Trofimov et al.

Although Trofimov did not comment on the mechanism of this addition it was similar enough to our own observations to deserve some scrutiny. Trofimov's system, unlike the TEMPO free additions mentioned above, adds  $Ph_2P(S)H$  to electron-rich alkenes as well as to Michael acceptors. This provided us with a simple way of determining whether Trofimov's additions involved radical intermediates. Having demonstrated in the previous chapter that dimethyl diallylmalonate cyclises in the presence of  $Ph_2P(S)^{\bullet}$  radicals, generated by TEMPO, we have also shown that the same reaction occurs in good yield at elevated temperatures in the absence of an initiator or a solvent (Figure 3.22).

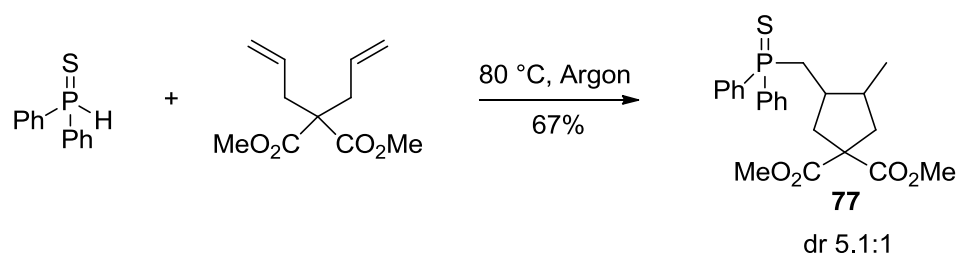
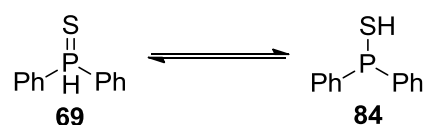


Figure 3.22: Radical cyclisation at elevated temperatures.

This 5-*exo-trig* cyclisation is typical of radical reactions suggesting that this cyclisation proceeds via a radical addition of  $Ph_2P(S)^{\bullet}$  which is formed by the homolytic thermolysis of the P-H bond. At room temperature in DCM however neither the cyclisation nor simple addition occurred suggesting that this mechanism

only occurs at higher temperatures. It is interesting to note the lower diastereoselectivity of this cyclisation compared to the TEMPO initiated version of the same reaction (5.1:1 compared to 9.4:1). This is due to the higher temperature increasing the proportion of molecules going through the higher energy boat-like transition state.

One final possibility was considered and that is the involvement of the tautomeric form of diphenylphosphine sulfide (Figure 3.23).



*Figure 3.23: Tautomerism of diphenylphosphine sulfide.*

This could potentially add more readily through the sulfur in a Michael addition than the phosphorus would in the other tautomer (Figure 3.24).

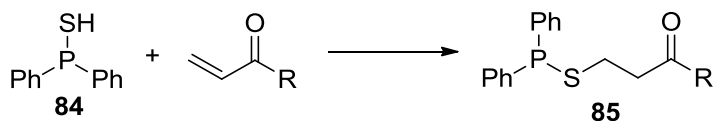


*Figure 3.24: Addition of diphenylphosphinothionous (**84**) acid to Michael acceptors.*

Since the  $^{31}\text{P}$  NMR shift and the  $^{13}\text{C}$  NMR P-C couplings do not support compound **85** as the product, some form of rearrangement would be necessary for the formation of the real product.

Overall, there is evidence to discount certain potential mechanisms but further work is required to determine the correct one.



## **4. TEMPO Ionic Liquids**

## 4. TEMPO Ionic Liquids

### 4.1. Introduction

#### 4.1.1. Nitroxide Ionic Liquids

As mentioned in the introduction, ionic liquids have gained a reputation as green solvents due to the ease with which they can be recycled. Since recycling organic catalysts is less trivial than heterogeneous inorganic catalysts it is unsurprising that organic catalysts have been incorporated into ionic liquids to ease their isolation and reuse. To this end several research groups have set to work creating ionic liquids which incorporate nitroxides allowing for catalyst recovery. For example in 2010 Fall et al. attached a TEMPO derivative to an imidazolium ion to create the ionic liquid shown in Figure 4.1.<sup>147</sup>

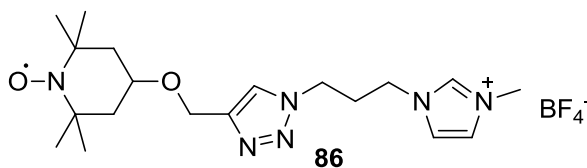


Figure 4.1: TEMPO ionic liquid **86**.

The synthesis of ionic liquid **86** is achieved using Click chemistry (a copper-catalysed azide-alkyne cycloaddition) between an azide attached to an imidazolium ion and an alkyne incorporated into a TEMPO derivative (Figure 4.2).

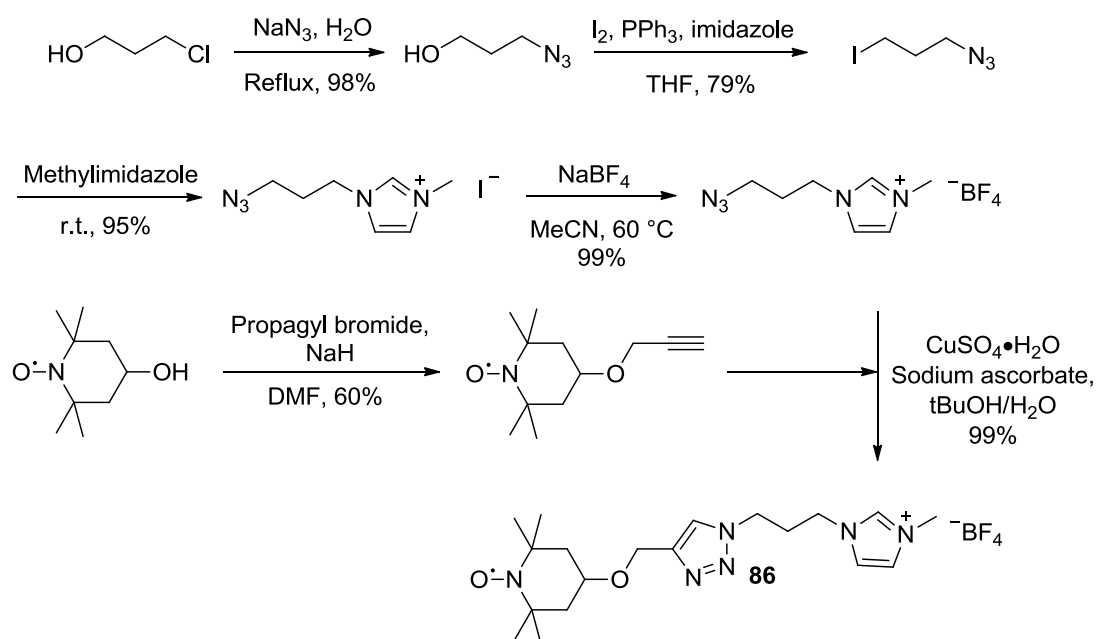


Figure 4.2: Synthesis of TEMPO ionic liquid **86** by Click chemistry.

The approach chosen here was to covalently attach the nitroxide functionality to an imidazolium cation, which is commonly used for ionic liquids and use a conventional counterion. Other examples of this approach include that published by He et al. in 2009 who joined the TEMPO moiety to an imidazolium group by an ester linkage (Figure 4.3).<sup>148</sup>

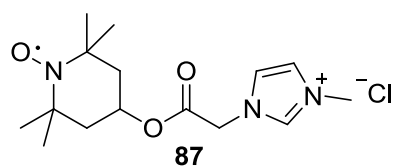


Figure 4.3: TEMPO ionic liquid **87**.

The ionic liquid **87** was used by He et al. to perform oxidations of primary and secondary alcohols (Table 4.1).

Table 4.1: Oxidation of aldehydes by TEMPO ionic liquid **87**.<sup>148</sup>

Entry	Product	Temp (°C)	Time (min)	Yield (%)
1	Benzaldehyde	60	30	99
2	Benzaldehyde	100	10	99
3	4-Methoxybenzaldehyde	60	60	96
4	2-Methoxybenzaldehyde	60	30	85
5	4-Methybenzaldehyde	60	20	92
6	4-Nitrobenzaldehyde	100	20	94
7	2-Nitrobenzaldehyde	80	60	72
8	Acetophenone	60	180	96
9	1-Heptaldehyde	60	360	45
10	2-Octanone	60	360	23

Conditions: Alcohol, **87** (5 mol%), NaNO<sub>2</sub> (5 mol%), H<sub>2</sub>O, O<sub>2</sub> (1 MPa), 60 °C, 0.5-12 h.

As would be expected, primary benzyl alcohols proved to be the most susceptible to oxidation whereas alkyl and secondary alcohols produced lower yields or required longer reaction times and higher temperatures.

An alternative approach to the task of creating ionic liquids incorporating the TEMPO moiety is to use the functionality available on TEMPO derivatives to create an anion on the 4-position by functional group interconversion. In 2007 Saito et al. synthesised a set of ionic liquids with TEMPO sulfate as the anion (Figure 4.4).<sup>149</sup>

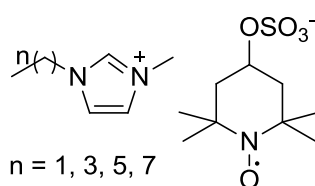


Figure 4.4: Imidazolium TEMPO sulfonates.

### 4.1.2. Aims

The aim of this particular project was to synthesise a TEMPO derived novel ionic liquid which could be easily and cheaply made in high yields with low cost and which could be used as a catalyst in the same way as TEMPO.

## 4.2. Synthesis of Nitroxide Ionic Liquids

### 4.2.1. [BMIM][Carboxy-TEMPO]

The first ionic liquid we attempted to synthesise was [BMIM][Carboxy-TEMPO]. 4-Carboxy-TEMPO is a commercially available derivative of TEMPO, but due to its prohibitive cost we chose to synthesise it from the much cheaper derivative 4-oxo-TEMPO using the method developed by Rosen et al.<sup>150</sup> The first step of the synthesis was a Van Leusen reaction where the carbonyl of oxo-TEMPO is converted into a nitrile group to give 4-cyano-TEMPO (**88**) (Figure 4.5).<sup>151</sup>

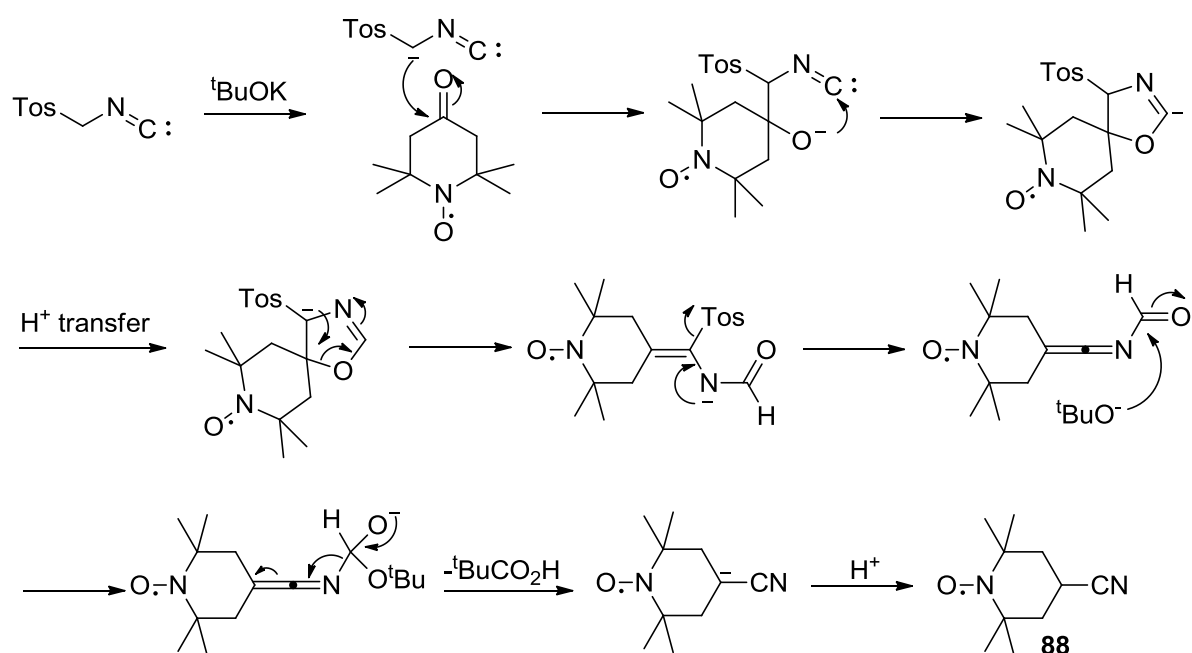


Figure 4.5: Synthesis of cyano-TEMPO.

The cyano-TEMPO (**88**) was then hydrolysed under basic conditions to give the desired carboxy-TEMPO (Figure 4.6).<sup>150</sup>

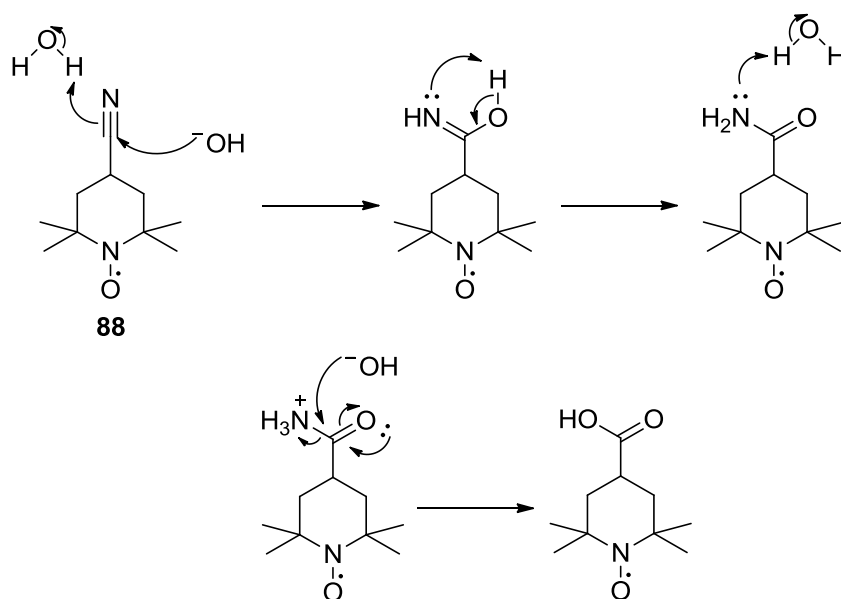


Figure 4.6: Hydrolysis of cyano-TEMPO (**88**).

The carboxy-TEMPO was then coupled with an imidazolium cation to form the novel ionic liquid **89** (Figure 4.7).

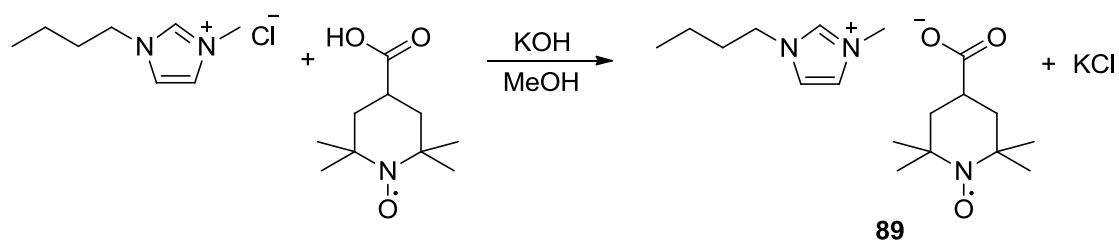


Figure 4.7: Synthesis of [BMIM][Carboxy-TEMPO] (**89**).

[BMIM][Carboxy-TEMPO] (**89**) was synthesised from oxo-TEMPO (without isolation or characterisation of intermediates) in a 17% overall yield. The final product was an orange oil which was not further purified due to the difficulties of distilling ionic liquids or purifying using a silica column. Compounds such as **89** are difficult to characterise by NMR spectroscopy due to their paramagnetic nature. Mass spectrometry of **89** is also not straightforward since the signals arising from the electrospray ionised starting materials would be indistinguishable from the signals corresponding to the product. As a result of these problems **89** has not been well characterised. Nonetheless oxidation reactions with **89** were carried out to determine its synthetic usefulness.

Table 4.2: Oxidation of benzyl alcohol by [BMIM][Carboxy-TEMPO] (**89**).

Entry	Oxidant	Equivalents of oxidant	Yield (%)
1	TEMPO	0.025	29 <sup>a</sup>
2	[BMIM][Carboxy-TEMPO] ( <b>89</b> )	0.01	36 <sup>b</sup>
3	[BMIM][Carboxy-TEMPO] ( <b>89</b> ) (Recycled)	0.01	12 <sup>b</sup>

*Conditions: Benzyl alcohol (1 eq), oxidant, NaBr (0.01 eq), NCS (1.1 eq) in [BMIM][BF<sub>4</sub>] and K<sub>2</sub>CO<sub>3</sub>/NaHCO<sub>3</sub> buffer for 24 h. <sup>a</sup>Isolated yield. <sup>b</sup>Conversion as determined from <sup>1</sup>H NMR.*

Table 4.2 shows that [BMIM][Carboxy-TEMPO] (**89**) is capable of performing oxidations of alcohols in [BMIM][BF<sub>4</sub>] and that to a certain degree at least can be recycled. In the instance shown here, the recycling was achieved by simply subjecting the mixture of [BMIM][BF<sub>4</sub>] and [BMIM][Carboxy-TEMPO] (**89**) to reduced pressure to remove any residual water and then adding more buffer and NaBr. No attempt was made to remove left over buffer, NaBr or succinimide from the previous reaction, and this would clearly be the next step in optimising the system.

#### 4.2.2. Horner-Wadsworth-Emmons

Due the expense of carboxy-TEMPO and the low yields achieved when synthesising an ionic liquid from it an alternative method was sought for synthesising an anion incorporating a TEMPO moiety. Since TEMPO and its derivatives are all synthesised from triacetoneamine (**33**) this was the obvious place to start from. Research conducted by Zabza et al. in 1987 showed that an ester group could be added to triacetoneamine (**33**) by a Horner-Wadsworth-Emmons reaction by the mechanism shown in Figure 4.8.<sup>152</sup>

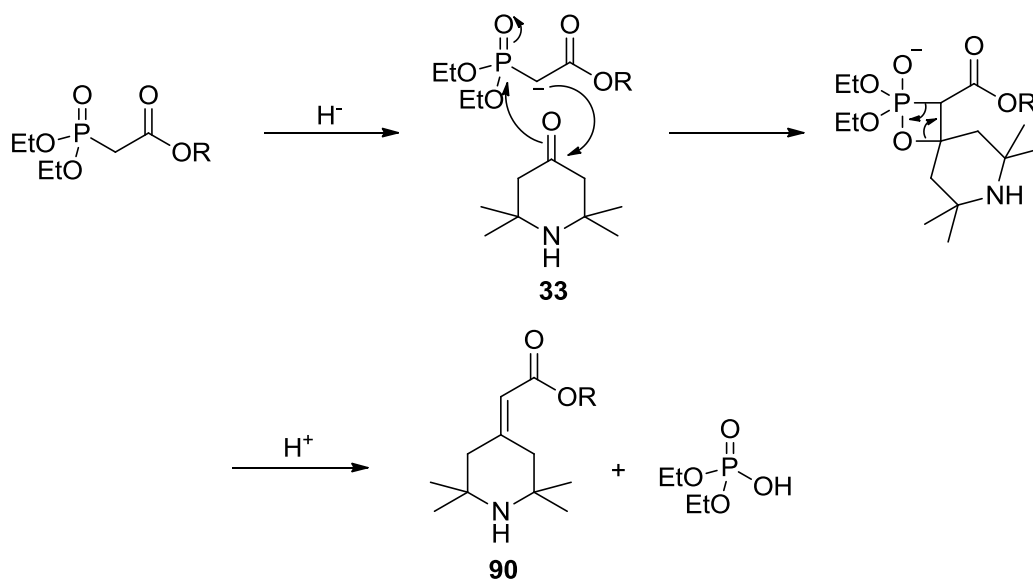


Figure 4.8: Mechanism of the HWE of triacetoneamine (**33**).

The ester produced by this reaction could be easily hydrolysed to the equivalent carboxylic acid and form the anion of a nitroxide ionic liquid (Figure 4.9).

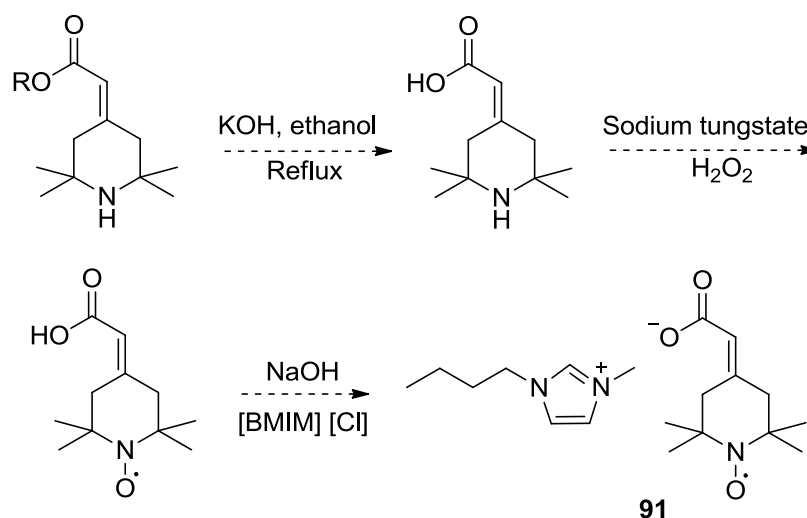


Figure 4.9: Proposed route for the formation of **91**.

Initial studies showed that the HWE step was viable although the yields were relatively low at only 29% (Figure 4.10). One possible reason for the low yield is the deprotonation of the amine competing for the 1 equivalent of sodium hydride available but since the pK<sub>a</sub> of the phosphonoacetate (~18.6) is so much lower than the pK<sub>a</sub> of the triacetoneamine (**33**) (~37) this seems unlikely to have much of an effect.<sup>153</sup>



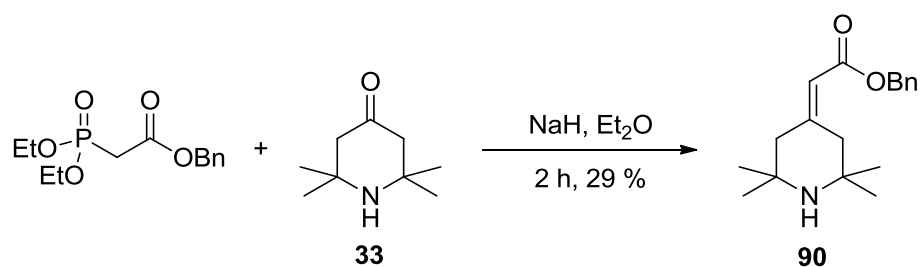


Figure 4.10: HWE of triacetoneamine (**33**).

In order for this synthesis to be a viable alternative to carboxy TEMPO this reaction will require some optimisation to increase the yield.

It still remains for the oxidation of the amine to a nitroxide and the subsequent ion pairing to be attempted.

## **5. Kinetic Resolution of Secondary Alcohols**

## 5. Kinetic Resolution of Secondary Alcohols

### 5.1. Introduction

Chiral molecules have long been of major interest due to their importance in biological systems and therefore the need for enantiomerically pure pharmaceuticals and agrichemicals. One method by which an enantiomerically pure compound can be obtained is kinetic resolution which involves submitting a racemic sample to conditions which result in the reaction of one enantiomer, leaving the other unchanged. For example in 2012 Birman et al. performed the kinetic resolution of secondary alcohols using catalysts derived from amidine (Figure 5.1).<sup>154</sup>

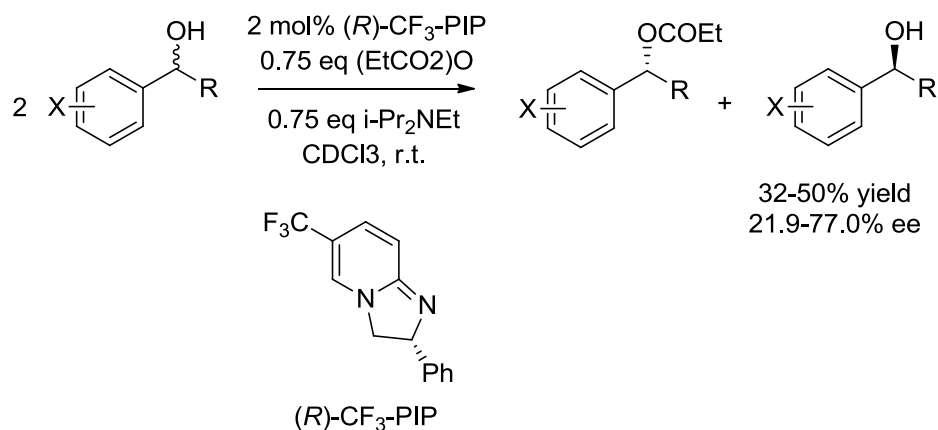


Figure 5.1: Kinetic resolution of secondary alcohols by (R)-CF<sub>3</sub>-PIP.

The disadvantage of this approach is that the maximum yield that can be achieved is 50% and therefore a kinetic resolution step should always come early in a synthetic sequence in order to reduce the impact of the low yielding step.

### 5.2. Kinetic Resolution

#### 5.2.1. Camphorsulfonic Acid

Reactions were carried out to determine if an *R*-camphorsulfonate counterion to TEMPO oxoammonium **35** could convey enantioselectivity on the oxidation of racemic 1-phenylethanol. The ion pair (**92**) was synthesised in situ by disproportionation of TEMPO using camphorsulfonic acid (Figure 5.2).<sup>155</sup>

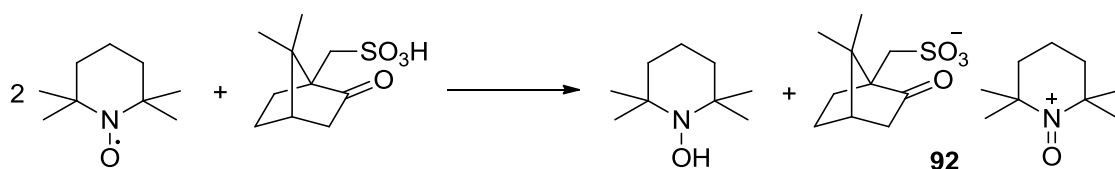


Figure 5.2: Formation of oxoammonium/camphorsulfonate ion pair (**92**) by disproportionation of TEMPO.

It was hoped that the oxoammonium/sulfonate ion pair (**92**) would selectively oxidise one enantiomer of 1-phenylethanol (**93**) into acetophenone leaving behind enantioenriched 1-phenylethanol (**93**) (Figure 5.3).

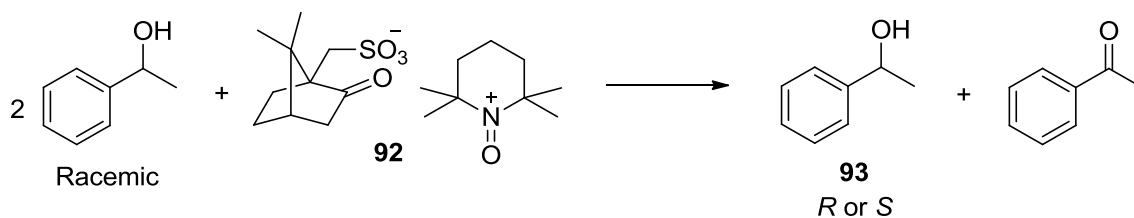
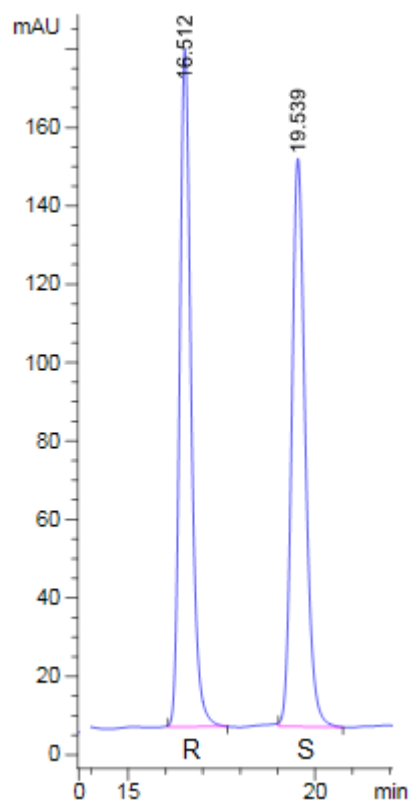


Figure 5.3: Scheme for the kinetic resolution of 1-phenylethanol (**93**).

Oxidations performed with the oxoammonium/sulfonate ion pair **92** in acetonitrile showed no stereoselectivity, leaving behind a racemic mixture of 1-phenylethanol as determined by chiral HPLC (Figure 5.4).



*Figure 5.4: Chiral HPLC trace of 1-phenylethanol (**93**). ee = 0.1%. Chiralcel OD-H column (95:5 hexane:IPA, 0.5 mL/min). R and S assignments determined by use of commercial (S)-1-phenylethanol.*

One possible reason for the lack of chiral induction could be that the oxoammonium and the camphorsulfonate are not forming a close ion pair which would reduce the impact of the chiral centre on the sulfonate. In order to try and resolve this, less polar solvents were used to encourage a stronger and therefore shorter ionic bond (Table 5.1).

Table 5.1: Yields and enantiomeric excesses of chiral oxidations.

Entry	Solvent	Isolated Yield of <b>93</b> (%)	ee (%) <sup>a</sup>
1	Acetonitrile	38	0.1
2	DCM	26	1.4
3	Toluene	28	2.0

Conditions: 1-Phenylethanol (**93**) (1 eq), TEMPO (1 eq) and R-camphorsulfonic acid for 24 h.

Table 5.1 shows that changing the polarity of the solvent appears to have slightly improved the ee but certainly not by any significant amount.

It was thought that the excess of camphor sulfonic acid used in the oxidation reactions could be racemizing the 1-phenylethanol, via an S<sub>N</sub>1 mechanism as shown in Figure 5.5.

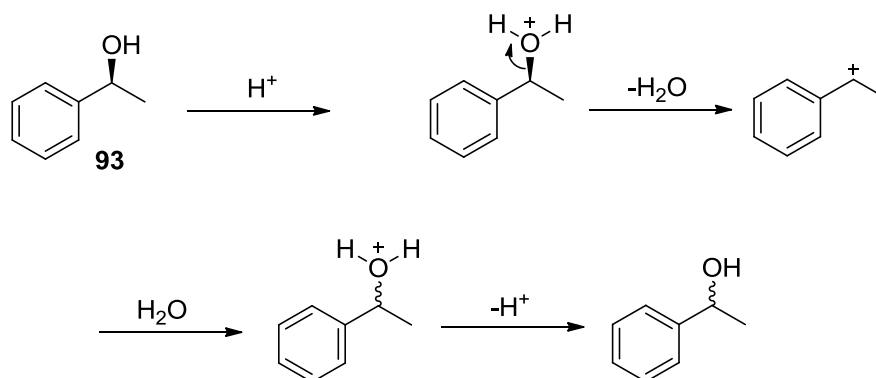


Figure 5.5: Acid catalysed racemization of (S)-1-phenylethanol.

In order to test this, (S)-1-phenylethanol was stirred with camphorsulfonic acid in acetonitrile for 2 h and the product analysed by chiral HPLC. After 2 h the enantiomeric excess had decreased from >99% to 76% demonstrating that 1-phenylethanol can be racemized by camphorsulfonic acid.

Overall it seems that the oxoammonium/sulfonate ion pair **92** is not conferring enantioselectivity to the oxidation process. This could be due to the fact that the chiral centre is possibly too far away from the oxoammonium active site to have a

significant impact and any enantiomeric excess that is achieved is at least partially undone by camphorsulfonic acid catalysed racemization.

### 5.2.2. Ionic Liquids

As an alternative to camphorsulfonate, chiral ionic liquids were considered as a possible way of creating a chiral environment which could enable the kinetic resolution of 1-phenylethanol by TEMPO mediated oxidation.<sup>156</sup> Using a chiral solvent means there will be a large excess of the chiral agent present in the reaction mixture and the racemization issues associated with camphorsulfonic acid should not be a problem.

Probably the easiest way to synthesise a chiral ionic liquid is to use a deprotonated amino acid as the anion coupled with a suitable cation. In this case the known ionic liquid [BMIM][Leu] (**94**) was chosen for the initial testing of the concept. [BMIM][Leu] (**94**) is formed from leucine, one of the simplest and least functionalised amino acids and 1-butyl-3-methylimidazolium (Figure 5.6).<sup>157</sup>

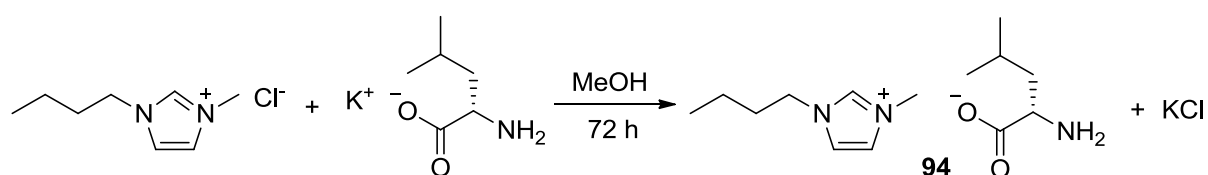


Figure 5.6: Synthesis of [BMIM][Leu] (**94**) from [BMIM][Cl].

It quickly became apparent though that the oxidation of 1-phenylethanol by TEMPO oxoammonium **35** did not proceed well in [BMIM][Leu] (**94**), even at elevated temperatures or when mixed with water or DMF (Table 5.2).

Table 5.2: Oxidation of 1-phenylethanol by oxoammonium **35** in ionic liquids.

Entry	Chiral Solvent	Temperature	Isolated Yield of <b>93</b> (%)
1	[BMIM][Leu]	r.t.	9
2	[BMIM][Leu]	60 °C	3
3	50% [BMIM][Leu]/H <sub>2</sub> O	r.t.	2
4	50% [BMIM][Leu]/DMF	r.t.	3

Conditions: 1-Phenylethanol (**93**) (1 eq), oxoammonium **35** (0.5 eq) in chiral solvent for 24 h.

The same reaction carried out in [BMIM][BF<sub>4</sub>] gave a respectable yield of 57% suggesting that the anion is causing the problem since the imidazolium ion is clearly compatible with the oxidation process. It was thought that the lone pair on leucine's nitrogen, as the only functional group, could be interfering with the reaction. In order to test this idea, two novel protected leucine ionic liquids (**95** and **96**) were synthesised (Figure 5.7).

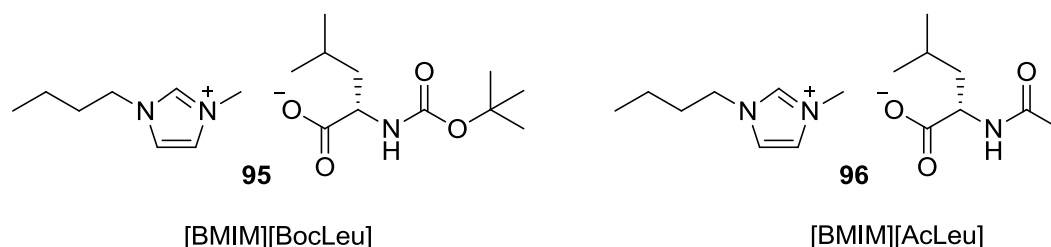


Figure 5.7: Structure of [BMIM][BocLeu] and [BMIM][AcLeu].

[BMIM][BocLeu] (**95**) turned out to be solid at temperatures up to 100 °C and had to be dissolved in DMF (50% at 100 °C) and used as a mixture at 60 °C. Both of the protected leucine ionic liquids suffered from the same lack of yield of **93** observed for the unprotected version (Table 5.3).



Table 5.3: Oxidation of 1-phenylethanol in protected amino acid ionic liquids.

Entry	Solvent	Temperature	Yield (%)
1	50% [BMIM][BocLeu] ( <b>95</b> )/DMF	60 °C	3
2	[BMIM][AcLeu] ( <b>96</b> )	r.t.	1

In order to test the suitability of carboxylate based ionic liquids, the reaction was performed in a simpler solvent, namely [BMIM][AcO] (**97**) (Figure 5.8).<sup>158</sup>

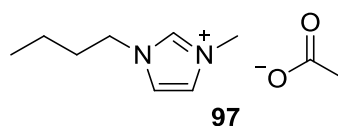


Figure 5.8: Structure of [BIMIM][AcO] (**97**).

No product was observed leading to the conclusion that ionic liquids with a carboxylate as the anion are not compatible with the oxidation of alcohols by TEMPO oxoammonium (**35**).

In conclusion the kinetic resolution of 1-phenylethanol (**93**) via TEMPO mediated oxidation with camphorsulfonate as a chiral auxiliary or in leucine based ionic liquids has been unsuccessful, however a novel acetyl protected amino acid ionic liquid ([BMIM][AcLeu]) (**96**) has been developed.

## **6. Conclusions**

## 6. Conclusions

### 6.1 Acetal Oxidation

The work on the oxidation of acetals has shown that TEMPO/MgBr<sub>2</sub> is capable of oxidising a variety of acetals to benzoate esters in moderate to good yields at room temperature. The oxidation is mild, non-hazardous and does not appear to be particularly sensitive to air or water, making it fairly robust. The mechanism of the acetal oxidation has been investigated and two possible radical routes have been identified on the basis of literature precedent and the regioselectivity of a certain oxidation. Preliminary studies of TEMPO/LA mixtures by EPR have not shown any evidence of complexes forming in solution contrary to our initial assumptions. A screen of different Lewis acids has shown that others are capable of performing similar oxidations under the same conditions but as of yet these have not been fully explored.

### 6.2 Phosphorus Hydrides

TEMPO has also been shown to act as a radical initiator for phosphorus hydrides, although so far this is limited to diphenylphosphine sulfide (**69**). TEMPO is considerably easier to handle and safer than more traditional initiators such as AIBN and Et<sub>3</sub>B and allows reactions to take place under very mild conditions. TEMPO initiated diphenylphosphine sulfide was successfully added to several alkenes and alkynes and used in C-C bond forming reactions in the form of radical cyclisations. The mechanism for all these reactions is believed to be the same radical mechanism observed with other initiators in similar reactions. An excess of TEMPO has been shown to inhibit the addition of phosphine radicals to alkenes and is believed to be the result of the formation of a phosphine/TEMPO adduct although this has yet to be confirmed. In the case of additions of diphenylphosphine sulfide to Michael acceptors it has been found that radical initiators are not necessary and will proceed at room temperature with moderate to good yields. It is not currently clear what the mechanism of this addition is, but it thought that it is unlikely to be radical.

### 6.3 TEMPO Ionic Liquids

The novel ionic liquid [BMIM][carboxy-TEMPO] (**89**) was successfully synthesised and used to oxidise a primary alcohol. Although in the early stages of investigation, this new compound shows promise as a recyclable catalyst which could be used in conjunction with ionic liquid solvents to create environmentally friendly analogues of existing oxidation processes. Work has also begun on creating a similar ionic liquid via a Horner-Wadsworth-Emmons reaction, potentially providing an easier, cheaper and higher yielding synthetic route.

### 6.4 Kinetic Resolution of Secondary Alcohols

Attempts were made to perform the kinetic resolution of 1-phenylethanol (**93**) by oxidising one enantiomer with TEMPO in the presence of a chiral auxiliary. Camphorsulfonate proved to convey no chiral selectivity to the oxidation reaction and reactions carried out in leucine based ionic liquids did not proceed at all. In the course of these investigations however, a novel protected amino acid ionic liquid ([BMIM][AcLeu]) was developed (**96**) as well as [BMIM][BocLeu] (**95**) a novel solid.

## **7. Future Work**

## 7. Future Work

Although this thesis has brought to light some interesting reactions it is by no means comprehensive and there is much work that can be done to expand on the ideas introduced by these projects.

### 7.1 Acetal Oxidation

The oxidation of acetals by TEMPO/MgBr<sub>2</sub> is only one example of many Lewis acids which could be used to catalyse this reaction, some of which have been explored in this thesis. Stronger Lewis acids than MgBr<sub>2</sub> would be expected to act as better catalysts and reduce reaction times and/or increase yields. Lewis acids which are soluble in organic solvents or form soluble complexes with acetals or TEMPO would eliminate the inherent problems of heterogeneous catalysis such as the high Lewis acid stoichiometry due to low surface area. An ideal situation would be to find a Lewis acid capable of catalysing the both the synthesis of acetals and their oxidation to esters in one pot (Figure 7.1).

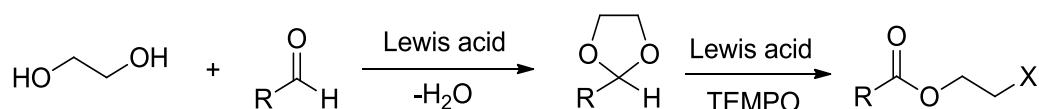


Figure 7.1: One pot TEMPO/Lewis acid mediated synthesis of esters from aldehydes.

The introduction of a mild stoichiometric oxidising agent could possibly regenerate TEMPO from hydroxylamine (**36**) in a similar way to the regeneration of the oxoammonium (**35**) from hydroxylamine (**36**) in TEMPO-mediated alcohol oxidations (Figure 7.2).

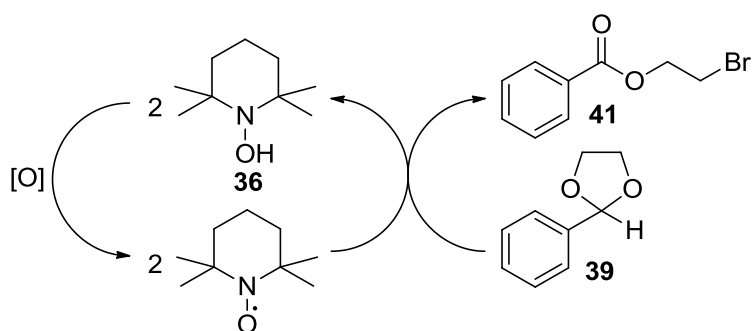


Figure 7.2: Oxidation of acetals to esters with catalytic TEMPO.

This would replace the two equivalents of TEMPO with a cheaper oxidising agent. The challenge here is to find an oxidising agent which is capable of regenerating TEMPO from the hydroxylamine (**36**) without over oxidation to the oxoammonium (**35**) which is not the active reagent in this system.

## 7.2 Phosphorus Hydrides

One of the uses for phosphane sulfides is to perform HWE reactions which have been shown to proceed in one pot with the addition step.<sup>6</sup> In order for TEMPO to compete with AIBN or Et<sub>3</sub>B as an initiator in these reactions it is important that it is compatible with these one-pot additions/HWE reactions (Figure 7.3).

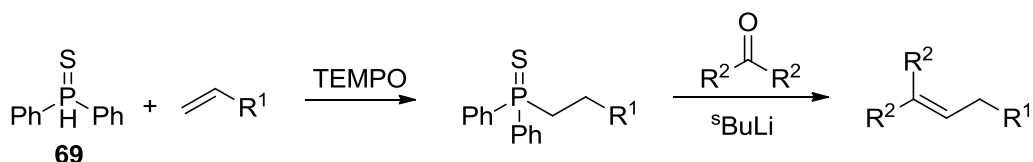


Figure 7.3: One pot TEMPO initiated phosphorous hydride addition and HWE reaction.

This Thesis has covered the use of TEMPO as an initiator for the addition of phosphorus hydrides to alkenes and alkynes but there is much more chemistry that phosphorus hydrides are capable of performing as discussed in the introduction. Being able to use TEMPO as an initiator not only for addition reactions but reductions of functional groups could see it as a commonly accepted replacement for AIBN and Et<sub>3</sub>B. Diphenylphosphine sulfide (**69**) is not a commonly used reagent for functional group reductions and may not be suitable for these sorts of reactions

so further investigation into the types of phosphorus hydride that TEMPO can initiate would also prove to be beneficial.

### 7.3 TEMPO Ionic Liquids

The ionic liquid [BMIM][Carboxy-TEMPO] (**89**) has been shown in an initial test to oxidise benzyl alcohol in [BMIM][BF<sub>4</sub>] and has also been shown to be recyclable at least to some degree. The next stage here is clearly to try and optimise the yield of this reaction, to demonstrate its scope, in particular with alcohols with poor solubility in organic solvents, and to improve the method of recycling and demonstrate its effectiveness over several iterations.

Compound **90**, the intermediate on route to the other ionic liquid needs to be hydrolysed, oxidised to a nitroxide and coupled with a suitable counterion such as [BMIM] (Figure 7.4) so its effectiveness as a catalyst can be determined.

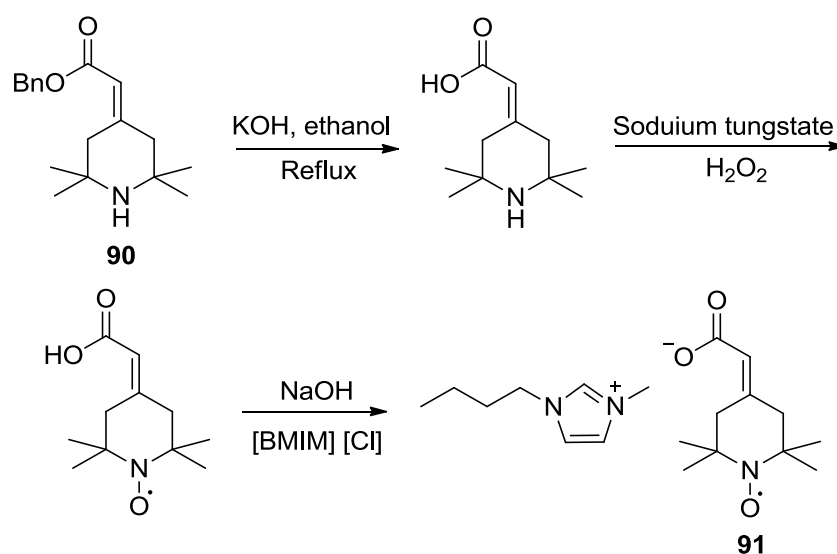


Figure 7.4: Route to ionic liquid **91**.

### 7.4 Kinetic Resolution of Secondary Alcohols

Although the kinetic resolution of 1-phenylethanol was unsuccessful, the acetyl protected amino acid based ionic liquid [BMIM][AcLeu] (**96**) or similar ionic liquids based on other amino acids could be used as chiral solvents/auxiliaries in different reactions where the presence of a free amine is undesirable.



## **8. Experimental**

## 8. Experimental

### 8.1. General Methods

All reagents were used as purchased unless otherwise stated. Dry solvents (DCM, diethyl ether, DMF, hexane, THF and toluene) were obtained from a Pure Solv solvent purification system.

TLC was performed using Merck aluminium backed 0.2 mm Kieselgel 60 (F<sub>254</sub>) pre-coated plates. Spot visualisation was achieved through the use of UV irradiation (254 nm) and staining with KMnO<sub>4</sub> followed by heating. Flash column chromatography was performed on Fluka 60 (F<sub>254</sub>) silica gel, with the column pre-loaded with a solvent-silica slurry.

NMR spectra were recorded on a Jeol ECX 400 (<sup>1</sup>H, 400 MHz; <sup>31</sup>P, 131 MHz; <sup>13</sup>C, 100 MHz). Chemical shifts are reported in parts per million (ppm) downfield of trimethylsilane with residual solvent acting as the internal standard. Coupling constants (*J*) are reported to the nearest 0.5 Hz. Assignments were based on chemical shifts and coupling constants.

Mass spectra were recorded on a Bruker Daltonics microTOF (ESI) instrument.

Infra-red spectra were recorded on a Perkin Elmer Spectrum Two FTIR fitted with a UATR Two.

Chiral stationary phase HPLC was performed on an Agilent 1200 series chromatograph. Chiralcel OD-H column (95:5 hexane:IPA, 0.5 mL/min).

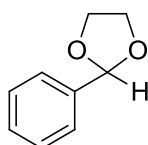
### 8.2. Acetal Oxidation

#### General Procedure 1 for acetal formation<sup>159</sup>

Aldehyde (2.0 mmol, 1 eq), diol (3.0 mmol, 1.5 eq), Ce(OTf)<sub>3</sub> (11.8 mg, 0.02 mmol, 0.01 eq), hexane (4 mL), triisopropyl orthoformate (0.67 mL, 3.0 mmol, 1.5 eq) were stirred in a round bottom flask under nitrogen at r.t. for 24 h. The reaction mixture was quenched with triethylamine (0.14 mL, 1.0 mmol, 0.5 eq) and saturated

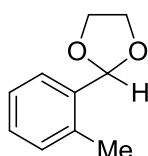
NaHCO<sub>3</sub> (5 mL). The mixture was separated and the aqueous phase extracted with diethyl ether (3 × 5 mL). The combined organic extracts were washed with saturated NaCl (5 mL), dried over MgSO<sub>4</sub> and concentrated under reduced pressure to yield crude product.

### 2-Phenyl-1,3-dioxolane (39)



Benzaldehyde (4.2 mL, 41 mmol, 1 eq), ethane-1,2-diol (5 mL, 90 mmol, 2.2 eq), *p*-toluenesulfonic acid monohydrate (0.1527 g, 0.08 mmol, 0.002 eq) and toluene (75 mL) were refluxed under Dean-Stark conditions (115°C) for 4 h. The reaction mixture was cooled, washed with saturated NaHCO<sub>3</sub> (2 × 50 mL) and brine (50 mL), dried over magnesium sulfate and concentrated under vacuum to yield **39** as a straw coloured oil (6.0 g, 98%). <sup>1</sup>H NMR (400 MHz, acetone-d<sub>6</sub>) δ<sub>H</sub> 4.00-4.08 (m, 2H, CHH'CHH'), 4.09-4.17 (m, 2 × 1H, CHH'CHH'), 5.82 (s, 1H, CH), 7.34-7.41 (m, 3H, Ph), 7.47-7.50 (m, 2H, Ph). <sup>13</sup>C NMR (100 MHz, acetone-d<sub>6</sub>) δ<sub>C</sub> 66.0 (2 × CH<sub>2</sub>), 104.4 (PhCH), 127.5 (Ph), 129.0 (Ph), 129.8 (Ph), 139.7 (Ph). ESI-MS *m/z* calcd for C<sub>9</sub>H<sub>10</sub>O<sub>2</sub> (M + H)<sup>+</sup> 151.0746, found 151.0754 (-1.2 ppm error). Spectroscopic data were consistent with the literature.<sup>160</sup>

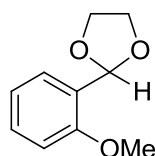
### 2-(2-Methylphenyl)-1,3-dioxolane (44)



Using General Procedure 1, 2-methylbenzaldehyde (0.23 mL, 2.0 mmol 1.0 eq), ethane-1,2-diol (0.17 mL, 3.0 mmol, 1.5 eq), Ce(OTf)<sub>3</sub> (12.1 mg, 0.02 mmol, 0.01 eq) gave crude product. The crude mixture was purified by flash column chromatography (95% hexane, 4.9% ethyl acetate, 0.1% triethylamine) to yield **44** as a straw coloured oil (47 mg, 14%). R<sub>f</sub> 0.18 (95% hexane, 5% ethyl acetate). <sup>1</sup>H NMR (400 MHz, acetone-d<sub>6</sub>) δ<sub>H</sub> 2.46 (s, 3H, CH<sub>3</sub>) 4.04-4.12 (m, 2H, CHH'CHH'), 4.13-

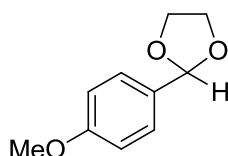
4.21 (m, 2H, CHH'CHH'), 5.97 (s, 1H, CHO<sub>2</sub>), 7.24-7.34 (m, 2H, Ph), 7.56-7.58 (m, 2H, Ph). <sup>13</sup>C NMR (100 MHz, acetone d<sub>6</sub>) δ<sub>c</sub> 19.0 (CH<sub>3</sub>), 65.8 (2 × CH<sub>2</sub>), 102.8 (CO<sub>2</sub>), 126.4 (Ph), 129.6 (Ph), 131.3 (Ph), 137.0 (Ph). Spectroscopic data were consistent with the literature.<sup>161</sup>

### 2-(2-Methoxyphenyl)-1,3-dioxolane (46)



Using General Procedure 1, 2-methoxybenzaldehyde (280 mg, 2.1 mmol 1.0 eq), ethane-1,2-diol (0.17 mL, 3.0 mmol, 1.4 eq), Ce(OTf)<sub>3</sub> (11.7 mg, 0.02 mmol, 0.01 eq) gave crude product. The crude mixture was purified by flash column chromatography (90% hexane, 9.9% ethyl acetate, 0.1% triethylamine) to yield **46** as a straw coloured oil (344 mg, 91%). R<sub>f</sub> 0.11 (90% petroleum ether, 10% ethyl acetate). <sup>1</sup>H NMR (400 MHz, acetone-d<sub>6</sub>) δ<sub>H</sub> 4.01-4.08 (m, 2H, CHH'CHH'), 4.10-4.18 (m, 2H, CHH'CHH'), 6.17 (s, 1H, CHO<sub>2</sub>), 6.91 (d, 1H, *J* = 8.5 Hz, Ph), 6.98 (t, 1H, *J* = 7.5 Hz, Ph), 7.33 (dt, 1H, *J* = 1.5 and 8.5 Hz, Ph), 7.54 (dd, 1H, *J* = 1.5 and 7.5 Hz, Ph). <sup>13</sup>C NMR (100 MHz, acetone-d<sub>6</sub>) δ<sub>c</sub> 55.9 (CH<sub>3</sub>), 65.8 (2 × CH<sub>2</sub>), 99.5 (CO<sub>2</sub>), 111.8 (Ph), 121.0 (Ph), 127.3 (Ph), 128.0 (Ph), 131.1 (Ph), 158.9 (Ph). Spectroscopic data were consistent with the literature.<sup>161</sup>

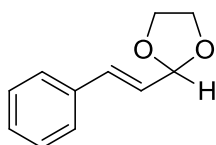
### 2-(4-Methoxyphenyl)-1,3-dioxolane (48)



Using General Procedure 1, 4-methoxybenzaldehyde (0.24 mL, 2.0 mmol 1.0 eq), ethane-1,2-diol (0.17 mL, 3.0 mmol, 1.5 eq), Ce(OTf)<sub>3</sub> (13.8 mg, 0.02 mmol, 0.01 eq) gave product **48** as a straw coloured oil without further purification (428 mg, >99%). <sup>1</sup>H NMR (400 MHz, acetone-d<sub>6</sub>) δ<sub>H</sub> 3.81 (s, 3H, CH<sub>3</sub>), 3.98-4.06 (m, 2H, CHH'CHH'), 4.09-4.17 (m, 2H, CHH'CHH'), 5.76 (s, 1H, CH), 6.91 (d, 2H, *J* = 8.5 Hz, Ph), 7.41 (d, 1H, *J* = 8.5 Hz). <sup>13</sup>C NMR (100 MHz, acetone-d<sub>6</sub>) δ<sub>c</sub> 55.6 (CH<sub>3</sub>), 65.8 (2 × CH<sub>2</sub>), 104.4

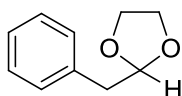
(CO<sub>2</sub>), 114.3 (Ph), 129.0 (Ph), 131.6 (Ph), 161.3 (Ph). ESI-MS *m/z* calcd for C<sub>10</sub>H<sub>12</sub>O<sub>3</sub> (M + Na)<sup>+</sup> 203.0679, found 203.0683 (-2.1 ppm error). Spectroscopic data were consistent with the literature.<sup>162</sup>

### (*E*)-2-(2-Phenylethenyl)-1,4-dioxolane (51)



Using General Procedure 1, (*E*)-cinnamaldehyde (0.25 mL, 2.0 mmol 1.0 eq), ethane-1,2-diol (0.17 mL, 3.0 mmol, 1.5 eq), Ce(OTf)<sub>3</sub> (13.8 mg, 0.02 mmol, 0.01 eq) gave crude product. The crude mixture was purified by flash column chromatography (50% hexane, 49.9% DCM, 0.1% triethylamine) to yield **51** as a yellow oil (305 mg, 87%). R<sub>f</sub> 0.24 (50% hexane, 50% DCM) <sup>1</sup>H NMR (400 MHz, acetone-*d*<sub>6</sub>) δ<sub>H</sub> 3.94-4.00 (m, 2H, CHH'CHH'), 4.01-4.08 (m, 2H, CHH'CHH'), 5.43 (dd, 1H, *J* = 1.0 and 6.0 Hz, CHO<sub>2</sub>), 6.16 (dd, 1H, *J* = 6.0 and 16.0, CCHCH), 6.77, (d, 1H, *J* = 16.0, CCHCH), 7.27-7.35 (m, 3H, Ph), 7.41-7.47 (m, 2H, Ph). <sup>13</sup>C NMR (100 MHz, CDCl<sub>3</sub>) δ<sub>C</sub> 65.6 (2 × CH<sub>2</sub>), 104.6 (CO<sub>2</sub>), 127.0 (CHCO<sub>2</sub>), 127.7 (Ph), 129.2 (Ph), 129.6 (Ph), 134.9 (PhCH), 137.1 (Ph). Spectroscopic data were consistent with the literature.<sup>163</sup>

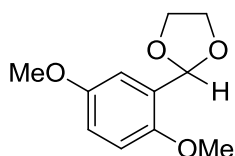
### 2-Benzyl-1,3-dioxolane (53)



Phenylacetaldehyde (1.6 mL, 14 mmol, 1 eq), ethane-1,2-diol (1.7 mL, 30 mmol, 2.2 eq), *p*-toluenesulfonic acid monohydrate (0.0500 g, 0.03 mmol, 0.002 eq) and toluene (25 mL) were refluxed under Dean-Stark conditions (115 °C) for 4 h. The reaction mixture was cooled, washed with saturated NaHCO<sub>3</sub> (2 × 50 mL) and brine (50 mL), dried over magnesium sulfate and concentrated under vacuum to yield crude **53**. The crude product was purified by flash column chromatography (50% hexane, 50% DCM) to yield **53** as a colourless oil (0.64 g, 28%). R<sub>f</sub> 0.22 (50% hexane, 50% DCM). <sup>1</sup>H NMR (400 MHz, acetone-*d*<sub>6</sub>) δ<sub>H</sub> 2.80 (d, 2H, *J* = 5.0 Hz, PhCH<sub>2</sub>), 3.80-

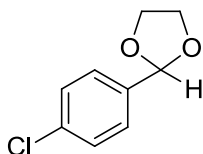
3.88 (m, 2H,  $\text{CHH}'\text{CHH}'$ ), 3.90-3.98 (m, 2H,  $\text{CHH}'\text{CHH}'$ ), 5.06 (t, 1H,  $J = 5.0$  Hz), 7.21-7.39 (m, 5H, Ph).  $^{13}\text{C}$  NMR (100 MHz,  $\text{CDCl}_3$ )  $\delta_{\text{C}}$  41.0 ( $\text{PhCH}_2$ ), 65.2 ( $\text{OCH}_2$ ), 104.9 (CH), 126.8 (Ph), 128.5 (Ph), 129.8 (Ph), 136.3 (Ph). Spectroscopic data were consistent with the literature.<sup>164</sup>

### 2-(2,5-Dimethoxyphenyl)-1,3-dioxolane (55)



Using General Procedure 1, 2,5-dimethoxybenzaldehyde (336 mg, 2.0 mmol 1.0 eq), ethane-1,2-diol (0.17 mL, 3.0 mmol, 1.5 eq),  $\text{Ce}(\text{OTf})_3$  (13.3 mg, 0.02 mmol, 0.01 eq) gave crude product. The crude mixture was purified by flash column chromatography (90% hexane, 9.9% ethyl acetate, 0.1% triethylamine) to yield **55** as a colourless oil (301 mg, 72%).  $R_f$  0.08 (90% hexane, 10% ethyl acetate)  $^1\text{H}$  NMR (400 MHz, acetone- $d_6$ )  $\delta_{\text{H}}$  3.72 (s, 3H,  $\text{CH}_3$ ), 3.76 (s, 3H,  $\text{CH}_3$ ) 3.89-3.97 (m, 2H,  $\text{CHH}'\text{CHH}'$ ), 4.02-4.10 (m, 2H,  $\text{CHH}'\text{CHH}'$ ), 5.99 (s, 1H, CH), 6.85-6.93 (m, 3H, Ph), 7.03 (d, 1H,  $J = 3.2$  Hz).  $^{13}\text{C}$  NMR (100 MHz, acetone- $d_6$ )  $\delta_{\text{C}}$  55.9 ( $\text{CH}_3$ ), 56.6 ( $\text{CH}_3$ ), 65.8 ( $2 \times \text{CH}_2$ ), 99.4 ( $\text{CO}_2$ ), 113.2 (Ph), 115.6 (Ph), 128.4 (Ph), 153.1 (Ph), 154.6 (Ph). Spectroscopic data were consistent with the literature.<sup>165</sup>

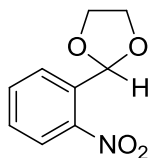
### 2-(4-Chlorophenyl)-1,3-dioxolane (57)



Using General Procedure 1, 4-chlorobenzaldehyde (285 mg, 2.0 mmol 1.0 eq), ethane-1,2-diol (0.17 mL, 3.0 mmol, 1.5 eq),  $\text{Ce}(\text{OTf})_3$  (12.9 mg, 0.02 mmol, 0.01 eq) gave crude product. The crude mixture was purified by flash column chromatography (90% hexane, 9.9% ethyl acetate, 0.1% triethylamine) to yield **57** as a colourless oil (290 mg, 79%).  $R_f$  0.19 (90% hexane, 10% ethyl acetate).  $^1\text{H}$  NMR (400 MHz, acetone- $d_6$ )  $\delta_{\text{H}}$  3.93-4.01 (m, 2H,  $\text{CHH}'\text{CHH}'$ ), 4.02-4.10 (m, 2H,  $\text{CHH}'\text{CHH}'$ ), 5.72 (s, 1H,  $\text{CHO}_2$ ), 7.37-7.41 (m, 2H, Ph), 7.44-7.48 (m, 2H, Ph).  $^{13}\text{C}$  NMR

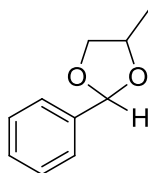
(100 MHz, acetone d<sub>6</sub>)  $\delta_c$  66.9 (2 × CH<sub>2</sub>), 104.5 (Ph), 130.1 (Ph), 136.1 (Ph), 139.6 (Ph). Spectroscopic data were consistent with the literature.<sup>161</sup>

### 2-(2-Nitrophenyl)-1,3-dioxolane (59)



2-Nitrobenzaldehyde (0.7518 g, 5.0 mmol, 1 eq), ethane-1,2-diol (1.5 mL, 27 mmol, 5.4 eq), *p*-toluenesulfonic acid monohydrate (0.0108 g, 0.06 mmol, 0.012 eq) and toluene (10 mL) were refluxed under Dean-Stark conditions (115°C) for 17 h. The reaction mixture was cooled, washed with saturated NaHCO<sub>3</sub> (5 mL). The aqueous layer was washed with DCM (3 × 5 mL). The combined organic layer were washed with brine (5 mL), dried over magnesium sulfate and concentrated under vacuum to yield **59** as a brown oil (0.95 g, 97%). <sup>1</sup>H NMR (400 MHz, CDCl<sub>3</sub>)  $\delta_H$  3.99-4.09 (m, 4H, CH<sub>2</sub>CH<sub>2</sub>), 6.49 (s, 1H, CHO<sub>2</sub>), 7.50 (td, 1H, *J* = 8.0 and 1.5 Hz, Ph), 7.62 (td, 1H, *J* = 7.5 and 1.0 Hz, Ph), 7.80 (dd, 1H, *J* = 8.0 and 1.5 Hz, Ph), 7.90 (dd, 1H, *J* = 8.0 and 1.0 Hz). <sup>13</sup>C NMR (100 MHz, CDCl<sub>3</sub>)  $\delta_c$  65.5 (2 × OCH<sub>2</sub>), 99.8 (PhCH), 124.6 (Ph), 127.8 (Ph), 129.9 (Ph), 133.1 (Ph), 149.1 (Ph). *m/z* calcd for C<sub>9</sub>H<sub>9</sub>NO<sub>4</sub> (M + Na)<sup>+</sup> 218.0424, found 218.0427 (-1.5 ppm error). Spectroscopic data were consistent with the literature.<sup>161</sup>

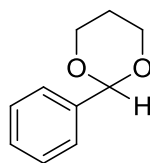
### 2-Phenyl-4-methyl-1,3-dioxolane (61)



Benzaldehyde (4.2 mL, 41 mmol, 1 eq), propane-1,2-diol (6.6 mL, 90 mmol, 2.2 eq), *p*-toluenesulfonic acid monohydrate (0.1538 g, 0.08 mmol, 0.002 eq) and toluene (75 mL) were refluxed under Dean-Stark conditions (115 °C) for 4 h. The reaction mixture was cooled, washed with saturated NaHCO<sub>3</sub> (2 × 50 mL) and brine (50 mL), dried over magnesium sulfate and concentrated under vacuum to yield product **61**

as a 1:1 mixture of diastereomers (6.8 g, 100%). Diastereomer A  $^1\text{H}$  NMR (400 MHz,  $\text{CDCl}_3$ )  $\delta_{\text{H}}$  1.36 (d, 3H,  $J = 6.0$  Hz,  $\text{CH}_3$ ), 3.57 (dd, 1H,  $J = 8$  Hz and 7.5 Hz,  $\text{OCH}_2\text{H}'$ ), 4.28 (dd, 1H,  $J = 8$  Hz and 6 Hz,  $\text{OCH}_2\text{H}'$ ), 4.37 (m, 1H,  $\text{CH}_2\text{CH}$ ), 5.97 (s, 1H,  $\text{PhCH}$ ), 7.37 (m, 3H, Ph), 7.49 (m, 2H, Ph). Diastereomer A  $^{13}\text{C}$  NMR (100 MHz, acetone- $d_6$ )  $\delta_{\text{C}}$  19.0 ( $\text{CH}_3$ ), 71.0 ( $\text{CH}_2$ ), 72.4 ( $\text{CHCH}_3$ ), 103.7 ( $\text{PhCH}$ ), 129.9 (Ph), 130.2 (Ph), 130.3 (Ph), 135.2 (Ph). Diastereomer B  $^1\text{H}$  NMR (400 MHz,  $\text{CDCl}_3$ )  $\delta_{\text{H}}$  1.41 (d, 3H,  $J = 6.0$  Hz,  $\text{CH}_3$ ), 3.62 (t, 1H,  $J = 7.5$  Hz,  $\text{OCH}_2\text{H}'$ ), 4.13 (dd, 1H,  $J = 7.5$  and 6.5 Hz,  $\text{OCH}_2\text{H}'$ ), 4.37 (m, 1H,  $\text{CH}_2\text{CH}$ ), 5.82 (s, 1H,  $\text{PhCH}$ ), 7.37 (m, 3H, Ph), 7.49 (m, 2H, Ph). Diastereomer B  $^{13}\text{C}$  NMR (100 MHz, acetone- $d_6$ )  $\delta_{\text{C}}$  18.7 ( $\text{CH}_3$ ), 65.4 ( $\text{CH}_2$ ), 71.0 ( $\text{CHCH}_3$ ), 104.7 ( $\text{PhCH}$ ), 129.9 (Ph), 130.2 (Ph), 130.3 (Ph), 135.2 (Ph). ESI-MS  $m/z$  calcd for  $\text{C}_{10}\text{H}_{12}\text{O}_2$  ( $\text{M} + \text{Na}$ ) $^+$  187.0730, found 187.0730 (0.9 ppm error). Spectroscopic data were consistent with the literature.<sup>166</sup>

### 2-Phenyl-1,3-dioxane (63)



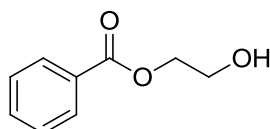
Benzaldehyde (4.2 mL, 41 mmol, 1 eq), propane-1,3-diol (6.7 mL, 90 mmol, 2.2 eq), *p*-toluenesulfonic acid monohydrate (0.1532 g, 0.08 mmol, 0.002 eq) and toluene (75 mL) were refluxed under Dean-Stark conditions (115°C) for 5 h. The reaction mixture was cooled, washed with saturated  $\text{NaHCO}_3$  (2  $\times$  50 mL) and brine (50 mL), dried over magnesium sulfate and concentrated under vacuum to yield product **63** as an off white crystalline solid (6.8 g, 100%). m.p. 37-43 °C (lit. 39-42 °C).<sup>167</sup>  $^1\text{H}$  NMR (400 MHz,  $\text{CDCl}_3$ )  $\delta_{\text{H}}$  1.43-1.48 (m, 1H,  $\text{CHH}'\text{CHH}'\text{CHH}'$ ), 2.18-2.30 (m, 1H,  $\text{CHH}'\text{CHH}'\text{CHH}'$ ), 3.97-4.03 (m, 2H,  $\text{CHH}'\text{CHH}'\text{CHH}'$ ), 4.25-4.30 (m, 2H,  $\text{CHH}'\text{CHH}'\text{CHH}'$ ), 5.51 (s, 1H, CH), 7.33-7.39 (m, 3H, Ph), 7.47-7.49 (m, 2H, Ph).  $^{13}\text{C}$  NMR (100 MHz,  $\text{CDCl}_3$ )  $\delta_{\text{C}}$  26.0 ( $\text{CH}_2\text{CH}_2\text{CH}_2$ ), 67.6 ( $\text{CH}_2\text{CH}_2\text{CH}_2$ ), 101.9 ( $\text{CO}_2$ ), 126.2 (Ph), 128.5 (Ph), 129.0 (Ph), 138.9 (Ph). Spectroscopic data were consistent with the literature.<sup>160</sup>



## General Procedure 2 for acetal oxidation

2-Phenyl-1,3-dioxolane (45  $\mu$ L, 0.33 mmol, 1 eq), TEMPO (100 mg, 0.64 mmol, 2 eq) and Lewis acid (2 eq), were stirred in toluene (5 mL) at r.t. for 17 h. The reaction mixture was quenched with H<sub>2</sub>O (5 mL), separated and the aqueous layer extracted with DCM (2  $\times$  5 mL). The combined organic layers were washed with brine (5 mL), dried over MgSO<sub>4</sub> and concentrated *in vacuo* to yield crude product. Yields (0-91%) were estimated by comparing integrations of product, starting material and side product in the <sup>1</sup>H NMR spectrum.

## 2-Hydroxyethyl benzoate (40)



R<sub>f</sub> 0.13 (50% hexane, 50% diethyl ether). <sup>1</sup>H NMR (400 MHz, CDCl<sub>3</sub>)  $\delta$ <sub>H</sub> 1.97 (s, 1H, OH), 3.94-3.98 (m, 2H, CH<sub>2</sub>OH), 4.45-4.49 (m, 2H, CO<sub>2</sub>CH<sub>2</sub>), 7.44 (t, 2H, *J* = 7.5 Hz, Ph), 7.54-7.60 (m, 1H, Ph), 8.06 (dd, 2H, *J* = 1.5 and 8.5 Hz, Ph). <sup>13</sup>C NMR (100 MHz, CDCl<sub>3</sub>)  $\delta$ <sub>C</sub> 61.2 (CH<sub>2</sub>OH), 66.5 (CO<sub>2</sub>CH<sub>2</sub>), 128.3 (Ph), 129.6 (Ph), 129.7 (Ph), 166.9 (CO<sub>2</sub>). Spectroscopic data were consistent with the literature.<sup>168</sup>

### Table 2.1, Entry 1

Using General Procedure **2**, 2-phenyl-1,3-dioxolane (45  $\mu$ L, 0.33 mmol, 1 eq), TEMPO (100 mg, 0.64 mmol, 2 eq) and boron trifluoride etherate (0.1 mL, 0.64 mmol, 2 eq) in toluene at r.t. stirred for 17 h gave crude product **40** (105.0 mg, 91% yield as indicated by <sup>1</sup>H NMR spectroscopy). Spectroscopic data were consistent with the data detailed above.

### Table 2.1, Entry 2

Using General Procedure **2**, 2-phenyl-1,3-dioxolane (45  $\mu$ L, 0.33 mmol, 1 eq), TEMPO (100 mg, 0.64 mmol, 2 eq) and iron(III) chloride (100.3 mg, 0.64 mmol, 2 eq) in toluene at r.t. stirred for 17 h gave crude product **40** (137.7 mg, 89% yield as

indicated by  $^1\text{H}$  NMR spectroscopy). Spectroscopic data were consistent with the data detailed above.

#### **Table 2.1, Entry 3**

Using General Procedure **2**, 2-phenyl-1,3-dioxolane (45  $\mu\text{L}$ , 0.33 mmol, 1 eq), TEMPO (100 mg, 0.64 mmol, 2 eq) and aluminium chloride (88.2 mg, 0.64 mmol, 2 eq) in toluene at r.t. stirred for 17 h gave crude product **40** (186.4 mg, 86% yield as indicated by  $^1\text{H}$  NMR spectroscopy). Spectroscopic data were consistent with the data detailed above.

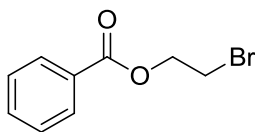
#### **Table 2.1, Entry 4**

Using General Procedure **2**, 2-phenyl-1,3-dioxolane (45  $\mu\text{L}$ , 0.33 mmol, 1 eq), TEMPO (100 mg, 0.64 mmol, 2 eq) and copper(II) triflate (232.7 mg, 0.64 mmol, 2 eq) in toluene at r.t. stirred for 17 h gave crude product **40** (160.8 mg, 86% yield as indicated by  $^1\text{H}$  NMR spectroscopy). Spectroscopic data were consistent with the data detailed above.

#### **General Procedure 3 for oxidation of acetals**

2-Phenyl-1,3-dioxolane (0.32 mmol, 1 eq), TEMPO (1, 2 or 3 eq) and magnesium bromide (1, 2, 3, 4 or 8 eq), were stirred in dry, degassed toluene, DCM, diethyl ether, THF, acetonitrile or hexane (5 mL) at r.t. or 50  $^\circ\text{C}$  under argon for 4, 8, 17 or 24 h. The reaction mixture was quenched with  $\text{H}_2\text{O}$  (5 mL), separated and the aqueous layer extracted with ethyl acetate (2  $\times$  5 mL). The combined organic layers were washed with brine (5 mL), dried over  $\text{MgSO}_4$  and concentrated *in vacuo* to yield crude product. Yields were calculated by  $^1\text{H}$  NMR spectroscopy in  $\text{CDCl}_3$  with dry DMF as an internal standard.

## 2-Bromoethyl benzoate (**41**)



$R_f$  0.14 (97.5% Hexane, 2.5% Et<sub>2</sub>O). <sup>1</sup>H NMR (400 MHz, CDCl<sub>3</sub>)  $\delta_H$  8.05-8.08 (m, 2H, Ph), 7.58 (tt, 1H,  $J = 7.5$  and 1.0 Hz, Ph), 7.45 (t, 2H,  $J = 7.5$  Hz, Ph), 4.63 (t, 2H,  $J = 6.0$  Hz, CO<sub>2</sub>CH<sub>2</sub>), 3.64 (t,  $J = 6.0$  Hz, CH<sub>2</sub> Br). <sup>13</sup>C NMR (100 MHz, CDCl<sub>3</sub>)  $\delta_C$  166.1 (CO<sub>2</sub>), 133.3 (Ph), 129.7 (Ph), 129.6 (Ph), 128.4 (Ph), 64.2 (CO<sub>2</sub>CH<sub>2</sub>), 28.8 (CH<sub>2</sub>Br). ESI-MS  $m/z$  calcd for C<sub>9</sub>H<sub>9</sub><sup>79</sup>BrO<sub>2</sub> (M + Na)<sup>+</sup> 250.9678, found 250.9684 (-2.4 ppm error). Spectroscopic data were consistent with the literature.<sup>169</sup>

### Table 2.1, Entry 5

Using General Procedure **2**, 2-phenyl-1,3-dioxolane (45  $\mu$ L, 0.33 mmol, 1 eq), TEMPO (100 mg, 0.64 mmol, 2 eq) and magnesium bromide (125.5 mg, 0.68 mmol, 2 eq) in toluene at r.t. stirred for 17 h gave crude product **41** (127.7 mg, 67% yield as indicated by <sup>1</sup>H NMR spectroscopy). Spectroscopic data were consistent with the data detailed above.

### Table 2.2, Entry 1; Table 2.6, Entry 2; Table 2.7, Entry 2; 2.8, Entry 2 and Table 2.12, Entry 1

Using General Procedure **3**, 2-phenyl-1,3-dioxolane (45  $\mu$ L, 0.33 mmol, 1 eq), TEMPO (100.5 mg, 0.64 mmol, 2 eq) and magnesium bromide (119.1 mg, 0.64 mmol, 2 eq) in toluene at r.t. stirred for 17 h gave crude product **41** (379.1 mg, 59% yield as indicated by <sup>1</sup>H NMR spectroscopy). Spectroscopic data were consistent with the data detailed above.

### Table 2.2, Entry 2 and Table 2.12, Entry 2

2-Phenyl-1,3-dioxolane (0.22 mL, 1.6 mmol, 1 eq), TEMPO (500.5 mg, 3.2 mmol, 2 eq) and magnesium bromide (591.8 mg, 3.2 mmol, 2 eq), were stirred in dry, degassed toluene (25 mL) at r.t. under argon for 17 h. The reaction mixture was quenched with H<sub>2</sub>O (25 mL), separated and the aqueous layer extracted with ethyl

acetate (2 × 25 mL). The combined organic layers were washed with brine (25 mL), dried over MgSO<sub>4</sub> and concentrated *in vacuo* to yield crude product **41** (636.8 mg, 42% yield as indicated by <sup>1</sup>H NMR spectroscopy). Yield was calculated by <sup>1</sup>H NMR in CDCl<sub>3</sub> with dry DMF as an internal standard. The crude mixture was purified by flash column chromatography (97.5% hexane, 2.5% diethyl ether) to yield **41** as colourless oil (135.6 mg, 37%). Spectroscopic data were consistent with the data detailed above.

**Table 2.4, Entry 1; Table 2.5, Entry 1 and Table 2.10, Entry 1**

Using General Procedure **3**, 2-phenyl-1,3-dioxolane (45 μL, 0.33 mmol, 1 eq), TEMPO (100.1 mg, 0.64 mmol, 2 eq) and magnesium bromide (118.6 mg, 0.64 mmol, 2 eq) in toluene at r.t. stirred for 17 h gave crude product **41** (144.5 mg, 50% yield as indicated by <sup>1</sup>H NMR spectroscopy). Spectroscopic data were consistent with the data detailed above.

**Table 2.4, Entry 2**

2-Phenyl-1,3-dioxolane (45 μL, 0.33 mmol, 1 eq), TEMPO oxoammonium chloride (122.6 mg, mmol, eq) and magnesium bromide (118.4 mg, 0.32 mmol, 2 eq), were stirred in dry, degassed toluene (5 mL) at r.t. under argon for 17 h. The reaction mixture was quenched with H<sub>2</sub>O (5 mL), separated and the aqueous layer extracted with ethyl acetate (2 × 5 mL). The combined organic layers were washed with brine (5 mL), dried over MgSO<sub>4</sub> and concentrated *in vacuo* to yield crude product **41** (72.9 mg, 22% yield as indicated by <sup>1</sup>H NMR spectroscopy). Yield was calculated by <sup>1</sup>H NMR in CDCl<sub>3</sub> with dry DMF as an internal standard. Spectroscopic data were consistent with the data detailed above.

**Table 2.5, Entry 2**

Using General Procedure **3**, 2-phenyl-1,3-dioxolane (45 μL, 0.33 mmol, 1 eq), TEMPO (100.1 mg, 0.64 mmol, 2 eq) and magnesium bromide (118.4 mg, 0.64 mmol, 2 eq) in toluene at r.t. stirred for 17 h gave crude product **41** (106.7 mg, 45% yield as indicated by <sup>1</sup>H NMR spectroscopy). Spectroscopic data were consistent with the data detailed above.

**Table 2.5, Entry 3**

Using General Procedure **3**, 2-phenyl-1,3-dioxolane (45  $\mu$ L, 0.33 mmol, 1 eq), TEMPO (100.0 mg, 0.64 mmol, 2 eq) and magnesium bromide (118.1 mg, 0.64 mmol, 2 eq) in diethyl ether at r.t. stirred for 17 h gave crude product **41** (135.9 mg, 33% yield as indicated by  $^1\text{H}$  NMR spectroscopy). Spectroscopic data were consistent with the data detailed above.

**Table 2.5, Entry 4**

Using General Procedure **3**, 2-phenyl-1,3-dioxolane (45  $\mu$ L, 0.33 mmol, 1 eq), TEMPO (100.5 mg, 0.64 mmol, 2 eq) and magnesium bromide (118.4 mg, 0.64 mmol, 2 eq) in THF at r.t. stirred for 17 h gave crude product **41** (100.3 mg, 5% yield as indicated by  $^1\text{H}$  NMR spectroscopy). Spectroscopic data were consistent with the data detailed above.

**Table 2.5, Entry 5**

Using General Procedure **3**, 2-phenyl-1,3-dioxolane (45  $\mu$ L, 0.33 mmol, 1 eq), TEMPO (100.1 mg, 0.64 mmol, 2 eq) and magnesium bromide (118.4 mg, 0.64 mmol, 2 eq) in acetonitrile at r.t. stirred for 17 h gave crude product **41** (100.3 mg, 4% yield as indicated by  $^1\text{H}$  NMR spectroscopy). Spectroscopic data were consistent with the data detailed above.

**Table 2.5, Entry 6**

Using General Procedure **3**, 2-phenyl-1,3-dioxolane (45  $\mu$ L, 0.33 mmol, 1 eq), TEMPO (100.1 mg, 0.64 mmol, 2 eq) and magnesium bromide (118.4 mg, 0.64 mmol, 2 eq) in hexane at r.t. stirred for 17 h gave crude product **41** (116.3 mg, 4% yield as indicated by  $^1\text{H}$  NMR spectroscopy). Spectroscopic data were consistent with the data detailed above.

**Table 2.6, Entry 1**

Using General Procedure **3**, 2-phenyl-1,3-dioxolane (45  $\mu$ L, 0.33 mmol, 1 eq), TEMPO (50.4 mg, 0.32 mmol, 1 eq) and magnesium bromide (59.4 mg, 0.32 mmol, 1

eq) in toluene at r.t. stirred for 17 h gave crude product **41** (105.7 mg, 25% yield as indicated by  $^1\text{H}$  NMR spectroscopy). Spectroscopic data were consistent with the data detailed above.

**Table 2.6, Entry 3**

Using General Procedure **3**, 2-phenyl-1,3-dioxolane (45  $\mu\text{L}$ , 0.33 mmol, 1 eq), TEMPO (150.7 mg, 0.96 mmol, 3 eq) and magnesium bromide (177.6 mg, 0.96 mmol, 3 eq) in toluene at r.t. stirred for 17 h gave crude product **41** (182.1 mg, 74% yield as indicated by  $^1\text{H}$  NMR spectroscopy). Spectroscopic data were consistent with the data detailed above.

**Table 2.7, Entry 1**

Using General Procedure **3**, 2-phenyl-1,3-dioxolane (45  $\mu\text{L}$ , 0.33 mmol, 1 eq), TEMPO (50.1 mg, 0.32 mmol, 1 eq) and magnesium bromide (118.9 mg, 0.64 mmol, 2 eq) in toluene at r.t. stirred for 17 h gave crude product **41** (87.2 mg, 46% yield as indicated by  $^1\text{H}$  NMR spectroscopy). Spectroscopic data were consistent with the data detailed above.

**Table 2.7, Entry 3**

Using General Procedure **3**, 2-phenyl-1,3-dioxolane (45  $\mu\text{L}$ , 0.33 mmol, 1 eq), TEMPO (150.6 mg, 0.96 mmol, 3 eq) and magnesium bromide (118.6 mg, 0.64 mmol, 2 eq) in toluene at r.t. stirred for 17 h gave crude product **41** (365.5 mg, 50% yield as indicated by  $^1\text{H}$  NMR spectroscopy). Spectroscopic data were consistent with the data detailed above.

**Table 2.8, Entry 1**

Using General Procedure **3**, 2-phenyl-1,3-dioxolane (45  $\mu\text{L}$ , 0.33 mmol, 1 eq), TEMPO (100.4 mg, 0.64 mmol, 2 eq) and magnesium bromide (59.6 mg, 0.32 mmol, 1 eq) in toluene at r.t. stirred for 17 h gave crude product **41** (212.2 mg, 37% yield as indicated by  $^1\text{H}$  NMR spectroscopy). Spectroscopic data were consistent with the data detailed above.

**Table 2.8, Entry 3**

Using General Procedure **3**, 2-phenyl-1,3-dioxolane (45  $\mu$ L, 0.33 mmol, 1 eq), TEMPO (100.4 mg, 0.64 mmol, 1 eq) and magnesium bromide (177.2 mg, 0.96 mmol, 3 eq) in toluene at r.t. stirred for 17 h gave crude product **41** (244.0 mg, 72% yield as indicated by  $^1\text{H}$  NMR spectroscopy). Spectroscopic data were consistent with the data detailed above.

**Table 2.8, Entry 4**

Using General Procedure **3**, 2-phenyl-1,3-dioxolane (47.9 mg, 0.32 mmol, 1 eq), TEMPO (100.1 mg, 0.64 mmol, 1 eq) and magnesium bromide (236.3 mg, 1.3 mmol, 4 eq) in DCM at r.t. stirred for 17 h gave crude product **41** (142.7 mg, 76% yield as indicated by  $^1\text{H}$  NMR spectroscopy). Spectroscopic data were consistent with the data detailed above.

**Table 2.8, Entry 5**

Using General Procedure **3**, 2-phenyl-1,3-dioxolane (48.1 mg, 0.32 mmol, 1 eq), TEMPO (100.4 mg, 0.64 mmol, 1 eq) and magnesium bromide (470.8 mg, 1.3 mmol, 4 eq) in DCM at r.t. stirred for 17 h gave crude product **41** (150.9 mg, 82% yield as indicated by  $^1\text{H}$  NMR spectroscopy). Spectroscopic data were consistent with the data detailed above.

**Table 2.9, Entry 1**

Using General Procedure **3**, 2-phenyl-1,3-dioxolane (45  $\mu$ L, 0.33 mmol, 1 eq), TEMPO (100.0 mg, 0.64 mmol, 2 eq) and magnesium bromide (118.0 mg, 0.64 mmol, 2 eq) in toluene at r.t. stirred for 4 h gave crude product **41** (156.8 mg, 21% yield as indicated by  $^1\text{H}$  NMR spectroscopy). Spectroscopic data were consistent with the data detailed above.

**Table 2.9, Entry 2**

Using General Procedure **3**, 2-phenyl-1,3-dioxolane (45  $\mu$ L, 0.33 mmol, 1 eq), TEMPO (100.3 mg, 0.64 mmol, 2 eq) and magnesium bromide (118.0 mg, 0.64

mmol, 2 eq) in toluene at r.t. stirred for 8 h gave crude product **41** (167.3 mg, 48% yield as indicated by <sup>1</sup>H NMR spectroscopy). Spectroscopic data were consistent with the data detailed above.

**Table 2.9, Entry 3**

Using General Procedure **3**, 2-phenyl-1,3-dioxolane (45 μL, 0.33 mmol, 1 eq), TEMPO (100.3 mg, 0.64 mmol, 2 eq) and magnesium bromide (118.4 mg, 0.64 mmol, 2 eq) in toluene at r.t. stirred for 17 h gave crude product **41** (339.4 mg, 59% yield as indicated by <sup>1</sup>H NMR spectroscopy). Spectroscopic data were consistent with the data detailed above.

**Table 2.9, Entry 4**

Using General Procedure **3**, 2-phenyl-1,3-dioxolane (45 μL, 0.33 mmol, 1 eq), TEMPO (100.2 mg, 0.64 mmol, 2 eq) and magnesium bromide (118.2 mg, 0.64 mmol, 2 eq) in toluene at r.t. stirred for 24 h gave crude product **41** (43.9 mg, 53% yield as indicated by <sup>1</sup>H NMR spectroscopy). Spectroscopic data were consistent with the data detailed above.

**Table 2.10, Entry 2**

2-Phenyl-1,3-dioxolane (45 μL, 0.33 mmol, 1 eq), TEMPO (100.0 mg, 0.64 mmol, 2 eq) and magnesium bromide (118.7 mg, 0.64 mmol, 2 eq), were stirred in dry toluene (5 mL) at r.t. under air for 17 h. The reaction mixture was quenched with H<sub>2</sub>O (5 mL), separated and the aqueous layer extracted with ethyl acetate (2 × 5 mL). The combined organic layers were washed with brine (5 mL), dried over MgSO<sub>4</sub> and concentrated *in vacuo* to yield crude product **41** (157.1 mg, 48% yield as indicated by <sup>1</sup>H NMR spectroscopy). Yield was calculated by <sup>1</sup>H NMR in CDCl<sub>3</sub> with dry DMF as an internal standard. Spectroscopic data were consistent with the data detailed above.

**Table 2.10, Entry 3**

2-Phenyl-1,3-dioxolane (45 μL, 0.33 mmol, 1 eq), TEMPO (100.4 mg, 0.64 mmol, 2 eq) and magnesium bromide (118.9 mg, 0.64 mmol, 2 eq), were stirred in dry



toluene (5 mL) degassed with O<sub>2</sub> at r.t. under O<sub>2</sub> for 17 h. The reaction mixture was quenched with H<sub>2</sub>O (5 mL), separated and the aqueous layer extracted with ethyl acetate (2 × 5 mL). The combined organic layers were washed with brine (5 mL), dried over MgSO<sub>4</sub> and concentrated *in vacuo* to yield crude product **41** (171.9 mg, 57% yield as indicated by <sup>1</sup>H NMR spectroscopy). Yield was calculated by <sup>1</sup>H NMR in CDCl<sub>3</sub> with dry DMF as an internal standard. Spectroscopic data were consistent with the data detailed above.

**Table 2.10, Entry 3**

2-Phenyl-1,3-dioxolane (45 μL, 0.33 mmol, 1 eq), TEMPO (100.1 mg, 0.64 mmol, 2 eq) and magnesium bromide (118.4 mg, 0.64 mmol, 2 eq), were stirred in toluene (5 mL) degassed with argon at r.t. under argon for 17 h. The reaction mixture was quenched with H<sub>2</sub>O (5 mL), separated and the aqueous layer extracted with ethyl acetate (2 × 5 mL). The combined organic layers were washed with brine (5 mL), dried over MgSO<sub>4</sub> and concentrated *in vacuo* to yield crude product **41** (147.1 mg, 57% yield as indicated by <sup>1</sup>H NMR spectroscopy). Yield was calculated by <sup>1</sup>H NMR in CDCl<sub>3</sub> with dry DMF as an internal standard. Spectroscopic data were consistent with the data detailed above.

**Table 2.11, Entry 1**

Using General Procedure **3**, 2-phenyl-1,3-dioxolane (45 μL, 0.33 mmol, 1 eq), TEMPO (100.5 mg, 0.64 mmol, 2 eq) and magnesium bromide (118.1 mg, 0.64 mmol, 2 eq) in toluene at r.t. stirred for 17 h gave crude product **41** (339.9 mg, 39% yield as indicated by <sup>1</sup>H NMR spectroscopy). Spectroscopic data were consistent with the data detailed above.

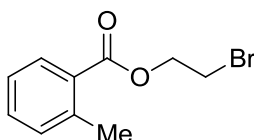
**Table 2.11, Entry 2**

Using General Procedure **3**, 2-phenyl-1,3-dioxolane (45 μL, 0.33 mmol, 1 eq), TEMPO (100.3 mg, 0.64 mmol, 2 eq) and magnesium bromide (118.0 mg, 0.64 mmol, 2 eq) in toluene at 50 °C stirred for 17 h gave crude product **41** (532.6 mg, 49% yield as indicated by <sup>1</sup>H NMR spectroscopy). Spectroscopic data were consistent with the data detailed above.

### General Procedure 4 for the oxidation of acetals

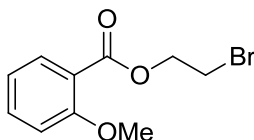
Acetal (0.32 mmol, 1 eq), TEMPO (100 mg, 0.64 mmol, 2 eq) and magnesium bromide (236 mg, 1.28 mmol, 4 eq), were stirred in DCM (5 mL) at r.t. for 17 h. The reaction mixture was quenched with H<sub>2</sub>O (5 mL), separated and the aqueous layer extracted with DCM (2 × 5 mL). The combined organic layers were washed with brine (5 mL), dried over MgSO<sub>4</sub> and concentrated *in vacuo* to yield crude product. Yields were calculated by <sup>1</sup>H NMR spectroscopy in CDCl<sub>3</sub> with dry DMF as an internal standard.

### 2-Bromoethyl 2-methylbenzoate (45)



Using General Procedure 4, 2-(2-methylphenyl)-1,3-dioxolane (52.9 mg, 0.32 mmol, 1 eq), TEMPO (100.1 mg, 0.64 mmol, 2 eq) and magnesium bromide (226.6 mg, 1.23 mmol, 4 eq) gave crude product **45** (80% NMR yield). <sup>1</sup>H NMR (400 MHz, CDCl<sub>3</sub>) δ<sub>H</sub> 2.62 (s, 3H, CH<sub>3</sub>), 3.64 (t, 2H, *J* = 6.0 Hz, CH<sub>2</sub>Br), 4.61 (t, 2H, 6.0 Hz, CO<sub>2</sub>CH<sub>2</sub>), 7.18-7.31 (m, 2H, Ph), 7.35-7.52 (m, 1H, Ph), 7.91-8.03 (m, 1H, Ph). <sup>13</sup>C NMR (100 MHz, CDCl<sub>3</sub>) δ<sub>C</sub> 21.9 (CH<sub>3</sub>), 28.9 (CH<sub>2</sub>Br), 64.0 (CO<sub>2</sub>CH<sub>2</sub>), 125.8 (Ph), 128.9 (Ph), 130.8 (Ph), 132.3 (Ph), 166.9 (CO<sub>2</sub>). ESI-MS *m/z* calcd for C<sub>10</sub>H<sub>11</sub><sup>79</sup>BrO<sub>2</sub> (M + Na)<sup>+</sup> 264.9835, found 264.9842 (-2.4 ppm error).

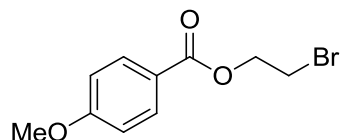
### 2-Bromoethyl 2-methoxybenzoate (47)



Using General Procedure 4, 2-(2-methoxyphenyl)-1,3-dioxolane (58.1 mg, 0.32 mmol, 1 eq), TEMPO (100.0 mg, 0.64 mmol, 2 eq) and magnesium bromide (236.3 mg, 1.28 mmol, 4 eq) gave crude product **47** (60% NMR yield). <sup>1</sup>H NMR (400 MHz, CDCl<sub>3</sub>) δ<sub>H</sub> 7.79 (d, 1H, *J* = 7.5 Hz, Ph), 7.41-7.46 (m, 1H, Ph), 6.91-6.93 (m, 2H, Ph), 4.53 (t, 2H, *J* = 5.0 Hz, CO<sub>2</sub>CH<sub>2</sub>), 3.85 (s, 3H, CH<sub>3</sub>), 3.57 (t, 2H, *J* = 5.0 Hz, CH<sub>2</sub>Br).

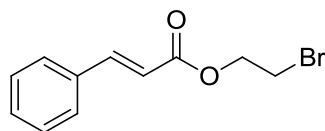
Structure was assigned based on the evidence of  $^1\text{H}$  NMR spectroscopy and reactions of similar substrates under the same conditions.

### 2-Bromoethyl 4-methoxybenzoate (**49**)



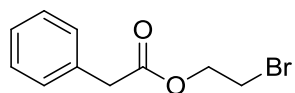
Using General Procedure **4**, 2-(4-methoxyphenyl)-1,3-dioxolane (58.1 mg, 0.32 mmol, 1 eq), TEMPO (100.4 mg, 0.64 mmol, 2 eq) and magnesium bromide (236.6 mg, 1.29 mmol, 4 eq) gave crude product **49** (54% NMR yield).  $^1\text{H}$  NMR (400 MHz,  $\text{CDCl}_3$ )  $\delta_{\text{H}}$  3.72 (bs, 2H,  $\text{CH}_2\text{Br}$ ), 3.96 (s, 3H,  $\text{CH}_3$ ), 4.69 (bs, 2H,  $\text{CO}_2\text{CH}_2$ ), 6.99-7.03 (m, 2H, Ph), 8.09-8.15 (m, 2H, Ph). Structure was assigned based on the evidence of  $^1\text{H}$  NMR spectroscopy and reactions of similar substrates under the same conditions. Spectroscopic data were consistent with the literature.<sup>169</sup>

### 2-Bromoethyl (*E*)-cinnamate (**52**)



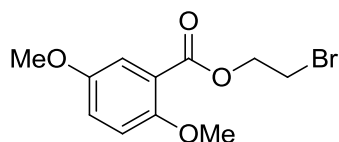
Using General Procedure **4**, (*E*)-2-(2-phenylethenyl)-1,3-dioxolane (56.5 mg, 0.32 mmol, 1 eq), TEMPO (100.0 mg, 0.64 mmol, 2 eq) and magnesium bromide (236.4 mg, 1.28 mmol, 4 eq) gave crude product **52** (47% NMR yield).  $^1\text{H}$  NMR (400 MHz,  $\text{CDCl}_3$ )  $\delta_{\text{H}}$  3.59 (t, 2H,  $J = 6.0$  Hz,  $\text{CH}_2\text{Br}$ ), 4.52 (t, 2H,  $J = 6.0$  Hz,  $\text{CO}_2\text{CH}_2$ ), 6.47 (d, 1H,  $J = 16.0$  Hz,  $\text{CHCO}_2$ ), 7.37-7.42 (m, 3H, Ph), 7.52-7.56 (m, 2H, Ph), 7.74 (d, 1H,  $J = 16.0$  Hz,  $\text{PhCH}$ ).  $^{13}\text{C}$  NMR (100 MHz,  $\text{CDCl}_3$ )  $\delta_{\text{C}}$  29.1 ( $\text{CH}_2\text{Br}$ ), 64.1 ( $\text{CO}_2\text{CH}_2$ ), 117.5 ( $\text{CHCO}_2$ ), 128.4 (Ph), 130.7 (Ph), 134.4 (Ph), 146.0 ( $\text{PhCH}$ ), 166.3 ( $\text{CO}_2$ ). ESI-MS  $m/z$  calcd for  $\text{C}_{11}\text{H}_{11}^{79}\text{BrO}_2$  ( $\text{M} + \text{Na}$ ) $^+$  276.9835, found 276.9840 (-1.9 ppm error). Spectroscopic data were consistent with the literature.<sup>170</sup>

### 2-Bromoethyl phenylacetate (**54**)



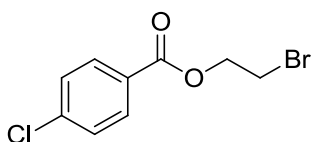
Using General Procedure **4**, 2-benzyl-1,3-dioxolane (52.8 mg, 0.32 mmol, 1 eq), TEMPO (100.0 mg, 0.64 mmol, 2 eq) and magnesium bromide (238.1 mg, 1.29 mmol, 4 eq) gave crude product **54** (27% NMR yield).  $^1\text{H}$  NMR (400 MHz,  $\text{CDCl}_3$ )  $\delta_{\text{H}}$  3.42 (t, 2H,  $J = 6.0$  Hz,  $\text{CH}_2\text{Br}$ ), 3.59 (s, 2H,  $\text{PhCH}_2$ ), 4.32 (t, 2H,  $J = 6.0$  Hz  $\text{CO}_2\text{CH}_2$ ), 7.13-7.29 (m, 5H, Ph).  $m/z$  calcd for  $\text{C}_{10}\text{H}_{11}^{79}\text{BrO}_2$  ( $\text{M} + \text{Na}$ ) $^+$  264.9835, found 264.9873 (-10.7 ppm error). Spectroscopic data were consistent with the literature.<sup>171</sup>

### 2-Bromoethyl 2,5-dimethoxybenzoate (**56**)



Using General Procedure **4**, 2-(2,5-dimethoxyphenyl)-1,3-dioxolane (69.9 mg, 0.33 mmol, 1 eq), TEMPO (100.5 mg, 0.64 mmol, 2 eq) and magnesium bromide (236.5 mg, 1.28 mmol, 4 eq) gave crude product **56** (41% NMR yield).  $^1\text{H}$  NMR (400 MHz,  $\text{CDCl}_3$ )  $\delta_{\text{H}}$  3.69 (t, 2H,  $J = 6.0$  Hz,  $\text{CH}_2\text{Br}$ ), 3.86 (s, 3H,  $\text{OCH}_3$ ), 3.93 (s, 3H,  $\text{OCH}_3$ ), 4.66 (t, 2H,  $J = 6.0$  Hz,  $\text{CO}_2\text{CH}_2$ ), 6.99 (d, 1H,  $J = 9.0$  Hz, Ph), 7.11 (dd, 1H,  $J = 9.0, 3.0$  Hz, Ph), 7.45 (d, 1H,  $J = 3.0$  Hz, Ph). Structure was assigned based on the evidence of  $^1\text{H}$  NMR and reactions of similar substrates under the same conditions.

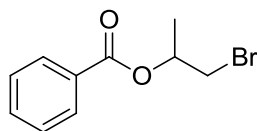
### 2-Bromoethyl 2-chlorobenzoate (**58**)



Using General Procedure **4**, 2-(4-chlorophenyl)-1,3-dioxolane (52.1 mg, 0.28 mmol, 1 eq), TEMPO (88.5 mg, 0.57 mmol, 2 eq) and magnesium bromide (208.8 mg, 1.13 mmol, 4 eq) gave crude product **58** (35% NMR yield).  $^1\text{H}$  NMR (400 MHz,  $\text{CDCl}_3$ )  $\delta_{\text{H}}$

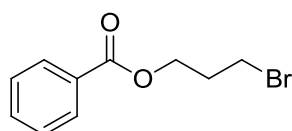
3.82 (bs, 2H, CH<sub>2</sub>Br), 4.81 (bs, 2H, CO<sub>2</sub>CH<sub>2</sub>), 7.41-7.68 (m, 4H, Ph). Structure was assigned based on the evidence of <sup>1</sup>H NMR spectroscopy and reactions of similar substrates under the same conditions. Spectroscopic data were consistent with the literature.<sup>169</sup>

### 1-Bromopropan-2-yl benzoate (**62**)



Using General Procedure **4**, 2-phenyl-4-methyl-1,3-dioxolane (52.8 mg, 0.32 mmol, 1 eq), TEMPO (100.5 mg, 0.64 mmol, 2 eq) and magnesium bromide (236.6 mg, 1.28 mmol, 4 eq) gave crude product **62** (73% NMR yield). <sup>1</sup>H NMR (400 MHz, CDCl<sub>3</sub>) δ<sub>H</sub> 7.99 (d, 2H, *J* = 7.5 Hz, Ph), 7.51 (t, 1H, *J* = 7.5 Hz, Ph), 7.38 (t, 7.0 Hz, Ph), 5.22-5.37 (m, 1H, CO<sub>2</sub>CH), 3.48-3.55 (m, 2H, CH<sub>2</sub>Br), 1.21 (d, 3H, *J* = 6.0, CH<sub>3</sub>). <sup>13</sup>C NMR (100 MHz, CDCl<sub>3</sub>) δ<sub>C</sub> 19.0 (CH<sub>3</sub>), 35.7 (CH<sub>2</sub>Br), 69.9 (CO<sub>2</sub>CH<sub>2</sub>), 128.6 (Ph), 129.9 (Ph), 130.2 (Ph), 133.4 (Ph), 166.9 (CO<sub>2</sub>). ESI-MS *m/z* calcd C<sub>10</sub>H<sub>11</sub>BrO<sub>2</sub> (M + Na)<sup>+</sup> 264.9835, found 264.9843 (-3.3 ppm error). Spectroscopic data were consistent with the literature.<sup>172</sup>

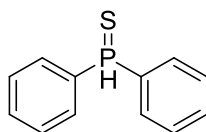
### 3-Bromopropyl benzoate (**64**)



Using General Procedure **4**, 2-phenyl-1,3-dioxane (51.8 mg, 0.32 mmol, 1 eq), TEMPO (100.0 mg, 0.64 mmol, 2 eq) and magnesium bromide (236.2 mg, 1.28 mmol, 4 eq) gave crude product **64** (19% NMR yield). <sup>1</sup>H NMR (400 MHz, CDCl<sub>3</sub>) δ<sub>H</sub> 2.33 (p, 2H, *J* = 6.5 Hz, CH<sub>2</sub>CH<sub>2</sub>CH<sub>2</sub>), 3.56 (t, 2H, *J* = 6.5 Hz, CH<sub>2</sub>Br), 4.47 (t, 2H, *J* = 6.0 Hz, CO<sub>2</sub>CH<sub>2</sub>), 7.45 (t, 2H, *J* = 7.5 Hz, Ph), 7.54-7.61 (m, 1H, Ph), 8.02-8.05 (m, 2H, Ph). <sup>13</sup>C NMR (100 MHz, CDCl<sub>3</sub>) δ<sub>C</sub> 29.7 (CH<sub>2</sub>Br), 32.1 (CH<sub>2</sub>CH<sub>2</sub>Br), 62.9 (CO<sub>2</sub>CH<sub>2</sub>), 128.6 (Ph), 129.8 (CH<sub>2</sub>), 130.2 (Ph), 133.3 (CH<sub>2</sub>), 166.6 (CH<sub>2</sub>). ESI-MS *m/z* calcd C<sub>10</sub>H<sub>11</sub><sup>79</sup>BrO<sub>2</sub> (M + Na)<sup>+</sup> 264.9835, found 264.9826 (3.7 ppm error). Spectroscopic data were consistent with the literature.<sup>173</sup>

## 8.3 Phosphorus Hydrides

### Diphenylphosphine sulfide (**69**)<sup>137</sup>



Diphenylphosphine (4.2 mL, 24 mmol, 1 eq) was added to a solution of sulfur S<sub>8</sub> (0.8772 g, 3.4 mmol, 0.14 eq) in dry, degassed toluene under N<sub>2</sub> and refluxed for 4 h. The solvent was removed *in vacuo* and the crude product recrystallized from acetonitrile to yield **69** as a white crystalline solid (4.10 g, 78%). m.p. 88-91 °C (lit. 98-99 °C).<sup>136</sup> <sup>1</sup>H NMR (400 MHz, CDCl<sub>3</sub>) δ<sub>H</sub> 7.46-7.56 (m, 6H, Ph), 7.74-7.80 (m, 4H, Ph), 7.74-7.80 (m, 4H, Ph), 8.04 (d, 1H, *J* = 544.0 Hz, PH). <sup>31</sup>P NMR (162 MHz, CDCl<sub>3</sub>) δ<sub>P</sub> 23.5 (Ph<sub>2</sub>P(S)H). <sup>13</sup>C NMR (100 MHz, CDCl<sub>3</sub>) δ<sub>C</sub> 129.0 (d, *J* = 13.0 Hz), 131.0 (d, *J* = 83.5 Hz), 131.1 (d, *J* = 11.5 Hz), 132.2 (d, *J* = 3.0 Hz). Spectroscopic data were consistent with the literature.<sup>136</sup>

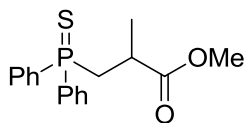
#### General Procedure 5 for the addition of diphenylphosphine sulfide to alkenes/alkynes

Alkene/alkyne (0.5 mmol, 1 eq), diphenylphosphine sulfide (327 mg, 1.5 mmol, 3 eq) and TEMPO (15.6 mg, 0.1 mmol, 0.2 eq) in dry, degassed DCM or toluene were stirred under argon for 24 h. Distilled water (5 mL) was added and the layers separated. The aqueous layer was washed with DCM (2 × 5 mL). The combined organic layers were washed with brine, dried over MgSO<sub>4</sub> and concentrated *in vacuo* to yield crude product.

#### General Procedure 6 for the addition of diphenylphosphine sulfide to alkenes

Alkene (0.5 mmol, 1 eq) and diphenylphosphine sulfide (327 mg, 1.5 mmol, 3 eq) in dry, degassed DCM or toluene were stirred under argon for 24 h. Distilled water (5 mL) was added and the layers separated. The aqueous layer was washed with DCM (2 × 5 mL). The combined organic layers were washed with brine, dried over MgSO<sub>4</sub> and concentrated *in vacuo* to yield crude product.

### Methyl 3-(diphenylphosphorothionyl)-2-methylpropanoate (**70**)



R<sub>f</sub> 0.18 (80% hexane, 20% ethyl acetate). <sup>1</sup>H NMR (400 MHz, CDCl<sub>3</sub>) δ<sub>H</sub> 1.19 (d, 3H, *J* = 4 Hz, CHCH<sub>3</sub>), 2.42-2.51 (m, 1H, CH), 3.09-3.20 (m, 2H, CH<sub>2</sub>), 3.45 (s, 3H, OCH<sub>3</sub>), 7.44-7.50 (m, 6H, Ph), 7.81-7.90 (m, 4H, Ph). <sup>31</sup>P NMR (162 MHz, CDCl<sub>3</sub>) δ<sub>P</sub> 41.3 (Ph<sub>2</sub>P(S)CH<sub>2</sub>). <sup>13</sup>C NMR (100 MHz, CDCl<sub>3</sub>) δ<sub>C</sub> 19.6 (d, *J* = 8.5 Hz, CH<sub>3</sub>CHCO<sub>2</sub>), 34.6 (CH<sub>3</sub>CH), 35.7 (d, *J* = 57.0 Hz, (P(S)CH<sub>2</sub>), 52.1 (OCH<sub>3</sub>), 128.7 (d, *J* = 12.5 Hz, Ph), 131.2 (d, *J* = 10.5 Hz, Ph), 131.5 (d, *J* = 10.5 Hz, Ph), 131.7 (d, *J* = 3.0 Hz, Ph), 131.8 (d, *J* = 3.0 Hz, Ph), 132.5 (d, *J* = 75.5 Hz, Ph), 133.3 (d, *J* = 75.5 Hz, Ph), 176.1 (d, *J* = 9.0 Hz, CO<sub>2</sub>CH<sub>3</sub>). Spectroscopic data were consistent with the literature.<sup>133</sup>

#### Table 3.1, Entry 4 and Table 3.2 Entry 1

Methyl methacrylate (0.5 mmol, 1 eq), diphenylphosphine sulfide (326.2 mg, 1.5 mmol, 3 eq), TEMPO (16.1 mg, 0.1 mmol, 0.2 eq) and MgBr<sub>2</sub> (18.7 mg, 0.1 mmol, 0.2 eq) in dry, degassed DCM were stirred under argon for 24 h. Distilled water (5 mL) was added and the layers separated. The aqueous layer was washed with DCM (2 × 5 mL). The combined organic layers were washed with brine, dried over MgSO<sub>4</sub> and concentrated *in vacuo* to yield crude product. The crude mixture was purified by flash column chromatography (80% hexane, 20% ethyl acetate) to yield **70** as a colourless oil (111.9 mg, 75%). Spectroscopic data were consistent with the data detailed above.

#### Table 3.2, Entry 2 and Table 3.3, Entry 1

Using general procedure **5**, methyl methacrylate (0.05 mL, 0.5 mmol, 1 eq), diphenylphosphine (307.7 mg, 1.4 mmol, 3 eq) and TEMPO (15.0 mg, 0.1 mmol, 0.2 eq) in DCM (2 mL) gave crude product. The crude mixture was purified by flash column chromatography (80% hexane, 20% ethyl acetate) to yield **70** as a colourless oil (163.8 mg, 100%). Spectroscopic data were consistent with the data detailed above.

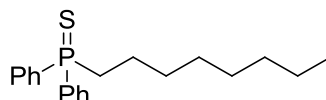
### Table 3.3, Entry 2

Methyl methacrylate (0.5 mmol, 1 eq), diphenylphosphine sulfide (109.7 mg, 0.5 mmol, 1 eq) TEMPO (4.9 mg, 0.03 mmol, 0.06 eq) in dry, degassed DCM were stirred under argon for 24 h. Distilled water (5 mL) was added and the layers separated. The aqueous layer was washed with DCM (2 × 5 mL). The combined organic layers were washed with brine, dried over MgSO<sub>4</sub> and concentrated *in vacuo* to yield crude product. The crude mixture was purified by flash column chromatography (80% hexane, 20% ethyl acetate) to yield **70** as a colourless oil (83.2 mg, 52%). Spectroscopic data were consistent with the data detailed above.

### Table 3.6 Entry 1

Using general procedure **6**, methyl methacrylate (0.05 mL, 0.5 mmol, 1 eq) and diphenylphosphine (327.0 mg, 1.5 mmol, 3 eq) in DCM (2 mL) gave crude product. The crude mixture was purified by flash column chromatography (80% hexane, 20% ethyl acetate) to yield **70** as a colourless oil (132.5 mg, 89%). Spectroscopic data were consistent with the data detailed above.

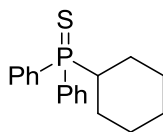
### Octyl(diphenyl)phosphane sulfide (**72**)



Using general procedure **5**, 1-octene (0.08 mL, 0.5 mmol, 1 eq), diphenylphosphine (326.8 mg, 1.5 mmol, 3 eq) and TEMPO (15.4 mg, 0.1 mmol, 0.2 eq) in DCM (2 mL) gave crude product. The crude mixture was purified by flash column chromatography (90% hexane, 10% ethyl acetate) to yield **72** as a colourless oil (160.6 mg, 95%). R<sub>f</sub> 0.20 (90% hexane, 10% diethyl ether). <sup>1</sup>H NMR (400 MHz, CDCl<sub>3</sub>) δ<sub>H</sub> 0.85 (t, 3H, *J* = 7.0, CH<sub>3</sub>), 1.17-1.30 (m, 8H, 4 × CH<sub>2</sub>), 1.34-1.41 (m, 2H, P(S)CH<sub>2</sub>CH<sub>2</sub>CH<sub>2</sub>), 1.57-1.66 (m, 2H, P(S)CH<sub>2</sub>CH<sub>2</sub>), 2.40-2.47 (m, 2H, P(S)CH<sub>2</sub>), 7.42-7.49 (m, 6H, Ph), 7.79-7.85 (m, 4H, Ph). <sup>13</sup>C NMR (100 MHz, CDCl<sub>3</sub>) δ<sub>C</sub> 14.3, 22.3 (d, *J* = 2.5 Hz), 22.8, 29.3, 30.9 (d, *J* = 16.5 Hz), 32.0, 32.8 (d, *J* = 56.5 Hz), 128.8 (d, *J* = 12.0), 131.3 (d, *J* = 10.0 Hz), 131.6 (d, *J* = 3.0 Hz), 133.2 (d, *J* = 79.5 Hz). Spectroscopic data were consistent with the literature.<sup>138</sup>

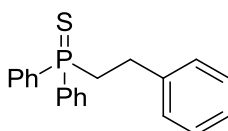


### Cyclohexyl(diphenyl)phosphane sulfide (**73**)



Using general procedure **5** cyclohexene (0.05 mL, 0.5 mmol, 1 eq), diphenylphosphine sulfide (328 mg, 1.5 mmol, 3 eq) and TEMPO (15.4 mg, 0.1 mmol, 0.2 eq) gave crude product. The crude mixture was purified by flash column chromatography (90% hexane, 10% ethyl acetate) to yield **73** as a white solid (39.5 mg, 26%). Rf 0.33 (90% hexane, 10% ethyl acetate).  $^1\text{H}$  NMR (400 MHz,  $\text{CDCl}_3$ )  $\delta_{\text{H}}$  1.22 (m, 3H,  $\text{CH}_2$ ), 1.57-1.61 (m, 4H,  $\text{CH}_2$ ), 1.68-1.71 (m, 1H,  $\text{CH}_2$ ), 1.79-1.83 (m, 2H,  $\text{CH}_2$ ), 2.51-2.64 (m, 1H,  $\text{P(S)CH}_2$ ), 7.43-7.48, (m, 6H, Ph), 7.89-7.94 (m, 4H, Ph).  $^{31}\text{P}$  NMR (162 MHz,  $\text{CDCl}_3$ )  $\delta_{\text{P}}$  50.3 ( $\text{Ph}_2\text{P(S)CH}$ ).  $^{13}\text{C}$  NMR(100 MHz,  $\text{CDCl}_3$ )  $\delta_{\text{C}}$  25.0 (2  $\times$   $\text{P(S)CHCH}_2\text{CH}_2$ ), 25.5 (d,  $J = 1.0$  Hz,  $\text{CHC}(\text{CH}_2)_2\text{CH}_2$ ), 25.9  $\text{P(S)CHCH}_2$ ), 38.1 (d,  $J = 56.0$  Hz,  $\text{P(S)CH}$ ), 128.7 (d,  $J = 11.5$  Hz, Ph) 131.5 (d,  $J = 3.0$  Hz, Ph), 131.5 (d,  $J = 9.0$  Hz, Ph), 131.8 (d,  $J = 75.0$  Hz, Ph). Spectroscopic data were consistent with the literature.<sup>146</sup>

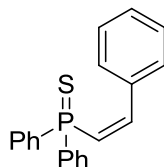
### Diphenyl(2-phenylethyl)phosphane sulfide (**74**)



Using general procedure **5** styrene (0.06 mL, 0.5 mmol, 1 eq), diphenylphosphine sulfide (327.6 mg, 1.5 mmol, 3 eq) and TEMPO (15.3 mg, 0.1 mmol, 0.2 eq) gave crude product. The crude mixture was purified by flash column chromatography (90% hexane, 10% ethyl acetate) to yield **74** as a white solid (141.6 mg, 88%). Rf 0.26 (90% hexane, 10% ethyl acetate). m.p. 86-88 °C (lit. 94 °C).<sup>141</sup>  $^1\text{H}$  NMR (400 MHz,  $\text{CDCl}_3$ )  $\delta_{\text{H}}$  2.71-2.80 (m, 2H,  $\text{P(S)CH}_2$ ), 2.88-2.97 (m, 2H,  $\text{CH}_2\text{Ph}$ ), 7.14-7.21 (m, 3H, Ph), 7.23-7.29 (m, 2H, Ph), 7.42-7.54 (m, 6H, Ph), 7.79-7.91 (m, 4H, Ph).  $^{31}\text{P}$  NMR (162 MHz,  $\text{CDCl}_3$ )  $\delta_{\text{P}}$  42.5 ( $\text{Ph}_2\text{P(S)CH}_2$ ).  $^{13}\text{C}$  NMR(100 MHz,  $\text{CDCl}_3$ )  $\delta_{\text{C}}$  28.6 (d,  $J = 1.0$  Hz,  $\text{CH}_2\text{Ph}$ ), 34.8 (d,  $J = 4.5$  Hz,  $\text{P(S)CH}_2$ ), 126.6 (Ph), 128.4 (Ph), 128.8 (Ph), 128.9 (Ph), 129.0 (Ph), 131.3 (d,  $J = 10.5$  Hz, Ph), 131.8 (d,  $J = 2.5$  Hz, Ph), 132.8 (d,  $J = 80.0$

Hz, Ph), 141.4 (d,  $J = 17.0$  Hz, Ph). Spectroscopic data were consistent with the literature.<sup>141</sup>

### Diphenyl(2-phenylethenyl)phosphane sulfide (75)

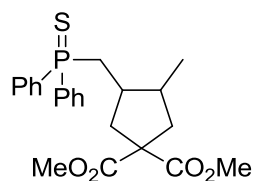


Using general procedure **5** phenylacetylene (0.05 mL, 0.5 mmol, 1 eq), diphenylphosphine sulfide (327.3 mg, 1.5 mmol, 3 eq) and TEMPO (15.3 mg, 0.1 mmol, 0.2 eq) gave crude product. The crude mixture was purified by flash column chromatography (90% hexane, 10% ethyl acetate) to yield **75** as a white solid (96.3 mg, 43%).  $R_f$  0.19 (90% hexane, 10% ethyl acetate). m.p. 87-90 °C (lit. 98-99 °C).<sup>142</sup>  $^1\text{H}$  NMR (400 MHz,  $\text{CDCl}_3$ )  $\delta_{\text{H}}$  6.42 (dd, 1H,  $J = 13.5$  and 17.6 Hz, P(S)CH), 7.00-7.09 (m, 2H, Ph), 7.28-7.56 (m, 9H, Ph), 7.39 (d, 1H,  $J = 13.5$  Hz, P(S)CHCH), 7.83-7.91 (m, 4H, Ph).  $^{31}\text{P}$  NMR (162 MHz,  $\text{CDCl}_3$ )  $\delta_{\text{P}}$  30.89 ( $\text{Ph}_2\text{P(S)CH}$ ).  $^{13}\text{C}$  NMR (100 MHz,  $\text{CDCl}_3$ )  $\delta_{\text{C}}$  122.9 (d,  $J = 82.0$  Hz, P(S)CH=CH), 127.7 (Ph), 128.5 (d,  $J = 12.5$  Hz, Ph), 129.0 (Ph), 130.4 (Ph), 131.4 (d,  $J = 3.0$  Hz, Ph), 131.4 (d,  $J = 10.5$  Hz, Ph), 132.9 (d,  $J = 85.5$  Hz, Ph), 134.6 (d,  $J = 7.0$  Hz, Ph), 146.7 (d,  $J = 2.5$  Hz, P(S)CH=CH). Spectroscopic data were consistent with the literature.<sup>142</sup>

### General Procedure 7 for the addition of diphenylphosphine sulfide to dienes

Diphenylphosphine sulfide (0.5 mmol, 1 eq or 1.5 mmol, 3 eq), TEMPO (0.03 mmol, 0.06 eq) and diene were stirred under argon in dry, degassed DCM for 24 h. 5 mL of  $\text{H}_2\text{O}$  were added, the layers were separated and the aqueous washed with DCM (2  $\times$  5mL). The combined organic layers were washed with brine (5 mL), dried over  $\text{MgSO}_4$  and concentrated *in vacuo* to yield crude product.

**Dimethyl 3-[(diphenylphosphorothioyl)methyl]-4-methylcyclopentane-1,1-dicarboxylate (**77**)**



R<sub>f</sub> 0.15 (80% hexane, 20% ethyl acetate). Major *cis*-isomer: <sup>1</sup>H NMR (400 MHz, CDCl<sub>3</sub>) δ<sub>H</sub> 0.82 (d, 3H, *J* = 7.0 Hz, CH<sub>3</sub>CH), 1.92 (dd, 2H, *J* = 14.0 Hz and 6.5 Hz, CH<sub>3</sub>CHCHH' and Ph<sub>2</sub>P(S)CH<sub>2</sub>CHCHH'), 2.14-2.26 (m, 2H, Ph<sub>2</sub>P(S)CH<sub>2</sub>CH and Ph<sub>2</sub>P(S)CH<sub>2</sub>CHCHH'), 2.38 (dd, 1H, *J* = 14.0 Hz and 7.0 Hz, CH<sub>3</sub>CHCHH'), 2.44-2.58 (m, 3H, Ph<sub>2</sub>P(S)CH<sub>2</sub> and CH<sub>3</sub>CH), 3.61-3.67 (m, 6H, 2 × CO<sub>2</sub>Me), 7.44-7.49 (m, 6H, Ph), 7.80-7.89 (m, 4H, Ph). <sup>31</sup>P NMR (162 MHz, CDCl<sub>3</sub>) δ<sub>P</sub> 42.51 (Ph<sub>2</sub>P(S)CH<sub>2</sub>). <sup>13</sup>C NMR (100 MHz, CDCl<sub>3</sub>) δ<sub>C</sub> 15.2 (CH<sub>3</sub>CH), 32.6 (d, *J* = 56.5 Hz, Ph<sub>2</sub>P(S)CH<sub>2</sub>), 37.3 (d, *J* = 10.5 Hz, Ph<sub>2</sub>P(S)CH<sub>2</sub>CH), 37.4 (d, *J* = 2.5 Hz, CH<sub>3</sub>CH), 39.1 (d, *J* = 5.5 Hz, Ph<sub>2</sub>P(S)CH<sub>2</sub>CHCH<sub>2</sub>), 41.3 (CH<sub>3</sub>CHCH<sub>2</sub>), 53.0 (2 × CO<sub>2</sub>CH<sub>3</sub>), 58.7 ((CH<sub>3</sub>O<sub>2</sub>C)<sub>2</sub>C), 128.7 (d, *J* = 2.0 Hz, Ph), 128.9 (d, *J* = 2.0 Hz, Ph), 131.2 (d, *J* = 10.0 Hz, Ph), 131.4 (d, *J* = 10.5 Hz, Ph), 131.5 (d, *J* = 10.0 Hz, Ph), 131.6 (d, *J* = 3.0 Hz, Ph), 131.7 (d, *J* = 3.0 Hz, Ph), 132.6 (Ph), 133.4 (d, *J* = 14.0 Hz, Ph), 134.1 (Ph), 173.1 (CO<sub>2</sub>CH<sub>3</sub>), 173.4 (CO<sub>2</sub>CH<sub>3</sub>). The presence of the minor *trans* isomer was indicated by the following data: <sup>1</sup>H NMR (400 MHz, CDCl<sub>3</sub>) δ<sub>H</sub> 0.95 (d, 3H, *J* = 6.0 Hz, CH<sub>3</sub>CH). <sup>31</sup>P NMR (162 MHz, CDCl<sub>3</sub>) δ<sub>P</sub> 41.55 (Ph<sub>2</sub>P(S)CH<sub>2</sub>). IR ATR 2953, 1728 (C=O), 1435, 1253, 1101, 739, 691, 624, 611 cm<sup>-1</sup>. *m/z* calcd for C<sub>23</sub>H<sub>27</sub>O<sub>4</sub>PS (M + Na)<sup>+</sup> 453.1260, found 453.1259 (0.3 ppm error).

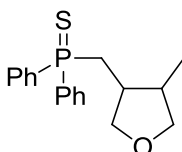
**Table 3.5, Entry 1**

Using General Procedure **7** diphenylphosphine sulfide (327.9 mg, 1.5 mmol, 3 eq), TEMPO (15.1 mg, 0.1 mmol, 0.2 eq) and dimethyl diallylmalonate (119.3 mg, 0.56 mmol, 1 eq) gave crude product. The crude mixture was purified by flash column chromatography (80% hexane, 20% ethyl acetate) to yield **77** as a colourless oil (233 mg, 97%, 9.4:1 dr *cis:trans*). Spectroscopic data were consistent with the data detailed above.

### Figure 3.6

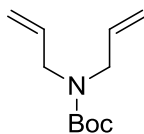
Dimethyl diallylmalonate (212.1 mg, 1 mmol, 1 eq) and diphenylphosphine sulfide (217.8 mg, 1 mmol, 1 eq) were stirred at 80 °C for 48 h to give crude product. The crude mixture was purified by flash column chromatography (80% hexane, 20% ethyl acetate) to yield **77** as a colourless oil (288 mg, 67%, 5.1:1 dr *cis:trans*). Spectroscopic data were consistent with the data detailed above.

### [(4-Methyltetrahydrofuran-3-yl)methyl](diphenyl)phosphane sulfide (**78**)



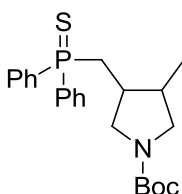
Using General Procedure **7** diphenylphosphine sulfide (109.4 mg, 0.5 mmol, 1 eq), TEMPO (5.0 mg, 0.03 mmol, 0.06 eq) and diallylether (0.06 mL, 0.5 mmol, 1 eq) gave crude product. The crude mixture was purified by flash column chromatography (80% hexane, 20% ethyl acetate) to yield **78** as a colourless oil (233 mg, 52%, 3.7:1 dr *cis:trans*). R<sub>f</sub> 0.08 (80% hexane, 20% ethyl acetate). Major *cis* isomer: <sup>1</sup>H NMR (400 MHz, CDCl<sub>3</sub>) δ<sub>H</sub> 0.94 (d, 3H, *J* = 7.0 Hz, CH<sub>3</sub>), 2.32 (m, 1H, CH<sub>3</sub>CH), 2.49 (m, 1H, P(S)CH<sub>2</sub>CH'), 2.62 (m, 1H, P(S)CHCH'), 2.73 (m, 1H, P(S)CH<sub>2</sub>CH), 3.26 (t, *J* = 8.5 Hz, P(S)CH<sub>2</sub>CHCH'), 3.42 (dd, *J* = 4.0 and 8.0 Hz, CH<sub>3</sub>CHCH'), 3.66 (t, *J* = 8.5 Hz, P(S)CH<sub>2</sub>CHCH'), 3.83 (dd, *J* = 6.0 and 8.0 Hz), 7.38-7.53 (m, 6H, Ph), 7.78-7.90 (m, 4H, Ph). <sup>31</sup>P NMR (162 MHz, CDCl<sub>3</sub>) δ<sub>P</sub> 42.5 (Ph<sub>2</sub>P(S)CH<sub>2</sub>). <sup>13</sup>C NMR (100 MHz, CDCl<sub>3</sub>) δ<sub>C</sub> 13.7 (CH<sub>3</sub>), 31.2 (d, *J* = 57.5 Hz, P(S)CH<sub>2</sub>), 36.9 (d, *J* = 10.5 Hz, P(S)CH<sub>2</sub>CH), 37.1 (d, *J* = 2.0 Hz, CH<sub>3</sub>CH), 71.6 (d, *J* = 5.0 Hz, P(S)CH<sub>2</sub>CH<sub>2</sub>), 74.7 (CH<sub>3</sub>CH<sub>2</sub>), 128.5-128.7 (m, Ph), 130.9-131.6 (m, Ph), 132.4 (d, *J* = 79.5 Hz, Ph), 132.7 (d, *J* = 80.0 Hz, Ph), 133.3 (d, *J* = 81.0 Hz). The presence of the minor *trans* isomer was indicated by the following data: <sup>1</sup>H NMR (400 MHz, CDCl<sub>3</sub>) δ<sub>H</sub> 0.97 (d, 3H, *J* = 6.5 Hz, CH<sub>3</sub>CH). <sup>31</sup>P NMR (162 MHz, CDCl<sub>3</sub>) δ<sub>P</sub> 41.38 (Ph<sub>2</sub>P(S)CH<sub>2</sub>). IR ATR 3053, 2960, 2921, 2851, 1435, 1100, 740, 690, 623, 610, 509 cm<sup>-1</sup>. *m/z* calcd for C<sub>11</sub>H<sub>19</sub>NO<sub>2</sub> (M + Na)<sup>+</sup> 317.1123, found 317.116 (1.0 ppm error).

### ***tert*-Butyl diprop-2-en-1-ylcarbamate (79)**



Diallylamine (0.74 ml, 6.0 mmol, 1.2 eq) was added to a solution of di-*tert*-butyl dicarbonate (1.0934 g, 5.0 mmol, 1 eq) in DCM at 0 °C under N<sub>2</sub>. The reaction was warmed to room temperature and stirred for 18 h. The reaction was washed with 2 M HCl (3 × 5 mL), saturated NaHCO<sub>3</sub> (3 × 5 mL), dried over MgSO<sub>4</sub> and concentrated under reduced pressure to yield **79** as a white crystalline solid (0.83 g, 84%). <sup>1</sup>H NMR (400 MHz, CDCl<sub>3</sub>) δ<sub>H</sub> 1.41 (s, 9H, 3 × CH<sub>3</sub>), 3.76 (d, 4H, *J* = 8.5 Hz, 2 × NCH<sub>2</sub>CHCH<sub>2</sub>), 4.99-5.13 (m, 4H, NCH<sub>2</sub>CHCH<sub>2</sub>), 5.72 (ddt, 2H, *J* = 16.0, 11.0, 5.5 Hz, 2 × CH). <sup>13</sup>C NMR(100 MHz, CDCl<sub>3</sub>) δ<sub>C</sub> 28.6 (3 × CH<sub>3</sub>), 48.9 (2 × NCH<sub>2</sub>), 79.8 (CO<sub>2</sub>C), 116.6 (CH=C<sub>2</sub>H<sub>2</sub>), 134.2 (C<sub>2</sub>H=CH<sub>2</sub>), 155.6 (CO<sub>2</sub>). *m/z* calcd for C<sub>11</sub>H<sub>19</sub>NO<sub>2</sub> (M + Na)<sup>+</sup> 220.1308, found 220.1306 (0.8 ppm error). Spectroscopic data were consistent with the literature.<sup>174</sup>

### ***tert*-Butyl 3-[(diphenylphosphorothioyl)methyl]-4-methylpyrrolidine-1-carbamate (80)**



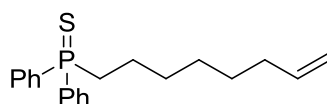
Using General Procedure **7** diphenylphosphine sulfide (110.4 mg, 0.5 mmol, 1 eq), TEMPO (5.1 mg, 0.03 mmol, 0.06 eq) and *N*-Boc-diallylamine (98.6 mg, 0.5 mmol, 1 eq) gave crude product. The crude mixture was purified by flash column chromatography (80% hexane, 20% ethyl acetate) to yield **80** as a viscous oil (233 mg, 51%, 2.1:1 dr *cis:trans*). R<sub>f</sub> 0.08 (80% hexane, 20% ethyl acetate). Major *cis* isomer: <sup>1</sup>H NMR (400 MHz, DMSO d<sub>6</sub>) δ<sub>H</sub> 0.90 (d, 3H, *J* = 7.0 Hz, CHCH<sub>3</sub>), 1.35 (s, 9H, 3 × CCH<sub>3</sub>), 2.19-2.30 (m, 1H, CHCH<sub>3</sub>), 2.55 (dd, 1H, *J* = 13.0 Hz, P(S)CH<sub>2</sub>CH), 2.64-2.74 (m, 2H, P(S)CH<sub>2</sub>), 2.82-2.90 (m, 1H, P(S)CH<sub>2</sub>CHCH'), 2.99 (dd, 1H *J* = 3.0 and 10.5 Hz, CH<sub>3</sub>CHCH'), 3.11-3.19 (m, 1H, P(S)CH<sub>2</sub>CHCH'), 3.25 (dd, 1H, *J* = 6.0 and 10.5

Hz, CH<sub>3</sub>CHCHH'), 7.48-7.59 (m, 6H, Ph), 7.87-8.04 (m, 4H, Ph). <sup>31</sup>P NMR (162 MHz, CDCl<sub>3</sub>) δ<sub>P</sub> 42.0 (Ph<sub>2</sub>P(S)CH<sub>2</sub>). <sup>13</sup>C NMR(100 MHz, CDCl<sub>3</sub>) δ<sub>C</sub> 13.5 (3 × CCH<sub>3</sub>), 30.9 (d, J = 12.2 Hz, P(S)CH<sub>2</sub>CH), 36.0 (d, J = 1.5 Hz, CH<sub>3</sub>CH), 48.81 (d, J = 41.9 Hz, P(S)CH<sub>2</sub>), 49.0 (d, J = 4.5 Hz, NCH<sub>2</sub>CHCH<sub>2</sub>P(S)), 52.6 (NCH<sub>2</sub>CHCH<sub>3</sub>), 78.7 (3 × CCH<sub>3</sub>), 128.6-127.9 (m, Ph), 130.4-131.6 (m, Ph), 131.7-134.0 (m, Ph), 154.2 (CO<sub>2</sub>). The presence of the minor *trans* isomer was indicated by the following data: <sup>1</sup>H NMR (400 MHz, CDCl<sub>3</sub>) δ<sub>H</sub> 0.95 (d, 3H, J = 6.0 Hz, CH<sub>3</sub>CH). <sup>31</sup>P NMR (162 MHz, CDCl<sub>3</sub>) δ<sub>P</sub> 41.90 (Ph<sub>2</sub>P(S)CH<sub>2</sub>). IR ATR 3054, 2973, 2872, 1684, 1403, 1131, 1102, 734, 691, 624, 612, 512 cm<sup>-1</sup>. *m/z* calcd for C<sub>23</sub>H<sub>30</sub>NO<sub>2</sub>PS (M + Na)<sup>+</sup> 438.1627, found 438.1614 (2.8 ppm error).

### Addition of diphenylphosphine sulfide to 1,7-octadiene

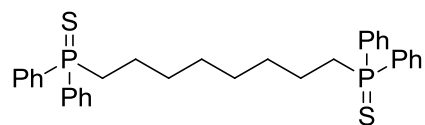
Using General Procedure **7** diphenylphosphine sulfide (109.3 mg, 0.5 mmol, 1 eq), TEMPO (5.0 mg, 0.03 mmol, 0.06 eq) and 1,7-octadiene (0.07 mL 0.5 mmol, 1 eq) gave crude product. The crude mixture was purified by flash column chromatography (80% hexane, 20% ethyl acetate) to yield **81** (53.3 mg, 32%) and **98** (28.7 mg, 10%) as colourless oils.

### Oct-7-en-1-yl(diphenyl)phosphane sulfide (**81**)



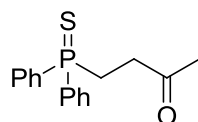
R<sub>f</sub> 0.35 (90% hexane, 10% ethyl acetate). <sup>1</sup>H NMR (400 MHz, CDCl<sub>3</sub>) δ<sub>H</sub> 1.22-1.44 (m, 6H, 3 × CH<sub>2</sub>), 1.57-1.68 (m, 2H, P(S)CH<sub>2</sub>CH<sub>2</sub>), 1.99 (q, 2H, J = 7.0 Hz, CH<sub>2</sub>CH=CH<sub>2</sub>), 2.38-2.49 (m, 2H, P(S)CH<sub>2</sub>), 4.89-5.00 (m, 2H, CH=CH<sub>2</sub>), 5.76 (ddt, 1H, J = 6.5, 10.0 and 17.0 Hz, CH=CH<sub>2</sub>), 7.41-7.52 (m, 6H, Ph), 7.77-7.86 (m, 4H, Ph). <sup>31</sup>P NMR (162 MHz, CDCl<sub>3</sub>) δ<sub>P</sub> 43.31 (Ph<sub>2</sub>P(S)CH<sub>2</sub>). <sup>13</sup>C NMR(100 MHz, CDCl<sub>3</sub>) δ<sub>C</sub> 22.3 (d, J = 2.5 Hz, P(S)CH<sub>2</sub>CH<sub>2</sub>), 28.8 (P(S)CH<sub>2</sub>)<sub>3</sub>CH<sub>2</sub>), 28.85 (CH<sub>2</sub>CH<sub>2</sub>CH=CH<sub>2</sub>), 30.7 (d, J = 16.5 Hz, P(S)CH<sub>2</sub>CH<sub>2</sub>CH<sub>2</sub>), 32.8 (d, J = 56.5 Hz, P(S)CH<sub>2</sub>), 33.9 (CH<sub>2</sub>CH=CH<sub>2</sub>), 114.5 (CH=CH<sub>2</sub>), 128.8 (d, J = 12.0 Hz, Ph), 131.3 (d, J = 10.0 Hz, Ph), 131.6 (d, J = 3.0 Hz, Ph), 133.2 (d, J = 79.5 Hz, Ph), 139.11 (Ph).<sup>175</sup>

### 8-(Diphenylphosphorothioyl)octyl(diphenyl)phosphine sulfide (98)



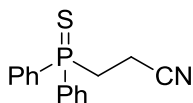
Rf 0.08 (90% hexane, 10% ethyl acetate).  $^1\text{H}$  NMR (400 MHz,  $\text{CDCl}_3$ )  $\delta_{\text{H}}$  1.19-1.23 (m, 4H, 2  $\times$   $\text{CH}_2$ ), 1.30-1.36 (m, 4H, 2  $\times$   $\text{CH}_2$ ), 1.53-1.63 (m, 4H, 2  $\times$   $\text{P(S)CH}_2\text{CH}_2$ ), 2.40 (ddd, 4H,  $J = 11.5, 8.5$  and  $4.5$  Hz,  $\text{P(S)CH}_2$ ), 7.43-7.50 (m, 12 H, Ph), 7.78-7.84 (m, 8H, Ph).  $^{31}\text{P}$  NMR (162 MHz,  $\text{CDCl}_3$ )  $\delta_{\text{P}}$  43.32 (2  $\times$   $\text{Ph}_2\text{P(S)CH}_2$ ).  $^{13}\text{C}$  NMR (100 MHz,  $\text{CDCl}_3$ )  $\delta_{\text{C}}$  22.2 (d,  $J = 2.5$  Hz, 2  $\times$   $\text{P(S)CH}_2\text{CH}_2$ ), 29.0 (2  $\times$   $\text{P(S)CH}_2\text{CH}_2\text{CH}_2\text{CH}_2$ ), 30.6 (d,  $J = 16.5$  Hz, 2  $\times$   $\text{P(S)CH}_2\text{CH}_2\text{CH}_2$ ), 32.7 (d,  $J = 56.5$  Hz,  $\text{P(S)CH}_2$ ), 128.8 (d,  $J = 12.0$  Hz, Ph), 131.3 (d,  $J = 10.0$  Hz, Ph), 131.6 (d,  $J = 3.0$  Hz, Ph), 133.1 (d,  $J = 79.5$  Hz, Ph).

### 4-(diphenylphosphorothioyl)butan-2-one (82)



Using general procedure **6**, diphenylphosphine sulfide (328.3 mg, 1.5 mmol, 3 eq) and methyl vinyl ketone (0.04 mL, 0.48 mmol, 1 eq) gave crude product. The crude mixture was purified by flash column chromatography (80% hexane, 20% ethyl acetate) to yield **82** as a colourless oil (67.6 mg, 47%). Rf 0.12 (80% hexane, 20% ethyl acetate).  $^1\text{H}$  NMR (400 MHz,  $\text{CDCl}_3$ )  $\delta_{\text{H}}$  2.10 (s, 3H,  $\text{CH}_3$ ), 2.64-2.83 (m, 4H, 2  $\times$   $\text{CH}_2$ ), 7.36-7.55 (m, 6H, Ph), 7.81 (ddd, 4H,  $J = 8.5$  Hz, 5.0 Hz and 3.0 Hz, Ph).  $^{31}\text{P}$  NMR (162 MHz,  $\text{CDCl}_3$ )  $\delta_{\text{P}}$  43.39 ( $\text{Ph}_2\text{P(S)CH}_2$ ).  $^{13}\text{C}$  NMR (100 MHz,  $\text{CDCl}_3$ )  $\delta_{\text{C}}$  26.3 (d,  $J = 60.0$  Hz,  $\text{Ph}_2\text{P(S)CH}_2$ ), 30.0 ( $\text{CH}_3$ ), 36.5 ( $\text{CH}_2\text{C(O)}$ ), 128.8 (d,  $J = 12.5$  Hz, Ph), 131.1 (d,  $J = 10.4$  Hz, Ph), 131.8 (d,  $J = 3.0$  Hz, Ph), 131.9 (Ph), 132.7 (Ph), 206.4 (d,  $J = 15.0$  Hz,  $\text{C(O)}$ ).  $m/z$  calcd for  $\text{C}_{16}\text{H}_{17}\text{OPS}$  ( $\text{M} + \text{Na}$ ) $^+$  311.0630, found 311.0619 (3.5 ppm error). IR ATR 3054, 2917, 1715 ( $\text{C=O}$ ), 1436, 1265, 1103, 729, 691, 625, 612, 507, 493, 409  $\text{cm}^{-1}$ .

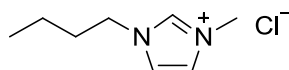
### 3-(Diphenylphosphorothioyl)propanenitrile (**83**)



Using general procedure **6**, diphenylphosphine sulfide (327.5 mg, 1.5 mmol, 3 eq) and acrylonitrile (0.03 mL, 0.5 mmol, 1 eq) gave crude product. The crude mixture was purified by flash column chromatography (80% hexane, 20% ethyl acetate) to yield **83** as a white solid (64.0 mg, 52%). Rf 0.14 (80% hexane, 20% ethyl acetate). m.p. 117-119 °C (lit. 119-124 °C).<sup>176</sup> <sup>1</sup>H NMR (400 MHz, CDCl<sub>3</sub>) δ<sub>H</sub> 2.65-2.83 (m, 4H, 2 × CH<sub>2</sub>), 7.48-7.60 (m, 6H, Ph), 7.78-7.86 (m, 4H, Ph). <sup>31</sup>P NMR (162 MHz, CDCl<sub>3</sub>) δ<sub>P</sub> 41.65 (Ph<sub>2</sub>P(S)CH<sub>2</sub>). <sup>13</sup>C NMR (100 MHz, CDCl<sub>3</sub>) δ<sub>C</sub> 11.5 (CH<sub>2</sub>CN), 29.2 (d, *J* = 56.5 Hz, P(S)CH<sub>2</sub>), 119.0 (d, *J* = 22.0 Hz, CN), 129.2 (d, *J* = 12.5 Hz, Ph), 131.1 (d, *J* = 82.0 Hz, Ph), 131.3 (d, *J* = 10.5 Hz, Ph), 132.5 (d, *J* = 3.0 Hz, Ph).<sup>136</sup>

## 8.4. TEMPO Ionic Liquids

### 1-Butyl-3-methylimidazolium chloride (**99**)<sup>177</sup>

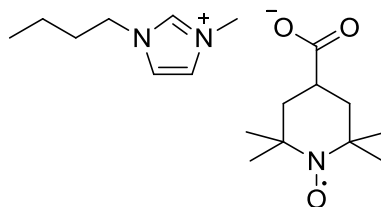


In a flame dried round bottom flask and condenser under nitrogen was refluxed *N*-methylimidazole (15.6 mL, 0.2 mol, 1 eq), and 1-chlorobutane (22 mL, 0.21 mol, 1.05 eq) in dry acetonitrile (10 mL) at 90 °C for 48 h. The reaction mixture was concentrated under vacuum and re-dissolved in dry acetonitrile (25 mL). The solution was added via cannula transfer to ethyl acetate (100 mL) containing a seed crystal of 1-butyl-3-methylimidazolium chloride and cooled at -15 °C for 3 h. The solvent was removed by cannula filtration and the product washed with ice cold ethyl acetate (20 mL) and concentrated under vacuum to yield **99** as a white crystalline solid (30.32 g, 89%). <sup>1</sup>H NMR (400 MHz, D<sub>2</sub>O) δ<sub>H</sub> 0.75 (t, 3H, *J* = 7.5 Hz, CH<sub>3</sub>CH<sub>2</sub>), 1.10-1.19 (m, 2H, CH<sub>3</sub>CH<sub>2</sub>), 1.64-1.72 (m, 2H, CH<sub>3</sub>CH<sub>2</sub>CH<sub>2</sub>), 3.72 (s, 3H, CH<sub>3</sub>N), 4.03 (t, 2H, *J* = 7.0, CH<sub>2</sub>N), 7.25 (s, 1H, CHN), 7.30 (s, 1H, CHN), 8.54 (s, 1H,



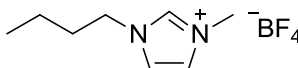
NCHN).  $^{13}\text{C}$  NMR (100 MHz,  $\text{D}_2\text{O}$ )  $\delta_{\text{C}}$  12.6 ( $\underline{\text{C}}\text{H}_3\text{C}\underline{\text{H}}_2$ ), 18.8 ( $\text{C}\underline{\text{H}}_3\underline{\text{C}}\text{H}_2$ ), 31.3 ( $\text{C}\underline{\text{H}}_3\text{C}\underline{\text{H}}_2\underline{\text{C}}\text{H}_2$ ), 35.6 ( $\text{C}\underline{\text{H}}_3\text{N}$ ), 49.3 ( $\text{C}\underline{\text{H}}_2\text{N}$ ), 122.2 ( $\text{C}\underline{\text{H}}\text{N}$ ), 123.5 ( $\text{C}\underline{\text{H}}\text{N}$ ), 135.9 ( $\text{N}\underline{\text{C}}\text{H}\text{N}$ ).<sup>177</sup>

**1-Butyl-3-methylimidazolium 2,2,6,6-tetramethylpiperidine-*N*-oxyl-4-carboxylate (89)**



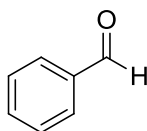
Potassium *tert*-butoxide (0.13 g, 1.2 mmol, 2 eq) in dimethoxyethane (1 mL) and *tert*-butanol was added dropwise over 45 min to a stirred solution of 4-oxo-2,2,6,6-tetramethylpiperidine-*N*-oxyl (0.10 g, 0.6 mmol, 1 eq) and *p*-toluenesulfonylmethyl isocyanide (0.11 g, 0.6 mmol, 1 eq) in dimethoxyethane (4 mL) at 0 °C and stirred for 1 h at room temperature.  $\text{H}_2\text{O}$  (10 mL) was added and washed with diethyl ether (4  $\times$  2.5 mL). The organic layers were concentrated under vacuum and re-dissolved in MeOH (2 mL). To this was added a solution of NaOH (0.035 g, 0.9 mmol, 1.5 eq) and  $\text{Ba}(\text{OH})_2 \cdot 8\text{H}_2\text{O}$  (0.731, 2.3 mmol, 4 eq) in  $\text{H}_2\text{O}$  (7 mL). The mixture was stirred at reflux for 24 h, cooled, acidified to pH 1 with 2M HCl, extracted with  $\text{CHCl}_3$  (3  $\times$  10 mL) and concentrated under vacuum. The 4-carboxy-TEMPO intermediate (21 mg, 0.1 mmol, 0.2 eq) was re-dissolved in a solution of KOH (5.6 mg, 0.1 mmol, 0.2 eq) in MeOH (2 mL) and stirred for 2.5 h. [BMIM][Cl] (18.4 mg, 0.1 mmol, 0.2 eq) was added and stirred for 72 h. The mixture was concentrated under vacuum, dissolved in  $\text{CHCl}_3$  (5 mL), filtered through Celite and concentrated under vacuum to yield **89** as an orange oil (34.2 mg, 17%).  $m/z$  calcd for  $\text{C}_{10}\text{H}_{18}\text{NO}_3$  ( $\text{M} - \text{H}$ )<sup>-</sup> 199.1214, found 199.1214 (0.0 ppm error).  $m/z$  calcd for  $\text{C}_8\text{H}_{15}\text{N}_2$  ( $\text{M} + \text{H}$ )<sup>+</sup> 139.1230, found 139.1225 (3.8 ppm error).

### 1-Butyl-3-methylimidazolium tetrafluoroborate (100)<sup>177</sup>



To 1-butyl-3-methylimidazolium chloride (12.13 g, 69 mmol, 1 eq) was added a solution of sodium tetrafluoroborate (7.62 g, 69 mmol, 1 eq) in distilled water (20 mL) and stirred for 2 h. The reaction mixture was concentrated under reduced pressure, dissolved in dichloromethane (20 mL), dried over magnesium sulfate and concentrated to yield a colourless oil (15.33 g, 98%). <sup>1</sup>H NMR (400 MHz, D<sub>2</sub>O) δ<sub>H</sub> 0.75 (t, 3H, *J* = 7.4 Hz, CH<sub>3</sub>CH<sub>2</sub>), 1.14 (m, 2H, *J* = 7.5 Hz, CH<sub>3</sub>CH<sub>2</sub>), 1.67 (m, 2H, *J* = 7.5 Hz, CH<sub>3</sub>CH<sub>2</sub>CH<sub>2</sub>), 3.71 (s, 3H, CH<sub>3</sub>N), 4.02 (t, 2H, *J* = 7.0, CH<sub>2</sub>N), 7.24 (d, 1H, *J* = 1.5 Hz, CHN), 7.29 (d, 1H, *J* = 1.5 Hz, CHN), 8.52, (s, 1H, NCHN). <sup>13</sup>C NMR (100 MHz, D<sub>2</sub>O) δ<sub>C</sub> 12.6 (CH<sub>3</sub>CH<sub>2</sub>), 18.8 (CH<sub>3</sub>CH<sub>2</sub>), 31.3 (CH<sub>3</sub>CH<sub>2</sub>CH<sub>2</sub>), 35.6 (CH<sub>3</sub>N), 49.3 (CH<sub>2</sub>N), 122.2 (CHN), 123.5 (CHN), 135.9 (NCHN). IR ATR 3122, 3161, 2964, 2877, 1575, 1467, 1170, 1034, 848, 754 cm<sup>-1</sup>. Spectroscopic data were consistent with the literature.<sup>177</sup>

### Benzaldehyde (101)



<sup>1</sup>H NMR (400 MHz, CDCl<sub>3</sub>) δ<sub>H</sub> 7.54 (t, 2H, Ph), 7.60-7.66 (m, 1H, Ph), 7.85-7.91 (m, 2H, Ph), 10.02 (s, 1H, CHO). <sup>13</sup>C NMR (100 MHz, CDCl<sub>3</sub>) δ<sub>C</sub> 129.0 (Ph), 129.7 (Ph), 134.5 (Ph), 136.4 (Ph), 192.4 (C=O). Spectroscopic data were consistent with the literature.<sup>178</sup>

### Table 4.2, Entry 1

Benzyl alcohol (0.41 mL, 4.0 mmol, 1 eq), TEMPO (18.1 mg, 0.1 mmol, 0.025eq), NaBr (4.0 mg, 0.04 mmol, 0.01 eq) and *N*-chlorosuccinimide (0.59 g, 4.4 mmol, 1.1 eq) were stirred in a mixture of [BMIM][BF<sub>4</sub>] (5 mL) and buffer (34.9 mg K<sub>2</sub>CO<sub>3</sub> and 209.0 mg NaHCO<sub>3</sub> in 5 mL H<sub>2</sub>O) for 24 h. The reaction mixture was extracted with diethyl ether (3 × 30 mL). The combined organic layers were dried over MgSO<sub>4</sub> and

concentrated under reduced pressure. The crude mixture was purified by column chromatography (80% petrol, 20% ethyl acetate) to yield (**101**) as a colourless oil (120.6 mg, 29%). Spectroscopic data were consistent with the data detailed above.

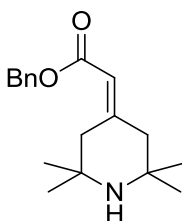
#### Table 4.2, Entry 2

Benzyl alcohol (0.21 mL, 2.0 mmol, 1 eq), [BMIM][Carboxy-TEMPO] (6.9 mg, 0.02 mmol, 0.01 eq), NaBr (2.1 mg, 0.02 mmol, 0.01 eq) and *N*-chlorosuccinimide (0.29 g, 2.2 mmol, 1.1 eq) were stirred in a mixture of [BMIM][BF<sub>4</sub>] (5 mL) and buffer (35.0 mg K<sub>2</sub>CO<sub>3</sub> and 209.9 mg NaHCO<sub>3</sub> in 5 mL H<sub>2</sub>O) for 24 h. The reaction mixture was extracted with diethyl ether (4 × 30 mL). The combined organic layers were dried over MgSO<sub>4</sub> and concentrated under reduced pressure to yield crude (**101**) (236.9 mg, 36% conversion as estimated by <sup>1</sup>H NMR). Spectroscopic data were consistent with the data detailed above.

#### Table 4.2, Entry 3

Benzyl alcohol (0.21 mL, 2.0 mmol, 1 eq), recycled [BMIM][Carboxy-TEMPO] and [BMIM][BF<sub>4</sub>] (5 mL), NaBr (2.0 mg, 0.02 mmol, 0.01 eq) and *N*-chlorosuccinimide (0.29 g, 2.2 mmol, 1.1 eq) were stirred in a mixture of recycled [BMIM][Carboxy-TEMPO] and [BMIM][BF<sub>4</sub>] (5 mL) and buffer (35.2 mg K<sub>2</sub>CO<sub>3</sub> and 210.1 mg NaHCO<sub>3</sub> in 5 mL H<sub>2</sub>O) for 24 h. The reaction mixture was extracted with diethyl ether (4 × 30 mL). The combined organic layers were dried over MgSO<sub>4</sub> and concentrated under reduced pressure to yield crude (**101**) (323.6 mg, 11% conversion as estimated by <sup>1</sup>H NMR). Spectroscopic data were consistent with the data detailed above.

#### Benzyl-2-(2,2,6,6-tetramethylpiperidin-4-ylidene)acetate (**90**)

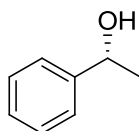


Sodium hydride (1.36 g, 34 mmol, 1 eq, 60% suspension in oil) in a flame dried flask under argon was washed with dry hexane (40 mL), and dry diethyl ether (20 mL). To

the flask was added dry diethyl ether (25 mL) and diethyl benzyl phosphonoacetate (16.86 g, 74 mmol, 2.2 eq) over 1 h and stirred for 30 min. To the mixture was added triacetoneamine (6.41 g, 41 mmol, 1.2 eq) in dry diethyl ether (20 mL) over 10 min. The mixture was stirred for 2 h, quenched with H<sub>2</sub>O (40 mL), separated, washed with diethyl ether (2 × 40 mL), dried over MgSO<sub>4</sub> and concentrated under vacuum. The crude mixture was purified by flash column chromatography (95% DCM, 5% methanol) to yield **90** as a brown oil (3.00 g, 29%). R<sub>f</sub> 0.10 (95% DCM, 5% methanol). <sup>1</sup>H NMR (400 MHz, CDCl<sub>3</sub>) δ<sub>H</sub> 1.17 (s, 6H, 2 × CH<sub>3</sub>), 1.18 (s, 6H, 2 × CH<sub>3</sub>), 2.08 (s, 2H, CH<sub>2</sub>CCH<sub>2</sub> *trans*), 2.77 (s, 2H, CH<sub>2</sub>CCH<sub>2</sub>), 5.14 (s, 2H, CH<sub>2</sub>Ph), 5.82 (s, 1H, CHCO<sub>2</sub>), 7.29-7.38 (m, 5H, Ph). <sup>13</sup>C NMR (100 MHz, CDCl<sub>3</sub>) δ<sub>C</sub> 31.1 (2 × CH<sub>3</sub>), 31.2 (2 × CH<sub>3</sub>), 42.9 (CH<sub>2</sub>CCH<sub>2</sub>), 50.6 (CH<sub>2</sub>CCH<sub>2</sub>), 54.1 (CNHC), 54.3 (CNHC), 65.7 (CO<sub>2</sub>CH<sub>2</sub>), 116.0 (CHCO<sub>2</sub>), 128.2 (Ph), 128.3 (Ph), 128.7 (Ph), 136.4 (Ph), 159.3 (CH<sub>2</sub>CCH<sub>2</sub>), 166.3 (CO<sub>2</sub>). ESI-MS *m/z* calcd C<sub>18</sub>H<sub>25</sub>NO<sub>2</sub> (M + H)<sup>+</sup> 288.1958, found 288.1949 (3.2 ppm error).

## 8.5. Chiral Resolution of Secondary Alcohols

### (S)-1-Phenylethanol (**93**)



R<sub>f</sub> 0.17 (75% petrol, 25% diethyl ether). <sup>1</sup>H NMR (400 MHz, CDCl<sub>3</sub>) δ<sub>H</sub> 1.49 (d, 3H, *J* = 6.5 Hz, CH<sub>3</sub>), 1.94 (bs, 1H, OH), 4.89 (q, 1H, *J* = 6.5 Hz, CH), 7.25-7.39 (m, 5H, Ph). <sup>13</sup>C NMR (100 MHz, CDCl<sub>3</sub>) δ<sub>C</sub> 25.2 (CH<sub>3</sub>), 70.4 (PhCH), 125.4 (Ph), 127.5 (Ph), 128.5 (Ph), 145.8 (Ph). Spectroscopic data were consistent with the literature.<sup>179</sup>

#### Table 5.1, Entry 1

(*R*)-Camphor-10-sulfonic acid (1.5 g, 6.5 mmol, 5 eq) and TEMPO (0.20 g, 1.3 mmol, 1 eq) were dissolved in acetonitrile (40 mL) and stirred for 2 h. 1-Phenylethanol (1.6 mL, 1.3 mmol, 1 eq) was added and stirred for 24 h. The crude reaction mixture was concentrated under reduced pressure and purified by flash column chromatography (75% petrol, 25% diethyl ether) yielding (**93**) as a colourless oil (51

mg, 32%, 0.1% ee by CSP-HPLC). CSP-HPLC Chiralcel OD-H column (95:5 hexane:IPA, 0.5 mL/min) (*R*) 16.5 min, (*S*) (**93**) 19.5 min. Spectroscopic data were consistent with the data detailed above.

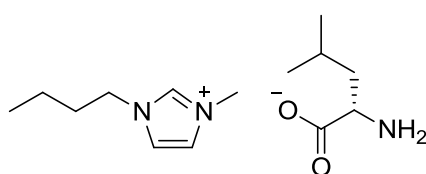
#### Table 5.1, Entry 2

(*R*)-Camphor-10-sulfonic acid (0.15 g, 0.65 mmol, 5 eq) and TEMPO (20.0 mg, 0.13 mmol, 1 eq) were dissolved in DCM (20 mL) and stirred for 2 h. 1-Phenylethanol (16  $\mu$ L, 0.13 mmol, 1 eq) was added and stirred for 24 h. The crude reaction mixture was concentrated under reduced pressure and purified by flash column chromatography (75% petrol, 25% diethyl ether) to yield **93** as a colourless oil (1.4 mg, 9%, 1.4% ee by CSP-HPLC). CSP-HPLC Chiralcel OD-H column (95:5 hexane:IPA, 0.5 mL/min) (*R*) 16.5 min, (*S*) (**93**) 19.5 min. Spectroscopic data were consistent with the data detailed above.

#### Table 5.1, Entry 3

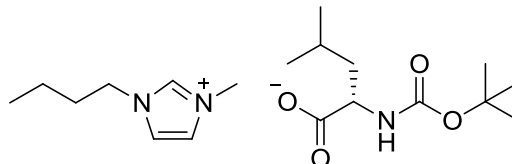
(*R*)-Camphor-10-sulfonic acid (0.45 g, 1.9 mmol, 5 eq) and TEMPO (60.0 mg, 0.4 mmol, 1 eq) were dissolved in toluene (60 mL), stirred for 2 h and concentrated under vacuum. Toluene (30 mL) and 1-phenylethanol (48.9 mg, 0.4 mmol, 1 eq) were added and stirred for 21 h. The crude reaction mixture was concentrated under reduced pressure and purified by flash column chromatography (75% petrol, 25% diethyl ether) yielding (**93**) as a colourless oil (16.8 mg, 35%, 2% ee by CSP-HPLC: Chiralcel OD-H (95:5 hexane: propan-2-ol, 0.5 mL/min) (*R*)-phenylethanol 16.1 min, (*S*)-phenylethanol 18.7 min). CSP-HPLC Chiralcel OD-H column (95:5 hexane:IPA, 0.5 mL/min) (*R*) 16.5 min, (*S*) (**93**) 19.5 min. Spectroscopic data were consistent with the data detailed above.

#### 1-Butyl-3-methylimidazolium L-leucinate (**94**)



L-Leucine (4.02 g, 31 mmol, 1 eq) and potassium hydroxide (1.72 g, 31 mmol, 1 eq) were dissolved in methanol (75 mL) and stirred for 20 min. A solution of [BMIM][Cl] (5.41 g, 31 mmol, 1 eq) in methanol (15 mL) was added and stirred for 5 h. The reaction mixture was filtered through Celite and concentrated under reduced pressure to yield (**94**) as a pale yellow oil (7.46 g, 89%).  $^1\text{H}$  NMR (400 MHz,  $\text{D}_2\text{O}$ )  $\delta_{\text{H}}$  0.73-0.78 (m, 9H,  $2 \times \text{CH}_3\text{CH}$ ,  $\text{CH}_3\text{CH}_2$ ), 1.11-1.20 (m, 2H,  $\text{CH}_3\text{CH}_2$ ), 1.21-1.37 (m, 2H,  $\text{CH}_2\text{CH}$ ), 1.43-1.57 (m, 1H,  $\text{CH}_3\text{CH}$ ), 1.65-1.72 (m, 2H,  $\text{CH}_2\text{CH}_2\text{N}$ ), 3.15 (dd, 1H,  $J = 8.0$  and 8.5 Hz,  $\text{CHCO}_2$ ), 3.72 (s, 3H,  $\text{CH}_3\text{N}$ ), 4.03 (t, 2H,  $J = 7.0$  Hz,  $\text{CH}_2\text{N}$ ), 7.26 (d, 1H,  $J = 2.0$  Hz, CHN), 7.31 (d, 1H,  $J = 2.0$  Hz, CHN).  $^{13}\text{C}$  NMR (100 MHz,  $\text{D}_2\text{O}$ )  $\delta_{\text{C}}$  12.6 ( $\text{CH}_3\text{CH}_2$ ), 18.8 ( $\text{CH}_3\text{CH}_2$ ), 21.3 ( $\text{CH}_3\text{CH}$ ), 22.4 ( $\text{CH}_3\text{CH}$ ), 24.4 ( $(\text{CH}_3)_2\text{CH}$ ), 31.3 ( $\text{CH}_3\text{CH}_2\text{CH}_2$ ), 35.6 ( $\text{CH}_3\text{N}$ ), 43.3 ( $\text{CHCH}_2\text{CH}$ ), 49.3 ( $\text{CH}_2\text{N}$ ), 54.4 ( $\text{CHNH}_2$ ), 122.2 (CHN), 123.4 (CHN), 182.6 (NCHN), one signal not resolved. IR ATR 3361 ( $\text{H}_2\text{O}$ ), 3058, 2955, 2868, 1563 (NH), 1466, 1382, 1339, 1171, 881, 145, 753, 700  $\text{cm}^{-1}$ . Spectroscopic data were consistent with the literature.<sup>157</sup>

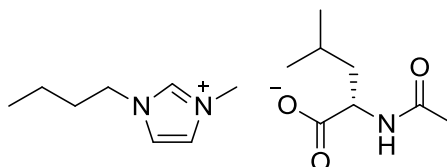
### 1-Butyl-3-methylimidazolium *N*-(*tert*-butoxycarbonyl)-L-leucinate (**95**)



Di-*tert*-butyl dicarbonate (1.24 g, 5.7 mmol, 2.3 eq) in THF (5 mL) was added dropwise over 15 min to a solution of L-leucine (0.33 g, 2.5 mmol, 1 eq) and NaOH (0.23 g, 5.8 mmol, 2.3 eq) in  $\text{H}_2\text{O}$  (5 mL). The mixture was stirred at 45 °C for 3.5 h and THF was removed under reduced pressure. The aqueous solution was extracted with cyclohexane (10 mL), acidified to pH 4 with citric acid and extracted with ethyl acetate (10 mL). The combined organic layers were washed with  $\text{H}_2\text{O}$  (5 mL) and brine (5 mL), dried over  $\text{MgSO}_4$  and concentrated under vacuum. The resultant solid was dissolved in MeOH (10 mL) with KOH (0.14g, 2.5 mmol, 1 eq), and stirred for 19 h. [BMIM][Cl] (0.44 g, 2.5 mmol, 1 eq) in MeOH (1 mL) was added to the solution and stirred for 24 h. The product was filtered through Celite and concentrated under pressure to yield (**95**) as a pale yellow solid (0.87 g, 94%).  $^1\text{H}$  NMR (400 MHz,  $\text{D}_2\text{O}$ )  $\delta_{\text{H}}$  0.74-0.79 (m, 9H,  $2 \times \text{CH}_3\text{CH}$ ,  $\text{CH}_3\text{CH}_2$ ), 1.16 (dq, 2H,  $J = 15.0, 7.5$  Hz,

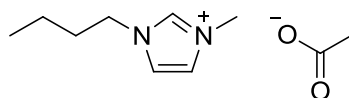
CH<sub>3</sub>CH<sub>2</sub>), 1.28 (s, 9H, 3 × CH<sub>3</sub>C), 1.33-1.40 (m, 1H, CHNH), 1.49 (dd, 2H, *J* = 13.5, 6.5 Hz, CHCH<sub>2</sub>CH), 1.64-1.74 (m, 2 H, CH<sub>2</sub>CH<sub>2</sub>N), 3.73 (s, 3H, CH<sub>3</sub>N), 4.04 (t, 2H, CH<sub>2</sub>N), 7.27 (t, 1H, *J* = 2.0 Hz, CHN), 7.32 (t, 1H, *J* = 2.0 Hz, CHN) 8.55 (s, 1 H, NCHN).

### 1-Butyl-3-methylimidazolium N-acetyl-L-leucinate (96)



N-Acetyl-L-leucine (1.91g, 11 mmol, 1 eq), and potassium hydrogen carbonate (1.10 g, 11 mmol, 1 eq) were dissolved in methanol (25 mL) and stirred for 3.5 h at 50 °C. The solution was cooled to room temperature and [BMIM] [Cl] (1.94 g, 11 mmol, 1 eq) in methanol (5 mL) was added and stirred for 5 h. The crude reaction mixture was filtered through Celite and concentrated under reduced pressure to yield (96) as a straw coloured oil (2.21 g, 68%). <sup>1</sup>H NMR (400 MHz, D<sub>2</sub>O) δ<sub>H</sub> 0.73-0.79 (m, 9H, 2 × CH<sub>3</sub>CH, CH<sub>3</sub>CH<sub>2</sub>), 1.12-1.21 (m, 2H, CH<sub>3</sub>CH<sub>2</sub>), 1.40-1.52 (m, 3H, (CH<sub>3</sub>)<sub>2</sub>CHCH<sub>2</sub>), 1.66-1.73 (m, 2 H, CH<sub>2</sub>CH<sub>2</sub>N), 1.87 (s, 3H, CH<sub>3</sub>CO), 3.73 (s, 3H, CH<sub>3</sub>N), 4.00-4.06 (m, 3H, CHCO<sub>2</sub>, CH<sub>2</sub>N), 7.27 (d, 1H, *J* = 2.0 Hz, CHN), 7.32 (d, 1H, *J* = 2.0 Hz, CHN). <sup>13</sup>C NMR (100 MHz, D<sub>2</sub>O) δ<sub>C</sub> 12.6 (CH<sub>3</sub>CH<sub>2</sub>), 18.7 (CH<sub>3</sub>CH<sub>2</sub>), 20.7, 21.9 (CH<sub>3</sub>C(O)NH), 22.5 (CH<sub>3</sub>CH), 24.6 ((CH<sub>3</sub>)<sub>2</sub>CH), 31.3 (CH<sub>3</sub>CH<sub>2</sub>CH<sub>2</sub>), 35.6 (CH<sub>3</sub>N), 40.7, 49.3 (CH<sub>2</sub>N), 54.0 (CHNH), 122.2 (CHN), 135.8 (CHN), 173.5 (C(O)NH), 180.3 (NCHN), one signal not resolved. IR ATR 3264 (H<sub>2</sub>O), 3075, 2957, 2870, 1647, 1583 (NH), 1468, 1382, 1293, 1169, 1030, 984, 750 cm<sup>-1</sup>.

### 1-Butyl-3-methylimidazolium acetate (97)



Acetic acid (4 mL, 70 mmol, 1 eq) and KOH (3.8980 g, 69 mmol, 1 eq), were stirred in MeOH (30 mL) at 50 °C for 1 h and cooled to room temperature. [BMIM][Cl] (12.12 g, 69 mmol, 1 eq) in MeOH (25 mL) was added and stirred for 19 h. The

mixture was concentrated under reduced pressure, dissolved in  $\text{CHCl}_3$  (30 mL), filtered and concentrated under reduced pressure to yield (**97**) as a straw coloured oil (14.41 g, 100%).  $^1\text{H}$  NMR (400 MHz,  $\text{D}_2\text{O}$ )  $\delta_{\text{H}}$  0.76 (t, 3H,  $J = 7.5$  Hz,  $\text{CH}_3\text{CH}_2$ ), 1.16 (dq, 2H,  $J = 15.0, 7.5$  Hz,  $\text{CH}_3\text{CH}_2$ ), 1.64-1.74 (m, 2H,  $\text{CH}_3\text{CH}_2\text{CH}_2$ ), 1.77 (s, 3H,  $\text{CH}_3\text{CO}_2$ ), 3.73 (s, 3H,  $\text{CH}_3\text{N}$ ), 4.04 (t, 2H,  $J = 7.0$ ,  $\text{CH}_2\text{N}$ ), 7.26 (d, 1H,  $J = 1.5$  Hz, CHN), 7.31 (d, 1H,  $J = 1.5$  Hz, CHN), 8.55, (s, 1H, NCHN). Spectroscopic data were consistent with the literature.<sup>158</sup>

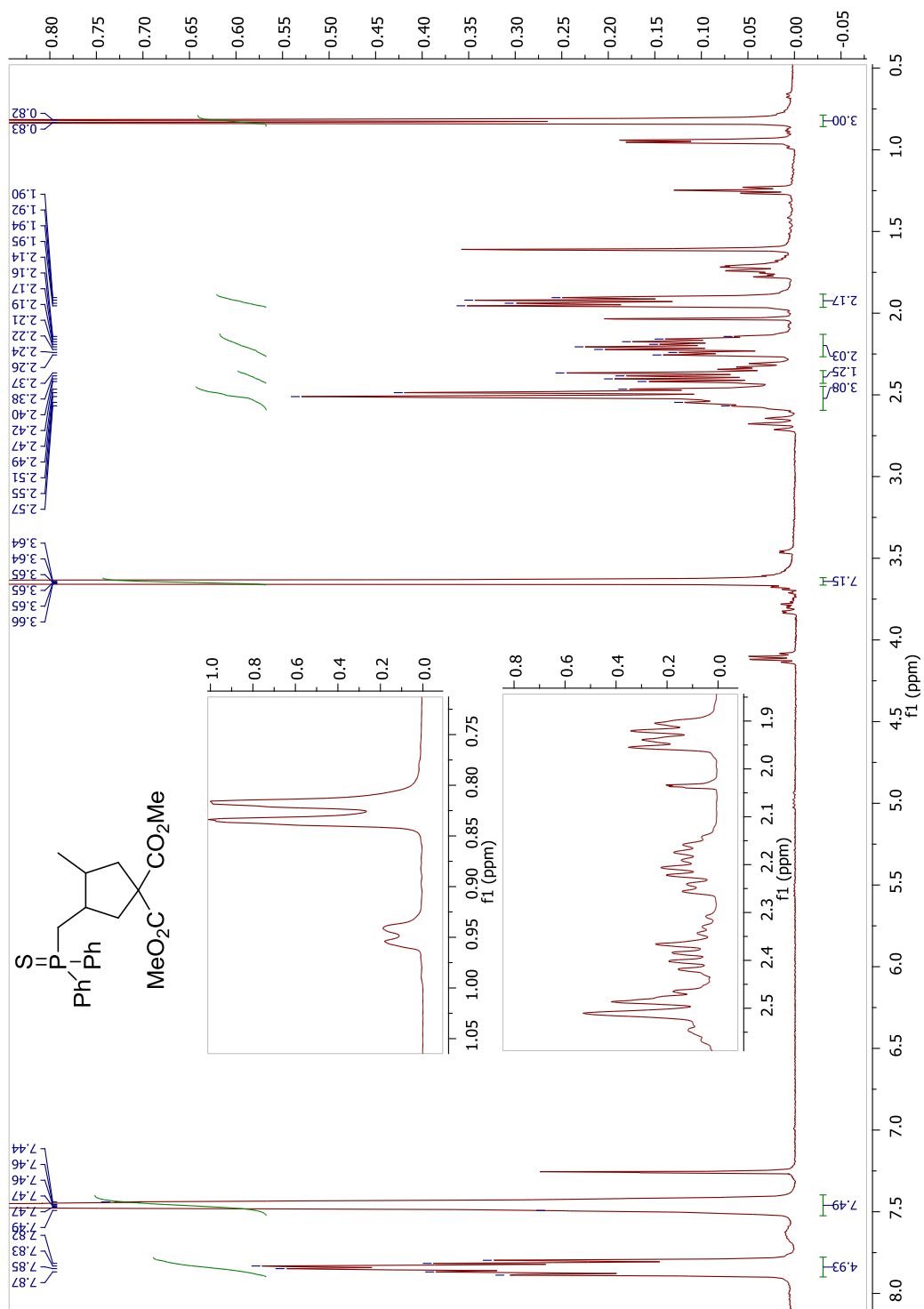


## **Appendices**

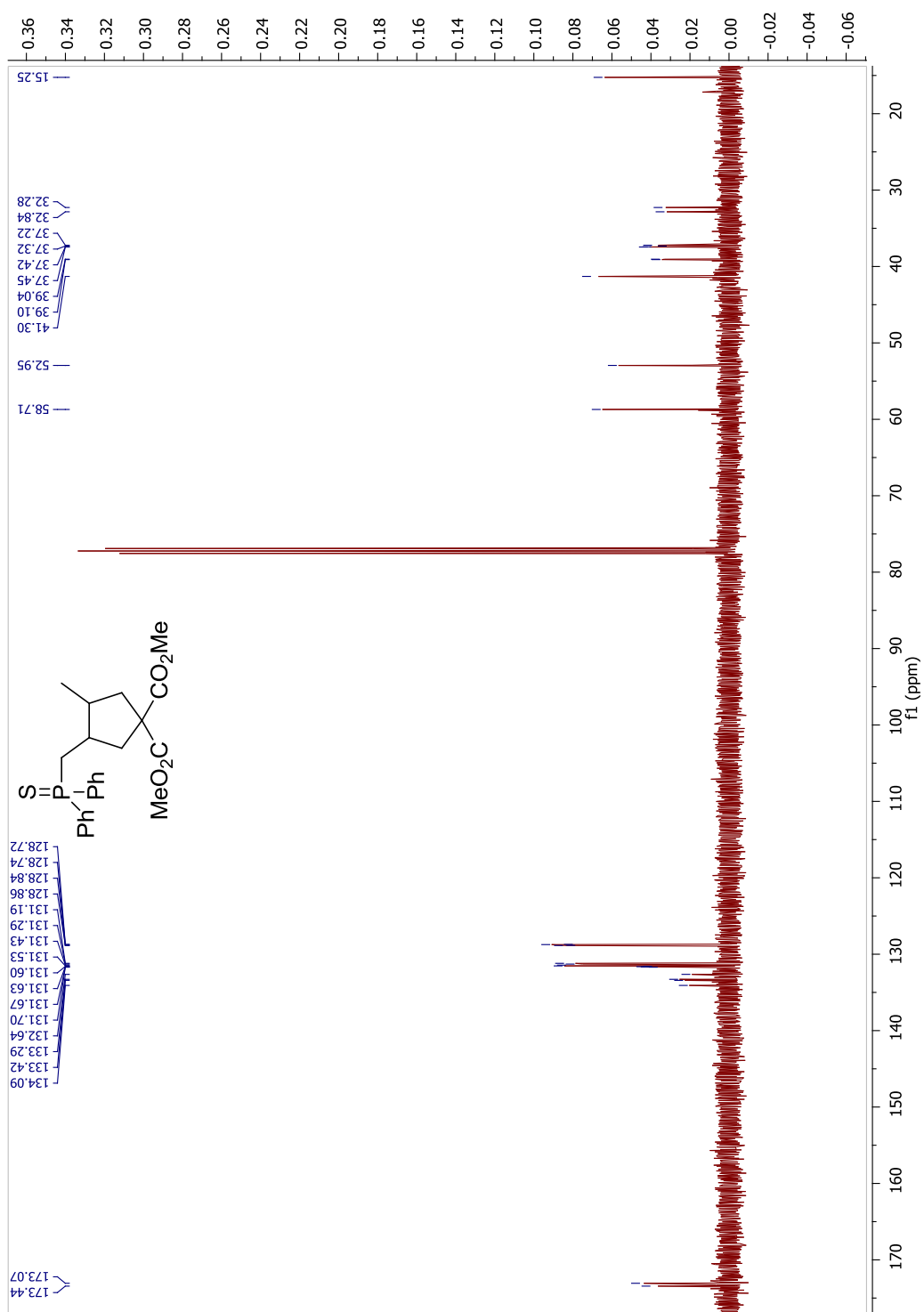
## Appendices

### *tert*-Butyl 3-[(diphenylphosphorothioyl)methyl]-4-methylpyrrolidine-1-carbamate (77)

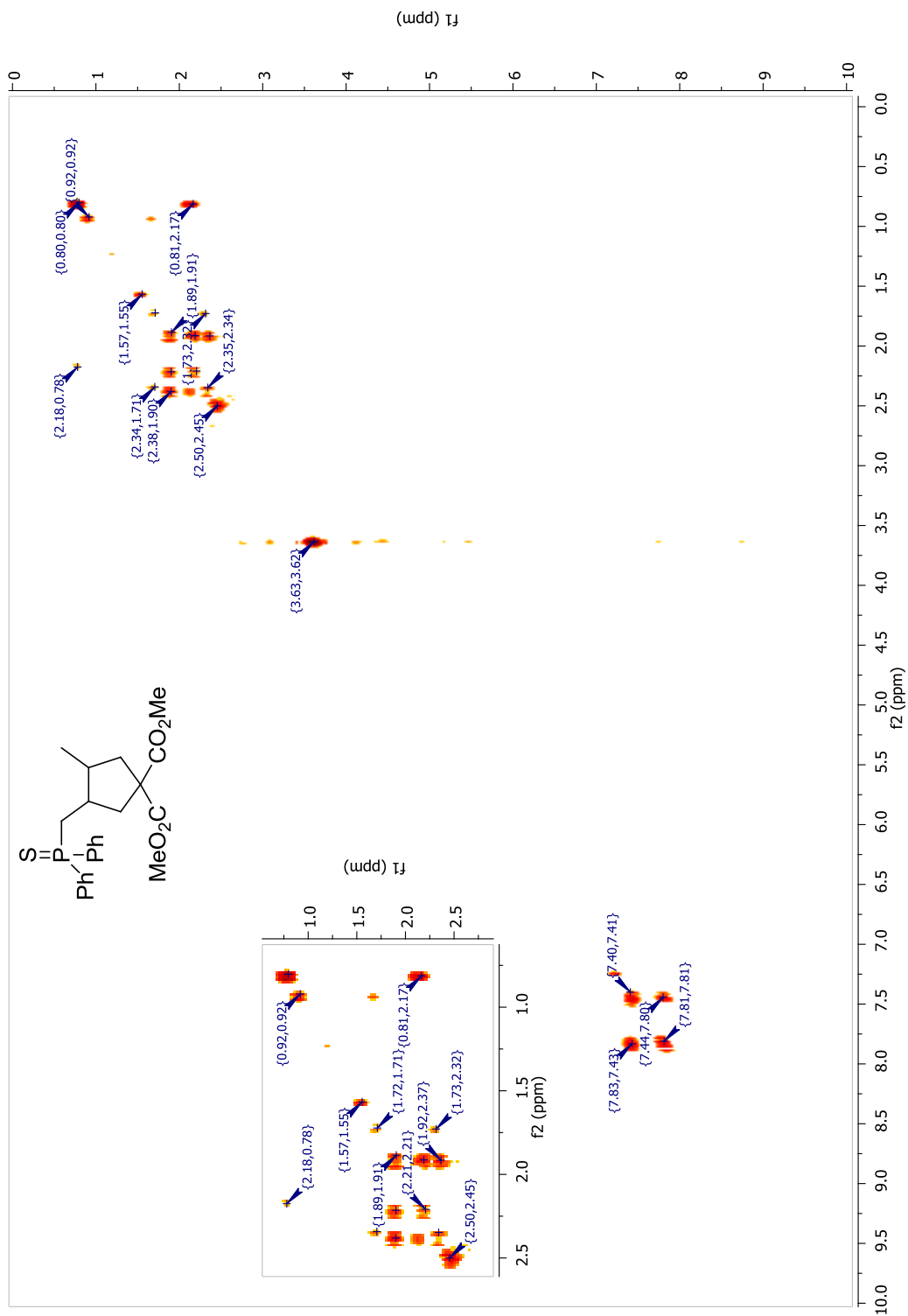
<sup>1</sup>H NMR



<sup>13</sup>C NMR

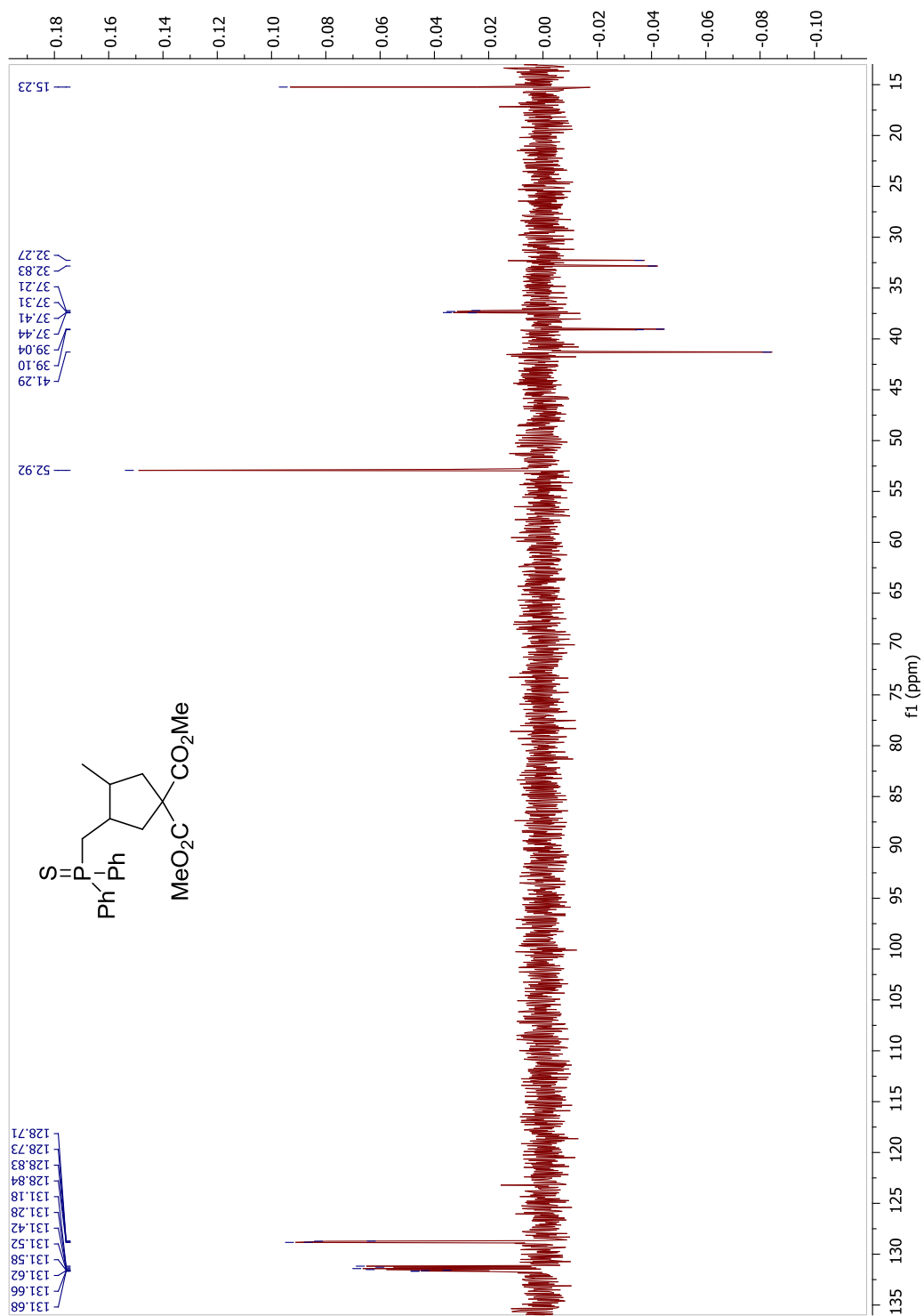


# COSY



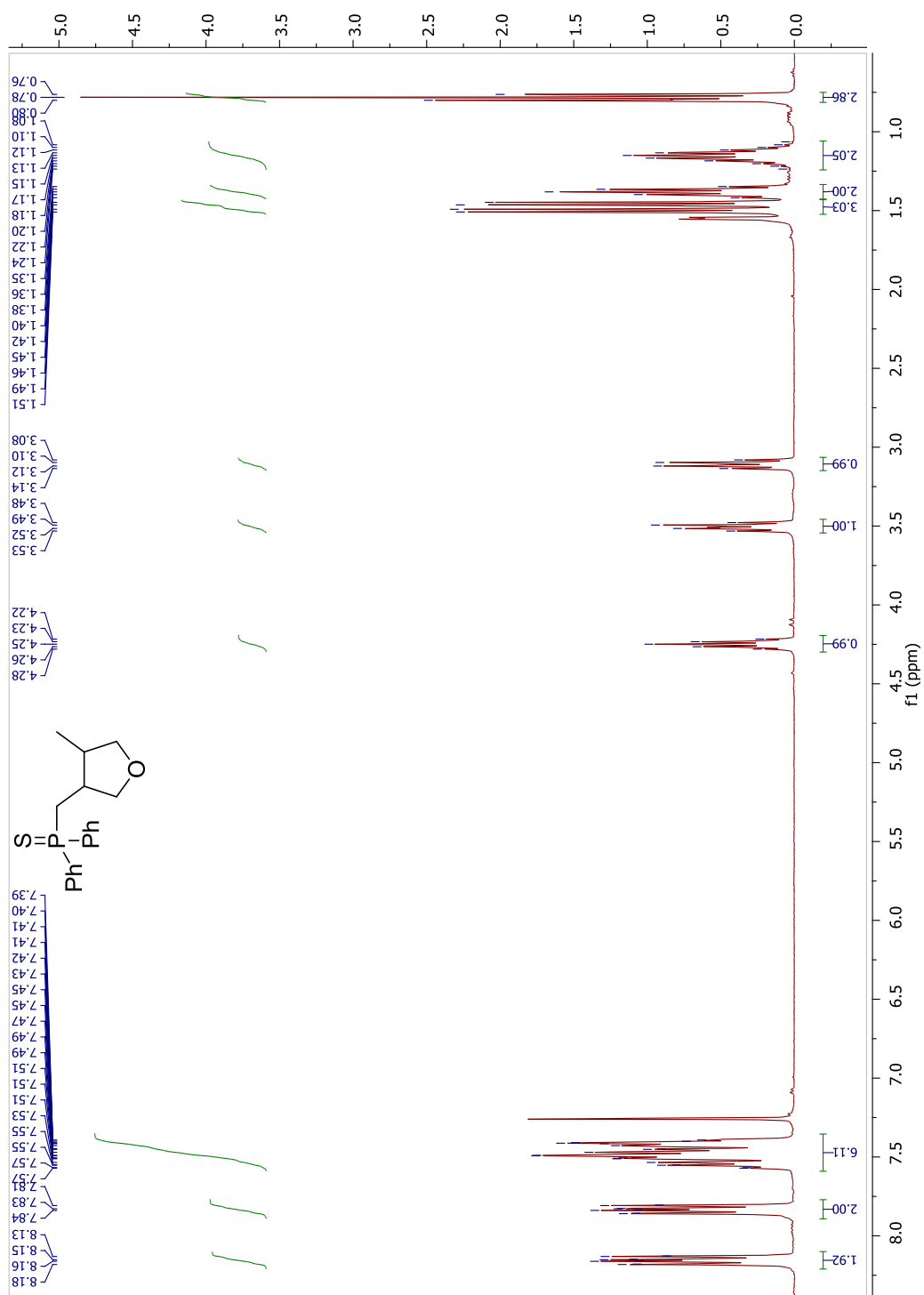


# 135 DEPT

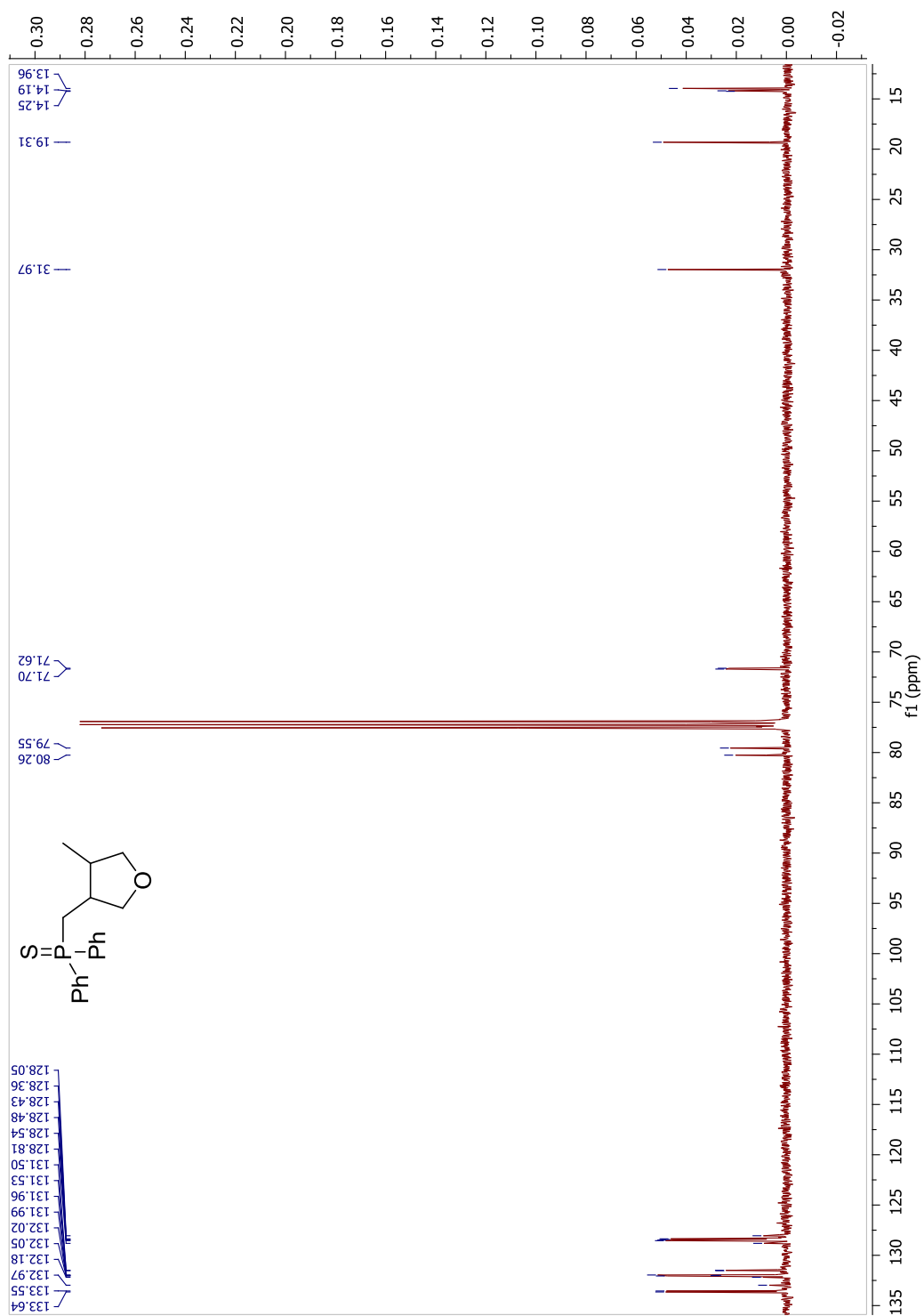


# [(4-Methyltetrahydrofuran-3-yl)methyl](diphenyl)phosphane sulfide (78)

$^1\text{H NMR}$

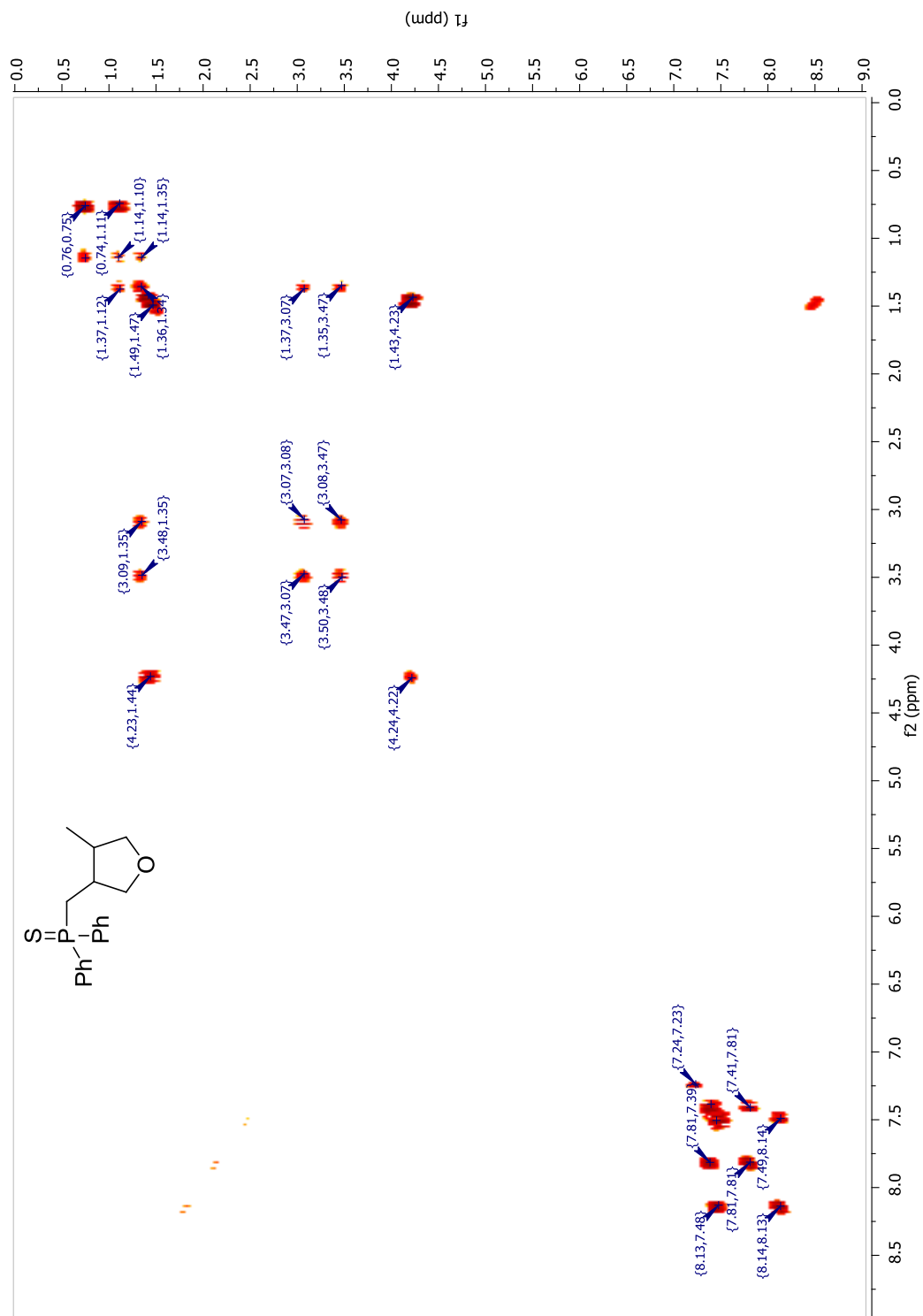


<sup>13</sup>C NMR

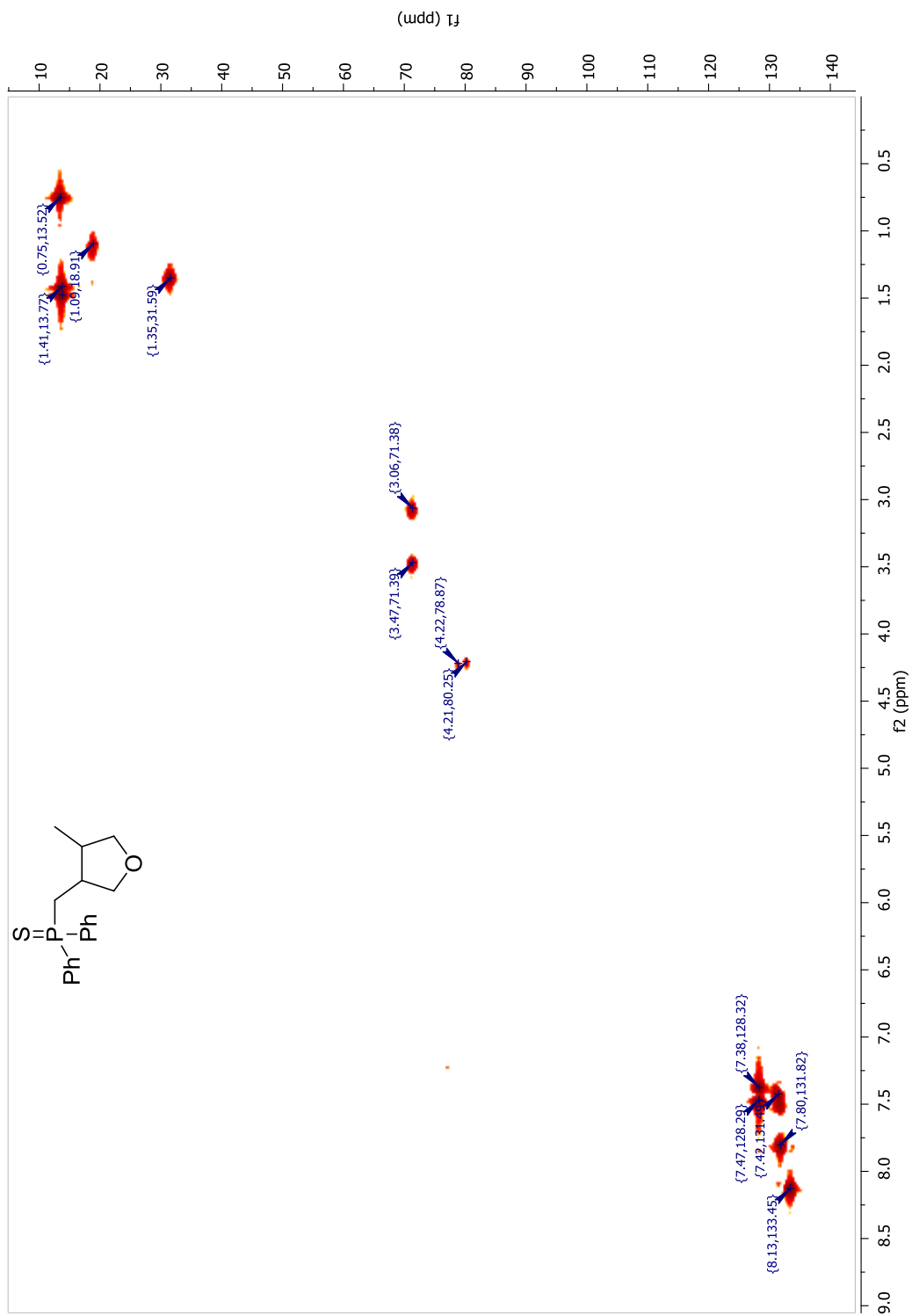




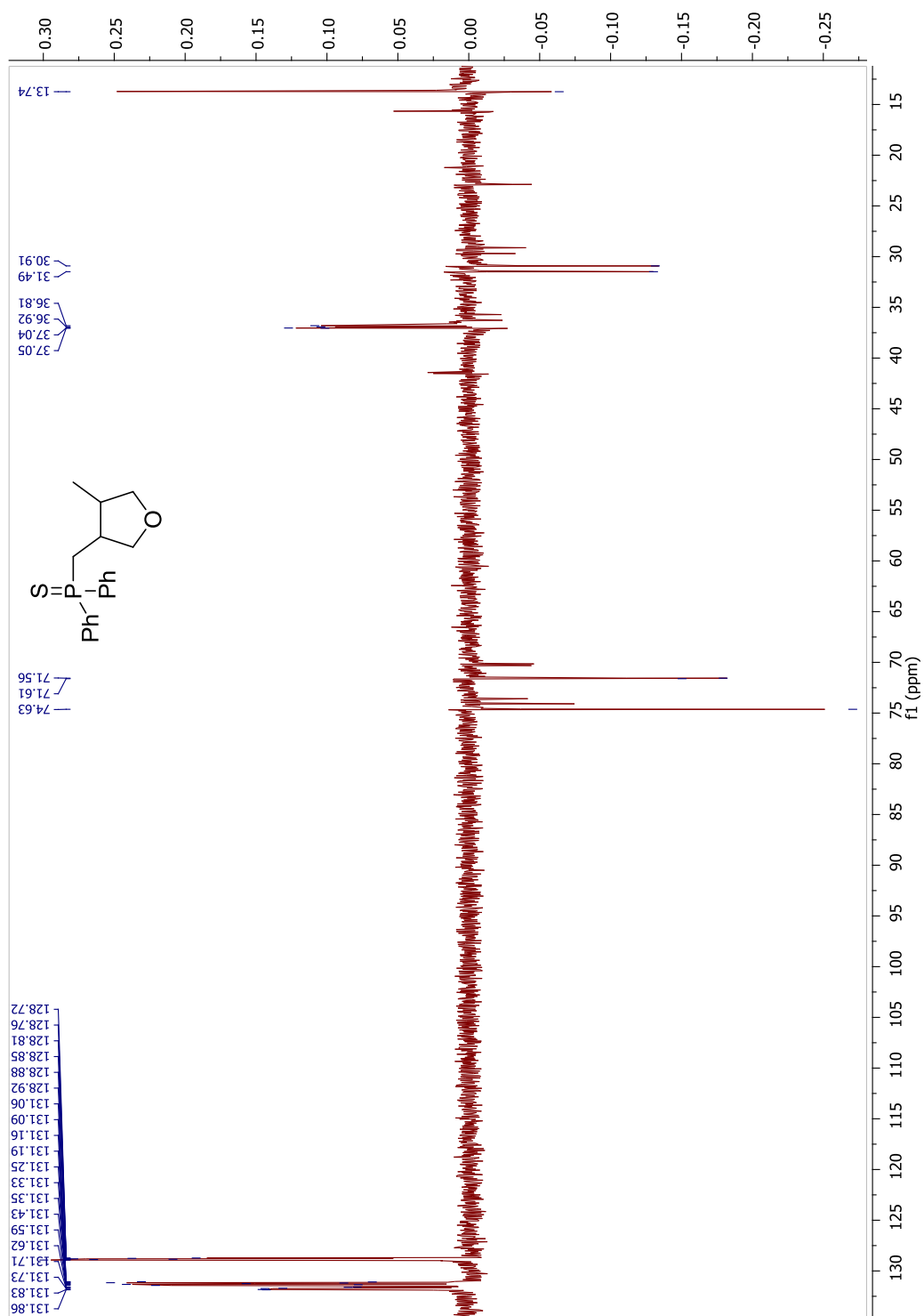
# COSY



# HMQC

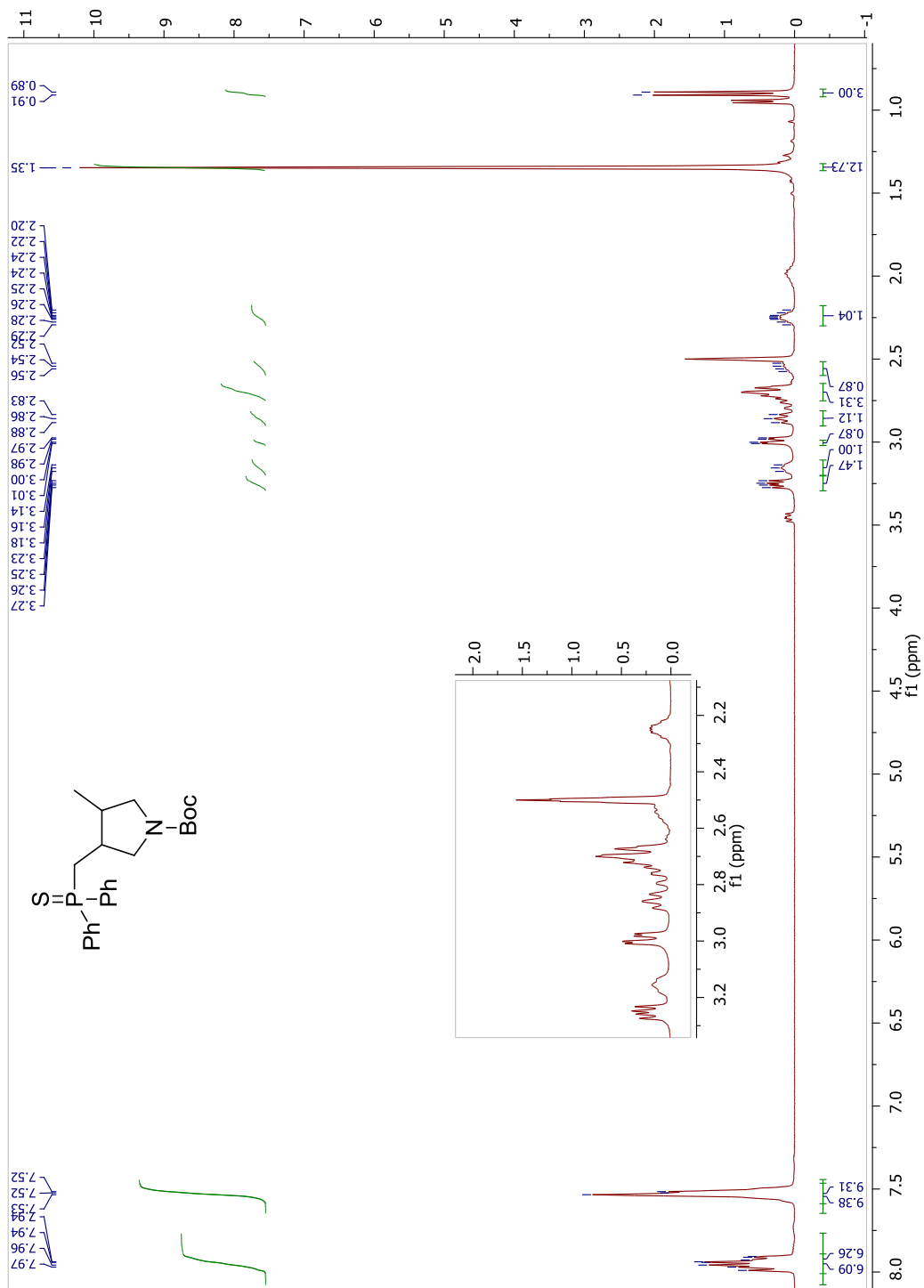


# 135 DEPT

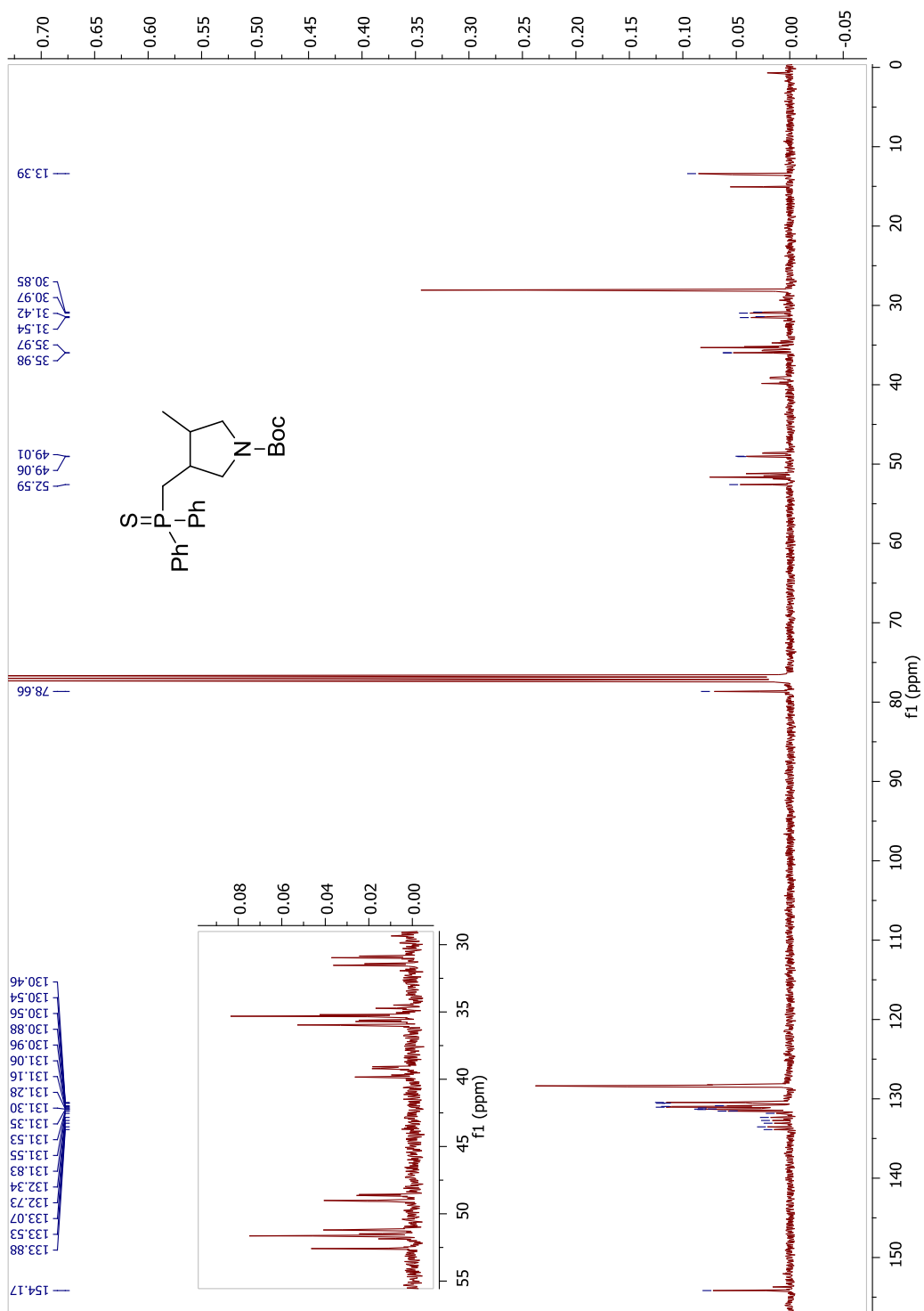


***tert*-Butyl 3-[(diphenylphosphorothioyl)methyl]-4-methylpyrrolidine-1-carbamate (80)**

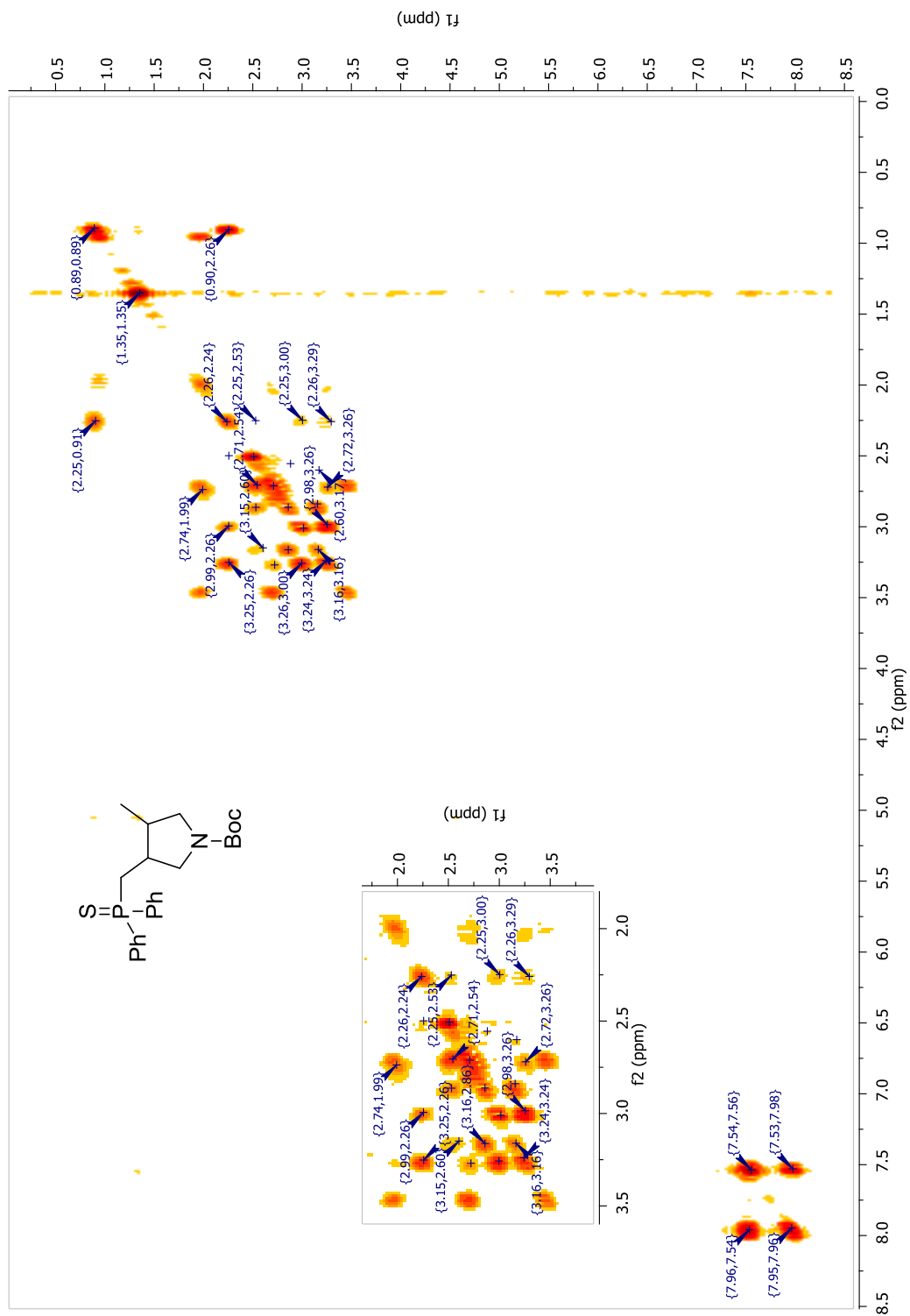
**<sup>1</sup>H NMR**



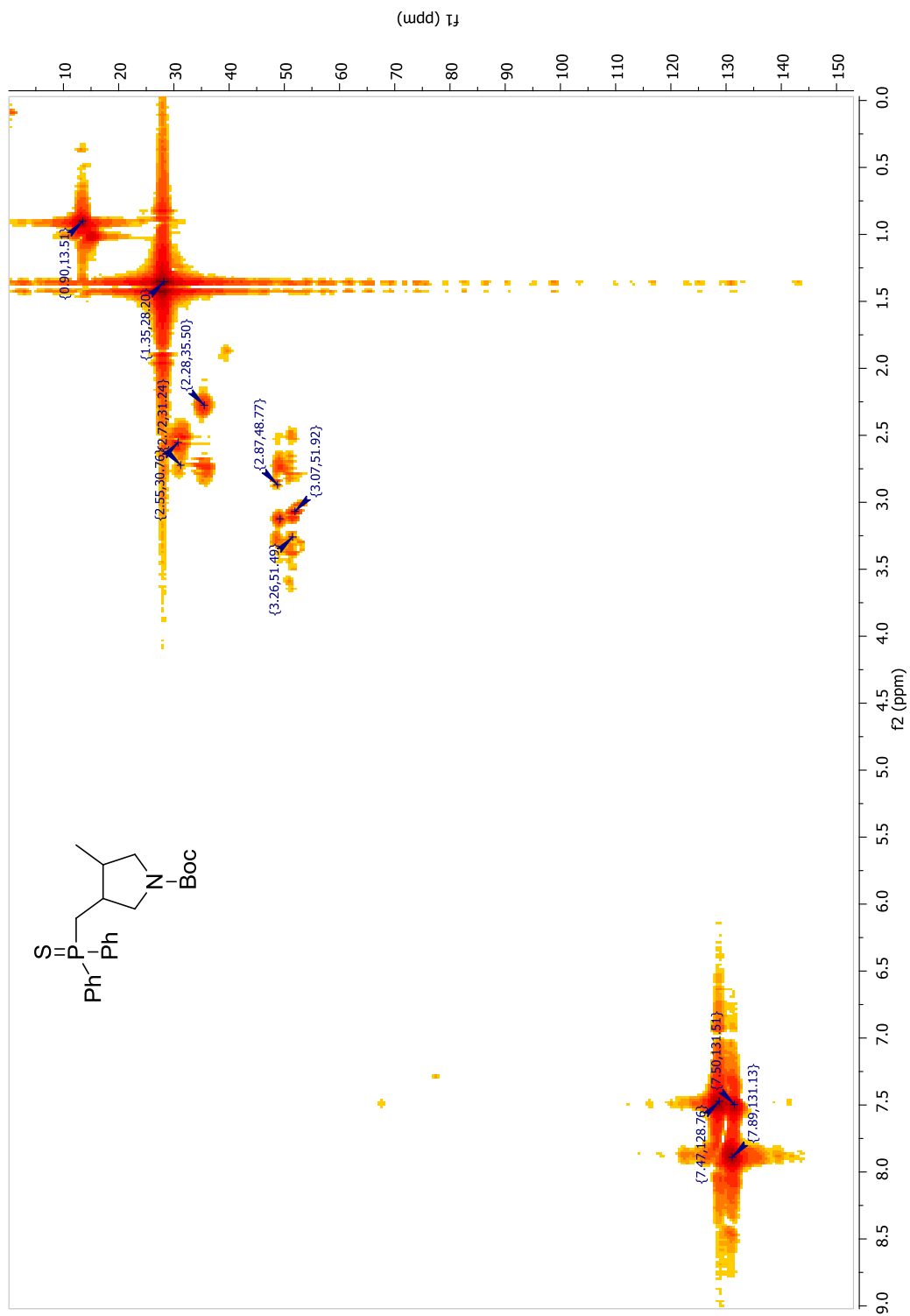
<sup>13</sup>C NMR



# COSY

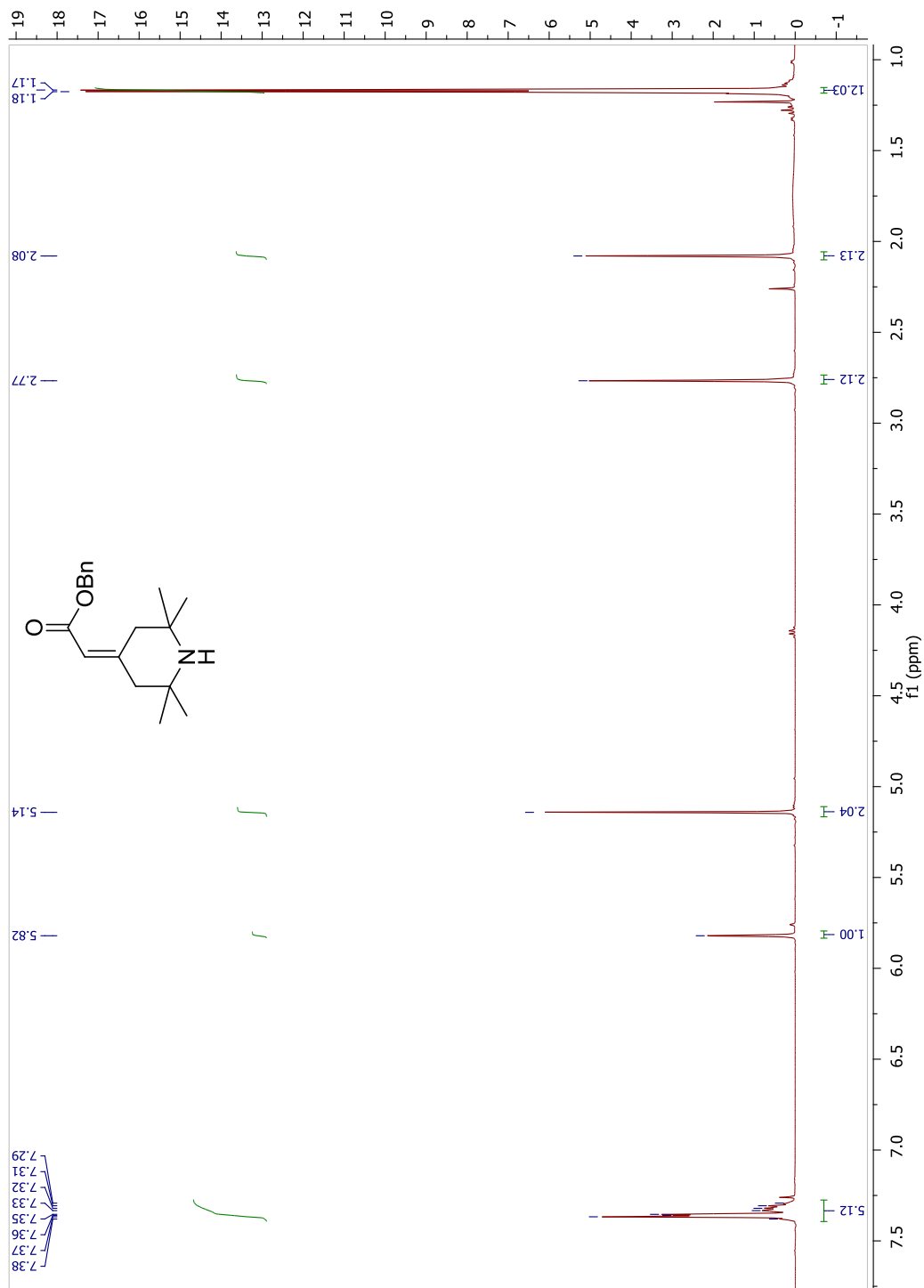


# HMQC



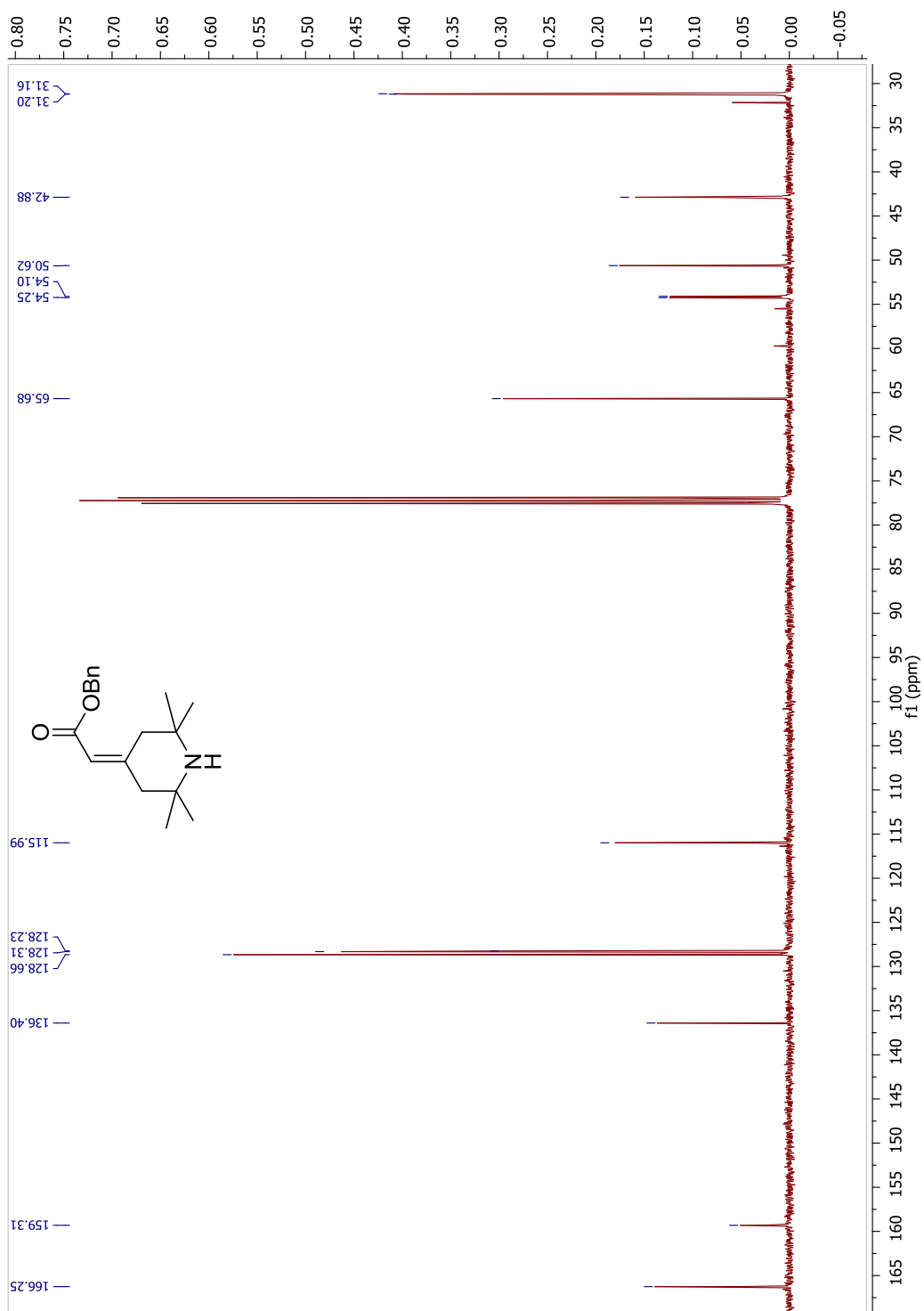
# Benzyl-2-(2,2,6,6-tetramethylpiperidin-4-ylidene)acetate (90)

## $^1\text{H NMR}$

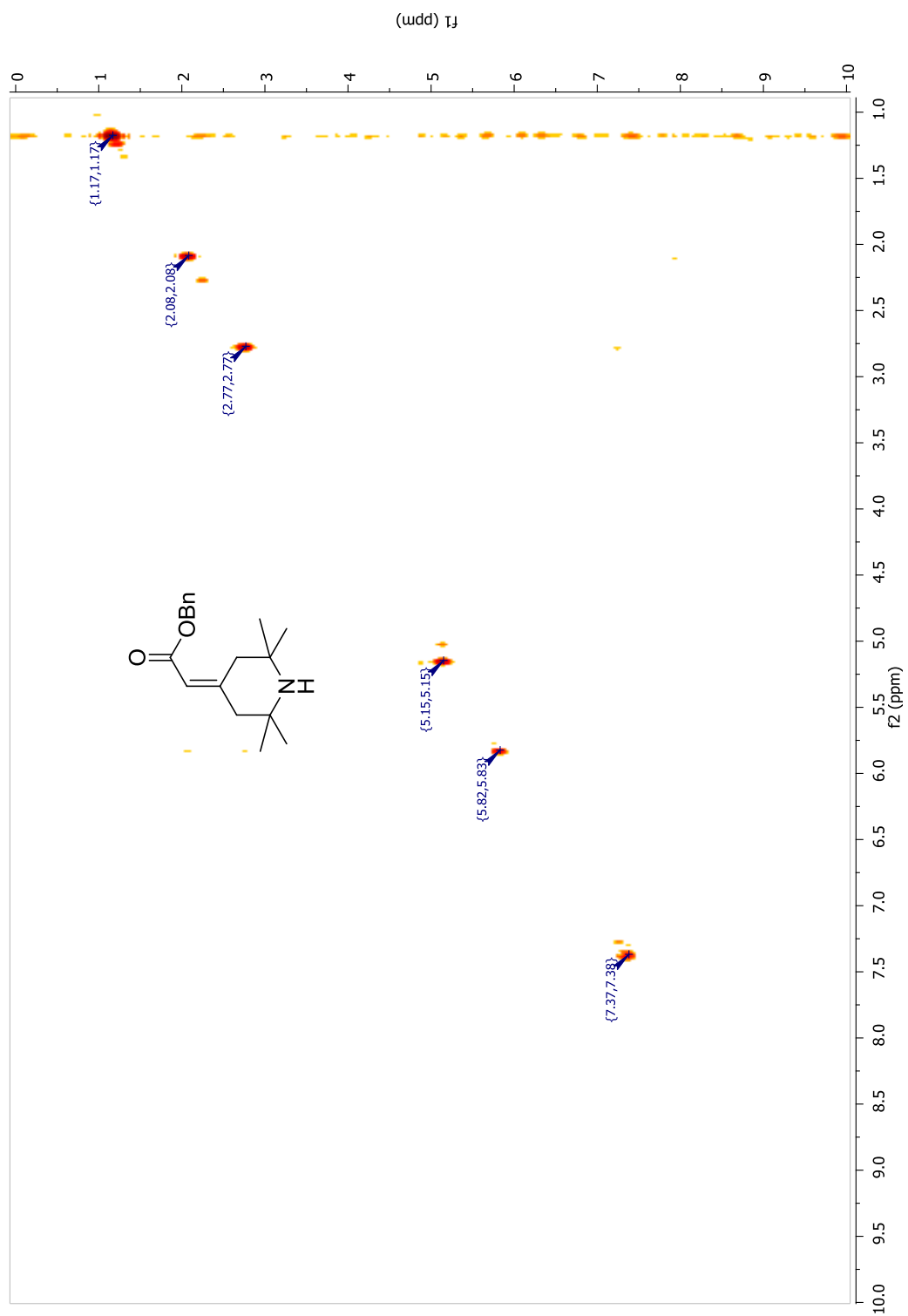




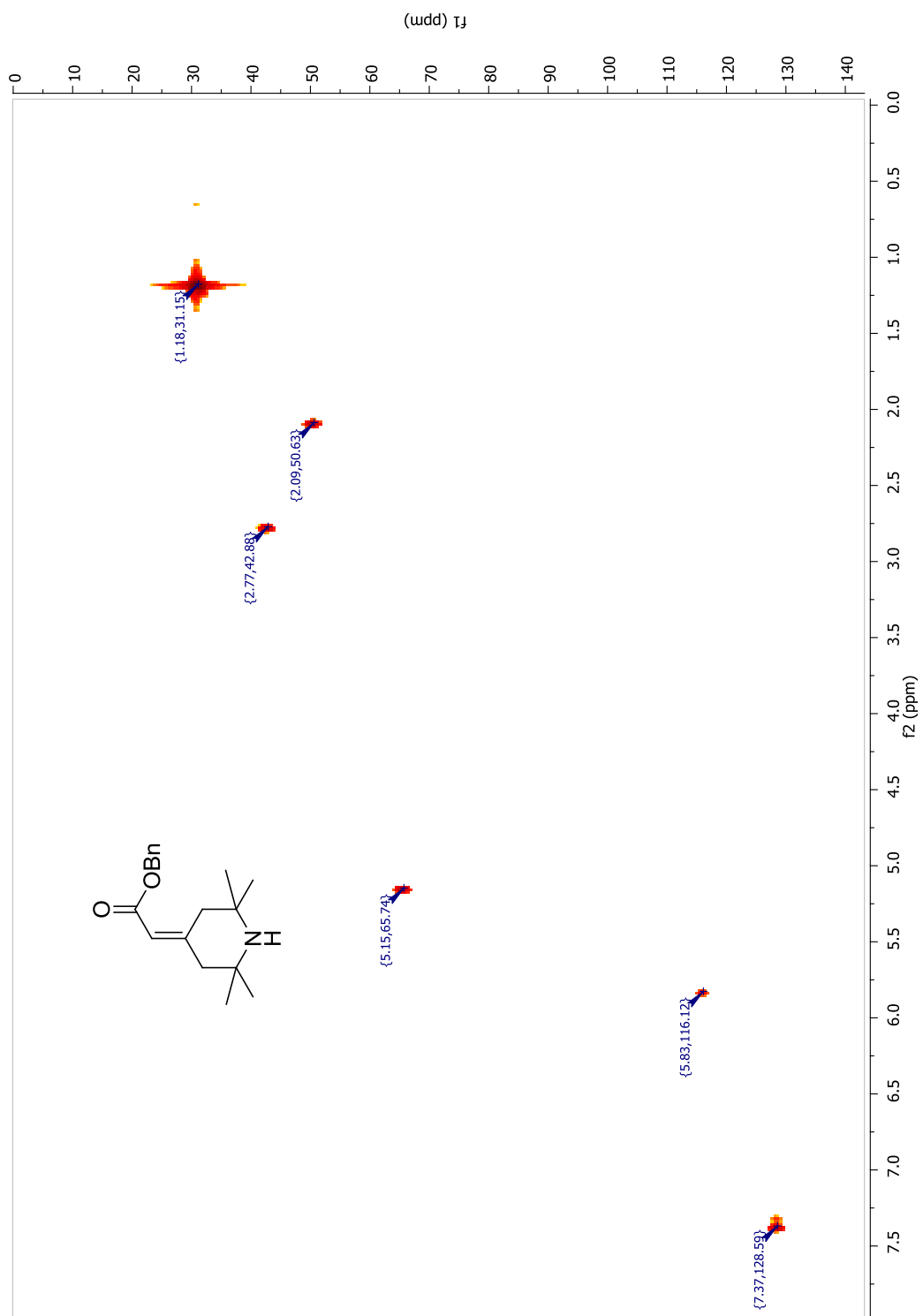
<sup>13</sup>C NMR



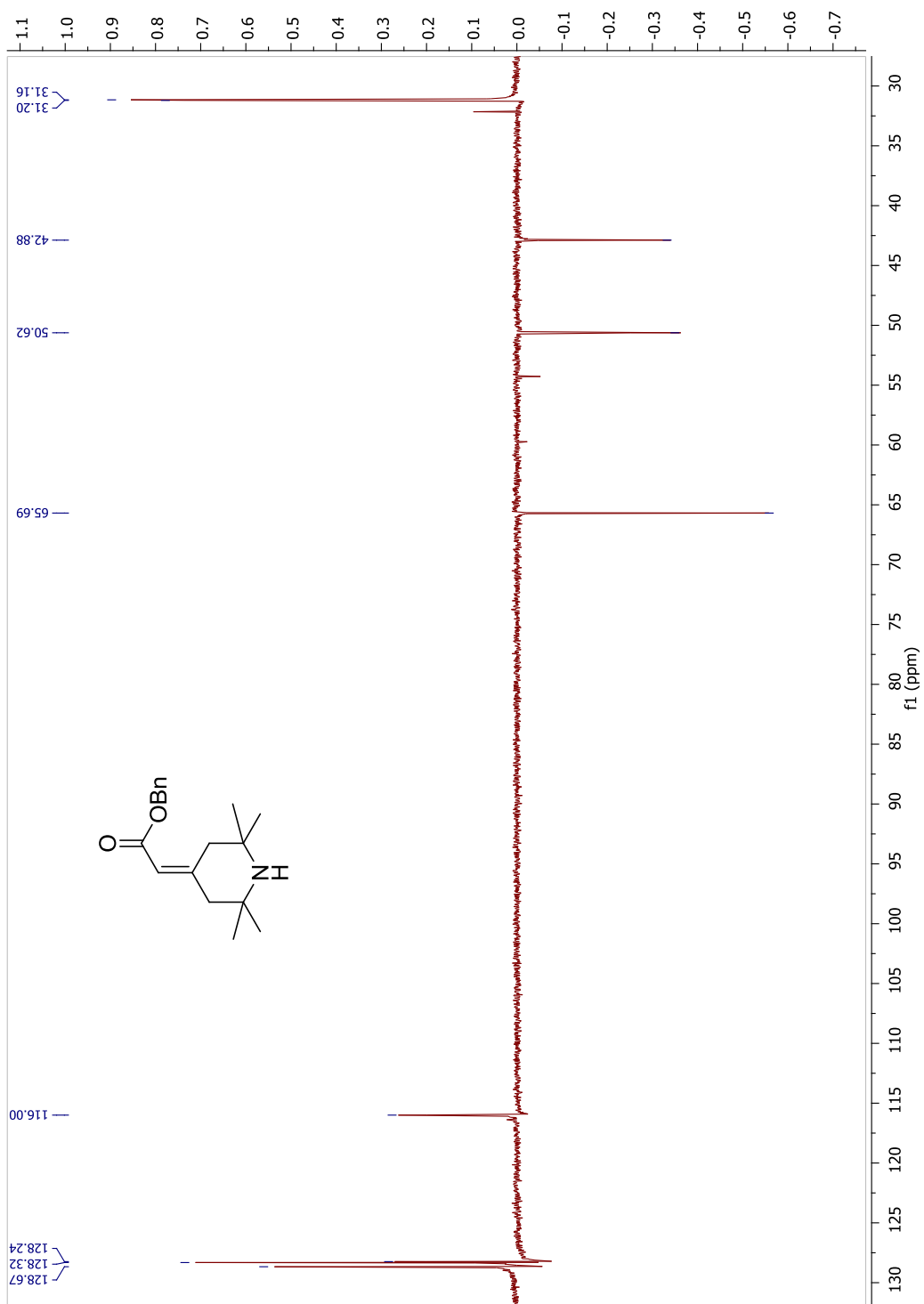
# COSY



# HMQC



135 DEPT



## **Abbreviations**

## Abbreviations

Ac	Acyl
AIBN	Azobisisobutyronitrile
Ar	Argon
BDE	Bond dissociation energy
[BMIM]	1-Butyl-3-methylimidazolium
[BMPyrd]	1-butyl-1-methylpyrrolidinium
Bn	Benzyl
Boc	<i>tert</i> -butyloxycarbonyl
BPO	Benzoyl peroxide
bpy	2,2'-Bipyridine
Bu	Butyl
Bz	Benzoate
°C	Degrees Celsius
calcd	Calculated
CAN	Cerium ammonium nitrate
COSY	Correlation spectroscopy
CSP	Chiral stationary phase
CTAB	Cetyltrimethylammonium bromide
$\Delta$	Thermal energy
d	Doublet
DCE	1,2-Dichloroethane

DCM	Dichloromethane
dd	Doublet of doublets
ddd	Double doublet of doublets
ddt	Double doublet of triplets
$\Delta E$	Change in energy
DEPT	Distortionless enhancement by polarisation transfer
DME	Dimethoxyethane
DMSO	Dimethylsulfoxide
dr	Diastereomeric ratio
dt	Doublet of triplets
$e^-$	Electron
EM	Electromagnetic
EPR	Electron paramagnetic resonance
ESI-MS	Electrospray ionisation mass spectrometry
Et	Ethyl
et al.	and others
eq	Equivalents
h	Hour(s)
h	Planck's constant
Hex	Hexyl
HMQC	Heteronuclear multiple-quantity correlation spectroscopy
HOMO	Highest occupied molecular orbital

HPLC	High performance liquid chromatography
Hz	Hertz
I	Inductive effect
IPA	Isopropyl alcohol
<i>J</i>	Coupling constant
kJ	Kilojoules
L	Ligand
LA	Lewis acid
LUMO	Lowest unoccupied molecular orbital
m	Multiplet
M	Mesomeric effect
Me	Methyl
mg	Milligram(s)
MHz	Megahertz
μL	Microlitres
mL	Millilitres
MO	Molecular orbital
mmol	Millimole(s)
mol	Mole(s)
m.p.	Melting point
$m_s$	Magnetic spin quantum number
m/z	mass to charge ratio



$\nu$	Frequency
NBS	<i>N</i> -Bromosuccinimide
NCS	<i>N</i> -Chlorosuccinimide
NHPI	<i>N</i> -Hydroxyphthalimide
nm	Nanometre(s)
NMI	<i>N</i> -Methylimidazole
NMP	Nitroxide mediated polymerisation
NMR	Nuclear magnetic resonance
[NTf <sub>2</sub> ]	Bis(trifluoroethanesulfonyl)imide
[O]	Oxidation
[ox]	Oxidised
OTf	Triflate
Ph	Phenyl
PINO	Phthalimide- <i>N</i> -oxyl
ppm	Parts per million
psi	Pounds per square inch
pTSA	<i>p</i> -Toluenesulfonic acid
q	Quartet
R	Generic organic group
R <sub>f</sub>	Retention factor
r.t.	Room temperature
s	Singlet

s	Spin quantum number
<sup>s</sup> BuLi	<i>sec</i> -Butyl-lithium
SOMO	Singly occupied molecular orbital
t	Triplet
T	Tesla
TEMPO	2,2,6,6-tetamethylpiperidine- <i>N</i> -oxyl
<i>tert</i>	Tertiary
THF	Tetrahydrofuran
TMS	Trimethylsilyl
td	Triplet of doublets
tt	Triplet of triplets
UV	Ultra-violet

## References

## References

- 1 M. Gomberg, *J. Am. Chem. Soc.*, 1900, **22**, 757–771.
- 2 M. Gomberg, *Chem. Rev.*, 1924, **1**, 91–141.
- 3 F. Dénès, M. Pichowicz, G. Povie and P. Renaud, *Chem. Rev.*, 2014, **114**, 2587–2693.
- 4 J. Iqbal, B. Bhatia and N. K. Nayyar, *Chem. Rev.*, 1994, **94**, 519–564.
- 5 F. Recupero and Carlo Punta, *Chem. Rev.*, 2007, **107**, 3800–3842.
- 6 M. P. Healy, A. F. Parsons and J. G. T. Rawlinson, *Org. Lett.*, 2005, **7**, 1597–1600.
- 7 M. S. Kharasch and F. R. Mayo, *J. Am. Chem. Soc.*, 1933, **55**, 2468–2496.
- 8 G. N. Lewis, D. Lipkin and T. T. Magel, *J. Am. Chem. Soc.*, 1944, **66**, 1579–1583.
- 9 W. Reints, D. A. Pratt, H.-G. Korth and P. Mulder, *J. Phys. Chem. A*, 2000, **104**, 10713–10720.
- 10 AIChE, <http://www3.aiche.org/proceedings/content/Annual-2013/extended-abstracts/P318455.pdf> (accessed September 2015).
- 11 A. D. Asandei, Y. Chen, I. W. Moran and G. Saha, *J. Organomet. Chem.*, 2007, **692**, 3174–3182.
- 12 G. Luft, H. Bitsch and H. Seidl, *J. Macromol. Sci. Part A - Chem.*, 2006, **11**, 1089–1112.
- 13 G. O. Wilson, J. W. Henderson, M. M. Caruso, B. J. Blaiszik, P. J. McIntire, N. R. Sottos, S. R. White and J. S. Moore, *J. Polym. Sci. Part A Polym. Chem.*, 2010, **48**, 2698–2708.
- 14 G. Ruggeri, M. Aglietto, A. Petraghani and F. Ciardelli, *Eur. Polym. J.*, 1983, **19**, 863–866.
- 15 M. Adamczyk, S. R. Akireddy and R. E. Reddy, *Tetrahedron: Asymmetry*, 2001, **12**, 2385–2387.
- 16 K. Miura, Y. Ichinose, K. Nozaki, K. Fugami, K. Oshima and K. Utimoto, *Bull. Chem. Soc. Jpn.*, 1989, **62**, 143–147.
- 17 B. Karimi and J. Rajabi, *Synthesis*, 2003, 2373–2377.
- 18 J. E. Baldwin, *J. Chem. Soc. Chem. Commun.*, 1976, 734.
- 19 J. E. Baldwin, R. C. Thomas, L. I. Kruse and L. Silberman, *J. Org. Chem.*, 1977, **42**, 3846–3852.
- 20 C. Chatgililoglu, C. Ferreri, M. Guerra, V. Timokhin, G. Froudakis and T. Gimisis, *J. Am. Chem. Soc.*, 2002, **124**, 10765–10772.
- 21 A. L. J. Beckwith, C. J. Easton and A. K. Serelis, *J. Chem. Soc. Chem. Commun.*, 1980, 482.
- 22 H. G. Kuivila, *Acc. Chem. Res.*, 1968, **1**, 299–305.

- 23 S. D. Burke, W. F. Fobare and D. M. Armistead, *J. Org. Chem.*, 1982, **47**, 3348–3350.
- 24 B. Giese, *Angew. Chemie Int. Ed. English*, 1983, **22**, 753–764.
- 25 G. E. Keck and J. B. Yates, *J. Am. Chem. Soc.*, 1982, **104**, 5829–5831.
- 26 P. Renaud and T. Bourquard, *Tetrahedron Lett.*, 1994, **35**, 1707–1710.
- 27 D. Griller and D. D. M. Wayner, *Pure Appl. Chem.*, 1989, **61**, 717–724.
- 28 UCSB, <https://labs.chem.ucsb.edu/zakarian/armen/11---bonddissociationenergy.pdf> (accessed September 2015).
- 29 A. Dobbs, *J. Org. Chem.*, 2001, **66**, 638–641.
- 30 C. Prakash, G. G. Rajeshwaran and A. K. Mohanakrishnan, *Synth. Commun.*, 2010, **40**, 2097–2107.
- 31 J. Lei, H. L. Cui, R. Li, L. Wu, Z. Y. Ding and Y. C. Chen, *Org. Biomol. Chem.*, 2010, **8**, 2840–2844.
- 32 P. Dowd and S. C. Choi, *J. Am. Chem. Soc.*, 1987, **109**, 3493–3494.
- 33 D. H. R. Barton and S. W. McCombie, *J. Chem. Soc. Perkin Trans. 1*, 1975, 1574.
- 34 J. Langhanki, K. Rudolph, G. Erkel and T. Opatz, *Org. Biomol. Chem.*, 2014, **12**, 9707–9715.
- 35 N. Asao, J. X. Liu, T. Sudoh and Y. Yamamoto, *J. Org. Chem.*, 1996, **61**, 4568–4571.
- 36 P. A. Baguley and J. C. Walton, *Angew. Chemie Int. Ed.*, 1998, **37**, 3072–3082.
- 37 D. Crich and S. Sun, *J. Org. Chem.*, 1996, **61**, 7200–7201.
- 38 E. J. Corey and J. W. Suggs, *J. Org. Chem.*, 1975, **40**, 2554–2555.
- 39 D. S. Hays and G. C. Fu, *J. Org. Chem.*, 1996, **61**, 4–5.
- 40 D. L. J. Clive and W. Yang, *J. Org. Chem.*, 1995, **60**, 2607–2609.
- 41 J. Light and R. Breslow, *Tetrahedron Lett.*, 1990, **31**, 2957–2958.
- 42 D. P. Curran and S. Hadida, *J. Am. Chem. Soc.*, 1996, **118**, 2531–2532.
- 43 W. Russell Bowman, S. L. Krintel and M. B. Schilling, *Org. Biomol. Chem.*, 2004, **2**, 585–592.
- 44 K. B. Clark and D. Griller, *Organometallics*, 1991, **10**, 746–750.
- 45 D. J. Carlsson, K. U. Ingold and L. C. Bray, *Int. J. Chem. Kinet.*, 1969, **1**, 315–323.
- 46 *Encyclopedia of Reagents for Organic Synthesis*, John Wiley & Sons, Ltd, Chichester, UK, 2001.
- 47 V. Gupta and D. Kahne, *Tetrahedron Lett.*, 1993, **34**, 591–594.
- 48 P. Pike, S. Hershberger and J. Hershberger, *Tetrahedron*, 1988, **44**, 6295–6304.
- 49 D. H. R. Barton, D. O. Jang and J. C. Jaszberenyi, *Tetrahedron Lett.*, 1991, **32**,

- 7187–7190.
- 50 S. J. Cole, J. N. Kirwan, B. P. Roberts and C. R. Willis, *J. Chem. Soc., Perkin Trans. 1*, 1991, 103–112.
- 51 H. S. Dang and B. P. Roberts, *Tetrahedron Lett.*, 1995, **36**, 2875–2878.
- 52 J. M. Kanabus-Kaminska, J. A. Hawari, D. Griller and C. Chatgililoglu, *J. Am. Chem. Soc.*, 1987, **109**, 5267–5268.
- 53 C. Chatgililoglu, D. Griller and M. Lesage, *J. Org. Chem.*, 1988, **53**, 3641–3642.
- 54 C. Chatgililoglu, *Acc. Chem. Res.*, 1992, **25**, 188–194.
- 55 M. Ballestri, C. Chatgililoglu, K. B. Clark, D. Griller, B. Giese and B. Kopping, *J. Org. Chem.*, 1991, **56**, 678–683.
- 56 B. Giese and B. Kopping, *Tetrahedron Lett.*, 1989, **30**, 681–684.
- 57 M. Ballestri, C. Chatgililoglu, N. Cardi and A. Sommazzi, *Tetrahedron Lett.*, 1992, **33**, 1787–1790.
- 58 M. Lesage, C. Chatgililoglu and D. Griller, *Tetrahedron Lett.*, 1989, **30**, 2733–2734.
- 59 D. Leca, L. Fensterbank, E. Lacôte and M. Malacria, *Chem. Soc. Rev.*, 2005, **34**, 858–865.
- 60 H. Yorimitsu, *Beilstein J. Org. Chem.*, 2013, **9**, 1269–1277.
- 61 D. H. R. Barton, D. O. Jang and J. C. Jaszberenyi, *J. Org. Chem.*, 1993, **58**, 6838–6842.
- 62 D. O. Jang, *Tetrahedron Lett.*, 1996, **37**, 5367–5368.
- 63 R. McCague, R. G. Pritchard, R. J. Stoodley and D. S. Williamson, *Chem. Commun.*, 1998, 2691–2692.
- 64 C. Gonzalez Martin, J. A. Murphy and C. R. Smith, *Tetrahedron Lett.*, 2000, **41**, 1833–1836.
- 65 H. Nambu, G. Anilkumar, M. Matsugi and Y. Kita, *Tetrahedron*, 2003, **59**, 77–85.
- 66 D. H. Cho and D. O. Jang, *Tetrahedron Lett.*, 2005, **46**, 1799–1802.
- 67 E. Fremy, *Ann. der Chemie und Pharm.*, 1845, **56**, 315–354.
- 68 S. Wertz and A. Studer, *Green Chem.*, 2013, **15**, 3116.
- 69 M. Holan and U. Jahn, *Org. Lett.*, 2013, **1**, 5–8.
- 70 K. Platkowski and K. H. Reichert, *Chem. Eng. Technol.*, 1999, **22**, 1035–1038.
- 71 E. Mezzina, R. Manoni, F. Romano and M. Lucarini, *Asian J. Org. Chem.*, 2015, **4**, 296–310.
- 72 R. B. Grubbs, *Polym. Rev.*, 2011, **51**, 104–137.
- 73 R. Briere and A. Rassat, *Tetrahedron*, 1976, **32**, 2891–2898.
- 74 M. Shibuya, M. Tomizawa, I. Suzuki and Y. Iwabuchi, *J. Am. Chem. Soc.*, 2006, **128**, 8412–8413.

- 75 J. Brecht, *Justus Liebigs Ann. Chem.*, 1924, **437**, 1–13.
- 76 V. A. Golubev, R. G. and M. B. Neiman, *Bull. Acad. Sci. USSR Div. Chem. Sci.*, 1965, **14**, 1898–1904.
- 77 Z. Ma and J. M. Bobbitt, *J. Org. Chem.*, 1991, **56**, 6110–6114.
- 78 M. Zhao, J. Li, E. Mano, Z. Song, D. M. Tschaen, E. J. J. Grabowski and P. J. Reider, *J. Org. Chem.*, 1999, **64**, 2564–2566.
- 79 Y. Kashiwagi, H. Ikezoe and T. Ono, *Synlett*, 2006, 69–72.
- 80 R. A. Miller and R. S. Hoerrner, *Org. Lett.*, 2003, **5**, 285–287.
- 81 C. Bolm, A. S. Magnus and J. P. Hildebrand, *Org. Lett.*, 2000, **2**, 1173–1175.
- 82 X. F. Zhao and C. Zhang, *Synthesis*, 2007, 551–557.
- 83 L. De Luca, G. Giacomelli, S. Masala, A. Porcheddu and D. Chimica, 2003, 14–16.
- 84 J. Einhorn, C. Einhorn, F. Ratajczak and J. L. Pierre, *J. Org. Chem.*, 1996, **61**, 7452–7454.
- 85 J. M. Hoover and S. S. Stahl, *J. Am. Chem. Soc.*, 2011, **133**, 16901–16910.
- 86 M. Fabbrini, C. Galli and P. Gentili, *J. Mol. Catal. - B Enzym.*, 2002, **16**, 231–240.
- 87 I. A. Ansari and R. Gree, *Org. Lett.*, 2002, **4**, 1507–1509.
- 88 R. Barhdadi, C. Comminges, A. P. Doherty, J. Y. Nédélec, S. O’Toole and M. Troupel, *J. Appl. Electrochem.*, 2007, **37**, 723–728.
- 89 P. J. Scammells, J. L. Scott and R. D. Singer, *Aust. J. Chem.*, 2005, **58**, 155–169.
- 90 E. L. Eliel, V. G. Badding and M. N. Rerick, *J. Am. Chem. Soc.*, 1962, **84**, 2371–2377.
- 91 P. Deslongchamps, P. Atlani, D. Fréhel, A. Malaval and C. Moreau, *Can. J. Chem.*, 1974, **52**, 3651–3664.
- 92 C. Van Doorslaer, A. Peeters, P. Mertens, C. Vinckier, K. Binnemans and D. De Vos, *Chem. Commun.*, 2009, 6439–6441.
- 93 J. Maślińska-Solich and A. Macionga, *React. Funct. Polym.*, 1997, **33**, 255–261.
- 94 R. Gopinath, A. R. Paital and B. K. Patel, *Tetrahedron Lett.*, 2002, **43**, 5123–5126.
- 95 J. D. Prugh and W. C. McCarthy, *Tetrahedron Lett.*, 1966, **7**, 1351–1356.
- 96 B. Karimi and J. Rajabi, *J. Mol. Catal. A Chem.*, 2005, **226**, 165–169.
- 97 J. T. Knudsen, R. Eriksson, J. Gershenzon and B. Ståhl, *Bot. Rev.*, 2006, **72**, 1–120.
- 98 H. Dreser, *Pflüger, Arch. für die Gesamte Physiol. des Menschen und der Thiere*, 1899, **76**, 306–318.
- 99 J. J. Scepaniak, A. M. Wright, R. A. Lewis, G. Wu and T. W. Hayton, *J. Am. Chem. Soc.*, 2012, **134**, 19350–19353.

- 100 K. L. Ford and E. J. Roskamp, *Tetrahedron Lett.*, 1992, **33**, 1135–1138.
- 101 U. Jahn, M. Müller and S. Aussieker, *J. Am. Chem. Soc.*, 2000, **122**, 5212–5213.
- 102 M. Pouliot, P. Renaud, K. Schenk, A. Studer and T. Vogler, *Angew. Chemie - Int. Ed.*, 2009, **48**, 6037–6040.
- 103 M. S. Tichenor, K. S. MacMillan, J. S. Stover, S. E. Wolkenberg, M. G. Pavani, L. Zanella, A. N. Zaid, G. Spalluto, T. J. Rayl, I. Hwang, P. G. Baraldi and D. L. Boger, *J. Am. Chem. Soc.*, 2007, **129**, 14092–14099.
- 104 R. A. Jackson, K. U. Ingold, D. Griller and A. S. Nazran, *J. Am. Chem. Soc.*, 1985, **107**, 208–211.
- 105 G. Henrich, V. M. Lynch and E. V. Anslyn, *Chem. Commun.*, 2001, 2436–2437.
- 106 J. Peterson, *J. Chem. Educ.*, 1992, **69**, 843.
- 107 U. V. Mallavadhani, A. Mahapatra, B. Pattnaik, N. Vanga, N. Suri and A. K. Saxena, *Med. Chem. Res.*, 2012, **22**, 1263–1269.
- 108 S. J. Yang, M. C. Liu, Q. Zhao, D. Y. Hu, W. Xue and S. Yang, *Eur. J. Med. Chem.*, 2015, **96**, 58–65.
- 109 N. P. Alza, V. Richmond, C. J. Baier, E. Freire, R. Baggio and A. P. Murray, *Bioorg. Med. Chem.*, 2014, **22**, 3838–3849.
- 110 D. Biedermann, B. Eignerova, M. Hajdich and J. Sarek, *Synthesis*, 2010, 3839–3848.
- 111 G. Rajabzadeh, S. Salehi and A. Jalalian, *Synth. React. Inorganic, Met. Nano-Metal Chem.*, 2010.
- 112 S. Sompech, A. Srion and A. Nuntiya, *Procedia Eng.*, 2012, **32**, 1012–1018.
- 113 M. D. Carrigan, D. Sarapa, R. C. Smith, L. C. Wieland and R. S. Mohan, *J. Org. Chem.*, 2002, **67**, 1027–1030.
- 114 R. Dalpozzo, A. De Nino, L. Maiuolo, A. Procopio, A. Tagarelli, G. Sindona and G. Bartoli, *J. Org. Chem.*, 2002, **67**, 9093–9095.
- 115 K. J. Eash, M. S. Pulia, L. C. Wieland and R. S. Mohan, *J. Org. Chem.*, 2000, **65**, 8399–8401.
- 116 C. Wiles, P. Watts and S. J. Haswell, *Tetrahedron*, 2005, **61**, 5209–5217.
- 117 S. C. W. Hook and B. Saville, *J. Chem. Soc. Perkin Trans. 2*, 1975, 589.
- 118 B. Karimi and J. Rajabi, *J. Mol. Catal. A Chem.*, 2005, **226**, 165–169.
- 119 J. McNulty, J. Wilson and A. C. Rochon, *J. Org. Chem.*, 2004, **69**, 563–565.
- 120 C. Xi, B. Yu, X. Yan and N. Tang, *Polyhedron*, 2013, **52**, 1323–1328.
- 121 S. Aizawa, M. Kondo, R. Miyatake and M. Tamai, *Inorganica Chim. Acta*, 2007, **360**, 2809–2813.
- 122 S. Aizawa, A. Majumder, Y. Yokoyama, M. Tamai, D. Maeda and A. Kitamura, *Organometallics*, 2009, **28**, 6067–6072.



- 123 P. Das, U. Bora, A. Tairai and C. Sharma, *Tetrahedron Lett.*, 2010, **51**, 1479–1482.
- 124 S. N. Arbuzova, P. A. Volkov, N. I. Ivanova, N. K. Gusarova, L. I. Larina, O. N. Kazheva, G. G. Alexandrov, O. A. Dyachenko and B. A. Trofimov, *J. Organomet. Chem.*, 2011, **696**, 2053–2058.
- 125 S. Aizawa, K. Fukumoto and T. Kawamoto, *Polyhedron*, 2013, **62**, 37–41.
- 126 D. Y. Vorobyev, V. F. Plyusnin, Y. V. Ivanov, V. P. Grivin, S. V. Larionov and H. Lemmetyinen, *Chem. Phys.*, 2003, **289**, 359–369.
- 127 Q. Jia, Q. Shang and W. Zhou, *Ind. Eng. Chem. Res.*, 2004, **43**, 6703–6707.
- 128 D. Gimes, D. Bertin, S. Marque, O. Guerret and P. Tordo, *Tetrahedron Lett.*, 2003, **44**, 1227–1229.
- 129 J. L. Hodgson, K. A. Green and M. L. Coote, *Org. Lett.*, 2005, **7**, 4581–4584.
- 130 N. Gusarova, N. Chernysheva, S. Yas'ko, T. Kazantseva, I. Ushakov and B. Trofimov, *Synthesis*, 2008, 2743–2746.
- 131 C. M. Jessop, A. F. Parsons, A. Routledge and D. J. Irvine, *Tetrahedron Lett.*, 2004, **45**, 5095–5098.
- 132 A. Gautier, G. Garipova, O. Dubert, H. Oulyadi and S. R. Piettre, *Tetrahedron Lett.*, 2001, **42**, 5673–5676.
- 133 A. F. Parsons, D. J. Sharpe and P. Taylor, *Synlett*, 2005, 2981–2983.
- 134 S. F. Malysheva, N. K. Gusarova, N. A. Belogorlova, T. V. Kashik, L. B. Krivdin, S. V. Fedorov and B. A. Trofimov, *Phosphorus. Sulfur. Silicon Relat. Elem.*, 2010, **185**, 1838–1844.
- 135 S. V. Fedorov, L. B. Krivdin, Y. Y. Rusakov, I. A. Ushakov, N. V. Istomina, N. A. Belogorlova, S. F. Malysheva, N. K. Gusarova and B. A. Trofimov, *Magn. Reson. Chem.*, 2009, **47**, 288–299.
- 136 D. Semenzin, G. Etemad-Moghadam, D. Albouy, O. Diallo and M. Koenig, *J. Org. Chem.*, 1997, **62**, 2414–2422.
- 137 G. Peters, *J. Am. Chem. Soc.*, 1960, **82**, 4751–4751.
- 138 C. M. Jessop, A. F. Parsons, A. Routledge and D. J. Irvine, *European J. Org. Chem.*, 2006, 1547–1554.
- 139 L. R. Mahoney, G. D. Mendenhall and K. U. Ingold, *J. Am. Chem. Soc.*, 1973, **95**, 8610–8614.
- 140 Y. Li, G. Qiu, Q. Ding and J. Wu, *Tetrahedron*, 2014, **70**, 4652–4656.
- 141 A. Perrier, V. Comte, C. Moïse, P. Richard and P. Le Gendre, *European J. Org. Chem.*, 2010, 1562–1568.
- 142 A. Artem'ev, S. Malysheva, N. Gusarova, N. Belogorlova, V. Shagun, A. Albanov and B. Trofimov, *Synthesis*, 2014, **47**, 263–271.
- 143 R. M. Kopchik and J. A. Kampmeier, *J. Am. Chem. Soc.*, 1968, **90**, 6733–6741.
- 144 J. S. Bryans, J. M. Large and A. F. Parsons, *J. Chem. Soc., Perkin Trans. 1*, 1999, 2897–2904.

- 145 J. S. Bryans, J. M. Large and A. F. Parsons, *J. Chem. Soc., Perkin Trans. 1*, 1999, 2905–2910.
- 146 S. F. Malysheva, N. K. Gusarova, A. V. Artem'ev, N. A. Belogorlova, A. I. Albanov, T. N. Borodina, V. I. Smirnov and B. A. Trofimov, *European J. Org. Chem.*, 2014, 2516–2521.
- 147 A. Fall, M. Sene, M. Gaye, G. Gómez and Y. Fall, *Tetrahedron Lett.*, 2010, **51**, 4501–4504.
- 148 C. X. Miao, L. N. He, J. Q. Wang and J. L. Wang, *Adv. Synth. Catal.*, 2009, **351**, 2209–2216.
- 149 Y. Yoshida, H. Tanaka and G. Saito, *Chem. Lett.*, 2007, **36**, 1096–1097.
- 150 E. J. Rauckman, G. M. Rosen and M. B. Abou-Donia, *J. Org. Chem.*, 1976, **41**, 564–565.
- 151 O. H. Oldenziel, D. Van Leusen and A. M. Van Leusen, *J. Org. Chem.*, 1977, **42**, 3114–3118.
- 152 E. Galera, J. Szykula and A. Zabż, *Liebigs Ann. der Chemie*, 1987, 777–780.
- 153 Harvard, [http://evans.harvard.edu/pdf/evans\\_pKa\\_table.pdf](http://evans.harvard.edu/pdf/evans_pKa_table.pdf) (accessed September 2015).
- 154 X. Li, H. Jiang, E. W. Uffman, L. Guo, Y. Zhang, X. Yang and V. B. Birman, *J. Org. Chem.*, 2012, **77**, 1722–1737.
- 155 V. D. Sen and V. A. Golubev, *J. Phys. Org. Chem.*, 2009, **22**, 138–143.
- 156 C. Baudequin, D. Brégeon, J. Levillain, F. Guillen, J. C. Plaquevent and A. C. Gaumont, *Tetrahedron Asymmetry*, 2005, **16**, 3921–3945.
- 157 F. Tang, K. Wu, Z. Nie, L. Ding, Q. Liu, J. Yuan, M. Guo and S. Yao, *J. Chromatogr. A*, 2008, **1208**, 175–181.
- 158 J. Hu, J. Ma, Z. Zhang, Q. Zhu, H. Zhou, W. Lu and B. Han, *Green Chem.*, 2015, **17**, 1219–1225.
- 159 F. Ono, H. Takenaka, T. Fujikawa, M. Mori and T. Sato, *Synthesis*, 2009, 1318–1322.
- 160 B. M. Smith, T. M. Kubczyk and A. E. Graham, *Tetrahedron*, 2012, **68**, 7775–7781.
- 161 M. Barbasiewicz and M. Makosza, *Org. Lett.*, 2006, **8**, 3745–3748.
- 162 B. T. Gregg, K. C. Golden and J. F. Quinn, *Tetrahedron*, 2008, **64**, 3287–3295.
- 163 M. Kurihara and W. Hakamata, *J. Org. Chem.*, 2003, **68**, 3413–3415.
- 164 M. A. Kumar, P. Swamy, M. Naresh, M. M. Reddy, C. N. Rohitha, S. Prabhakar, A. V. S. Sarma, J. R. P. Kumar and N. Narender, *Chem. Commun.*, 2013, **49**, 1711–1713.
- 165 D. R. Henton, R. A. McCreery and J. S. Swenton, *J. Org. Chem.*, 1980, **45**, 369–378.
- 166 M. Baruah and M. Bols, *Synlett*, 2002, 1111–1112.
- 167 B. Bartels and R. Hunter, *J. Org. Chem.*, 1993, **58**, 6756–6765.

- 168 S. Samanta, V. Pappula, M. Dinda and S. Adimurthy, *Org. Biomol. Chem.*, 2014, **12**, 9453–9456.
- 169 W. Bao and Z. Wang, *Green Chem.*, 2006, **8**, 1028.
- 170 J. P. Parrish, E. E. Dueno, S. I. Kim and K. W. Jung, *Synth. Commun.*, 2011, **30**, 2687–2700.
- 171 D. M. Denning and D. E. Falvey, *J. Org. Chem.*, 2013, **78**, 1934–1939.
- 172 US Patent US2010099761A1, 2010.
- 173 S. T. Heller, T. Fu and R. Sarpong, *Org. Lett.*, 2012, **14**, 1970–1973.
- 174 A. Millet and O. Baudoin, *Org. Lett.*, 2014, **16**, 3998–4000.
- 175 D. J. Sharpe, University of York PhD Thesis, 2005.
- 176 L. Maier, *Helv. Chim. Acta*, 1966, **49**, 1249–1259.
- 177 J. Dupont, C. S. Consorti, P. A. Z. Suarez and R. F. De Souza, *Org. Synth.*, 2002, **79**, 236.
- 178 A. Wang and H. Jiang, *J. Org. Chem.*, 2010, **75**, 2321–2326.
- 179 S. R. Roy, S. C. Sau and S. K. Mandal, *J. Org. Chem.*, 2014, **79**, 9150–9160.